



**HAL**  
open science

# The impact of exogenous IL-2 on the generation of CD8 memory precursor in vitro

Shaoying Wang

► **To cite this version:**

Shaoying Wang. The impact of exogenous IL-2 on the generation of CD8 memory precursor in vitro. Immunology. Université de Lyon; East China normal university (Shanghai), 2022. English. NNT : 2022LYSEN012 . tel-04099572

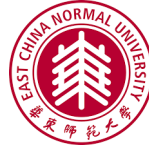
**HAL Id: tel-04099572**

**<https://theses.hal.science/tel-04099572>**

Submitted on 17 May 2023

**HAL** is a multi-disciplinary open access archive for the deposit and dissemination of scientific research documents, whether they are published or not. The documents may come from teaching and research institutions in France or abroad, or from public or private research centers.

L'archive ouverte pluridisciplinaire **HAL**, est destinée au dépôt et à la diffusion de documents scientifiques de niveau recherche, publiés ou non, émanant des établissements d'enseignement et de recherche français ou étrangers, des laboratoires publics ou privés.



Numéro National de Thèse : **2022LYSEN012**

## **THESE DE DOCTORAT DE L'UNIVERSITE DE LYON**

opérée par

**l'École Normale Supérieure de Lyon**

en cotutelle avec

**East China Normal University**

**Ecole Doctorale N° 340**

**Biologie Moléculaire, Intégrative et Cellulaire (BMIC)**

**Spécialité de doctorat** : Immunologie

**Discipline** : Sciences de la vie et de la santé

Soutenue publiquement le 16/05/2022, par :

**Shaoying WANG**

---

# **The impact of exogenous IL-2 on the generation of CD8 memory precursor *in vitro***

Impact de l'IL-2 exogène sur la génération de précurseurs de la CD8 mémoire *in vitro*

---

Devant le jury composé de :

|                    |                         |                        |                     |
|--------------------|-------------------------|------------------------|---------------------|
| ASTIER, Anne       | Directrice de recherche | INFINITY, INSERM       | Rapporteuse         |
| VERDEIL, Grégory   | Chargé de recherche     | Université de lausanne | Rapporteur          |
| FAURE, Mathias     | PR                      | UCBL, CIRI             | Examineur           |
| HASAN, Uzma        | Chargée de recherche    | CRCL, CIRI             | Examinatrice        |
| MARVEL, Jacqueline | Directrice de recherche | CIRI                   | Directrice de thèse |
| JIANG, wenzheng    | Professeur              | ECNU                   | Co-tuteur de thèse  |



## Abstract

The encounter of naive CD8 T cells with antigen presenting cells triggers their activation, proliferation and differentiation up to the memory state. To define the parameters necessary for the generation of memory precursors and to evaluate the impact of exogenous IL-2 (ex-IL-2) on this process, we have set-up an in vitro model of CD8 T cell activation. Our results indicate that cellular concentration strongly impacts the IL-2-dependency of CD8 T cell activation in vitro. Exogenous IL-2 is dispensable for cellular proliferation at high responding CD8 T concentration, but becomes essential at lower cell concentration. Exogenous IL-2 enhances the expression of CD25, EOMES and Bcl2 but downregulates TCF1 in all culture conditions. To assess the capacity of the in vitro activated CD8 T cells to participate in an ongoing effector response or to directly differentiate in memory cells we have transferred in vitro activated CD8 T cells in either virus-infected or naive mice. CD8 T cells activated with and without exogenous IL-2 have a similar capacity to participate in an ongoing immune response and to differentiate in memory cells following transfer in virus-infected mice. However, when transferred in naive hosts, CD8 T cells activated in the presence of exogenous IL-2 generate more memory cells that show enhanced functional memory features. Single cell transcriptomic analysis suggests that CD8 T cells activated without exogenous IL-2 generate more memory precursors 4 days after activation while cells activated with exogenous IL-2 acquire effector functions. Overall, the exogenous IL-2 delays the transition into memory precursor cells, allowing cells to acquire effector functions that imprint in the memory cells they generate. Finally, the role of other gamma-c cytokines on the activation of CD8 T cells was also studied, our results suggest that exogenous IL-7 and IL-15 drive a similar differentiation of CD8 as without any cytokine, while exogenous IL-4 and IL-21 induce a specific differentiation of CD8.



# Acknowledgements

First of all, I would like to thank all members of my thesis jury for accepting to evaluate my work. I would like to thank Dr. Anne ASTIER and Dr. Grégory VERDEIL for accepting to be the rapporteurs of this thesis. I also thank Pr. Mathias FAURE who accepted to be the president of the jury and Dr. Uzma HASAN for kindly examining my work.

I would certainly like to thank my thesis director Dr. Jacqueline MARVEL for agreeing to supervise me for this very interesting thesis. I really loved this multidisciplinary research project that links CD8 T cells, immunology and math model. During the past 4 years, I learned so many things that unfortunately I cannot mention everything here. I thank you for guiding me in the world of research, for teaching me how to do science correctly and rigorously, and how to organize myself professionally. I thank you for your help, your patience, your professionalism and the energy and time you have devoted.

I would also like to thank my thesis co-director Pr. Wenzheng JIANG for agreeing to supervise me during my PhD. I thank you for guiding me since my master work and your help during my PhD.

I would like to thank all the members of the ICL team, past and present, with whom I have worked during these years. So thanks: Daphné LAUBRETON, Margaux Prioux, Sophia DJEBALI, Maxence DUBOIS, Christophe ARPIN, Yann LEVERRIER, Séverine VALSESIA, Adèle FRIOT and Mélanie WENCKER.

I would particularly like to thank my colleague Daphné LAUBRETON for guiding my experiment at the beginning of my PhD, the help and encouragement during the past 4 years and advice, ideas to improve my thesis.

I would like to thank my colleague Margaux Prioux who did the single cell RNA-seq experiment and analysis, and wrote the results of the single cell RNA-seq data in the paper to enrich my work. I would also thank Simon de BERNARD for part of the analysis of the single cell RNA-seq data.

I would like to thank my colleague Sophia DJEBALI and Maxence DUBOIS for the help of some experiments.

I would like to thank my CST jury member Fabien CRAUSTE and Antoine MARÇAIS for the advice of my work and my life in France.

I would like to thank Pierre CONTARD and Jean-francois HENRY for the help of managing the mice.

Finally, I would like to thank china scholarship council (CSC), Pack ambition recherche, région Auvergne-Rhone-Alpes for funding my thesis.

## List of abbreviations

|                    |   |
|--------------------|---|
| ADA                | Adenosine deaminase                             |
| APC                | Antigen-presenting cell                         |
| Bcl-2              | B cell lymphoma 2                               |
| Bcl6               | B cell lymphoma 6                               |
| BCR                | B Cell Receptor                                 |
| BLIMP1             | B lymphocyte-induced maturation protein 1       |
| CCR7               | CC- chemokine receptor 7                        |
| CD62L              | L- selectin                                     |
| CMV                | Cytomegalovirus                                 |
| CTLA-4             | Cytotoxic T-Lymphocyte Antigen-4                |
| CTLs               | cytotoxic lymphocytes                           |
| CX3CR1             | CX3C chemokine receptor 1                       |
| CXCR3              | CXC-chemokine receptor 3                        |
| CXCR4              | CXC-chemokine receptor 4                        |
| DC                 | dendritic cell                                  |
| DN                 | double negative                                 |
| DP                 | double positive                                 |
| EOMES              | eomesodermin                                    |
| ETPs               | early thymocyte progenitors                     |
| Foxp3              | Forkhead box protein 3                          |
| GVHD               | graft-versus-host disease                       |
| HIV-1              | human immunodeficiency virus type 1             |
| HSCT               | Hematopoietic stem cell transplantation         |
| HTLV-1             | human T cell lymphotropic virus type 1          |
| ID2                | Inhibitor of DNA binding 2                      |
| ID3                | Inhibitor of DNA binding 3                      |
| IFN- $\gamma$      | Interferon- $\gamma$                            |
| IL-15              | Interleukin-15                                  |
| IL-2               | Interleukin-2                                   |
| IL-21              | Interleukin-21                                  |
| IL-4               | Interleukin-4                                   |
| IL-7               | Interleukin-7                                   |
| ITIMs              | immunoreceptor tyrosine-based inhibitory motifs |
| ITSMs              | immunoreceptor tyrosine-based switch motifs     |
| JNK                | c-Jun N-terminal Kinase                         |
| KLRG1              | Killer cell lectin-like receptor G1             |
| LAG-3              | Lymphocyte-activation gene 3                    |
| LCMV               | Lymphocytic choriomeningitis virus              |
| LN                 | lymph node                                      |
| MAP kinases (MAPK) | Mitogen-activated protein kinases               |
| MHC                | major histocompatibility complex                |

|                   |   |
|-------------------|---|
| MPEC              | memory precursor effector cell                                |
| mTECs             | medullary thymic epithelial cells                             |
| mTOR              | Mammalian target of rapamycin                                 |
| MuHV-4            | murid gammaherpesvirus 4                                      |
| PD-1              | Programmed cell Death 1                                       |
| PD-L              | Programmed Death-Ligand                                       |
| PI3K              | Phosphoinositide 3-Kinases                                    |
| pMHC              | peptide +MHC  |
| RSV               | respiratory syncytial virus                                   |
| Runx3             | Runt-related transcription factor 3                           |
| SCID              | Severe combined immunodeficiency disease                      |
| SLEC              | shorted-lived effector T cell                                 |
| SP                | single positive   |
| STAT              | Signal Transducer and Activator of Transcription              |
| T-bet             | T-box transcription factor                                    |
| TCF1/7            | T cell factor 1/7   |
| T <sub>CM</sub>   | T central memory T cell                                       |
| TCR               | T Cell Receptor   |
| T <sub>EM</sub>   | T effector memory cell  |
| T <sub>EMRA</sub> | T effector memory RA cell                                     |
| Tex               | T exhausted cells   |
| TGFβ              | Transforming Growth Factors β                                 |
| T <sub>H</sub>    | T helper cells  |
| ThPOK             | T-helper inducing POZ-Kruppel like factor                     |
| TIM3              | T cell immunoglobulin and mucin domain-containing protein 3   |
| T <sub>N</sub>    | T naive cell  |
| TNF-α             | Tumor necrosis factor α                                       |
| T <sub>PM</sub>   | T peripheral memory cell                                      |
| TRAIL             | Tumor-necrosis factor (TNF)-related apoptosis-inducing ligand |
| Treg              | regulatory T cells  |
| T <sub>RM</sub>   | T tissue-resident memory cell                                 |
| T <sub>SCM</sub>  | T memory stem cells   |
| T <sub>TE</sub>   | T terminally differentiated effector cell                     |
| T <sub>VM</sub>   | virtual memory CD8 T cell                                     |
| XCL1              | XC-chemokine ligand 1   |

## List of Figures

Figure 1. Scheme of T cell development and selection in the thymus.

Figure 2. Development of  $\gamma\delta$  and  $\alpha\beta$  T cell.

Figure 3. Model of T cell positive and negative selection and CD4 and CD8 T cell differentiation.

Figure 4. Dynamics of a T cell response and memory cell distribution.

Figure 5. The structure of TCR-CD3 complex.

Figure 6. Signal 3 alters the differentiation from tolerance to full activation of naive CD8 T cells.

Figure 7. CD4 T cell subsets.

Figure 8. Cellular interactions during the activation of CD8 T cells in vivo.

Figure 9. Key cell surface receptor–ligand and cytokine–receptor interactions during the T cell priming.

Figure 10. Relationship of  $T_{CM}$  and  $T_{EM}$ .

Figure 11. The phenotype of human naive and diverse memory T cell subsets.

Figure 12. T cell differentiation following acute infection/vaccination or chronic infection/cancer.

Figure 13. Molecular mechanisms of inhibitory receptors involved in T cell exhaustion.

Figure 14. Transcriptional factors associated with effector and memory T cell differentiation.

Figure 15. The role of TCF1 in CD8 T cell in response to acute and chronic infection.

Figure 16. Models for generation of effector and memory T cell.

Figure 17. NELM differentiation model.

Figure 18. Schematic of CD8 T cell differentiation.

Figure 19. Memory precursors are generated at multiple time points.

Figure 20. Receptors of  $\gamma c$  family cytokines.

Figure 21. IL-2 signaling modulates the differentiation of activated CD8.

Figure 22. The mode of IL-2 and IL-15 interacting with their receptors.

Figure 23. Activation signals by anti-CD3/anti-CD28 beads and DCs.

Figure 24. Number of activated CD8 T cells generated after 4 days following activation in different context.

Figure 25. Activation of CD8 T cells with BMDCs that had been matured with CpG reduced the expansion and memory formation in naive mice.

Figure 26. Impact of ex-IL-2 on the generation of memory precursors with time.

Figure 27. The expression of CD25 and TCF1 by CD8 T cells 4 days after activation.

Figure 28. The impact of ex-IL-2 in vitro activation on the activation and differentiation of CD8 T cells.

## List of Tables

Table 1. Surface markers expressed on human and mouse T cell.

Table 2. Memory T cell subsets.

Table 3. Expression of  $\gamma$ c family cytokine receptors.

## Table of Contents

|          |   |           |
|----------|---|-----------|
| <b>1</b> | <b>CD8 T cells</b> .....  | <b>1</b>  |
| 1.1      | The origin and development of T lymphocytes .....   | 1         |
| 1.2      | The role of CD8 T cell .....  | 5         |
| 1.2.1    | The dynamics of CD8 T cells following acute infection .....                               | 6         |
| 1.2.2    | Naive CD8 T cells .....   | 7         |
| 1.2.3    | Effector CD8 T cells .....  | 8         |
| 1.2.4    | Memory CD8 T cells .....  | 8         |
| 1.3      | The factors that drive the activation of naive CD8 T cells .....                          | 9         |
| 1.3.1    | Surface receptors involved in the activation of CD8 T cells .....                         | 9         |
| 1.3.2    | Cellular interactions involved in the activation of CD8 T cells .....                     | 13        |
| 1.4      | Effector and Memory CD8 T cell subsets.....   | 19        |
| 1.4.1    | T <sub>CM</sub> and T <sub>EM</sub> .....   | 20        |
| 1.4.2    | T <sub>SCM</sub> .....  | 22        |
| 1.4.3    | T <sub>EMRA</sub> .....   | 23        |
| 1.4.4    | T <sub>RM</sub> .....   | 24        |
| 1.4.5    | Other subsets .....   | 25        |
| 1.5      | T cell exhaustion.....  | 27        |
| 1.6      | Transcription factors important for the differentiation of CD8 during acute infection ... | 31        |
| 1.6.1    | T-bet and EOMES .....   | 32        |
| 1.6.2    | TCF1 .....  | 34        |
| 1.7      | The differentiation of CD8 .....  | 35        |
| 1.7.1    | Models of CD8 T cell differentiation .....  | 35        |
| 1.7.2    | New approaches to validate or revisit these models .....                                  | 39        |
| 1.7.3    | The Schematic of CD8 T cell differentiation.....  | 41        |
| <b>2</b> | <b>yc cytokines as important regulators of CD8</b> .....                                  | <b>43</b> |
| 2.1      | IL-2.....   | 44        |
| 2.1.1    | The role of IL-2 in regulating effector CD8 T cell response .....                         | 45        |
| 2.1.2    | The role of IL-2 in regulating memory CD8 T cell response.....                            | 45        |
| 2.1.3    | The role of IL-2 in regulating the differentiation of CD8 T cell .....                    | 47        |
| 2.2      | IL-4.....   | 49        |
| 2.2.1    | The impact of IL-4 on effector CD8 T cells .....  | 49        |
| 2.2.2    | The impact of IL-4 on memory CD8 T cells.....   | 50        |

|   |            |
|---|------------|
| <b>2.3 IL-7.....</b>  | <b>51</b>  |
| <b>2.3.1 The role of IL-7 in regulating the survival and homeostasis of naive and memory CD8 T cells.....</b>   | <b>51</b>  |
| <b>2.3.2 The role of IL-7 in regulating memory CD8 T cell differentiation .....</b>                             | <b>51</b>  |
| <b>2.3.3 The role of IL-7/IL-7R in cancer therapy .....</b>   | <b>52</b>  |
| <b>2.4 IL-15.....</b>   | <b>53</b>  |
| <b>2.4.1 The role of IL-15 in regulating the survival and homeostasis of naive and memory CD8 T cells .....</b> | <b>54</b>  |
| <b>2.4.2 The role of IL-15 in regulating CD8 T cell differentiation .....</b>                                   | <b>54</b>  |
| <b>2.4.3 The impact of IL-15 on CD8 T cells during chronic infection.....</b>                                   | <b>55</b>  |
| <b>2.5 IL-21.....</b>   | <b>55</b>  |
| <b>2.5.1 The impact of IL-21 on CD8 T cells during acute infection.....</b>                                     | <b>55</b>  |
| <b>2.5.2 The impact of IL-21 on CD8 T cells during chronic infection.....</b>                                   | <b>56</b>  |
| <b>3 Research projects.....</b>   | <b>58</b>  |
| <b>3.1 Scientific context and objectives .....</b>  | <b>58</b>  |
| <b>3.2 Model set up .....</b>   | <b>60</b>  |
| <b>3.3 Article .....</b>  | <b>72</b>  |
| <b>3.4 Extended results.....</b>  | <b>108</b> |
| <b>4 Discussion and perspectives .....</b>  | <b>115</b> |
| <b>4.1 Comparison of different culture conditions .....</b>   | <b>115</b> |
| <b>4.2 The role of IL-2 .....</b>   | <b>118</b> |
| <b>4.3 The role of IL-4, IL-7, IL-15 and IL-21 .....</b>  | <b>123</b> |
| <b>5 Conclusion .....</b>   | <b>124</b> |

# 1 CD8 T cells

The immune system can be divided into two categories: innate immunity and adaptive immunity. Innate immunity consists of hematopoietic cells including macrophages, neutrophils, dendritic cells, mast cells, eosinophils and natural killer (NK) cells and non-hematopoietic components such as skin or epithelial cells. They form the front line of defense and confer rapid inflammatory responses. Adaptive immunity is composed of adaptive immune cells including B cells and T cells. B lymphocytes produce antibodies, whereas the T lymphocytes confer the cellular immune responses (Bonilla and Oettgen, 2010). Adaptive immune cells develop a diverse repertoire of antigen-specific receptors (BCRs and TCRs) which increases the probability to recognize a given antigen and promote the generation of pathogen specific effector and memory cells (Kaur and Secord, 2019).

## 1.1 The origin and development of T lymphocytes

T cells develop in the thymus which provides a specialized microenvironment necessary for their differentiation and selection (Bonilla and Oettgen, 2010; Takahama, 2006; Taniuchi, 2018). At first, a small number of hematopoietic progenitors defined as early thymocyte progenitors (ETPs), that have the potential to become non-T lymphoid cells, migrates from the bone marrow or fetal liver to the thymus (Bonilla and Oettgen, 2010). Within the thymic microenvironment, progenitors proliferate and undergo the differentiation and selection processes that direct the development of mature T cells. The developing T lymphocytes classically undergo four differentiations stages that are defined based on the expression of the surface markers CD4 and CD8. First, ETPs are negative for both CD4 and CD8 and are termed as the CD4<sup>-</sup>CD8<sup>-</sup> double-negative (DN) cells that are further subdivided into four DN steps including DN1, DN2, DN3 and DN4 according to the surface expression of CD44 and CD25. Second, the transition from DN cells to CD4<sup>+</sup>CD8<sup>+</sup> double-positive (DP) thymocytes happens at the outer cortex of the thymus. Third, DP thymocytes acquire the capacity to survive and differentiate into CD4 or CD8 single positive (SP) thymocytes upon positive selection in the cortex. Fourth, single positive thymocytes interact with medullary thymic epithelial cells (mTECs) to complete their development. Mature T cells then egress from the thymus to peripheral lymphoid sites

where they will be called naive T cells (Figure 1) (Takahama, 2006; Taniuchi, 2018).

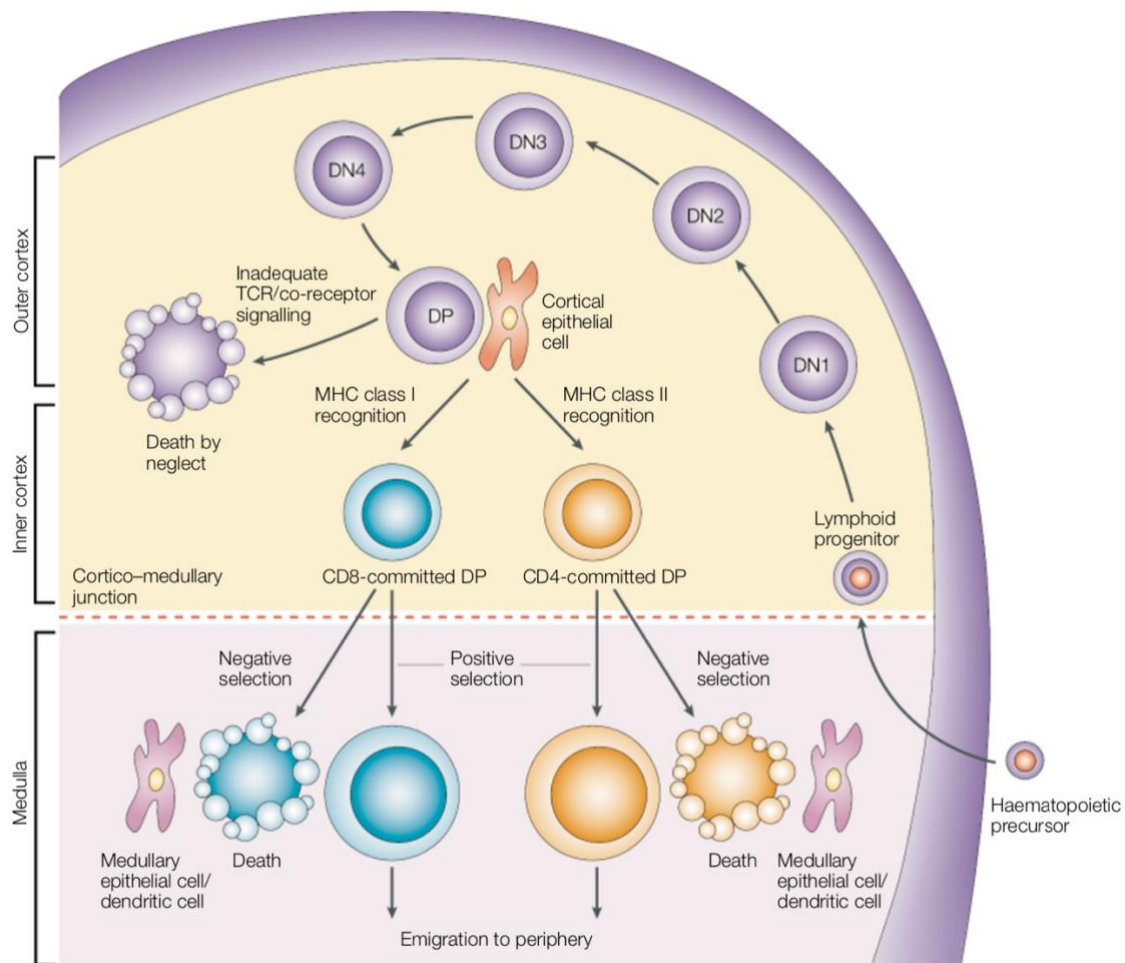


**Figure 1. Scheme of T cell development and selection in the thymus.** Common hematopoietic progenitors migrate to the thymus. Early progenitor T cells negative for T cell receptor (TCR), CD4 and CD8 are named double-negative (DN) thymocytes. Then DN cells undergo four phases of differentiation: DN1 (CD44+CD25-), DN2 (CD44+CD25+), DN3 (CD44-CD25+) and DN4 (CD44-CD25-) and further differentiate into double positive (DP) thymocytes. During this process, cells acquire a complete  $\alpha\beta$  TCR. Some of the DP thymocytes are then tuned to CD8 single positive cells or CD4 single positive cells or apoptotic death. Single positive cells migrate from the medulla to peripheral lymphoid sites. (Germain, 2002).

T lymphocytes are defined by the surface expression of  $\alpha\beta$  or  $\gamma\delta$  T cell receptor (TCR) complexes. T cells with  $\alpha\beta$  TCRs recognize the short peptides of foreign antigen presented on MHC class I or class II molecules. Typically, mature  $\alpha\beta$  T cells include two lineages that are defined by surface expression of either CD4 which binds MHC-class-II or CD8 which

binds MHC- class-I. CD4 T cells serve as helper or regulatory T cells, whereas CD8 T cells are mainly cytotoxic (Germain, 2002). The majority of the T lymphocytes that circulate in the blood and peripheral organs are  $\alpha\beta$  T cells,  $\gamma\delta$  T cells only accounting for a small fraction (1–5%) of them. However,  $\gamma\delta$  T cells constitute a high proportion of T cells (up to 50%) in epithelium and mucosa-associated tissues, such as the skin and intestine.  $\gamma\delta$  T cells differ from  $\alpha\beta$  T cells and recognize soluble protein and endogenous non-proteic antigen (Carding and Egan, 2002).

In mice, developmental transitions among DN thymocytes correlate to the modification of the expression of surface markers CD24, CD25, CD44 and CD117 (Figure 2). The DN compartment is heterogeneous and can be subdivided into 4 phases based on the expression of CD25 and CD44. During the transition from DN1 stage (CD44+CD25-) to DN2 cells (CD44+CD25+), DN thymocytes undergo irreversible gene rearrangements at the TCR $\beta$  or TCR $\gamma$ -TCR $\delta$  gene loci. The V and DJ segments successfully assembled at the TCR $\beta$  locus result in the functional TCR $\beta$  chain which forms pre-TCR complexes. At the DN3 stage (CD44-CD25+), signaling through pre-TCR complexes or  $\gamma\delta$  TCR leads to thymocyte proliferation and further differentiation. The transition from pre-selection DN3a to post-selection DN3b stage therefore corresponds to  $\beta$ -selection or  $\gamma\delta$ -selection. At DN4 stage, cells downregulate CD25 and are CD44-CD25-. The  $\gamma\delta$  lymphocytes remain DN and become mature. For  $\alpha\beta$  T cells, signaling through pre-TCR complexes activates the expression of the CD4 and CD8, consequently driving DN thymocytes into CD4 and CD8 double-positive (DP) thymocytes, which account for 80% of thymocytes. This process is accompanied by the recombination of the V and J segments of the TCR $\alpha$  gene. As a result, the DP thymocytes acquire  $\alpha\beta$ TCR complexes on the surface (Taniuchi, 2018). DP cells then undergo positive and negative selections leading to the appearance of CD4 or CD8 single-positive (SP) T cells (Ciofani and Zuniga-Pflucker, 2010).

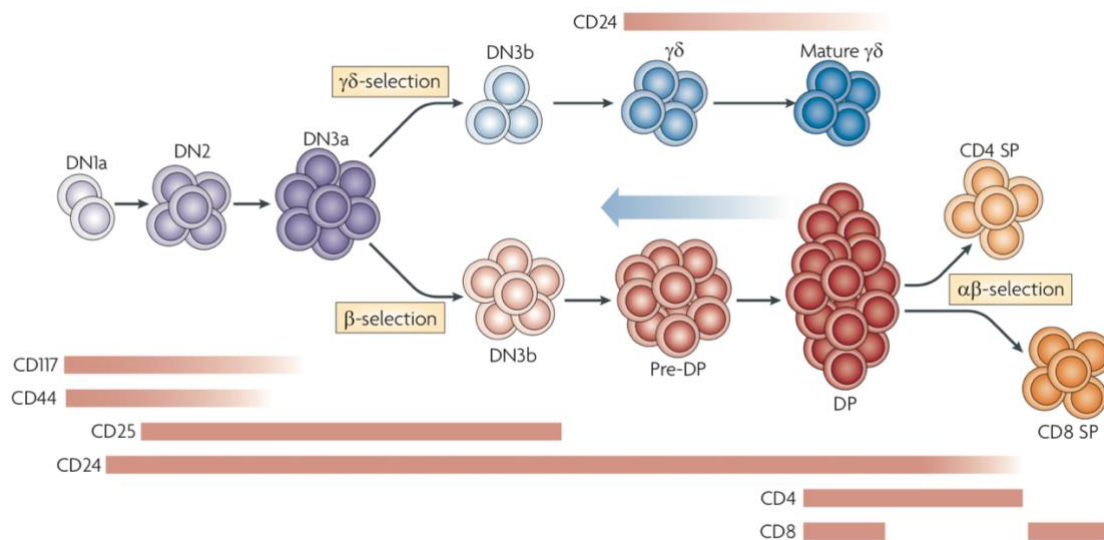


**Figure 2. Development of  $\gamma\delta$  and  $\alpha\beta$  T cell.** Illustration of significant surface markers used to distinguish the specific developmental subsets in the thymus. The main decision stage is the transition from the double-negative stage 3a (DN3a) to the DN3b stage, exerting the divergence of the TCR $\alpha\beta$  and TCR $\gamma\delta$  lineages. (Ciofani and Zuniga-Pflucker, 2010).

The positive and negative selection process is considered to depend on the affinity of the T cell receptor binding to self-peptide: self MHC complex (Figure 3a) (Murphy and Weaver, 2016). Rearrangements of TCR $\alpha$  and  $\beta$  chain gene lead to the generation a large pool of immature thymocytes that express a diverse repertoire of specificities. A lot of immature thymocytes receive no signals and die because their TCRs have very low affinity for self-peptide+MHC (pMHC) complexes. Another fraction of immature thymocytes possessing TCRs with intermediate affinity for self-pMHC complexes are positively selected and survive. The thymocytes whose receptors have excessively strong reactivity to self-pMHC complexes are negatively selected and removed by apoptosis. This negative selection establishes self-tolerance of the mature T cell population. A small fraction of positively selected cells receives a slightly lower level of signals than negatively selected cells and differentiates into regulatory T cells (Treg). This process is referred to as agonist selection (Murphy and Weaver, 2016).

The positive selection process determines whether an immature thymocyte will become a CD4 or CD8 single-positive T cell (Figure 3b) (Taniuchi, 2018). When recognizing the self-pMHC complexes, CD4 and CD8 double-positive T cells receive survival signals and

differentiate into CD4 or CD8 single-positive T cells according to the recognition of MHC class II and I, respectively. At the molecular level, this developmental choice is regulated by the expression of two antagonist transcription factors, ThPOK and Runx3. The recognition of MHC-I by the TCR thus leads to the expression of Runx3, which blocks the expression of ThPOK and the generation of CD4 single-positive T cells and promotes the generation of CD8 single-positive T cells while the recognition of MHC-II molecule induces ThPOK and inhibits Runx3 expression, resulting in the formation of CD4 single-positive T cells (Takaba and Takayanagi, 2017; Taniuchi, 2018).

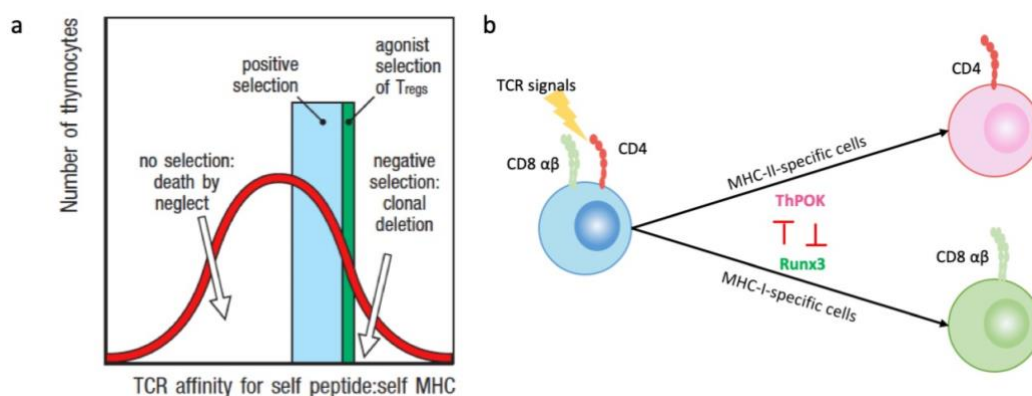


**Figure 3. Model of T cell positive and negative selection and CD4 and CD8 T cell differentiation.**  
**a.** Immature thymocytes having TCRs with very low or high affinity for self-pCMH complexes die by apoptosis while those possessing TCRs with intermediate affinity for self-pCMH complexes acquire survival signals and are positively selected. A small fraction of positively selected CD4 thymocytes differentiates into regulatory T cells (Treg). (Murphy and Weaver, 2016). **b.** DP precursors that express specific TCRs binding to MHC-class I or MHC- class II differentiate into either CD8 SP or CD4 SP thymocytes, respectively. Expression of the Runx3 and ThPOK in this differentiation process. Adapted from (Taniuchi, 2018).

## 1.2 The role of CD8 T cell

The function of the T lymphocytes is to destroy the intracellular invaders which cannot be detected by antibodies. Most of the CD4 T cells serve as helper cells ( $T_H$  cells) for the B cell response and the formation of functional CD8 cytotoxic T lymphocytes. CD8 T cells remove the targets in which intracellular pathogens, including viruses, some bacteria or parasites proliferate (Bonilla and Oettgen, 2010). CD8 T cells also play key roles in cancer

surveillance by their capacity to recognize and kill tumor cells (Shourian et al., 2019).

### 1.2.1 The dynamics of CD8 T cells following acute infection

Upon acute infection at a mucosal tissue site, dendritic cells (DCs) endocytose pathogen and travel to the draining secondary lymphoid organs where they present antigen to naive CD8 T cells, leading to their activation, proliferation and differentiation through TCR stimulation. DCs also provide co-stimulation and inflammatory cytokine signals necessary to CD8 activation (Bromley et al., 2008). Naive CD8 T cells divide 15-20 times and the number of activated CD8 T cell increase up to  $5 \cdot 10^4$ -fold. CD8 T cells then enter the blood and the effector CD8 T cells will subsequently migrate to the infected-site to eliminate the pathogen. Following antigen clearance, most of effector cells (90%-95%) die by apoptosis, but a small fraction (5%-10%) survives as long-lived memory T cells that confer the protection and can mount an enhanced response upon secondary challenge (Figure 4) (Dijkgraaf et al., 2021; Williams and Bevan, 2007).

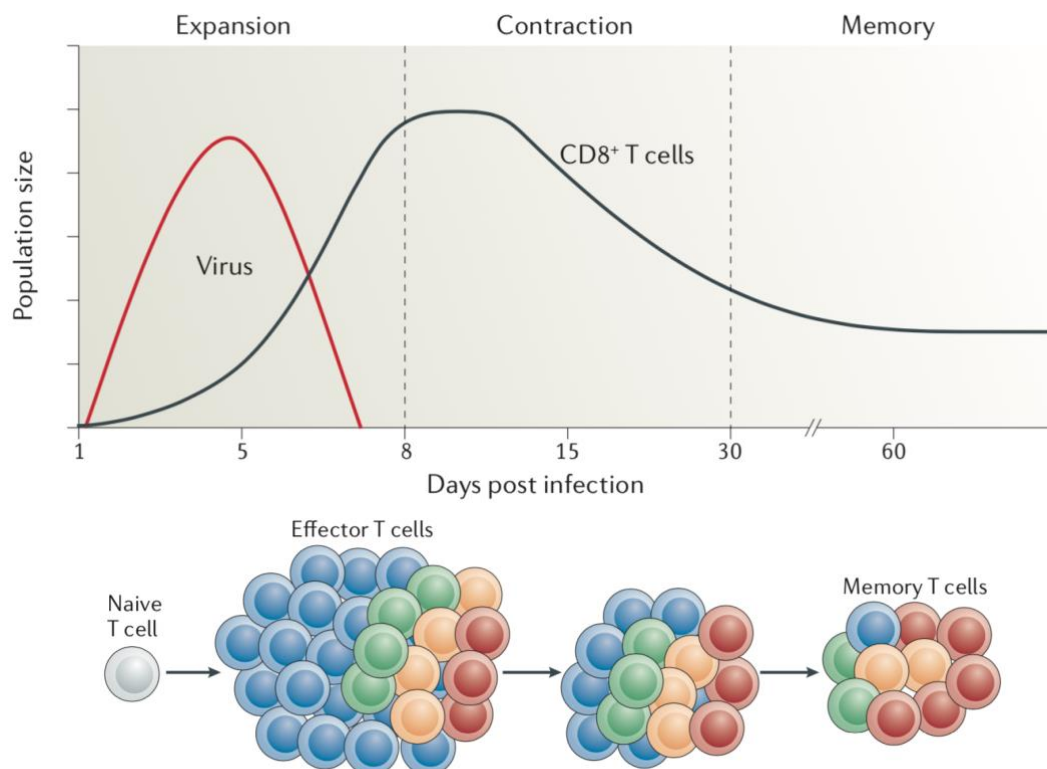


**Figure 4. Dynamics of a T cell response and memory cell distribution.** Following an acute infection of virus, antigen-specific T cells undergo three distinct phases: clonal expansion, contraction and memory generation. The pool of effector T cells can be classified in distinct subsets. Notably, not

all effector T cells differentiate into memory T cells. (Kaech and Cui, 2012).

### 1.2.2 Naive CD8 T cells

Naive CD8 T cells are quiescent cells that are released by the thymus into the circulation and have not yet encountered their cognate antigen. Human naive CD8 T cells are characterized by the surface expression of CD45RA (long isoform of CD45, naive marker), CC- chemokine receptor 7 (CCR7), L- selectin (CD62L) and IL-7R $\alpha$ , but are negative for CD25 and CD69 activation markers and memory marker-CD45RO (shorter isoform of CD45). Murine and human CD8 T cells express the same surface markers except for the expression for the CD45 isoforms that show a different expression pattern and are thus not used to identify murine naive cells. A key marker used only in mouse studies is the CD44 isoform recognized by the antibody IM7, which is expressed by effector and memory CD8 T cells but not by naive cells (Table 1) (De Rosa et al., 2001; van den Broek et al., 2018). Adequate numbers of naive CD8 T cells are required to ensure the efficient immune response against novel pathogens. Homeostatic proliferation and survival of naive T cells depending on IL-7 and IL-15 are critical for naive T cell pool maintenance (Rathmell et al., 2001; Takada and Jameson, 2009). Naive CD8 T cells keep on circulating between blood and secondary lymphoid organs (van den Broek *et al.*, 2018). When naive T cells encounter their specific antigen presented in an infection site-draining lymph node, they become activated, proliferates and differentiates into effector and memory cells. Antigen-specific effector CD8 T cells then leave the lymphoid tissue to re-enter into circulation (Dijkgraaf *et al.*, 2021).

|                     | human  | mouse                             |
|---------------------|--|-----------------------------------|
| naive               | CD45RO-, CD95-<br>CD45RA+, CCR7+, CD62L+       | CD44-, CD95-<br>CCR7+, CD62L+     |
| Effector/<br>memory | CD45RA-<br>CD45RO+, CD95+<br>CCR7+/-, CD62L+/- | CD44+, CD95+<br>CCR7+/-, CD62L+/- |

**Table 1. Surface markers expressed on human and mouse T cell.** Human naive T cells are CD45RO<sup>-</sup>, whereas mouse naive T cells are CD44<sup>-</sup>. And they are both negative for CD95 but positive for CCR7 and CD62L. Human effector and/or memory T cells are CD45RO<sup>+</sup>, whereas mouse effector and/or memory T cells are CD44<sup>+</sup>.

### **1.2.3 Effector CD8 T cells**

Naive CD8 T cells differentiate in CD8 cytotoxic T cells (also called cytotoxic T lymphocytes, or CTLs). CTLs mediate their effector function through cell contact-dependent killing of target host cells and secretion of pro-inflammatory cytokines (Bonilla and Oettgen, 2010). Indeed, CTLs recognize the peptide: MHC-class I complexes on a target cell and induce its apoptosis (Bonilla and Oettgen, 2010). This process requires the expression and secretion of cytotoxic proteins such as perforin and granzymes. Perforin induces the formation of pores on the membrane of the target cell, which allows for the entry of granzymes. Granzymes then induce the apoptotic cell death of the target cell (Ashton-Rickardt, 2005; Voskoboinik et al., 2015). The interaction of Fas-ligand on the CTL and Fas (CD95) on the target cell membrane also participate in the induction of apoptosis (Russell and Ley, 2002). CD8 cytotoxic T cells also produce cytokines, such as IFN- $\gamma$  and TNF- $\alpha$ , that contribute to the host protection (Dobrzanski et al., 2004). IFN- $\gamma$  enhances the expression of MHC class I molecule and antigen processing and presentation on cells, increasing their chance to be targeted by CTLs (Zhou, 2009).

### **1.2.4 Memory CD8 T cells**

Memory CD8 T cells are considered as the CD8 T cell pool that has responded to antigen and is maintained for a long time. Unlike naive cells which are unable to mount immediate effector function, memory cells perform immediate proliferation, cytotoxic functions and produce effector cytokines upon antigen re-encounter (Barber et al., 2003; Lalvani et al., 1997; Pihlgren et al., 1996; Veiga-Fernandes et al., 2000). Furthermore, they persist at a higher frequency than naive T cells. Finally, they share some similarities in gene expression and function with effector cells (Martin and Badovinac, 2018). In conclusion, memory CD8 T cells confer a more rapid and vigorous protection following secondary challenge with the same pathogen (Turner et al., 2021). Both the quantity and the quality of memory CD8

T cells determine the degree of memory CD8 T cell mediated protection (Martin and Badovinac, 2018). The memory CD8 T cell pool is heterogeneous in both phenotype and function (see section 1.4).

Besides the antigen-induced memory CD8 T cells described above, the memory CD8 T cell pool also includes innate memory CD8 T cells, also known as memory phenotype CD8 T cells or virtual memory CD8 T cells ( $T_{VM}$ ) (Martin and Badovinac, 2018). Innate memory CD8 T cells account for about 5%-15% of total circulating CD8 T cells and express high level of CD44 and CD122 (Turner et al., 2021). These cells are independent of foreign antigen exposure for their generation and are initially driven by the interaction of T cell precursors with self-peptide+MHC class I (pMHCI) in the thymus (Miller et al., 2020). In a lymphopenic environment, innate memory CD8 T cells also arise from naive cells in the periphery through homeostatic proliferation in response to various cytokines (Jameson et al., 2015). Antigen-induced memory CD8 T cells can be distinguished from innate memory CD8 T cells by NKG2D expression which serves as a costimulatory receptor inducing increased proliferation, as well as integrin expression (including CD29, CD49a and CD49d), which confer them the ability to migrate to the inflamed peripheral tissues (Grau et al., 2018). Similar to antigen-induced memory CD8 T cells, innate memory CD8 T cells proliferate and produce IFN- $\gamma$  following TCR stimulation or IL-12/IL-18 activation (Jameson et al., 2015) but at lower extent than antigen-induced memory CD8 T cells (Grau et al., 2018). Innate memory CD8 T cells also develop cytolytic functions and confer protection in several pathogen challenge models (Jameson et al., 2015). Innate memory CD8 T cells also exist in humans and show similarities with mouse innate memory CD8 T cells in terms of function and levels of CD122 expression (Turner et al., 2021).

## **1.3 The factors that drive the activation of naive CD8 T cells**

### **1.3.1 Surface receptors involved in the activation of CD8 T cells**

Upon the initial priming, naive CD8 T cell can acquire effector functions and give rise to memory cells. Three signals, including TCR (signal 1), co-stimulation (signal 2), such as

CD80/CD86-CD28 interactions, and inflammatory cytokines (signal 3), such as IL-12 and type I IFN, contribute to the activation, expansion and differentiation of naive CD8 T cells.

### Signal 1- TCR signal

The TCR expressed on the surface of CD8 T cells help recognize the multiple antigens and trigger the activation of CD8 T cells. TCR is a multiprotein complex composed of TCR  $\alpha\beta$  heterodimer and invariant CD3 polymers consisting of a CD3 $\delta\epsilon$  heterodimer, a CD3 $\gamma\epsilon$  heterodimer, and a CD3 $\zeta\zeta$  homodimer (Figure 5) (Mariuzza et al., 2020). The extracellular segments of the  $\alpha$  and  $\beta$  TCR chains mediate the recognition of pMHC while the CD3 molecules are responsible for transducing the activation signals to the T cells. The  $\alpha$  and  $\beta$  TCR chains have an immunoglobulin (Ig) -like structure with a constant region and a variable region which contains CDR (Complementarity Determining Region) loops. Each chain has three CDR loops called CDR1, CDR2 and CDR3 that directly bind to pMHC complex (Rossjohn et al., 2015). The CD3 $\gamma$ , CD3 $\delta$ , CD3 $\epsilon$  chains each contain one ITAMs and CD3 $\zeta$  chain has three ITAMs (Immunoreceptor Tyrosine-based Activation Motifs). The ITAMs are subjected to phosphorylation and transmit activation signals to T cells (Mariuzza et al., 2020).

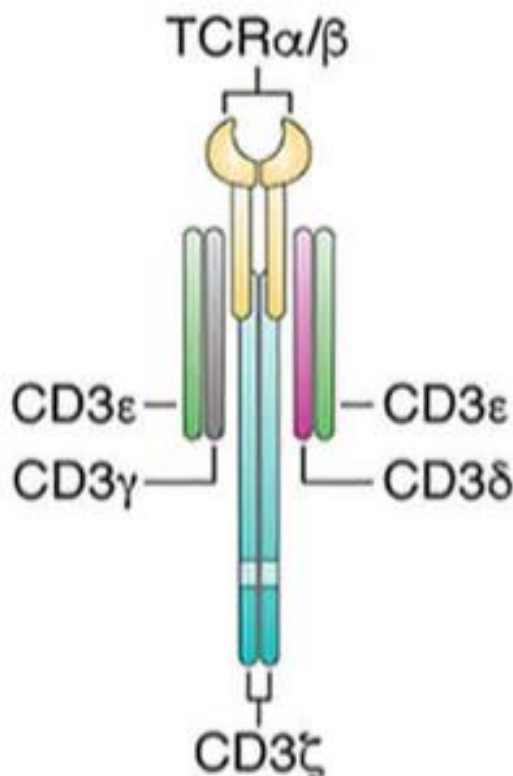


**Figure 5. The structure of TCR-CD3 complex.** The T cell receptor (TCR)-CD3 complex contains a  $\alpha\beta$  TCR and invariant CD3 dimers: CD3 $\delta\epsilon$ , CD3 $\gamma\epsilon$  and CD3 $\zeta\zeta$ . (Mariuzza et al., 2020).

## **Signal 2-costimulation**

### **CD80/CD86-CD28 interaction**

CD80 (B7.1) is generally not expressed on non-activated DCs, while CD86 (B7.2) is expressed at low level. Infections, tissue damage, inflammatory cytokines and lipopolysaccharide (LPS) promote the expression of both receptors (Acuto and Michel, 2003). CD80 and CD86 bind to the CD28 co-stimulatory receptor which is expressed on T cells to enhance T cells activation (McAdam et al., 1998). CD28 signaling, in conjunction with TCR signal, upregulates the expression by the T cell of multiple cytokines (for example, IL-2, IFN- $\gamma$ , IL-4), chemokines, receptors for cytokines and chemokines (such as IL-12R) (Acuto and Michel, 2003; McAdam *et al.*, 1998; Park et al., 2001). CD28 mainly serves as a quantitative rather than a qualitative supplier that amplifies the gene expression and signaling pathways induced by the TCR (Acuto and Michel, 2003). The proliferative response of CD28-deficient T cells to anti-CD3 is significantly disrupted (Green et al., 1994; Lenschow et al., 1996; Sigal et al., 1998). Blockade of CD80 and CD86 using monoclonal antibodies (Ab) inhibits the generation of CTLs in response to exogenous antigen and virus (Sigal *et al.*, 1998).

CD28 signaling plays a crucial role in enhancing the glycolytic rate in T cells through PI3K and Akt in response to activation, while neither CD3 nor CD28 alone could induce significant change in the expression of glucose transporter-Glut1. TCR activation in combination with CD28 co-stimulation could upregulate the expression of Akt and Glut1 (Frauwirth et al., 2002).

### **Signal 3-inflammatory cytokines**

Along with antigen and co-stimulation, CD8 T cell activation requires a third signal. Many studies suggest that signal 3 mainly contains IL-12 and type I IFN (IFN $\alpha/\beta$ ). Following the stimulation of CD40L, DCs produce high level of IL-12 (Cella et al., 1996). Type I IFNs are mainly produced by virus-infected cells and plasmacytoid DCs produce a large amount of this cytokine (Cella et al., 1999).

The two cytokines program the regulation of a common set of about 355 genes within 3

days of initial activation (Agarwal et al., 2009). In the absence of IL-12, the CD8 T cells develop minimal effector function, survive poorly, and fail to give rise to a functional memory pool. As a result, even though a small fraction of CD8 cells survive upon activation, they are tolerant (Figure 6) (Mescher et al., 2006). In response to peptide vaccination, type I IFN enhance the proliferation, effector function and survival of vaccine-induced CD8 T cells; the accumulation of CD8 T cells in tumor; the generation and long-term persistence of memory CD8 T cells and tumor suppression (Sikora et al., 2009). IL-12 and type I IFN upregulate the perforin and granzyme B mRNA and protein expression in CD8 T cells stimulated with anti-CD3/CD28 (Curtsinger et al., 2005). In peptide immunization models, high levels of B7 alone cannot compensate the requirement for IL-12 for inducing the differentiation of cytolytic CD8 T cells. Furthermore, IL-12 is essential for the production of IFN- $\gamma$  by effector CD8 T cells and memory CD8 T cells (Curtsinger et al., 2003).

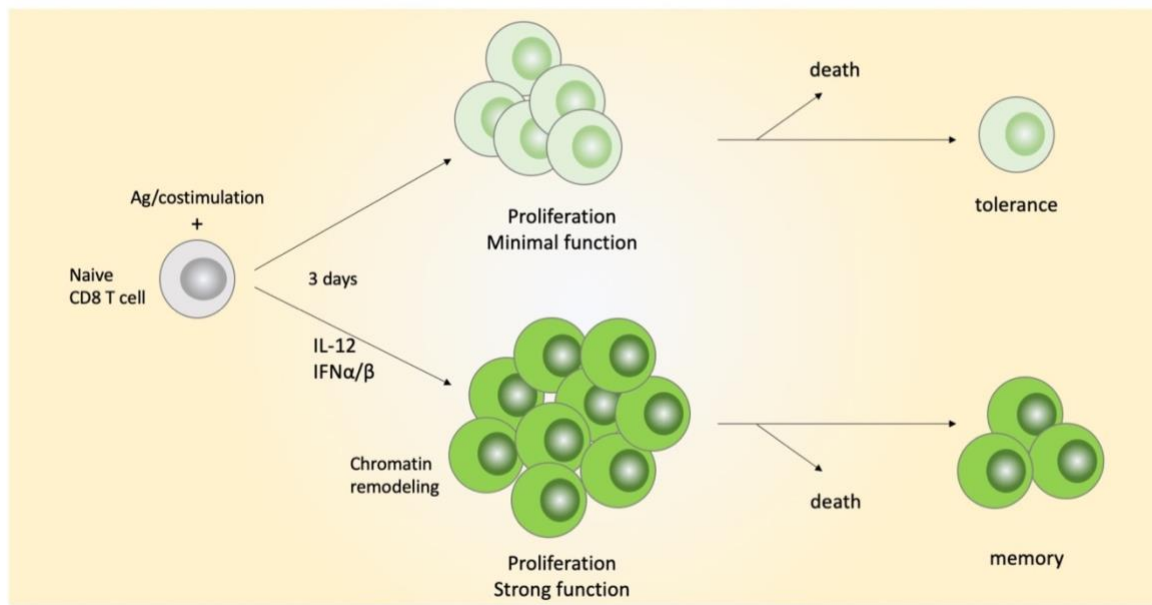


**Figure 6. Signal 3 alters the differentiation from tolerance to full activation of naive CD8 T cells.**

Three signals including antigen/TCR stimulation, co-stimulation, and inflammation cytokines (such as IL-12 and IFN $\alpha/\beta$ ) are required for the activation of naive CD8 T cells. Stimulation with antigen and co-stimulation induces extensive proliferation, but does not sustain the cell survival and the effector function acquisition. The small number of cells that are left behind and persist for a long time are tolerant. In the presence of either IL-12 or IFN $\alpha/\beta$ , cells perform comparable proliferation, increased survival, and the development of strong effector functions. Furthermore, protective memory cells are generated. **Adapted from (Curtsinger and Mescher, 2010).**

## 1.3.2 Cellular interactions involved in the activation of CD8 T cells

### Autopilot

Antigen presenting cells (APCs) activate naive CD8 T cells through providing signal 1,2 and 3. The activation of CD8 T cells has been called autopilot. Indeed, once the CD8 T cells are activated by APCs, they could continue proliferating and differentiating without further need of APCs. Van Stipdonk M. J., et al. found that a brief (even 2h) stimulation with APCs leads to the CD8 T cell expansion and induction of antigen-specific cytotoxic effector function. Moreover, the CD8 T cells primed in vivo for 24 hours could continue to expand in vitro in the absence of antigen. Similarly, the CD8 T cells activated for 4 hours in vitro, could divide upon transfer into antigen-free mice. Similar results were found by Kaech and Ahmed through transfer of purified CD8 T cells into naive mice 24h after stimulation (Kaech and Ahmed, 2001). Both groups demonstrated that once the CD8 T cells were primed, they could expand and differentiate in the absence of further antigen recognition (van Stipdonk et al., 2001). Furthermore, disparate initial antigen dose influences the number of CD8 T cells recruited into the response (Kaech and Ahmed, 2001).

### CD4 help

#### CD4 T cell subsets

CD4 T cells mainly serve as helper T cells ( $T_H$ ) and can be classified into several subsets according to the transcription factor expressed and the cytokines produced (Figure 7) (Bonilla and Oettgen, 2010).  $T_H1$  cells express T-box transcription factor (T-bet) and are able to produce IFN- $\gamma$  and IL-2. Their differentiation is mainly induced by IL-12. They regulate cell-mediated immunity, activate mononuclear phagocytes, and NK cells and promote CD8 T cell killing of intracellular pathogens.  $T_H2$  cells have the capacity to produce IL-4, IL-5, IL-10, and IL-13, which enhance B cell responses and antibody production. Naive precursors differentiate into  $T_H2$  cells under the influence of IL-4 and the expression of transcription factor GATA-3.  $T_H17$  cell differentiation is driven by IL-6 and TGF- $\beta$ , and  $T_H17$  cells are characterized by retinoic acid receptor related orphan receptor  $\gamma$  (ROR $\gamma$ t) expression and production of IL-17 cytokines, which comprise

homologous molecules named IL-17A-F.  $T_H17$  cells mainly produce IL-17A and IL-17F that induce IL-6 and TNF production and are important in granulocyte recruitment and tissue damage.  $T_H9$  cells are induced by IL-4 and TGF- $\beta$  and produce IL-9, which is regarded as a mast cell growth factor and plays a role in response to helminthic immunity. Regulatory CD4 T ( $T_{Reg}$ ) cells are induced by TGF- $\beta$  and express the transcription factor forkhead box protein 3 (FOXP3). They have the capacity to suppress T cell responses (Bonilla and Oettgen, 2010). Type 1 regulatory T cells ( $T_r1$ ) are negative for FOXP3 but produce IL-10 and TGF- $\beta$  and thus suppress T cell responses (Roncarolo et al., 2011). Finally, follicular T helper ( $T_{FH}$ ) cells are memory CD4 cells characterized by the expression of the chemokine receptor CXCR5 and reside in lymph nodes and the spleen where they regulate B-cell activation (Boehm and Swann, 2014; Bonilla and Oettgen, 2010).

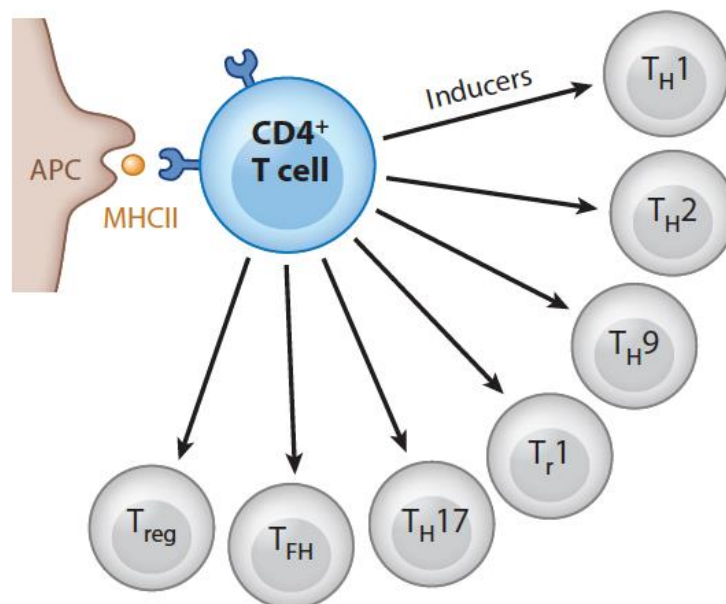


**Figure 7. CD4 T cell subsets.** Naive CD4 T cells are stimulated by APCs and different cytokines to expand. Depending on the type of the cytokines encountered, naive CD4 T cells can be driven to differentiate into different subsets. (Boehm and Swann, 2014).

#### CD4-DC-CD8 three-cell interaction model

Both DC activation and CD4 T cell help play essential roles in initiating the response of naive CD8 T cells. The priming of CD8 T cells occurs in two steps and CD4 T cells deliver their help during the second step of priming (Figure 8).

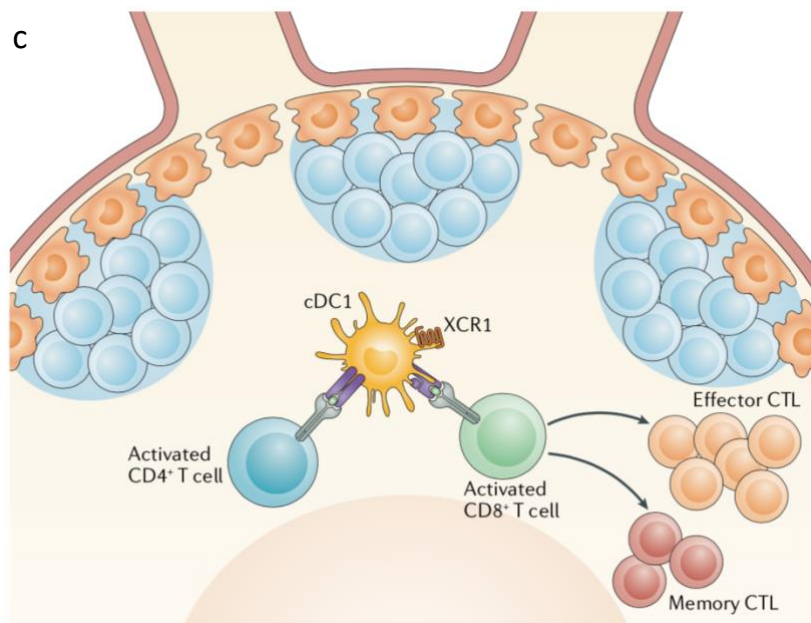
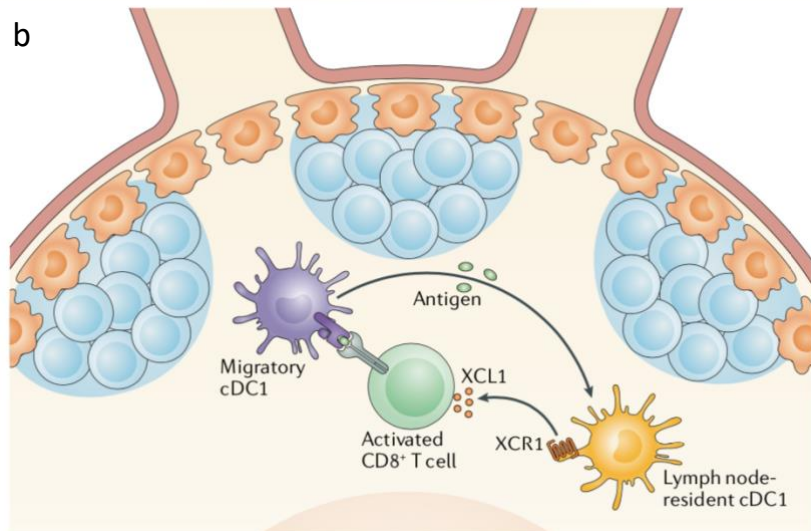
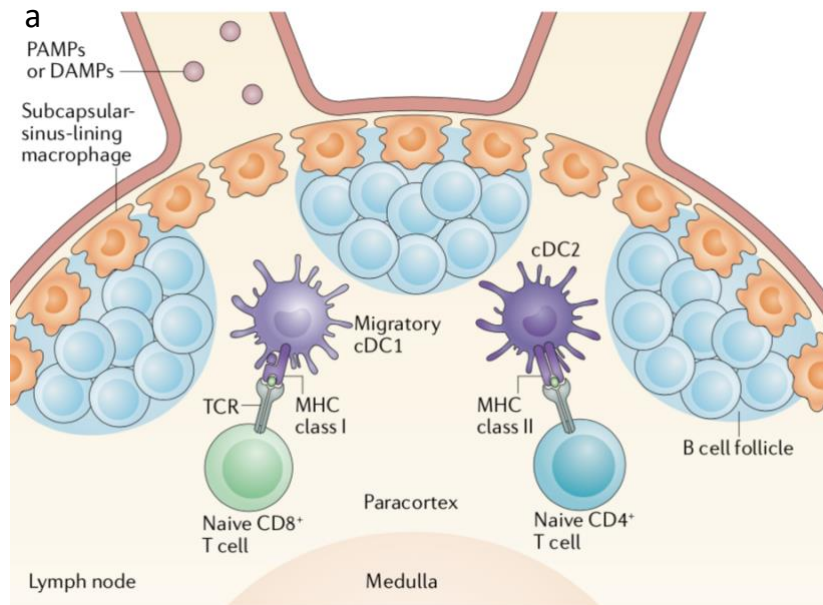


**Figure 8. Cellular interactions during the activation of CD8 T cells in vivo.** **a.** In mice, CD8 T cells and CD4 T cells are initially primed by different type of DCs. CD8 T cells are activated by infected conventional migratory DCs (cDC1) through MHC class I, but CD4 T cell are primed by uninfected conventional DCs (cDC2) via MHC class II. **b.** Activated CD8 T cells are able to secret XC-chemokine ligand 1 (XCL1). Thus, XC-chemokine receptor 1 + (XCR1+) resident cDC1s will then be recruited to the activation position where antigen from the migratory cDC1 can be transferred to XCR1+ cDC1. **c.** The XCR1+ cDC1s circulate to the deeper paracortical area of the lymph node and interact with both pre-activated CD4 T cells and pre-activated CD8 T cells. This interaction enables the help from CD4 T cells to CD8 T cells and induces the differentiation of effector and memory T cells. DAMP, damage-associated molecular pattern; PAMP, pathogen-associated molecular pattern. **(Borst et al., 2018).**

After immunization or infection, antigen-specific CD8 T cells and CD4 T cells are first activated by distinct type of conventional DCs (cDCs). CD4 T cells are mainly activated by non-infected cDC1, while CD8 T cells are initiated by infected cDC2. The two priming steps for CD4 T cells and CD8 T cells are segregated and occur in different areas within lymph node or spleen (Figure 8a) (Eickhoff et al., 2015). Next, CD8 T cells that have encountered the antigen presented by infected cDCs proliferate and produce XC-chemokine ligand 1 (XCL1) which help recruit the uninfected cross-presenting XCR1+ DCs. XCR1+ DCs migrate to the position where CD8 T cells are primed and cross-presented antigen from the cDC1 is transmitted to XCR1+ DCs (Figure 8b) (Brewitz et al., 2017). In a second priming step, the cross-presenting DCs present antigen to pre-activated CD4 T cells and pre-activated CD8 T cells via MHC-II and MHC-I separately. Both activated CD4 T cells and CD8 T cells bind XCR1+ DCs, and during this stage XCR1+ DCs relay CD4 T cell help signals for the differentiation of effector and memory CD8 T cells (Figure 8c) (Bennett et al., 1997; Eickhoff *et al.*, 2015). Antigen cross-presentation is essential for CD8 T cell response to vaccines and tumor generally, and large proteins of antigen must be phagocytosed and loaded on MHC-I and MHC-II molecules (Borst *et al.*, 2018).

Besides the three-cell interaction model, Ridge et al. also demonstrated a sequential two-cell interaction model in which CD4 T cells interact with DCs and drive their differentiation, then the licensed DCs could directly activate the CD8 T cells even in the absence of CD4 T cells (Ridge et al., 1998).

### **CD4 help through CD40-CD40L interaction**

The role of CD4 T cells in helping the promotion of an optimal primary CD8 T cell response is well appreciated. To do so, CD4 T cells enhance the activation of antigen-presenting cells (Bennett *et al.*, 1997) through the interaction of CD40 ligand (CD40L) with CD40 upregulated on pre-activated CD4 and DCs, respectively. This triggers IL-12 production by DCs, thus enhancing the proliferation of CD8 T cells (Figure 9) (Cella *et al.*, 1996). CD40 activation with an agonistic antibody could rescue the CTL response in the absence of CD4 T cells, for example through enhanced CD28 signaling (Prilliman *et al.*, 2002; Schoenberger *et al.*, 1998). Inversely, Blockade of CD28 or CD80/CD86 prevents the CTL response primed by CD40-activated APC (Prilliman *et al.*, 2002). Furthermore, CD80 and CD86 could be upregulated on activated DCs via CD40-CD40L signaling (Acuto and Michel, 2003; Borst *et al.*, 2018; McAdam *et al.*, 1998).

### **CD4 help through CD70-CD27 interaction**

Combined TCR/CD40 stimulation upregulates the surface expression of CD70 on DCs (Sanchez *et al.*, 2007). CD8 T cells express CD27 which is the ligand of CD70, and a large fraction of CD4 help provided to CD8 T cells depends on CD27 co-stimulation (Ahrends *et al.*, 2017). CD27 is a member of TNF receptor (TNFR) family. Unlike most other members of this TNFR family that are synthesized after T cell priming, CD27 is already expressed on naive CD4 and CD8 T cells (van de Ven and Borst, 2015; Wortzman *et al.*, 2013). CD27 is still expressed in the early antigen-primed CD8 T cells, however activated CD8 subsequently lose its expression via proteolytic cleavage following the differentiation from naive to antigen-primed cells (Appay *et al.*, 2002; Lens *et al.*, 1998). Soluble CD27 could serve as a monitor of T cells activation and immune response (Lens *et al.*, 1998). CD27 promotes the survival of activated T cells throughout their clonal expansion at the site of priming and contributes to the generation of both effector and memory CD8 T cells (Hendriks *et al.*, 2003). Indeed, CD27-deficient mice have decreased numbers of CD4 and CD8 effector T cells that infiltrate the lung in response to primary influenza virus infection as well as decreased numbers of CD4 and CD8 T cells and reduced memory T cell responses after secondary influenza infection (Hendriks *et al.*, 2000). The defective secondary expansion of CD8 T cells observed in CD27 deficient mice could be restored in

the absence of tumor-necrosis factor (TNF)-related apoptosis-inducing ligand (TRAIL) (Feau et al., 2012). Similarly, CD70 blockade during the primary response inhibits CD40-stimulated proliferation of CD8 T cells and memory generation (Bullock and Yagita, 2005; Taraban et al., 2004). Furthermore, co-stimulation of CD27 rescues CD28<sup>-/-</sup> T cells from death (Hendriks *et al.*, 2003). However, CD27 is dispensable for T cell division, IFN- $\gamma$  production and cytolytic T cell function (Hendriks *et al.*, 2000). Altogether, these studies show that CD70/CD27 interaction plays an important role in CD40-dependent CD8 T cell response (Bullock and Yagita, 2005; Taraban *et al.*, 2004).

### **CD4 help regulates the expression of TRAIL**

CD4 T cells regulate the expression of TRAIL, which play a key role in the differentiation of CD8 T cell memory (Janssen et al., 2005). Indeed, without CD4 T cell help, CD8 T cells are subjected to cell death regulated by TRAIL. Following in vitro re-stimulation, the mRNA of TRAIL which encode pro-apoptotic proteins is upregulated in CD8 T cells that have been primed in vivo in the absence of CD4 help. Autocrine TRAIL also impairs the secondary expansion of these helpless CD8 T cells (Janssen et al., 2005).

### **CD4 help through IL-2 (see section 2.1)**

CD4 T cells are the key producers of IL-2 which helps initiate the expansion of CD8 T cells during primary response (Sokke Umeshappa et al., 2012; Wilson and Livingstone, 2008). The role of IL-2 in CD8 T cell activation and memory formation will be covered in section 2.1.

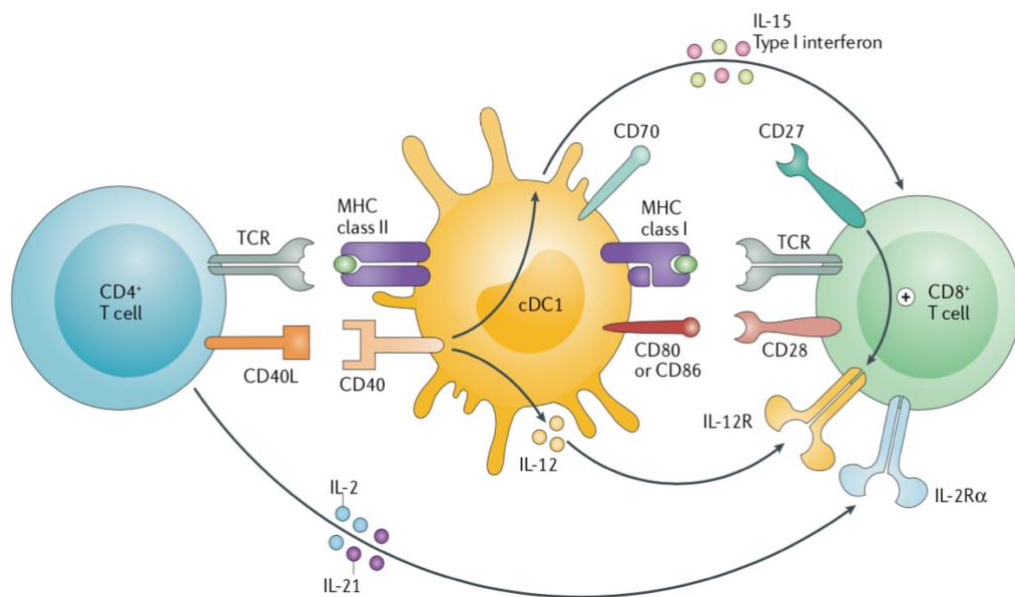


**Figure 9. Key cell surface receptor–ligand and cytokine-receptor interactions during the T cell priming.** Lymph node-resident cDC1 present antigen to CD4 T cells via MHC class II increasing the expression of CD40L. Then, CD40L–CD40 binding activates cDC1 to produce type I interferon, IL-12 and IL-15 that act directly on CD8 T cells. CD40L–CD40 interaction also increases the antigen presentation of cDC1 to CD8 through MHC class I. CD40 signaling increased the expression of CD80 and/or CD86 and CD70 on cDC1, which activate CD28 and CD27, respectively, on CD8 T cells. Activated CD4 T cells produce IL-2 and IL-21 that help prime CD8 T cells. (Borst *et al.*, 2018).

## 1.4 Effector and Memory CD8 T cell subsets

Following acute infection, activated precursors undergo the effector and memory differentiation. Typically, activated precursors differentiate into two subsets named short-lived effector T cells (SLECs) that are  $\text{KLRG1}^{\text{hi}}\text{IL-7R}\alpha^{\text{lo}}$  and memory precursor effector cells (MPECs) that are  $\text{KLRG1}^{\text{lo}}\text{IL-7R}\alpha^{\text{hi}}$  (Joshi *et al.*, 2007). MPECs have the capacity to become the long-lived memory cells and respond to the secondary challenge, while SLECs tend to become terminal differentiated effector cells and have a shortened lifespan (Joshi *et al.*, 2007). The decision between SLEC and MPEC fates could be altered by IL-2 and the strength of inflammatory cytokines such as IL-12 during the activation of T cells (Kalia and Sarkar, 2018). The high expression of the transcription factor T-bet induced by inflammation drives the formation of SLECs, while the low expression of T-bet promotes the generation of MPECs (Joshi *et al.*, 2007).

Memory T cells are a heterogeneous population and diverse subsets harboring different functional properties have been described according mainly to their surface phenotype (Jameson and Masopust, 2009; Mueller et al., 2013)

### **1.4.1 T<sub>CM</sub> and T<sub>EM</sub>**

In 1999, Sallusto et al., (Sallusto et al., 1999) found that human memory T cells could be divided in two subsets with different effector functions and homing capacities. One subset expressed high level of CCR7 and CD62L and was defined as central memory T cells (T<sub>CM</sub>) that could migrate into lymph nodes but lack inflammatory and cytotoxic function. Another subset with low levels of CCR7 and CD62L was named effector memory T cells (T<sub>EM</sub>) which are endowed with strong effector function and cytotoxicity but fail to home to lymph nodes as they do not express two major lymph-node-homing receptors CD62L and CCR7 (Weninger et al., 2001). The phenotype of T<sub>CM</sub> and T<sub>EM</sub> cells in mice is similar to that in human. In mice, it is demonstrated that T<sub>EM</sub> cells can enter into peripheral tissues to perform inflammatory reactions or cytotoxicity. However, their number decreases following antigen clearance and T<sub>EM</sub> cells are unable to mount an efficient response upon secondary challenge. In contrast, T<sub>CM</sub> cells that travel to secondary lymphoid organs could persist for a long-time following antigen clearance and clonally expand following a secondary challenge (Bouneaud et al., 2005; Sallusto *et al.*, 1999; Wherry *et al.*, 2003).

Based on the expression of CCR7 and CD45RA, human CD8 T cells could be classified into four subsets, naive (CCR7+CD45RA+), T<sub>CM</sub> (CCR7+CD45RA-), T<sub>EM</sub> (CCR7-CD45RA-), T<sub>EMRA</sub> (T effector memory RA cells, CCR7-CD45RA+). Compared to T<sub>EM</sub> cells and T<sub>EMRA</sub> cells, naive T cells and T<sub>CM</sub> cells show higher proliferation potential in response to antigen or cytokines implicated in homeostasis. T<sub>EM</sub> cells and T<sub>EMRA</sub> cells have high rate of cell death due to the low expression of Bcl2. Thus, from naive and T<sub>CM</sub> to T<sub>EM</sub> and T<sub>EMRA</sub> cells, antigen-dependent expansion, cell viability, and Bcl2 expression are progressively lost. (Geginat et al., 2003).

Numerous studies have been done to explain the relationship and differentiation pathway leading from naive cells to the generation of the different memory subsets and the interrelation between these subsets. Human naive T cells could generate both T<sub>CM</sub> and T<sub>EM</sub> cells under in vitro stimulation, whereas stimulation of T<sub>CM</sub> cells results in the

acquisition of effector function and differentiation to  $T_{EM}$  cells. This supports a linear differentiation model in which human naive T cells first generate  $T_{CM}$  and then to  $T_{EM}$  cells (Figure 10)(Sallusto *et al.*, 1999). In a murine model, adoptively transferring purified H-Y–specific  $T_{CM}$  and  $T_{EM}$  subsets to host mice that immediately receive a secondary immunization shows that  $T_{CM}$  subsets could mount a rapid recall response upon secondary challenge and generate both  $T_{CM}$  and  $T_{EM}$  cells, although only a fraction of  $T_{CM}$  differentiate into  $T_{EM}$  (Figure 10)(Bouneaud *et al.*, 2005).

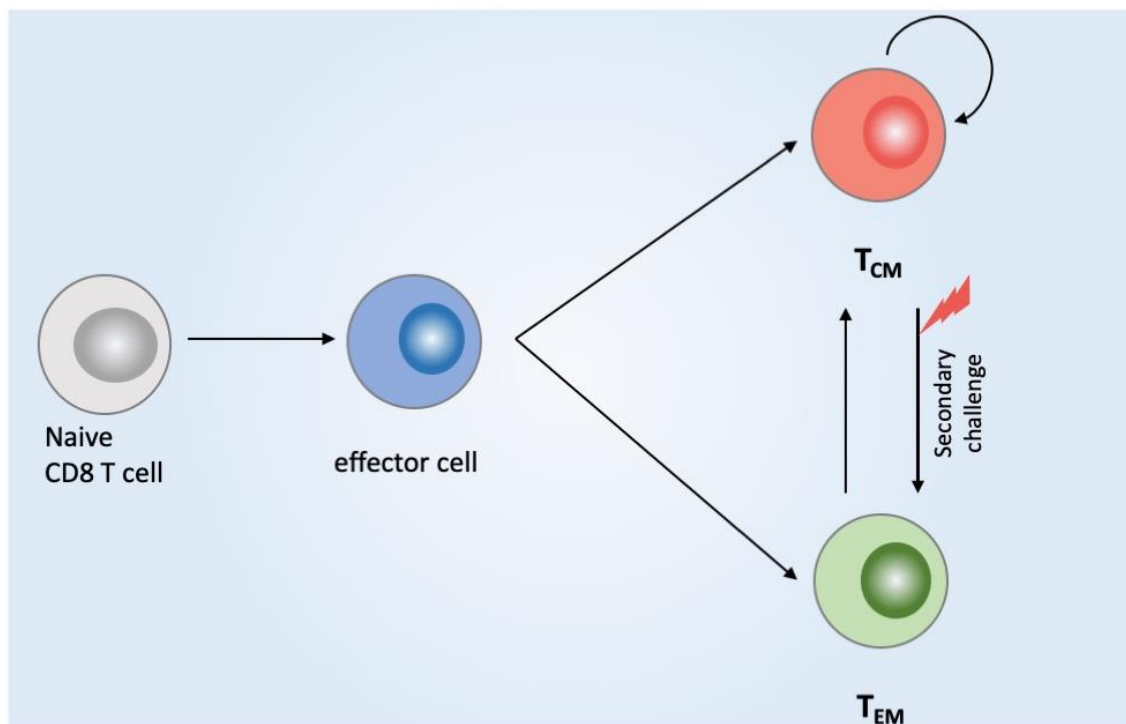


**Figure 10. Relationship of  $T_{CM}$  and  $T_{EM}$ .** Naive T cells generate both  $T_{CM}$  and  $T_{EM}$  cells.  $T_{EM}$  cells are then differentiated into  $T_{CM}$  cells following antigen clearance. Upon secondary challenge,  $T_{CM}$  cells could differentiate into  $T_{EM}$  cells.

Then, another differentiation pathway was put forward. In a murine model with LCMV infection, the conversion from  $T_{EM}$  to  $T_{CM}$  is found within 7 days after immunization. Between 1- and 3-months post infection, the total number of memory cells is stable but the absolute number of  $T_{EM}$  decline and the number of  $T_{CM}$  increase. Following adoptive transfer into naive mice,  $T_{CM}$  cells maintain high levels of CD62L while  $T_{EM}$  cells convert to  $T_{CM}$  cells. However,  $T_{CM}$  cells generate  $T_{EM}$  cells upon secondary challenge. Thus, naive cells can generate both  $T_{CM}$  and  $T_{EM}$ ,  $T_{CM}$  can differentiate into  $T_{EM}$  following re-stimulation by

antigen and T<sub>EM</sub> can convert in T<sub>CM</sub> under homeostatic conditions. (Figure 10) (Wherry *et al.*, 2003).

### 1.4.2 T<sub>SCM</sub>

A new subset of T memory stem cells (T<sub>SCM</sub>) was first identified in a mouse model of graft-versus-host disease (GVHD). In this model, T<sub>SCM</sub>, defined as CD44 low but CD62L, CD122, Bcl-2 and stem cell antigen-1 (Sca-1) positive, are generated in response to allo-antigens and DCs in an interleukin-15 (IL-15) dependent manner (Zhang *et al.*, 2005). In mouse, induction of Wnt signaling inhibits the proliferation and effector differentiation of CD8 T cell but promotes the generation of self-renewing multipotent CD8 T<sub>SCM</sub>. Furthermore, c-Myb promotes the CD8 T cell stemness via the induction of TCF1/7 and Bcl2 and repression of Zeb2 and c-Myb deficiency leads to the terminal differentiation of CD8 following viral infection (Gautam *et al.*, 2019).

In human, T<sub>SCM</sub> cells are identified by the expression of CD45RA, CCR7, CD27, CD28, CD62L and IL-7R $\alpha$  in conjunction with a range of memory markers, such as CXCR3, CD95, CD58, CD11a and IL-2R $\beta$  (CD122) (Figure 11) (Gattinoni *et al.*, 2017).

T<sub>SCM</sub> cells are regarded as the least differentiated T cell memory subset with increased self-renewal ability and multipotency to differentiate into all memory and effector CD8 T cell subsets (Gattinoni *et al.*, 2011). T<sub>SCM</sub> cells are also equipped with increased proliferative and survival capabilities and anti-tumor activity (Gattinoni *et al.*, 2011). In patients with haploidentical hematopoietic stem cell transplantation (HSCT), evidences show that human T<sub>SCM</sub> cells derive preferentially from naive precursors and emerge early following *in vivo* priming. Indeed, only naive T cells and T<sub>SCM</sub> cells had the capacity to regenerate the full spectrum of more differentiated T cell subsets (Cieri *et al.*, 2015). Despite being functionally distinct, T<sub>SCM</sub> cells are similar to naive cells in their distribution *in vivo* (Lugli *et al.*, 2013). T<sub>SCM</sub> cells possess the ability of long-term persistence. In patients with severe combined immunodeficiency disease (SCID) due to adenosine deaminase (ADA) deficiency, individual T<sub>SCM</sub> cells persist and preserve their functionality and differentiation potential for decades (Biasco *et al.*, 2015). Although the exact developmental origins of T<sub>SCM</sub> cells remains unclear, some evidence indicates that

T<sub>SCM</sub> cells may appear prior to fully differentiated effector or memory cells (Gattinoni et al., 2009; Lugli *et al.*, 2013).

T<sub>SCM</sub> cells are not identified in acute pathogen infection models. T<sub>SCM</sub> cells are well known in mouse model of GVHD and in human with HIV-1, HTLV-1 and some vaccinations (Gattinoni *et al.*, 2017).

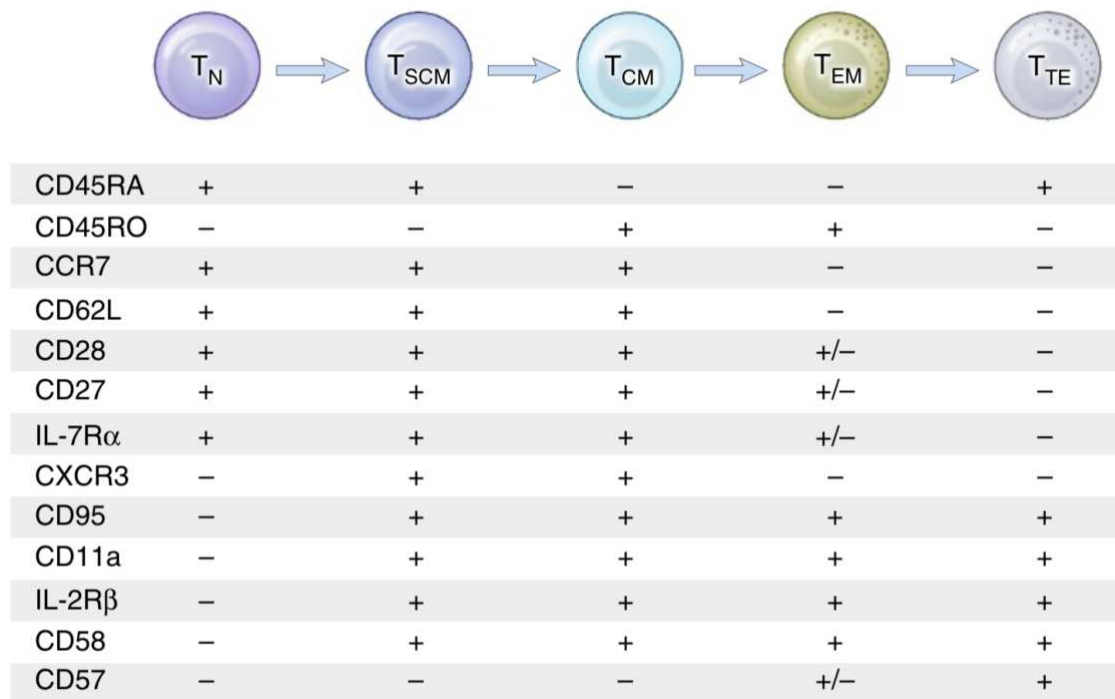


**Figure 11. The phenotype of human naive and diverse memory T cell subsets.** After antigen activation, naive T (T<sub>N</sub>) cells differentiate into T stem cells (T<sub>SCM</sub>), central memory T cells (T<sub>CM</sub>), effector memory cells (T<sub>EM</sub>), and ultimately, into terminally differentiated effector T (T<sub>TE</sub>) cells. The combinatorial expression of the indicated surface markers in naive and diverse memory T cell subsets is illustrated. (Gattinoni *et al.*, 2017).

### 1.4.3 T<sub>EMRA</sub>

T<sub>EMRA</sub> is a human CD8 T cell subset that is characterized by CD27<sup>-</sup>, CCR7<sup>-</sup>, CD62L<sup>-</sup>, CD28<sup>-</sup> and CD45RA<sup>+</sup> phenotype (Geginat *et al.*, 2003; Hamann et al., 1997; Mahnke et al., 2013). These cells have high cytotoxic capacity and produce perforin and granzyme B. Cytomegalovirus (CMV) infection triggers a strong proliferation and accumulation of a T<sub>EMRA</sub> subset in human (Patin et al., 2018). T<sub>EMRA</sub> cells are highly differentiated since they display the shortest telomeres which indicates the number of cell cycle performed, as

telomeres are progressively shortened following the cell division (Romero et al., 2007). Furthermore, T<sub>EMRA</sub> cells express high level of markers of terminal differentiation and senescence, such as KLRG1, CD57 and phosphorylation of histone H2AX (Mahnke *et al.*, 2013). So T<sub>EMRA</sub> cells in human are similar to terminal differentiated T effector cells in mice.

#### **1.4.4 T<sub>RM</sub>**

Tissue-resident memory T (T<sub>RM</sub>) cells, unlike naive and T<sub>CM</sub> cells that recirculate between blood, lymph nodes and secondary lymphoid organs or T<sub>EM</sub> cells that recirculate between non-lymphoid tissues and blood, don't recirculate but reside in non-lymphoid tissue, such as lungs, gut, skin, liver, brain, kidney, salivary glands, bladder, female reproductive tract, pancreas and heart in mice and human. (Gebhardt et al., 2018; Schenkel and Masopust, 2014). T<sub>RM</sub> cells are characterized by CD103 and CD69 expression, both induced by TCR triggering (Gebhardt et al., 2009; Wakim et al., 2010).

T<sub>RM</sub> cells are regarded as the first-line of defense and play a vital role in protecting tissue at the portal of reinfection. T<sub>RM</sub> cells could confer protective effect and directly kill the antigen-expressing cells by the secretion of cytotoxic molecules such as granzyme B and perforin (Steinbach et al., 2016). Activated TRM cells also protect tissue through cytokines production such as IFN- $\gamma$  to rapidly recruit other circulatory memory T cells and B cells (Schenkel et al., 2014; Schenkel et al., 2013). In addition, antigen activated T<sub>RM</sub> produce TNF- $\alpha$  that drive the maturation of local DCs and IL-2 which activates NK cells (Schenkel *et al.*, 2014). Lung or skin T<sub>RM</sub> cells provide superior protection in response to secondary acute lymphocytic choriomeningitis virus or vaccinia virus infections, as compared to circulating memory T cell subsets (Hofmann and Pircher, 2011; Jiang et al., 2012). Such protection depends on the local T<sub>RM</sub> cell density in the tissue. (Park et al., 2018). In conclusion, T<sub>RM</sub> cells act as tissue sentinels that rapidly alarm their surrounding environment to contribute to the local protection when secondary antigen invasion happens (Dijkgraaf *et al.*, 2021). The phenotype, location and function of T<sub>CM</sub>, T<sub>EM</sub> and T<sub>RM</sub> are compared in Table 2.

| Cell type            | Phenotype  | Location                   | Functional properties  |
|----------------------|--|----------------------------|--|
| T <sub>CM</sub> cell | CD62L <sup>hi</sup> CCR7 <sup>hi</sup>   | Lymph nodes, spleen, blood | ↑ Proliferative potential<br>↑ IL-2 production<br>↑ Migration<br>↓ Effector functions and cytotoxicity |
| T <sub>EM</sub> cell | CD62L <sup>low</sup> CCR7 <sup>low</sup>   | Spleen, blood, liver       | ↓ Proliferative potential<br>↓ IL-2 production<br>↑ Migration<br>↑ Effector functions and cytotoxicity |
| T <sub>RM</sub> cell | CD103 <sup>hi</sup> CD69 <sup>hi</sup> CD62L <sup>low</sup> CD27 <sup>low</sup> ; expression of tissue-specific chemokine receptors and integrins* | Skin, lung, gut, brain     | ↓ Proliferative potential<br>↓ IL-2 production<br>↓ Migration<br>↑ Effector functions and cytotoxicity |

**Table 2. Memory T cell subsets. (Kaech and Cui, 2012)**

### 1.4.5 Other subsets

#### Expression of CD27/CD43 defines 3 subsets in mice

In order to predict the capacity of memory T cells to regulate secondary responses, Hikono (Hikono et al., 2007) found that, based on the expression of CD27 and CD43, antigen-specific memory CD8 T cells could be divided into three distinct subpopulations that have different capacities to mount recall response. The three distinct subpopulations include CD27+/CD43+, CD27+/CD43- and CD27-/CD43- subsets. CXCR3 and CD127 were found both co-expressed with CD27, thereby the three major subsets of memory CD8 T cells could also be distinguished by CXCR3/CD43 or CD127/CD43 expression. The CD27-/CD43- subpopulation, expressing high level of KLRG1, exhibited low homeostatic proliferative capacity, thus progressively decreasing and disappearing by about 1 year after infection. In contrast, CD27+/CD43- subpopulation preferentially survived for a long time.

The classification of memory CD8 T cells into the three subpopulations is independent of T<sub>CM</sub> and T<sub>EM</sub> cells, since T<sub>CM</sub> and T<sub>EM</sub> cells were equally distributed in each subset (CXCR3+/CD43+, CXCR3+/CD43-, and CXCR3-/CD43-).

None of the three subsets expressed programmed cell death protein 1 (PD-1) which is a T cell exhaustion marker. And upon in vitro re-stimulation with antigen peptide, the three subsets showed similar effector functions in terms of the production of cytokines, such as IFN- $\gamma$  and TNF- $\alpha$ . Even though CD27+/CD43+ and CD27+/CD43- cells didn't express granzyme B during homeostatic state, granzyme B was produced by the three subsets upon the secondary infection.

Notably, after adoptive transfer of the three subsets isolated from a Sendai-virus-infected donor into naive mice that were then challenged with Sendai virus, CD27+/CD43- cells displayed the strongest recall response, whereas CD27-/CD43- cells exhibited the weakest protective efficacy. As a result, the capacity to mount a recall response of the different subsets was classified as CD27+/CD43- > CD27+/CD43+ > CD27-/CD43- (Hikono *et al.*, 2007).

### **CX3CR1 defines three CD8 T cell subsets**

Many CD8 T cells upregulate CX3CR1 upon pathogen challenge. And CX3CR1- and CX3CR1+ memory T cells exhibit profound differences at the transcriptome, proteome, and functional level (Bottcher *et al.*, 2015). Furthermore, Gerlach (Gerlach *et al.*, 2016) found CX3CR1+ cells can be divided into CX3CR1<sup>hi</sup> and CX3CR1<sup>int</sup> cells. As a result, the expression level of CX3CR1 could be used to define three distinct antigen-specific effector T cell subpopulations: CX3CR1<sup>hi</sup>, CX3CR1- and CX3CR1<sup>int</sup>.

The CX3CR1<sup>hi</sup> subsets have the potential to differentiate into terminally differentiated effector T cells, because they are CD27-, CD127- and KLRG+ and contain few IL-2 producing cells. IL-2 producers representing less differentiated cells are most frequent among CX3CR1- subsets. After adoptive transfer of the three subsets into infection-matched recipients, CX3CR1- cells give rise to more memory progeny than CX3CR1<sup>int</sup> effector T cells and even more than CX3CR1<sup>hi</sup> cells. Moreover, CX3CR1- subpopulations generate three memory subsets, whereas CX3CR1<sup>int</sup> cells give rise to CX3CR1<sup>int</sup> and CX3CR1<sup>hi</sup> offspring and CX3CR1<sup>hi</sup> cell exclusively differentiate into CX3CR1<sup>hi</sup> subsets. The progeny of CX3CR1- and CX3CR1<sup>hi</sup> effector cells are essentially T<sub>CM</sub> and T<sub>EM</sub> respectively while CX3CR1<sup>int</sup> effector cells generate both T<sub>CM</sub> and T<sub>EM</sub>. This demonstrates that the level of CX3CR1 expressed at effector phase could partially predict the type of memory subsets that the effector cell will give rise to.

Upon adoptively transferring naive CD8 T cells into naive mice followed by virus infection, CX3CR1- (T<sub>CM</sub>) cells are found in blood, spleen, LN and some peripheral tissues cells after more than 40 days. CX3CR1<sup>hi</sup> (T<sub>EM</sub>) cells are mainly found in blood and they are largely absent in peripheral tissues, which is contradictory to the previous founding that T<sub>EM</sub> cells

mainly circulate between blood and peripheral tissues. CX3CR1<sup>int</sup> memory cells circulate through peripheral tissues so that they are also defined as peripheral memory cells (T<sub>PM</sub>). These T<sub>PM</sub> cells account for a highest proportion in thoracic duct lymph, suggesting a role in the global surveillance of non-lymphoid tissues.

## 1.5 T cell exhaustion

During acute infection, naive CD8 T cells robustly proliferate and differentiate into effector CD8 T cells to control the infections. A small number of cells survives and differentiates into memory CD8 T cells that persist for a long time and confer the protective capacity in response to secondary response (Figure 12).

In contrast, during cancer or chronic infection, such as lymphocytic choriomeningitis virus (LCMV) clone 13 infection in mice and hepatitis B virus and hepatitis C virus infection in humans, CD8 T cells become exhausted due to the persistence exposure to the antigen or inflammatory cytokines (Figure 12) (Kaech and Cui, 2012). Exhausted T cells (Tex) display decreased effector functions (IL-2, TNF and IFN- $\gamma$  production and cytotoxic activity), increased expression of multiple inhibitory receptors (such as PD-1 and lymphocyte activation gene 3 (LAG-3)), impaired memory recall response and poor homeostatic proliferation. T cell exhaustion is also associated with a transcriptional program that differs from the one found in functional effector and memory T cells. Thus, T cell exhaustion is associated with an inefficient response, that leads to persisting infections (Kurachi, 2019).

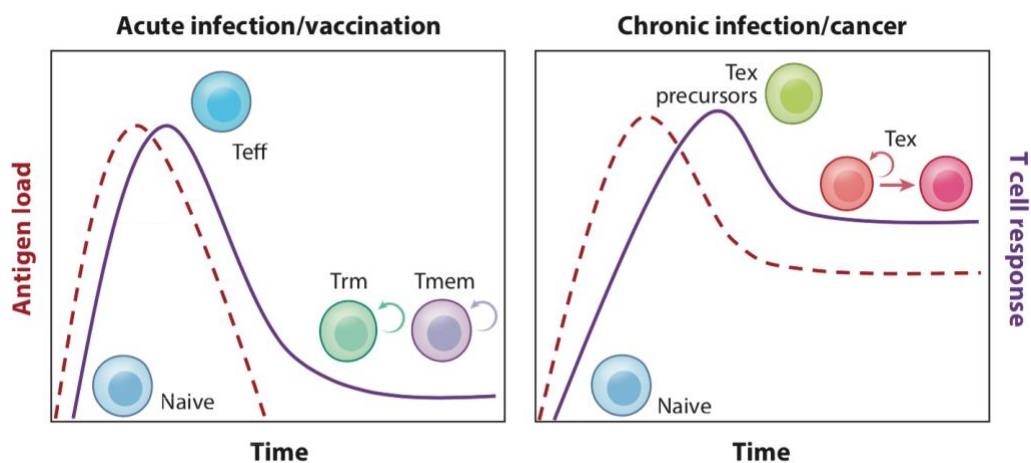


**Figure 12. T cell differentiation following acute infection/vaccination or chronic infection/cancer.**

After activation, naive CD8 T cells differentiate into effector cells to control antigen load. Following acute infection or vaccination, the majority of effector cells die following the elimination of antigen. A small fraction maintains and differentiates into circulating memory cells or tissue resident memory cells and respond to secondary challenges. In response to chronic infection or cancer, T exhausted memory precursors and exhausted effector are generated because of the failure to clear antigen. **Adapted from (McLane et al., 2019).**

Inhibitory receptors are critical in regulating T cell exhaustion. The inhibitory signaling pathway mediated by PD-1: PD-L1/L2 has been widely studied in T cell exhaustion. PD-1 is strikingly upregulated in exhausted CD8 T cells during chronic LCMV infection. Blocking the PD-1 inhibitory pathway promotes the proliferation and cytokine production of CD8 T cells and enhances the clearance of virus. Furthermore, treatment with anti-PD-L1 antibody in LCMV clone 13 infected mice that are depleted of CD4 T cell rescues the expansion and function of CD4-helpless exhausted CD8 T cells (Barber et al., 2006). PD-1 inhibits the activation of PI3K-AKT and Ras-MEK-ERK signaling pathways and PD-1 blocks cell cycle progression through arresting cell at G1 phase (Patsoukis et al., 2012). PD-1 upregulates the expression of basic leucine transcription factor BATF which results in the impaired T cell function (Quigley et al., 2010). In addition to PD-1, exhausted T cells also express a wide range of other inhibitory receptors such as LAG-3, CD244 (2B4), CD160, T cell immunoglobulin domain and mucin domain 3 (Tim-3), cytotoxic T lymphocyte antigen-4 (CTLA-4, CD152) and so on (Figure 13) (Blank et al., 2019; Kurachi, 2019). Individual expression of one inhibitory receptor is not sufficient to define exhaustion, co-expression of several distinct inhibitory receptors is needed. For example, simultaneous blockade of the inhibitory receptors PD-1 and LAG-3 restores the T cell responses and enhances viral control during chronic LCMV infection (Blackburn et al., 2009). Combined inhibition of PD-1 and Tim-3 pathways effectively reverses T cell exhaustion and facilitates the anti-tumor response in mice with solid tumor (Sakuishi et al., 2010). Synergistic blockade of PD-1 and CTLA-4 in human patients with melanoma successfully enhance the tumor regression (Wolchok et al., 2013). The molecular mechanisms by which the inhibitory receptors regulate T cell exhaustion are shown in Figure 13.

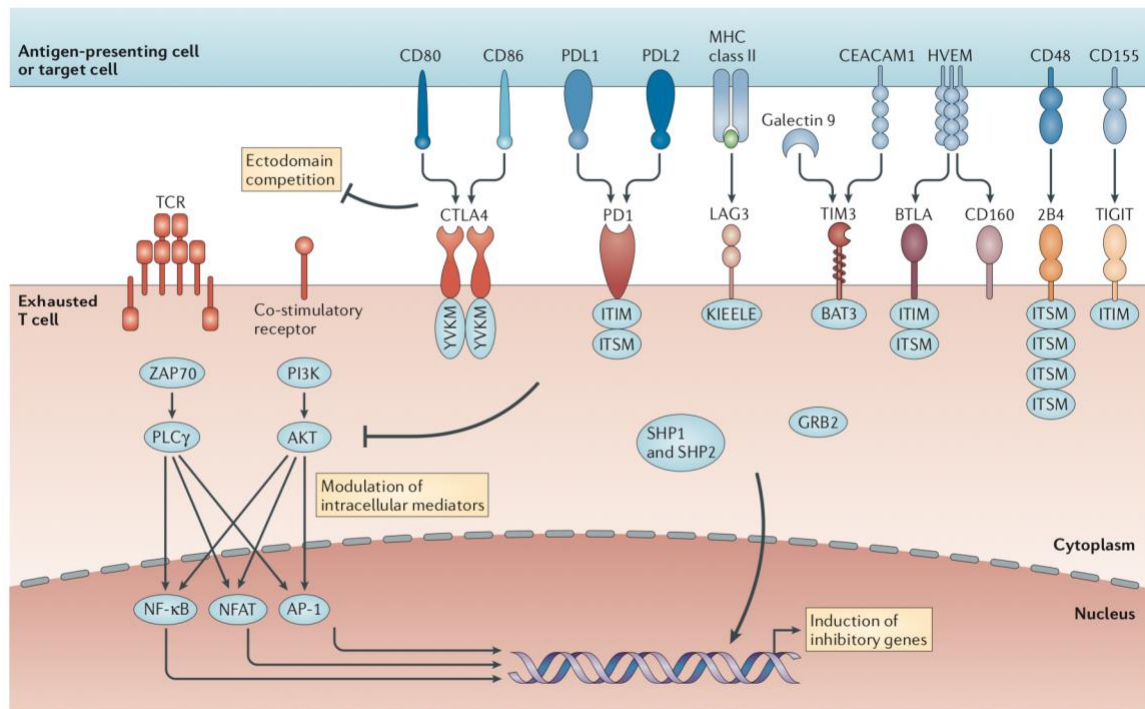


**Figure 13. Molecular mechanisms of inhibitory receptors involved in T cell exhaustion.** Most of the inhibitory receptors activate ITIMs and/or ITSMs which recruit SHP1 while some receptors signal through their specific intracellular motifs. For example, CTLA-4 activates YVKM and LAG-3 activates KIEELE. The inhibitory receptors mainly regulate ectodomain competition, modulation of intracellular mediators and induction of inhibitory genes. ITIM: immunoreceptor tyrosine-based inhibitory motifs; ITSM: immunoreceptor tyrosine-based switch motifs. **(Wherry and Kurachi, 2015).**

Signaling of inhibitory receptors is responsible for the T cell exhaustion through interference with co-stimulatory pathways. Co-receptor CD28 is targeted and dephosphorylated by PD-1. As a result, PD-1 suppresses T cell function primarily by inhibiting CD28 signaling pathway (Hui et al., 2017). PD-1 blockade fails to rescue the exhausted T cells when CD28 is conditionally deleted, suggesting that CD28/B7 costimulatory pathway is necessary for the effective PD-1 blockade therapy in the context of chronic viral infection and in tumor bearing mice (Kamphorst et al., 2017). CTLA-4 binding to CD86 negatively controls the T cell response (Freeman et al., 1993). Help from CD4 T cells is essential for the optimal CD8 T cell responses against infection and cancer (Sevilla et al., 2004). Treatment with agonistic anti-CD40 antibody ( $\alpha$ CD40) suppresses the induction of PD-1 and rescues the PD-1 mediated T cell exhaustion (Isogawa et al., 2013).

Blockade of CTLA-4 with Ab is unable to initiate the CTL response in the absence of CD4 T help. In other words, CTLA-4 blockade couldn't bypass the requirement for CD4 T help or CD40 activation (Prilliman et al., 2002). CD4-produced IL-21 is essential to prevent the exhaustion of CD8 T cell and to control the viral replication in HIV-infected human patient (Chevalier et al., 2011). Thus, loss of CD4 T cell help may lead to CD8 T cell exhaustion.

Soluble factors (such as IL-10, TGF- $\beta$  and IFN- $\alpha/\beta$ ) play crucial roles in regulating T cell exhaustion. Antibody blockade of type I interferon signaling reduces the expression of negative immune regulator IL-10 and PD-1 and promotes the control of persistent virus infection in mice with chronic LCMV infection (Teijaro et al., 2013).

Furthermore, the transcription factors T-bet, EOMES, Blimp1, NFAT, BATF, IRF4 and TCF1 that are implicated in T cell activation and differentiation following acute infection, they are also involved in the formation of exhausted T cells during chronic infection (see section 1.6) (Kurachi, 2019).

In chronic infection, exhausted T cells are heterogeneous with multiple subsets (McLane *et al.*, 2019). Exhausted virus-specific CD8 T cells derive from the KLRG1<sup>lo</sup> MPEC cells but not the terminally differentiated effector CD8 T cells (Angelosanto et al., 2012). T exhausted precursors progressively lose memory potential which is essentially ablated by day 30 post-infection. However, T exhausted precursors can regenerate T memory cells if moved from chronic infection to acute antigen stimulation (Angelosanto *et al.*, 2012). In the chronic LCMV infection model, PD1-exhausted CD8 can be divided in two subsets according to PD1 level of expression: PD-1<sup>int</sup>CD44<sup>hi</sup> and PD-1<sup>hi</sup>CD44<sup>int</sup> subsets. PD-1<sup>int</sup>CD44<sup>hi</sup> T exhausted cells are less functionally exhausted than PD-1<sup>hi</sup>CD44<sup>int</sup> subsets (Blackburn et al., 2008). PD-1<sup>int</sup>CD44<sup>hi</sup> cells maintain a proliferative potential, can be rescued by the PD-1 pathway blockade (Blackburn *et al.*, 2008). They possess progenitor capacity, since they can perform enhanced proliferation and directly differentiate in more terminal PD-1<sup>hi</sup> cells through extensive cell division (Paley et al., 2012).

In recent studies, single cell RNA-seq reveals a binary developmental bifurcation early during chronic viral infection describing a divergence of a T effector-like branch and a T exhausted precursor branch (Chen et al., 2019). T exhausted precursor cells are a

TCF1+Ly108+PD-1+ CD8 T cell population that seeds development of mature T exhausted cells. TCF1 serves as a mediator that represses the development of terminal KLRG1<sup>hi</sup> effectors while facilitating the establishment of KLRG1<sup>low</sup> T exhausted precursor cells, and PD-1 supports the development of this TCF1+ T exhausted precursor cell pool early during chronic infection (Chen *et al.*, 2019). T exhausted precursors proliferate and give rise to a terminal T exhausted cell population in response to persistent antigen stimulation (Paley *et al.*, 2012).

Thus, TCF1 that regulate the CD8 T cells activation and differentiation during acute infection (see next section) also play a role in regulating the differentiation of T cell exhaustion following chronic infection.

## 1.6 Transcription factors important for the differentiation of CD8 during acute infection

Several transcription factors that are involved in effector and memory CD8 T cell differentiation have been described. These transcription factors normally function in pairs to regulate the development of effector and memory cell. For example, T-bet and EOMES, BLIMP and Bcl6, ID2 and ID3, STAT3 and STAT4 counter regulate effector and memory cell potential (Figure 14) (Kaech and Cui, 2012). We mainly focus on the role of T-bet and EOMES.

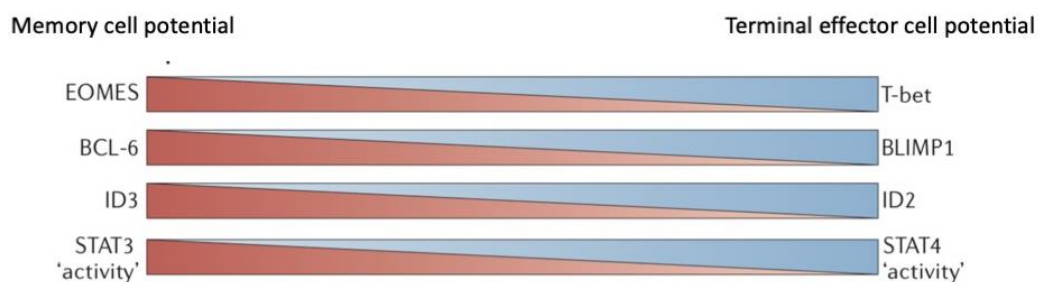


**Figure 14. Transcriptional factors associated with effector and memory T cell differentiation.** If the expression of T-bet, BLIMP1, ID2 and STAT4 increases, effector CD8 T cells tend to give rise to terminally differentiated cells that exhibit reduced proliferative capacity and longevity. Whereas, upregulation of EOMES, Bcl-6, ID3 and STAT3 facilitates memory cell properties and inhibits the differentiation in terminal effector cells. (Kaech and Cui, 2012).

### 1.6.1 T-bet and EOMES

T-bet and EOMES belong to a large T-box transcription factor family that possesses a conserved DNA-binding domain named T-box. T-box TFs exhibit widespread functions in cell fate decisions and organogenesis during development in vertebrate and EOMES and T-bet play important roles in the immune system (Papaioannou, 2014).

T-bet was first identified in 2000 and defined as a key transcription factor that directs the Th1 helper lineage commitment while repressing the differentiation of Th2 helper cells (Szabo et al., 2000). T-bet is encoded by the gene *Tbx21* (Svensson et al., 2008) and promotes the expression of IFN- $\gamma$  (Szabo *et al.*, 2000). T-bet is also expressed and has functions in multiple innate and adoptive lymphocytes, including DCs, B cells and NK cells (Kallies and Good-Jacobson, 2017). Finally, T-bet plays a key role in the development of effector and memory CD8 T cell populations and participates in mediating the long-term resistance to infection (Pritchard et al., 2019).

Eomesodermin (EOMES) was first defined as a key regulator in mesoderm formation of *Xenopus* in 1996 (Ryan et al., 1996). EOMES is highly expressed in conventional NK cells (Gordon et al., 2011), activated or memory CD8 T cells and activated CD4 T cells (Zhu et al., 2010).

T-bet and EOMES have central roles in the differentiation and function of effector and memory CD8 T cells (Intlekofer et al., 2005). The expression of T-bet is induced by TCR signaling and significantly enhanced by IL-12 and activation of mammalian target of rapamycin (mTOR) pathway in effector CD8 T cells (Rao et al., 2010; Takemoto et al., 2006). Conversely, EOMES expression is inhibited by IL-12 and the mTOR pathway but amplified by IL-2 (Pipkin et al., 2010; Rao *et al.*, 2010). T-bet is highly expressed in early effector CD8 T cells but its expression progressively decreases following the differentiation into memory cells. The expression of EOMES is delayed compared to T-bet expression in a Runx3-dependent manner (Cruz-Guilloty et al., 2009). Indeed, the expression of EOMES is enhanced by IL-2 in effector CD8 T cells but further increased during the transition from effector to memory cells (Joshi et al., 2011).

EOMES and T-bet have partially redundant functions and can compensate for each other

in CD8 T cells. Ectopic expression of EOMES is sufficient to invoke the function of effector CD8 T cells in the absence of T-bet, including cytotoxicity and production of interferon- $\gamma$  (IFN- $\gamma$ ), perforin, and granzyme B (Pearce et al., 2003). However, the expression of EOMES cannot compensate T-bet in terms of inducing the early cell expansion or effector cell differentiation during acute viral infections (Fixemer et al., 2020). Deficiency of both T-bet and EOMES in CD8 T cells impairs the formation of functional cytotoxic killers and decreases virus elimination during LCMV infection (Intlekofer et al., 2008). In memory CD8 T cells, T-bet cooperates with EOMES to induce the enhanced expression of IL-2R $\beta$  (CD122) which is responsible for the IL-15-mediated signaling and the long-term renewal of memory CD8 T cells (Intlekofer *et al.*, 2005). T-bet is necessary to induce the formation of short-lived KLRG1<sup>hi</sup>IL-7R $\alpha$ <sup>lo</sup> effector cells, suggesting a model in which high amounts of T-bet drive the terminal SLEC differentiation whereas low amounts of T-bet induce MPEC differentiation (Joshi *et al.*, 2007). Conversely, EOMES is dispensable for the generation of short-lived KLRG1<sup>hi</sup>IL-7R $\alpha$ <sup>lo</sup> effector cells and KLRG1<sup>lo</sup>IL-7R $\alpha$ <sup>hi</sup> memory precursor cells, but its deficiency decreases the formation of T<sub>CM</sub>. Furthermore, it impairs the homeostatic proliferation of memory cells and decreases the expression of chemokine receptors CXCR3 and CXCR4 implicated in homing to bone marrow (Banerjee et al., 2010).

The function of transcription factors T-bet and EOMES in chronic infection is distinct from that in acute infection (Doering et al., 2012). Deficiency of either T-bet or EOMES is not sufficient to completely impair the immune responses during acute infection, whereas the genetic elimination of either transcription factor impedes the formation of exhausted T cells following chronic infection (McLane *et al.*, 2019). Non-terminal exhausted progenitor cells are T-bet<sup>hi</sup> cells and proliferate in response to persisting antigen, giving rise to EOMES<sup>hi</sup> terminally differentiated exhausted T cells. This conversion from T-bet<sup>hi</sup> progenitors to EOMES<sup>hi</sup> progeny facilitates the virus control ability of CD8 T cell (Paley *et al.*, 2012). T-bet reduction is associated with T cell dysfunction, whereas EOMES upregulation correlates with enhanced CD8 T cell exhaustion during chronic viral infection. EOMES and T-bet are also involved in regulating T cell exhaustion in human cancer. High frequency of EOMES<sup>hi</sup>T-bet<sup>lo</sup> CD8 T cell subsets with reduced cytokines production and killing capacity is observed in patients with acute myeloid leukemia, and this correlates with poor response to chemotherapy and shorter overall survival (Jia et al., 2019).

## 1.6.2 TCF1

T cell factor 1 (TCF1, encoded by TCF7) was discovered as a T cell-specific transcription factor which regulates the development of T lymphocytes (van de Wetering et al., 1991). TCF1 is predominantly expressed in T cells and is activated through the Wnt/ $\beta$ -catenin signaling pathway (Molenaar et al., 1996; Zhao et al., 2021).

In early thymocyte development, TCF1 is highly expressed and sustained until maturation (Johnson et al., 2018). TCF1 deficiency impairs the transition from the double-negative to the double-positive stage of T cell development (Kovalovsky et al., 2009; Schilham et al., 1998). Moreover, TCF1 has a key role in regulating the differentiation of CD8 T cells (Figure 15).

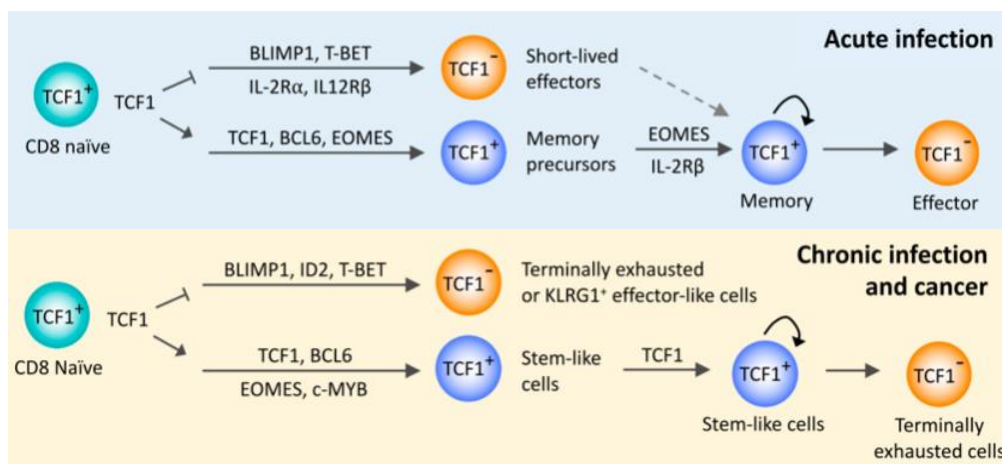


**Figure 15. The role of TCF1 in CD8 T cell in response to acute and chronic infection.** The role of TCF1 in promoting the generation of memory T cells following acute infections and stem-like T cells following chronic infection and cancer. (Kim et al., 2020).

TCF1 is highly expressed in naive CD8 T cells and decreased in most CD8 T cells during the effector phase (Danilo et al., 2018). However, the memory CD8 T cells re-acquire the expression of TCF1, which indicates an important role of TCF1 in the differentiation of memory CD8 T cells (Zhao et al., 2010).

TCF1 deficiency leads to a poor proliferation of antigen-specific effector CD8 T cells and impairs the differentiation toward T<sub>CM</sub>. Furthermore, the frequency of TCF-1-deficient memory CD8 T cells decrease progressively due to the low expression of Bcl-2 and IL-

2/15R $\beta$ . And TCF1 deficiency also leads to a significant reduction in secondary expansion (Jeannet et al., 2010; Zhou et al., 2010).

In human blood, the expression of TCF1 in CD8 T cells can be classified into 3 distinct levels: TCF1<sup>hi</sup>, TCF1<sup>int</sup> and TCF1<sup>lo</sup> cells. TCF1<sup>hi</sup> cells are found within both naive and memory pools and have a proliferative and self-renew potential. Moreover, TCF1<sup>hi</sup> cells lack immediate effector function but give rise to TCF1<sup>hi</sup> and TCF1<sup>lo</sup> cells following TCR stimulation. TCF1<sup>int</sup> cells are mainly found among memory pools, exhibiting robust immediate effector functions. TCF1<sup>lo</sup> cells mainly distribute in effector memory cells and are unable to generate TCF1<sup>hi</sup> cells (Kratchmarov et al., 2018).

TCF1 is an important determinant for the differentiation of CD8 T exhausted precursors under conditions of chronic infection and cancer (Figure 15). CD8 T exhausted precursors have self-renewal capacity and express TCF1, LEF1, Bcl6 and ID3 (Kim *et al.*, 2020). TCF1 represses the expression of ID-2 and Blimp1 but promotes the expression of EOMES and c-Myb (Chen *et al.*, 2019). TCF1 is essential to support the progenitor capacity in T exhausted cells, since cell-intrinsic TCF1 deficiency reduces the generation of CD8 T exhausted precursors. TCF1–Bcl6 axis may antagonize the pro-exhaustion effects of type I interferon and maintain T cell stemness (Wu et al., 2016).

Thus, TCF1 is essential for maintaining T cell stemness following both acute and chronic infection and for memory CD8 T cell differentiation.

## **1.7 The differentiation of CD8**

### **1.7.1 Models of CD8 T cell differentiation**

Many studies have been done on how naive CD8 T cells give rise to heterogeneous pools of effector and memory cells during infection. Several models illustrating the differentiation of T cells have been proposed (Figure 16).

#### **1.7.1.1 Decreasing-potential model**

This decreasing-potential model proposes that continued stimulation with antigens, co-stimulation and inflammatory cytokines on T cells drives differentiation process from

naive to T<sub>CM</sub>, transitional memory T (T<sub>TM</sub>), T<sub>EM</sub> progenitors and last to terminal effector T cells (Figure 16a). During this process, which is irreversible, cells progressively lose their memory cell properties including long-term survival, proliferative capacity and IL-7R $\alpha$  expression but acquire their effector function and cytolytic capacity. Several studies demonstrate this model. For example, curtailing antigen stimulation enhanced the generation of memory cells (Sarkar et al., 2008). Indeed, antibiotic treatment of mice, that are subsequently infected with *Listeria monocytogenes*, downregulates the early inflammation and IFN- $\gamma$  production but induces the generation of memory cells without experiencing contraction. Importantly, the quality and quantity of memory cells in these settings are similar to the one generated when antigen is maintained and when cells go through a contraction phase (Badovinac et al., 2005; Badovinac et al., 2004). Similar results are obtained in another experimental model where naive CD8 T cells are adoptively transferred to mice before and after virus infection. Indeed, CD8 T cells recruited later in antiviral response exhibit significantly reduced expansion but become functional memory cells (D'Souza and Hedrick, 2006). Thus, signal strength plays a key role in driving the differentiation of different quality of memory cells. However, these studies mentioned to favor the decreasing-potential model also fit with signal-strength model in section 1.7.1.2.

### **1.7.1.2 Signal-strength model**

This model also illustrates that the differentiation of multiple effector cell subsets is determined by the total strength of the three signals displayed during early T cell priming (Figure 16b) (Lanzavecchia and Sallusto, 2002). The amount of signal that T cells receive determines the transcriptional programs. This model is close to the decreasing-potential model. Strong signals direct the expansion and differentiation of terminal effector cells. For example, the presence of inflammatory cytokines IL-12 during priming drive the formation of terminal effector T cells (Joshi *et al.*, 2007). The major difference between this model and the decreasing-potential model is that, in this model, different cell fates are defined during the initial stimulation, depending on the divergent amount of the signals that the T cells received, rather than depending on a linear, repetitive stimulation in decreasing-potential hypothesis (Kaech and Cui, 2012). This corresponds to the fact that

autopilot memory cells are generated. However, it is contradictory to the in vivo cellular evidence in section 1.7.1.3 that one single cell could generate both effector and memory cells.

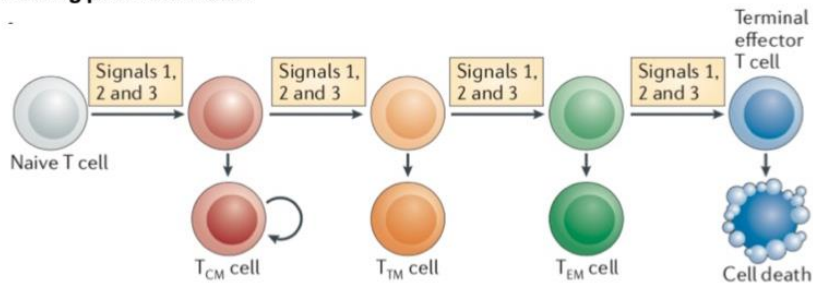
### **1.7.1.3 Asymmetric cell fate model**

The asymmetric cell fate model illustrates that when T cells are activated to expand, a single precursor T cell could give rise to both effector and memory T cells through asymmetric cell division (Figure 16c) (Arsenio et al., 2015; Chang et al., 2007). The unequal repartition of the capacity to receive stimulation signals in the single APC-activated initial cell leads to its asymmetric division. The proximal daughter cell that possesses the immunological synapse could perceive the strong TCR stimulation, co-stimulatory and pro-inflammatory cytokines, such as IL-12 and IFN- $\gamma$  provided by antigen-presenting cell (APC). In agreement with the notion that repetitive stimulation with antigen-bearing APCs (in the decreasing-potential model) and strong signals (in signal-strength model) enable the activated T cells to differentiate into terminal effector, the proximal daughter cell adopts an effector cell potential, whereas the distal cell, which does not segregate signaling complexes, preferentially acquire memory properties (Kaech and Cui, 2012).

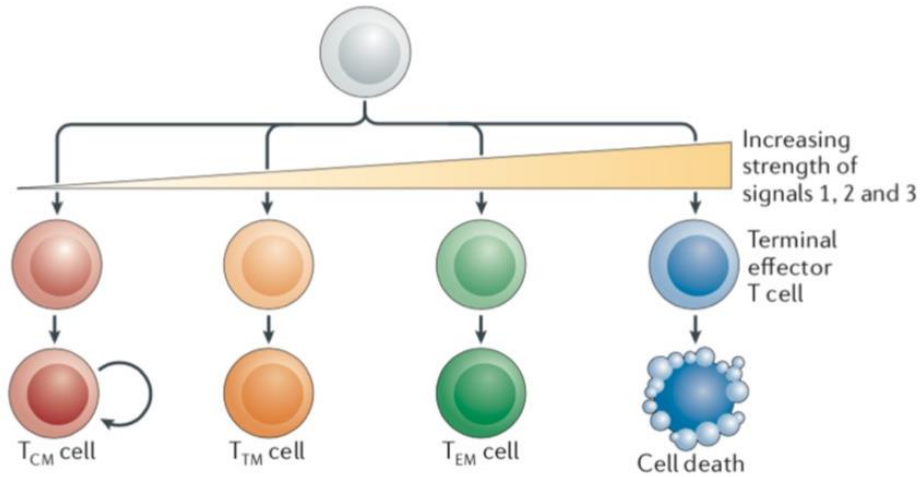
### **In vivo cellular evidence testing the models**

In favor of this model, studies show that the adoptive transfer of a single naive CD8 T cells, an individual naive T cell has multiple potentials and can generate both effector and memory progeny (Stemberger et al., 2007). Similarly, by introducing unique genetic barcodes into naive T cells and tracking the distribution of barcodes in antigen-specific effector and memory T cell populations, it was also demonstrated that one single naive T cell could differentiate into both effector and memory cells (Gerlach et al., 2010).

**a. Decreasing potential model**



**b. Signal strength model**



**c. Asymmetric cell fate model**

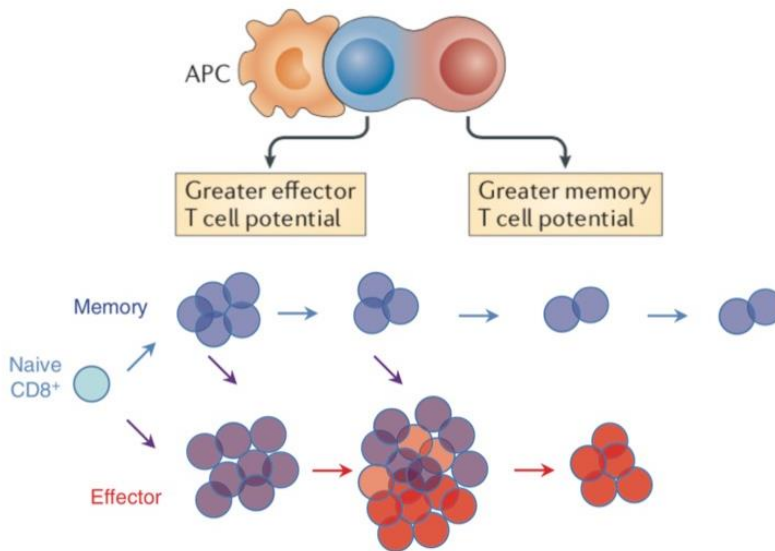


**Figure 16. Models for generation of effector and memory T cells.** **a.** The decreasing-potential model suggests that the repetitive history of signals during infection regulates the generation of various cell fates. Repetitive stimulation drives terminal effector differentiation. **b.** In the signal-strength model, the strength of signals early during T cell activation determines the various cell fates. Strong signals lead to terminal effector T cell differentiation. **c.** The asymmetric cell fate

model illustrates that a single naive precursor T cell undergoes asymmetric cell division. The proximal daughter of the initial cell, which is close to the APC, differentiates into an effector cell, in contrast, the distal daughter opposite to the APC becomes a memory cell. One single naive CD8 T cells could differentiate both effector and memory T cells.  $T_{CM}$ , central memory T;  $T_{EM}$ , effector memory T;  $T_{TM}$ , transitional memory T. (Kaech and Cui, 2012; Tsuda and Pipkin, 2021).

## 1.7.2 New approaches to validate or revisit these models

### 1.7.2.1 Mathematical modelling

Our team has established a mathematical model to identify the CD8 T cell differentiation stages during a primary response (Figure 17) (Crauste et al., 2017). Upon infection with vaccinia virus, based on the expression of CD44, Bcl-2 and Mki67, CD8 T cells can be divided into four stages: naive (CD44<sup>-</sup>, Bcl-2<sup>+</sup>, Mki67<sup>-</sup>), early effector (CD44<sup>+</sup>, Bcl-2<sup>-</sup>, Mki67<sup>+</sup>), later effector (CD44<sup>+</sup>, Bcl-2<sup>-</sup>, Mki67<sup>-</sup>) and memory (CD44<sup>+</sup>, Bcl-2<sup>+</sup>, Mki67<sup>-</sup>). These populations appear sequentially, i.e. naive CD8 T cells (N) first, early effector cells (E), then late effector cells appear (L) and at last memory cells (M) in the blood of infected mice. What Crauste et al. have tested is the capacity of different differentiation pathway to generate the total number of E and L effector and M memory cells (Crauste *et al.*, 2017). Cell number analysis support a model where N CD8 T cells first differentiate into E effectors then give rise to L effector cells and at last generate M CD8. The majority of memory CD8 T cells would emerge from this NELM pathway, except a small fraction that can be generated from N or E effectors. This model reconciles linear (sections 1.7.1.1 and 1.7.1.2) and branching (section 1.7.1.3) models.

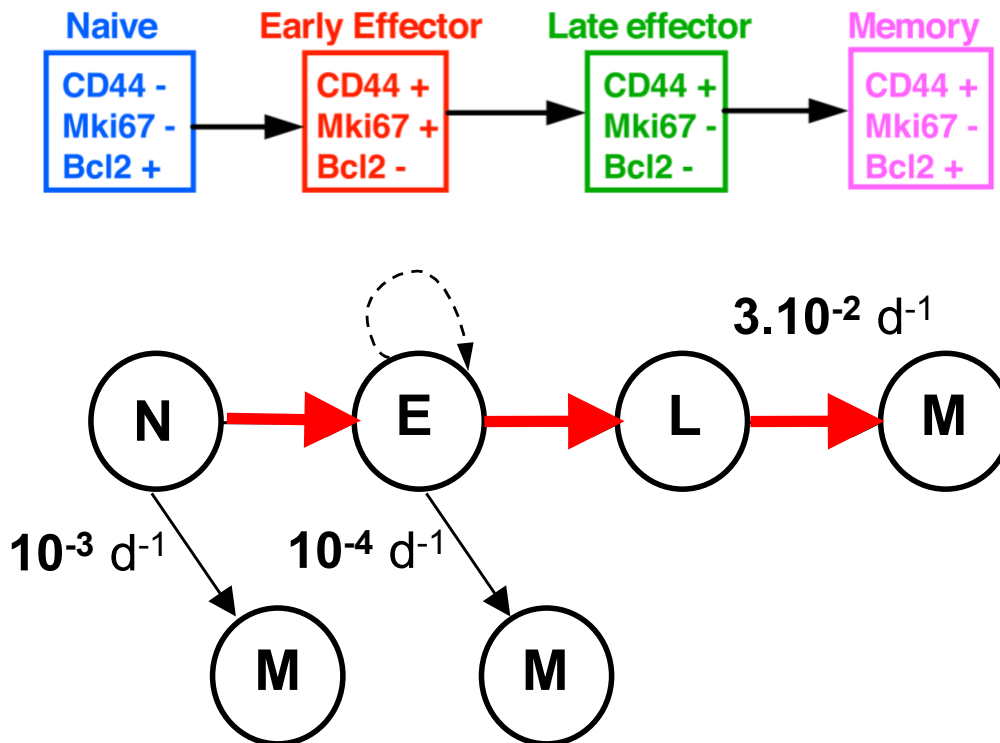


**Figure 17. NELM differentiation model.** The expression of CD44, Bcl-2 and Mki67 help identify four stages during primary infection: naive (N), early effector (E), later effector (L) and memory (M). The majority of the cells follow the liner NELM differentiation pathway. A small proportion of naive and early effector cells directly give rise to memory cells. (Crauste *et al.*, 2017).

### 1.7.2.2 Single-cell RNA sequencing of CD8 T cell differentiation

Models mentioned above have been revisited using single cell transcriptomic analysis. Sequencing of RNA, or RNA-Seq, is now a routine method to analyze gene expression in biomedical research. RNA-seq is typically performed in “bulk” to analyze the expression of RNAs from large populations of cells. And the data reveal an average of gene expression patterns across the large number of cells. In mixed cell populations, this measurement may obscure biological differences between individual cells (Olsen and Baryawno, 2018). Single-cell RNA sequencing (scRNA-seq) can illustrate RNA abundance and regulatory networks of genes, and track the trajectories of distinct cell lineages in cell development (Hwang et al., 2018).

Following microbial infection, single-cell RNA sequencing measurements in individual lymphocytes show that differences in the expression of IL-2R $\alpha$  during the first asymmetric

division may contribute to the acquisition of distinct gene-expression profiles in daughter lymphocytes and result in divergent cell fates. Proximal daughter cells encountering more IL-2 signaling may acquire characteristics of effector cells, whereas the distal daughter cells may acquire memory gene-expression program. The unequal partitioning of IL-2R $\alpha$  determines the effector versus memory cell fate (Arsenio et al., 2014). By performing scRNA-seq analysis on antigen-specific CD8 T cells isolated from different time points during a viral infection, Kakaradov et al. also found that cells that had undergone their first division exhibit transcriptional divergence. They identified a previously unknown molecular determinant called Ezh2 that regulates the differentiation of terminal effector cells (Kakaradov et al., 2017).

### **1.7.3 The Schematic of CD8 T cell differentiation**

Muroyama and Wherry proposed an overview of CD8 T cell subsets and a scheme of CD8 T cell differentiation (Figure 18). Upon activation, naive CD8 T cells are activated and give rise to T stem cell memory cells (T<sub>SCM</sub>) and a common precursor population with the potential to generate multiple CD8 T cell lineages. Then the differentiation pathway can be classified in three lineages: terminally differentiated T effector cell lineage, T memory cell lineage and T exhausted cell lineage. During chronic infection, activated precursors differentiate along the T exhausted cell lineage (Muroyama and Wherry, 2021).

Our team also explored the time point of the generation of memory precursor cells during an acute infection. We analysed the single cell RNA-seq data of CD8 T cell following acute infection and reconstructed the developmental trajectory of CD8 T cell response. The memory precursors were identified at multiple time points (Figure 19). Even as early as day4.5 post infection, a small fraction of memory precursors was generated. However, the majority of memory precursors arise at later time points when cells have undergone clonal expansion and become quiescent (Todorov et al. submitted 2022).

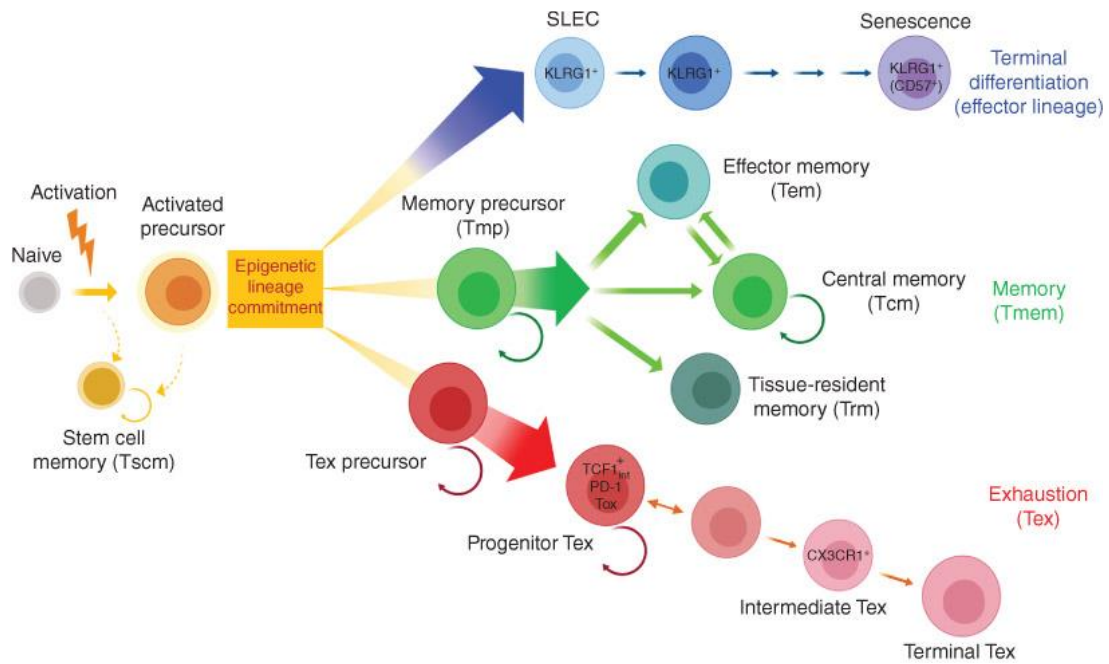
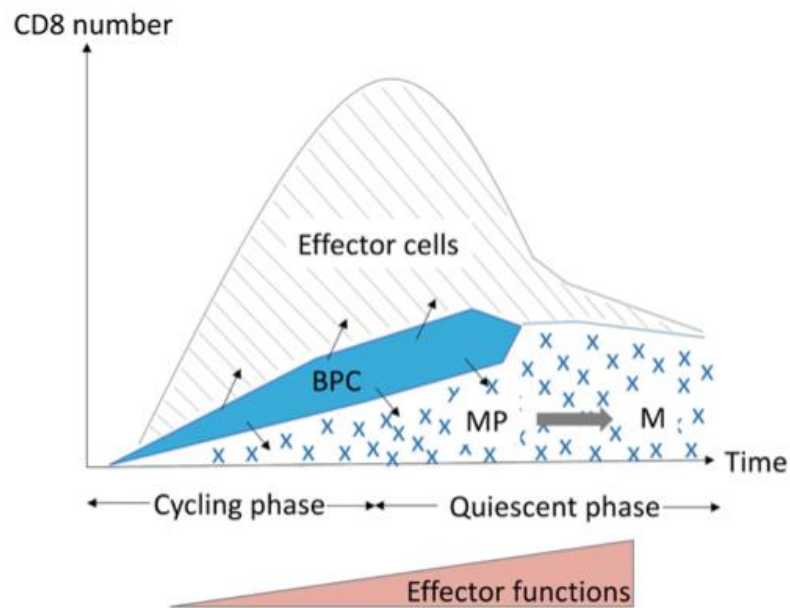


**Figure 18. Schematic of CD8 T cell differentiation.** Terminally differentiated T effector cell lineage, T memory cell lineage and T exhausted cell lineage are illustrated. **(Muroyama and Wherry, 2021).**



BPC: bipotent cells; MP: memory precursor; M: memory

**Figure 19. Memory precursors are generated at multiple time points.** Single cell transcriptomics analysis and in vivo memory precursors tracing reveal that memory precursors are generated continuously following activation. And the highest fraction of memory precursors is formed at the peak of expansion phase. **(Todorov et al. submitted 2022).**

## 2 $\gamma$ c cytokines as important regulators of CD8

Cytokines of the common cytokine-receptor  $\gamma$ -chain ( $\gamma$ c) family have a central role in cellular proliferation, differentiation and survival. The  $\gamma$ c cytokine family consists of IL-2, IL-4, IL-7, IL-9, IL-15 and IL-21. This family is named due to the  $\gamma$ c subunit (CD132) which is involved in receptor complexes of all these cytokines (Figure 20).

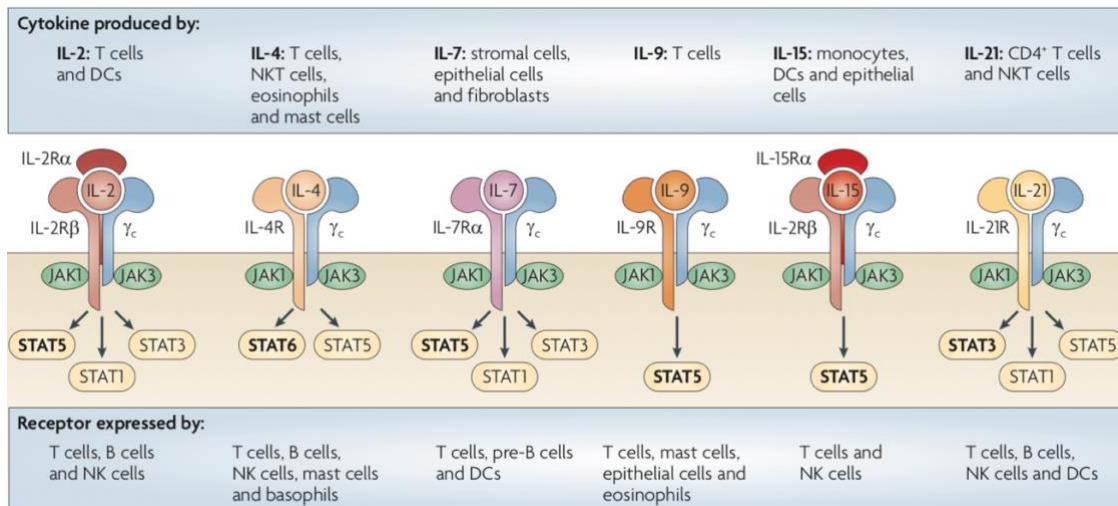


**Figure 20. Receptors of  $\gamma$ c family cytokines.** The receptors of IL-4, IL-7, IL-9 and IL-21 are composed of two chains including a specific  $\alpha$  chain and the common  $\gamma$  chain, while besides these two chains there is a  $\beta$  chain for the receptor of IL-2 and IL-15. The receptor for each  $\gamma$ c family cytokine transduces signals via the JAK–STAT pathway that subsequently activate or repress the gene expression in the nucleus. (Rochman et al., 2009).

IL-4, IL-7, IL-9 and IL-21 interact with their specific receptor composed of the  $\gamma$  chain and a unique  $\alpha$  chain: IL-4R $\alpha$ , IL-7R $\alpha$  (CD127), IL-9R $\alpha$  and IL-21R $\alpha$ , respectively. IL-2 and IL-15 interact with their receptor formed by three chains: the  $\gamma$  chain, the same IL-2/15R $\beta$  (CD122) and the specific subunits, IL-2R $\alpha$ (CD25) and IL-15R $\alpha$ , respectively. These  $\gamma$ c cytokine receptor complexes share a same subunit and lead to the recruitment and phosphorylation of JAK1 and JAK3 that subsequently activate the STAT family (Shuai and Liu, 2003). In general, IL-2, IL-7, IL-9 and IL-15 predominately prime STAT5, while IL-4 and IL-21 prime STAT6 and STAT3, respectively (Alves et al., 2007; Leonard and Spolski, 2005; Rochman et al., 2009; Shourian et al., 2019; Spolski and Leonard, 2008). The expression of  $\gamma$ c receptors is regulated during CD8 T cell activation and differentiation in memory

cells (Table 3).

| Receptor chain         | Level of expression |                   |                |
|------------------------|---------------------|-------------------|----------------|
|                        | Naive T cells       | Effector T cells  | Memory T cells |
| $\gamma_c$ (CD132)     | Intermediate        | Intermediate      | Intermediate   |
| IL-2R $\alpha$ (CD25)  | None                | High              | None           |
| IL-2R $\beta$ (CD122)  | Low                 | High              | High*          |
| IL-4R $\alpha$ (CD124) | None                | High              | ND             |
| IL-7R $\alpha$ (CD127) | Intermediate        | None <sup>‡</sup> | High           |
| IL-15R $\alpha$        | Low                 | High              | High           |
| IL-21R                 | Low                 | High              | ND             |

**Table 3. Expression of  $\gamma_c$  family cytokine receptors.** \*Maintained at a high-level expression on CD8 memory T cells. <sup>‡</sup> IL-7R $\alpha$  is expressed on a few effector T cells. (Rochman *et al.*, 2009).

The  $\gamma_c$  cytokines appear to be important for the differentiation of CD8 T cells (Cox *et al.*, 2011). Herein, we will discuss the impact of IL-2, IL-4, IL-7, IL-15 and IL-21 on the activation of naive CD8 T cells and proliferation and differentiation of effector and memory CD8 T cells.

## 2.1 IL-2

IL-2 has been viewed as a pleiotropic player in the CD8 T cell survival, proliferation, effector differentiation and the formation of long-lived memory cells (Kalia and Sarkar, 2018). IL-2 signals through its receptor formed by CD25 (IL-2R $\alpha$ ), CD122 (IL-2R $\beta$ ) and CD132 (IL-2R $\gamma$ ). IL-2 is produced by several lymphocytes, especially by CD4 and CD8 T cells. Indeed, during homeostasis, IL-2 is mainly produced by CD25<sup>int</sup> and CD25<sup>lo</sup> CD4 T cells, and by CD8 T cells to some extent. Furthermore, during an immune response, IL-2 is secreted by activated CD4 T cells in large amount, as well as by CD8 T cells and DCs (Kalia and Sarkar, 2018). Microarray experiments showed that DCs were also found to be able to produce IL-2 upon certain microbial stimuli (Granucci *et al.*, 2001). IL-2 production by CD8 T cells is also regulated along their differentiation. Indeed, memory-fated effector CD8 T cells are shown to potently produce IL-2 in response to antigen compared to the terminally differentiated effector cells (Kalia *et al.*, 2010). The capacity to produce IL-2 along with

IFN- $\gamma$  and TNF- $\alpha$  is a hall mark property of T<sub>CM</sub> (Kalia and Sarkar, 2018). The T<sub>RM</sub> cells in human skin and liver are also able to produce IL-2 (Pallett et al., 2017; Seidel et al., 2018).

IL-2 induce the expression of Blimp-1 which is a key regulator of short-lived effector differentiation (Boulet et al., 2014). IL-2 also promotes the perforin gene transcription in effector CD8 T cells through STAT5 and EOMES, but not T-bet (Pipkin *et al.*, 2010). The collaboration of IL-2 and IL-12 has been shown to drive the terminal effector differentiation of CD8 T cells through activation of Blimp-1 and T-bet (Xin et al., 2016).

### **2.1.1 The role of IL-2 in regulating effector CD8 T cell response**

IL-2 plays a critical role in driving optimal activation and expansion of CD8 T cells following TCR stimulation. Indeed, IL-2 can be used as a substitute for CD4 cells in a number of settings. For example, it is demonstrated that IL-2 addition could rescue the proliferative and functional capacity of CD4-helpless effector CD8 T cells extracted from CD4 depleted and mouse embryo cell lines (MEC)-immunized mice and cultured *in vitro*, by inhibiting the expression of TRAIL (Wolkers et al., 2011). Similarly, enhancing IL-2 signals by administration of IL-2/IL-2 antibody complexes to mice that have been immunized with DCs, potently enhances the number of antigen-specific effector and memory cells (Kim et al., 2016), indicating that IL-2 support activated-CD8-T cell proliferation and survival. In contrast, CD8 T cells proliferation (as measured by BrdU incorporation) was not affected by IL-2 deficiency following *in vivo* activation with peptide (Krämer et al., 1994). Furthermore, another study demonstrated that IL-2- or IL-2R $\alpha$ -deficient TCR transgenic CD8 T cells showed normal expansion in secondary lymphoid tissues following viral infection, which confirmed the capacity of CD8 T cells to proliferate in the absence of IL-2. However, IL-2 signal is essential for the optimal expansion of virus-specific CD8 T cells in non-lymphoid tissues (D'Souza et al., 2002). Moreover, IL-2-deficient CD8 T cells lack cytotoxic effector function which could be restored *in vitro* by the administration of exogenous IL-2 (Krämer *et al.*, 1994). In conclusion, the optimal activation of CD8 seem to be IL-2 independent only in certain experimental contexts.

### **2.1.2 The role of IL-2 in regulating memory CD8 T cell response**

In addition to its potential involvement in promoting the expansion, function and differentiation of effector CD8 T cells, IL-2 has also been shown to control the generation of memory cells. Indeed, using IL-2R $\alpha$ -deficient CD8 T cells it was shown that IL-2 signaling during the primary CD8 T cell activation was essential for the generation of efficient memory cells that could undergo secondary expansion (Williams et al., 2006). Although the absence of IL-2R $\alpha$  expression in CD8 does not significantly affect T cell expansion and memory transition, the memory CD8 cells generated in the absence of IL-2R $\alpha$  were unable to mount an effective recall response (Belz and Masson, 2010; Williams *et al.*, 2006). Boyman et al. had previously demonstrated that some IL-2 specific monoclonal antibodies in complex with recombinant IL-2 (IL-2/IL-2 mAb) could activate and transduce the signals through the  $\beta$  chain (CD122) and  $\gamma$  chain (CD132) subunits of the IL-2 receptor even in the absence of IL-2R $\alpha$  (Boyman et al., 2006). Williams et al. used the IL-2/IL-2 mAb complex during the primary infection to rescue the potential of IL-2R $\alpha$ -deficient primary memory CD8 T cells to mount a secondary expansion. So IL-2/IL-2 mAb during the primary infection signals through IL-2R $\beta$  and IL-2R $\gamma$  to help the generation of protective memory cells in the absence of IL-2R $\alpha$ . Importantly, treatment with IL-2/IL-2 mAb complexes during the secondary challenge, failed to restore the defective recall response of IL-2R $\alpha$ -deficient primary memory cells (Williams et al., 2006). As a result, IL-2 signaling through IL-2R $\beta$  and IL-2R $\gamma$  during the secondary challenge is unable to rescue the formation of protective memory cells. These data demonstrate the essential role of IL-2 in the generation of functional memory CD8 T cells.

IL-2 is considered to drive the effector and memory differentiation in an autocrine or paracrine manner. Since CD4 T cells are the main manufacturers of IL-2, it was long considered that CD4 T cells through their production of IL-2 provided help for the formation of protective memory CD8 T cells which could quickly respond to the secondary challenge (Kalia and Sarkar, 2018). However, studies on ablation of IL-2 in antigen-specific CD8 T cells following attenuated *Listeria Monocytogenes* immunization, demonstrated that the autocrine IL-2 is indispensable for the development of protective memory CD8 T cells even in the presence of helper CD4 T cells able to secrete paracrine IL-2 (Feau et al., 2011). Therefore, it is considered that first CD4 T cell help is mediated through CD40-CD40L interactions to license APCs, then the licensed APCs activate CD8 T cells and endow

them with the abilities to produce autocrine IL-2 (Feau et al., 2011). CD27 deficient CD8 T cells display reduced IL-2 production, and this autocrine IL-2 production directed by CD27 promotes the clonal expansion of activated CD8 T cells and is crucial to support the survival of virus-specific CTLs in non-lymphoid tissues (Peperzak et al., 2010). By comparing the transcriptome of CD4-helped and -unhelped-CD8 T cells, it was shown that autocrine IL-2 increases the expression of NGFI-A binding protein 2 (Nab2), which blocks TRAIL mediated apoptosis, promoting the secondary expansion of memory CD8 T cells (Wolkers et al., 2012). These data demonstrate a crucial role of autocrine IL-2 in the generation of protective memory CD8 T cells.

### **2.1.3 The role of IL-2 in regulating the differentiation of CD8 T cell**

IL-2 regulates CD25 expression on CD8 T cells. Indeed, higher CD25 expression correlates with increased IL-2 signal, while CD25 expression decreases when IL-2 signal is blocked. Activated CD8 T cells that express relatively high level of CD25 are more efficient to perceive and transduce IL-2 signal. The fate of effector CD8 T cells expressing different level of CD25 was thus studied (Kalia *et al.*, 2010). The CD25<sup>hi</sup> T cells express high level of KLRG1 and low level of CD62L and are more similar to effector cells. In contrast, CD25<sup>lo</sup> effector CD8 T cells show a low expression of perforin and Blimp-1 and a high expression of CD62L which is more similar to memory T cells in terms of gene expression (Cox *et al.*, 2011; Kalia *et al.*, 2010). To test their fate, the authors next transferred the CD25<sup>hi</sup> and CD25<sup>lo</sup> T cells effector cells into infection-matched recipient mice. The CD25<sup>hi</sup> donor cells tend to give rise to terminally differentiated effector cells that showed enhanced apoptosis and failed to accumulate as extensively as CD25<sup>lo</sup> cells in lymphoid and non-lymphoid organs. Furthermore, CD25<sup>hi</sup> progeny could not mount a recall response, indicating that these cells are defective in generating the protective memory cells. In contrast, the CD25<sup>lo</sup> CD8 T cells seem to survive for a long time, were able to settle in the lymph nodes and their progeny could respond to a secondary challenge, indicating that early during the initial priming phase the downregulation of CD25 in effector CD8 determines the differentiation to long lived functional memory cells (Cox *et al.*, 2011; Kalia and Sarkar, 2018; Kalia *et al.*, 2010). These data seem in contradiction with the IL-2 dependency described by others (Kim *et al.*, 2016). Alternatively, IL-2 dosage or timing of

delivery could differentially impact the fate of effector CD8 T cells. Indeed, it was shown by Kim et al., that following DC immunization of mice, early (days 1-3) or late (days 4-6) administration of IL-2/anti-IL-2 complexes to enhance IL-2 signals had a different impact on the differentiation of CD8 T cells. Indeed, the late administration enhanced the terminal differentiation without affecting the number of memory T cells generated, whereas early administration enhanced the memory formation. Furthermore, early treatment enhances CTLA-4 expression on regulatory T cells, which down regulates B7 ligands expression on DCs. Curtailed co-stimulation through B7-CD28 during CD8 T cell activation seemed to prevent terminal differentiation and promote memory CD8 T cell generation (Kim *et al.*, 2016).

The ambivalent role of IL-2 in regulating the differentiation program of naive CD8 T cells into effector and/or memory T cells has also been shown *in vitro* (Pipkin *et al.*, 2010). Strikingly, strong and prolonged IL-2 signal drives a higher level of STAT-5 and augments effector differentiation, while weak and curtailed IL-2 signal induces lower levels of STAT-5. Moreover, cell fate is tested by adoptively transferring the strong or weak IL-2-stimulated CD8 T cells in to naive mice. Strong IL-2 signal promotes the acquisition of effector T cell functions and the terminal differentiation of effector cells at the expense of the capacity to generate memory cells. In contrast, in the context of weak IL-2 signaling, T cells maintain a stem cell potential and convert to central memory-like features (Figure 21) (Belz and Masson, 2010; Pipkin *et al.*, 2010) .

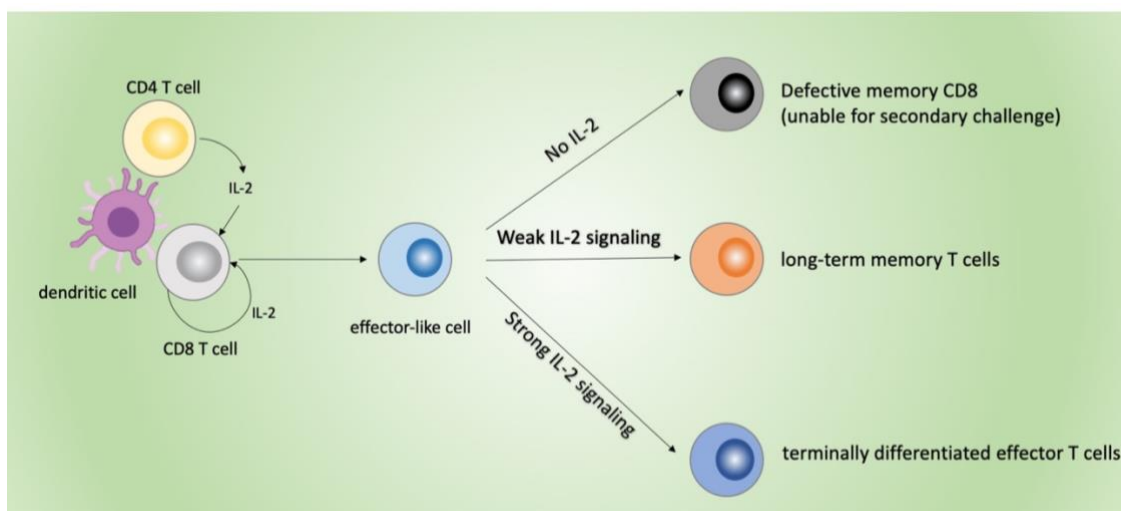


**Figure 21. IL-2 signaling modulates the differentiation of activated CD8.** Following initial

activation via TCR and co-stimulation provided by DCs, naive CD8 T cells begin to proliferate and differentiate into effector and memory cells along an intrinsic pathway. The amount of IL-2R signaling changes the subsequent transcriptional program of activated CD8 T cells. Without any IL-2 signal, the memory cells that are generated are unable to mount a secondary immune response. T cells will preferentially become terminally differentiated effector cells when IL-2 signaling is strong but maintain a stem cell potential and become memory cells when IL-2 signaling is weak.

## **2.2 IL-4**

IL-4, mainly produced by  $T_H2$  CD4 T cell and mast cell, was first defined as a factor that regulates B cell differentiation, the IgG class switch and the development of memory B cell (Howard et al., 1982; Isakson et al., 1982). IL-4 also plays a vital role in the differentiation of CD4  $T_H2$  T cells and inhibits the appearance of IFN- $\gamma$ -producing CD4  $T_H1$  T cells (Nelms et al., 1999). IL-4 leads to the activation of the IL-4R that subsequently signals through JAK1/STAT6 and PI-3K/protein kinase B pathways in naive, activated, and IFN- $\gamma$ -producing CD8 T cells. IL-4 also induces the phosphorylation of JAK3 and nuclear migration of STAT1, STAT3, and STAT5. This broad signaling activation of STAT family member in CD8 T cells results in reduced transcriptional activity of SOCS genes, which inhibit the cytokine-induced JAK/STAT pathway (Acacia de Sa Pinheiro et al., 2007). Several studies show that IL-4 performs different effects on the function and differentiation of CD8 T cells.

### **2.2.1 The impact of IL-4 on effector CD8 T cells**

CD8 T cells have the potential to generate type 1 and type 2 subsets that are similar to CD4  $T_H1$  and  $T_H2$  subsets in terms of cytokine production patterns (Croft et al., 1994; Li et al., 1997; Sad et al., 1995). IL-4 plays inhibitory effect on the type 1 cytokine secretion and CTL function of activated CD8 T cells both in vivo and in vitro and IL-4-deficient environment could enhance the cytolytic property of activated CD8 (Croft *et al.*, 1994; Sad and Mosmann, 1995; Villacres and Bergmann, 1999). Furthermore, IL-4 treatment during infection suppresses antiviral cytokine expression and cytotoxic responses and, as a result, delays virus clearance (Jackson et al., 2001; Moran et al., 1996; Sharma et al., 1996). In

addition, treatment with anti-IL-4 antibody of respiratory syncytial virus (RSV) infected mice augments the type 1 cytokine expression and CTL activity (Tang and Graham, 1994). IL-4 inhibits the expression of very late antigen (VLA)-4 (CD49d/ CD29) which imparts the migration of CD8 T cells into tumor lesions and leads to poor tumor infiltration (Sasaki et al., 2008). However, the disruption of IL-4 in mice does not significantly modulate the activation of CD8 T cells (Bachmann et al., 1995; Mo et al., 1997). In vitro, IL-4 enhances the IL-2-driven proliferation of CTL (Miller et al., 1990).

### **2.2.2 The impact of IL-4 on memory CD8 T cells**

As to the effect of IL-4 on antigen-specific memory cells, IL-4 exposure during initial antigen encounter is also shown to be essential for the generation of long term memory CD8 T cells (Huang et al., 2000). Following Malaria parasitic immunization, IL-4R knockout CD8 T cells are unable to generate a memory population in non-lymphoid tissues, even though they develop normal memory cells in lymphoid organs. Similarly, treatment with anti-IL-4 antibody early after immunization reduces the number of  $T_{RM}$  (Morrot et al., 2005). IL-4 inhibits the expression of NKG2D in memory CD8 T cells via the JAK/STAT6 pathway, and thereby impairs the NKG2D-dependent activation of memory CD8 T cells (Ventre et al., 2012). IL-4, through a STAT6-dependent pathway, suppresses the secretion of CCL5 which is immediately secreted by memory CD8 T cells upon antigen stimulation. This inhibition is reversible, as memory CD8 T cells reacquire their capacity of immediate CCL5 secretion when IL-4 is withdrawn (Marcais et al., 2006).

IL-4 plays a vital role in the development of innate memory cells (Lee et al., 2011). After helminths infection, IL-4 drives the expansion of  $T_{VM}$  which are conditioned and provide enhanced control of subsequent acute infection with the murine gammaherpesvirus 4 (MuHV-4) by raising antigen-specific CD8 T cell activation (Rolot et al., 2018). IL-4 produced by  $\gamma\delta$  T cells and invariant natural killer T cells is essential and sufficient for the generation of innate memory CD8 T cells in the thymus and inducing striking high levels of EOMES but not T-bet in these cells (Gordon *et al.*, 2011; Lai et al., 2011; Lee *et al.*, 2011; Renkema et al., 2016; Weinreich et al., 2009).

## 2.3 IL-7

IL-7, initially identified as a growth factor for B cell progenitors (Namen *et al.*, 1988), is predominately manufactured by fibroblastic reticular cells in the T cell zones of secondary lymphoid organs (Rochman *et al.*, 2009). The IL-7 receptor contains the IL7R $\alpha$ -chain (CD127) and the common  $\gamma$  chain (Shourian *et al.*, 2019). IL-7R stimulation enhances T cell survival through JAK/STAT and PI3K pathways by increasing the expression of Bcl-2 family member proteins (Tan *et al.*, 2001). In addition, IL-7 signals regulate the metabolism in part by activating mTOR and improving the expression of the glucose transporter GLUT1 in a PI3K/AKT pathway dependent manner (Wofford *et al.*, 2008).

### 2.3.1 The role of IL-7 in regulating the survival and homeostasis of naive and memory CD8 T cells

IL-7 plays multiple roles on T cells, such as regulating cell survival, homeostasis and cell cycle (Takada and Jameson, 2009). The absence of IL-7 or IL-7R $\alpha$  results in severe immune-deficiencies both in mice and humans. IL-7 plays a crucial role in maintaining the homeostatic proliferation and is critical for the survival of naive and memory CD8 T cells via Bcl-2 in a STAT5-dependent manner (Carrio *et al.*, 2007; Goldrath *et al.*, 2002; Osborne *et al.*, 2007; Schluns *et al.*, 2000; Tan *et al.*, 2001). Blocking of the biological activity of IL-7 results in the reduction of naive T cell survival and a severe decline in their numbers (Osborne *et al.*, 2007; Seddon and Zamoyska, 2002; Tan *et al.*, 2001; Vivien *et al.*, 2001). The homeostatic proliferation and long-term survival of naive T cells disappears upon adoptive transfer into IL-7-deficient mice (Tan *et al.*, 2001). Enhanced level of IL-7 facilitates TCR recognition of self-MHC ligands, leading to the differentiation from naive CD8 cells to memory phenotype cells (Kieper *et al.*, 2002).

### 2.3.2 The role of IL-7 in regulating memory CD8 T cell differentiation

IL-7 was dispensable for the growth of CD8 T cells but was essential for the generation of memory CD8 T cell following viral challenge (Schluns *et al.*, 2000). Mice that overexpress

IL-7 have an increased frequency of memory phenotype CD44<sup>hi</sup> CD122<sup>hi</sup> CD8 T cells even in the absence of IL-15. Memory precursor effector CD8 T cells that are characterized by high level of IL-7R $\alpha$  (CD127) expression show increased amounts of anti-apoptotic molecules (Kaech et al., 2003). CD127 combined with CD62L could further be used to distinguish two functionally distinct memory cell subsets: CD127<sup>hi</sup> and CD62L<sup>hi</sup> subsets that are similar to T<sub>CM</sub> and CD127<sup>hi</sup> and CD62L<sup>lo</sup> subsets that are described as T<sub>PM</sub> (Huster et al., 2004).

IL-7 also plays a central role in driving the memory differentiation in vitro. Following in vitro antigen activation and in vivo transfer in an Ag-free environment, CD8 maintained their function and phenotype of effector CTL in the presence IL-2, whereas they differentiate in memory cells in the presence of IL-7 or IL-15 (Carrio et al., 2004). The presence of IL-7 and IL-15 is required for the naive T cell precursors to differentiate to human long-lived T<sub>SCM</sub> following CD3/CD28 stimulation (Cieri et al., 2013).

### **2.3.3 The role of IL-7/IL-7R in cancer therapy**

In the context of chronic LCMV clone 13 infection, persistent antigen inhibits the expression of IL-7R $\alpha$ , which correlates to the severity of CD8 T cell exhaustion and decreased the expression of Bcl-2 (Lang et al., 2005). Furthermore, in tumor environment, PD-1<sup>+</sup> CD8 T cells that tend to become functionally exhausted cells lack of the expression of IL-7R $\alpha$  (Ahmadzadeh et al., 2009).

Thus, IL-7 could be used as an immunotherapeutic agent since it promotes homeostatic proliferation, T cell survival and the generation of memory cells and may reduce the probability of T cell exhaustion. IL-7 administration enhances the T cell effector function and reduces the expression of PD-1 on antigen-specific CD8 T cells, resulting in enhanced viral clearance in chronic viral infected mice (Pellegrini et al., 2011) and anti-tumor response in tumor hosts (Pellegrini et al., 2009). IL-7 treatment also prolongs the survival of tumor-bearing mice through improving the long-term responses of antigen-specific CD8 T cell and tumor control (Colombetti et al., 2009; Pellegrini *et al.*, 2009; Zhao et al., 2014). In patients with cancers, treatment with recombinant human IL-7 increases the amount of CD4 and CD8 T cells in peripheral blood in a dose dependent manner due to

the robust proliferation of T cells (Sportes et al., 2010). Similarly, culture of CD19 CAR T cells with IL-7 and IL-15 increases the frequency of CD45RA<sup>+</sup> CCR7<sup>+</sup> CD8 T cells in patients treated with these CAR T cells and improves the antitumor immunity by preserving their migration to secondary lymphoid organs through CCR7, while suppressing cell death (Xu et al., 2014). These observations demonstrate the potential role of IL-7 as an adjuvant in cancer immunotherapy.

## 2.4 IL-15

IL-15 was discovered as a T cell growth factor (Grabstein et al., 1994). DCs, macrophages and monocytes produce a large amount of IL-15, while mastocytes, B cells, T cells and epithelial and stromal cells produce IL-15 at low levels (Mishra et al., 2014; Shourian *et al.*, 2019). Unlike IL-2 which is a secreted cytokine, IL-15 is a membrane-associated molecule usually combined with the  $\alpha$  chain of its receptor and is trans-presented to T cells expressing the IL-2/15R $\beta$ - $\gamma_c$  receptor (Figure 22) (Jabri and Abadie, 2015; Waldmann, 2006). Like IL-2, IL-15 signaling triggers recruitment and activation of JAK1/JAK3-STAT5 that subsequently primes the AKT/P13K and RAS/MAPK signaling pathway activation in T cells (Steel et al., 2012).

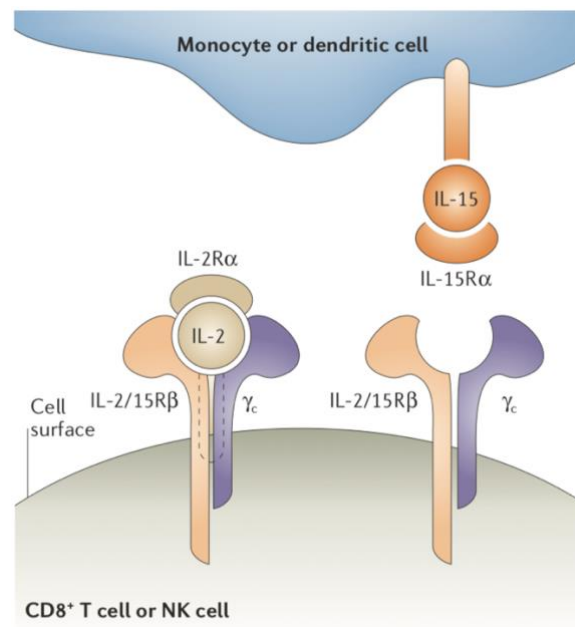


**Figure 22. The mode of IL-2 and IL-15 interacting with their receptors.** IL-2 directly binds different receptor chains either the IL-2R $\alpha$  chain and/or the IL-2/15R $\beta$  and the common  $\gamma_c$ -chain ( $\gamma_c$ )

complex. IL-15 complexes with IL-15R $\alpha$  which is on the surface of DCs or monocytes and IL-15/IL-15R $\alpha$  complex is presented to IL-2R $\beta$  and  $\gamma$ -chain that are expressed by CD8 T cells or NK cells. (Waldmann, 2006).

### **2.4.1 The role of IL-15 in regulating the survival and homeostasis of naive and memory CD8 T cells**

IL-15 has a central role in multiple biological processes such as enhancing the survival of naive and memory CD8 T cell (Berard et al., 2003), modulating the homeostatic maintenance of memory CD8 T cells (Burkett et al., 2004), and promoting the proliferation of memory CD8 T cells (Schluns et al., 2004). Like IL-7, IL-15 promotes the survival by inducing Bcl-2 and its family members in a JAK/STAT- and PI3K/AKT-dependent manner (Shenoy et al., 2014). When IL-2/15R $\beta$  is knockout, the number of antigen-experienced memory CD8 T cells is still maintained. However, their number severely declines when mice are deficient for the IL-15R $\alpha$  gene. This suggests that IL-15 and IL-15R $\alpha$  expression but not the expression of IL-2/15R $\beta$  are necessary to support the homeostasis of memory CD8 T cells (Burkett et al., 2004). Following viral infection, type I IFN-driven IL-15 endows the memory CD8 T cells with the ability to enter into cell-cycle in a mTORC1 dependent manner. Exposure to IL-15 also enhances the cell division of memory CD8 T cells and supports the optimal proliferation and protective response (Richer et al., 2015).

### **2.4.2 The role of IL-15 in regulating CD8 T cell differentiation**

Upon primary infection, IL-15 plays an important role in inhibiting the apoptosis and regulating the turnover of effector CD8 T cells during the contraction phase (Rubinstein et al., 2008; Yajima et al., 2006). IL-7 and IL-15 treatment during contraction phase both promote the accumulation of MPECs (KLRG1<sup>lo</sup> CD127<sup>hi</sup>), while administration of IL-15 or IL-2 enhances the accumulation of SLECs (KLRG1<sup>hi</sup> CD127<sup>lo</sup>) (Rubinstein *et al.*, 2008). Conversely, IL-15 deficient mice fail to generate CD127<sup>lo</sup> subset and preferentially accumulate CD127<sup>hi</sup> CD62L<sup>lo</sup> cells which are CD27<sup>hi</sup> but produce minimal level of granzyme B upon secondary response (Sandau et al., 2010). Since both IL-2 and IL-15 signal through IL-2/15R $\beta$ - $\gamma$ c, they share complementary or redundant functions during T cell responses. Indeed, acute viral infection of mice adoptively transferred with IL-2R $\beta$ -deficient CD8 T

cells suggests that IL-2R $\beta$ -dependent cytokines, in other words either IL-2 or IL-15 or both, promote the survival, proliferation of effector cells and drive the differentiation of KLRG1<sup>hi</sup> CD127<sup>lo</sup> SLECs upon both primary and secondary challenge. Furthermore, the IL-2R $\beta$ -dependent signals are essential for the maintenance of T<sub>EM</sub> cells but not T<sub>CM</sub> cells (Mathieu et al., 2015).

### **2.4.3 The impact of IL-15 on CD8 T cells during chronic infection**

Following chronic viral infection, IL-2/15R $\beta$  deficiency reduces the expression of some specific inhibitory receptors particularly 2B4 and Tim-3 on CD8 T cells, abrogates the formation of PD-1<sup>hi</sup> effectors, protects the CD8 T cells from exhaustion and rescues the memory CD8 T cell development (Beltra et al., 2016). Both exogenous and endogenous IL-15, but not IL-2, increase the in vivo tumor regression of adoptively transferred tumor-specific CD8 T cells (Klebanoff et al., 2004).

## **2.5 IL-21**

IL-21 is mainly produced by natural killer T (NKT) cells and some CD4 T cell subsets, such as T<sub>FH</sub> cells and T<sub>H</sub>17 cells. CD8 T cells could also synthesize IL-21 under specific conditions (Tian and Zajac, 2016). IL-21 receptor consists of IL-21R $\alpha$  and  $\gamma$ c and its expression on CD8 is activated by TCR and IL-21 itself. IL-21 signals through the JAK/ STAT, PI3K-AKT and MAPK signaling pathways and mainly induces the activation of STAT3 but it could also phosphorylate STAT1 and STAT5. Furthermore, IL-21 regulates the expression of some transcription factors such as EOMES, Bcl-6, Blimp-1 that have critical role in the differentiation of CD8 T cells (Shourian *et al.*, 2019).

### **2.5.1 The impact of IL-21 on CD8 T cells during acute infection**

IL-21 has diverse effects on the proliferation, differentiation, distribution and function of CD8 T cell subsets (Tian et al., 2016; Zeng et al., 2007). IL-21 alone is poorly effective on the proliferation of CD8 T cell, however, it promotes the expansion of CD8 T cells in concert with IL-7 or IL-15 but not with IL-2 (Zeng et al., 2005). Combination of IL-21 and IL-15 also enhances effector function of memory-phenotype CD8 T cells and accelerate

cell division of both naive and memory-phenotype CD8 T cells (Zeng *et al.*, 2005). IL-21 and IL-2 induce opposing differentiation of CD8 T cells (Hinrichs *et al.*, 2008). Indeed, IL-2 and IL-15 both induce the differentiation of effector CD8 subsets with enhanced cytolytic activity, while IL-21 preserves a less differentiated phenotype on CD8 T cells that fail to acquire effector function (Darcy, 2008; Hinrichs *et al.*, 2008). In vitro priming of CD8 T cells with IL-21 and transferring in tumor-bearing mice promotes T<sub>SCM</sub> generation and enhanced antitumor response while priming with IL-2 drives the generation of terminally differentiated cells that has minimal effect against tumors (Hermans *et al.*, 2020; Hinrichs *et al.*, 2008). IL-2 and IL-21 also drive distinct metabolic changes (Hermans *et al.*, 2020). Indeed, IL-2 induces the effector-like metabolism and glycolytic genes, promoting lactate dehydrogenase (LDH) production and lactate production, whereas IL-21 maintains metabolic quiescence. Abolishment of LDH production inhibits IL-2-induced terminal effector and exhaustion programs. IL-21 in combination with LDH inhibition promotes the generation of T<sub>SCM</sub> cells, resulting in increased antitumor responses and prolonged host survival (Hermans *et al.*, 2020). Furthermore, IL-21 programs the metabolic turnover from aerobic glycolysis towards fatty acid oxidation (FAO), increases the mitochondrial fitness and biogenesis, triggering the formation of T<sub>CM</sub>-like cells and decreases PD-1 expression (Loschinski *et al.*, 2018).

The requirement for IL-21 during acute viral infection is less strict (Yi *et al.*, 2010). After acute LCMV infection, IL-21 in cooperation with IL-10, promotes the generation and maturation of MPECs and the self-renewal of the protective memory T cell pool, through the expression of Bcl6 and EOMES in a STAT3 dependent manner. Minimal effects were observed on effector and memory CD8 T cell differentiation and function in mice lacking IL-21 only (Cui *et al.*, 2011).

### **2.5.2 The impact of IL-21 on CD8 T cells during chronic infection**

IL-21 is indispensable to prevent the CD8 T cell exhaustion and for the persistence of functional CD8 T cells in the context of chronic viral control (Johnson and Jameson, 2009). Indeed, in the absence of IL-21 signaling, CD8 T cells have decreased antiviral response and mice present defective control of chronic LCMV infection (Frohlich *et al.*, 2009). Furthermore, IL-21 suppress the IL-2 production by CD4 T cell and avoids CD8 T cell

exhaustion (Elsaesser et al., 2009). Administration of IL-21 to CD4 deficient mice following chronic infection enhances the generation of functional CD8 T cell and virus clearance (Yi et al., 2009). CD4 T cell-derived IL-21 sustains the antiviral function of CD8 T cell through the transcription factor BATF which depends on STAT3 signaling. BATF cooperates with IRF4 to promote the expression of Blimp-1 which support the CD8 T cell effector function development (Kwon et al., 2009; Xin et al., 2015). In tumor mouse model, IL-21 promotes the CD8 function and ability to infiltrate tumor resulting in reduced tumor growth and enhanced antitumor immunity, leading to mice survival (Moroz et al., 2004; Søndergaard et al., 2010).

In summary, among  $\gamma\text{c}$  cytokines, IL-7 and IL-15 play a critical role in mediating the homeostasis of naive and memory CD8 T cells and IL-2, IL-4, IL-7 and IL-15 participate in driving the activation of naive CD8 T cells. IL-7 and weak IL-2 signaling favor the differentiation of memory T cells. IL-15 and strong IL-2 signaling drive the terminal effector differentiation. Finally, IL-21 prevents T cell exhaustion during chronic infection and favors the generation of  $T_{\text{SCM}}$ .

## 3 Research projects

### 3.1 Scientific context and objectives

Common  $\gamma$ -chain cytokines, including IL-2, IL-4, IL-7, IL-15 and IL-21, play multiple roles in the activation of CD8 T cells. During my thesis, I mainly explored the role of exogenous IL-2 in the differentiation of CD8 T cells in vitro. Brief in vivo activation of CD8 T cells is sufficient to drive their differentiation into memory cells, and this is termed autopilot (van Stipdonk et al., 2001). The presence of exogenous IL-2 mimics the IL-2 provided by CD4 T cells in vivo. IL-2 plays an ambiguous role in the generation of memory cells as it is essential to generate efficient memory cells but can also favor the generation of terminal effector cells and as a consequence impair the generation of memory cells (Pipkin *et al.*, 2010; Williams *et al.*, 2006). Moreover, it was shown that the autocrine production of IL-2 by CD8 T cells plays an essential role in the generation of efficient CD8 memory cells (Feau *et al.*, 2011). Activation of T cells in vitro is classically performed in the presence of exogenous IL-2. Based on the current knowledge we wanted to determine the impact of exogenous IL-2 on the capacity of in vitro activated CD8 T cells to differentiate in memory cells.

To begin our project, our first aim was to set up an appropriate in vitro activation/ in vivo memory generation model. Therefore, I studied the impact of different in vitro activation conditions on the proliferation and phenotype of activated CD8 T cells. Then, in order to explore whether the cells activated in vitro had the capacity to differentiate into memory cells, we transferred the activated CD8 T cells activated with or without IL-2 in mice to let them pursue their differentiation in vivo. We then measured the number, phenotype, and function upon re-stimulation of the generated memory CD8 T cells. Next, we identified gene expression regulation by exogenous IL-2 at early time points by single cell RNA-sequencing. The data that we have generated will also support a more long-term goal which is to build a multiscale model of memory CD8 T cells development based on gene regulatory networks driving this process, which will be extracted from the single cell transcriptomic data.

I also compared the impact of other  $\gamma$ -chain cytokines in synergy with IL-2 or alone. The impact of IL-4, IL-7, IL-15 and IL-21 on the activation of naive CD8 T cells and the generation of memory CD8 T cells was compared.

## 3.2 Model set up

The goal was to set up an *in vitro* experiment model to study the impact of exogenous IL-2 on the activation of CD8 T cells and their capacity to further differentiate in effector and memory cells following *in vivo* transfer. First, in order to set up a suitable *in vitro* model in which we could study the activation of purified naive CD8 T cells, I tested different *in vitro* activation conditions.

### ***Impact of exogenous IL-2 on the activation of F5 CD8 T cells with different concentration of peptide***

The F5 TCR transgenic CD8 T cells recognizes the ASNENMDAM peptide (NP68) from the nucleoprotein of influenza virus A/NT/60/68 (NP366–374) in the context of H2-Db. In order to test whether CD8 T cells can be activated with NP68 peptide alone, we used four different concentrations of NP68 peptide to activate naive CD8 T cells *in vitro* in the presence or absence of exogenous IL-2. Naive CD8 T cells were purified with AutoMACS by negative selection and were then labeled with CTV before culture. The cells with the highest CTV signal correspond to undivided cells. The strength of CTV signal decreased as cells divided, every two-fold decrease represents one division. After 4 days of culture, naive CD8 T cells had divided in all conditions with the largest number of divided cells being found at the two lowest peptide concentration (Figure M1A). Addition of exogenous IL-2 did not significantly impact the number of divided CD8 T cells (Figure M1A, M1B). Therefore, we decided to use 10nM NP68 peptide to activate purified naive CD8 T cells *in vitro*.

### ***Comparison of naive CD8 T cells activation by soluble peptide or peptide-loaded mature dendritic cells***

Considering that CD8 T cells primed by matured, peptide-loaded dendritic cells (DCs) receive co-stimulations signals that are not provided when NP68 peptide alone is used to trigger CD8 T cells activation, we have compared these two activation methods. NP68 peptide loaded and CpG matured DCs were used to activate purified CD8 T cells, and T cell division was analyzed after 3 and 4 days. As expected DCs loaded with peptide are

superior to NP68 peptide alone, in terms of cell activation and proliferation, since more activated T cells were generated and T cells divided more times when activated by DCs (Figure M2A and M2B).

Similarly, when total unpurified F5 spleen cells were activated with NP68 peptide or CpG-matured, peptide-loaded DCs, DCs induced higher number of divided CD8 T cells (Figure M2C). Furthermore, in all conditions CD8 T cells divided more times when not purified (Figure M2D) indicating that splenocytes cooperated in the activation of CD8 T cells by peptide or peptide loaded dendritic cells. Therefore, to use a simplified, optimal activation system we decided to use CpG matured, peptide loaded DCs to activate purified CD8 T cells in vitro.

### ***Characterization of Flt3 generated Bone marrow derived dendritic cells***

Flt3-driven DCs are immature and they provide weak signal 2. To induce the expression of CD86/CD80 and CD40, DCs should be matured with a TLR ligand. CpG ODNs are short synthetic single-strand DNA molecules that contain unmethylated CpG dinucleotides in specific sequence contexts (CpG motifs) that bind TLR9. Purified CD8 T cells could be activated with CpG mature or immature DCs. Therefore, the DCs that are activated with and without CpG ODNs were compared. CpG maturation increased the expression of CD86 and CD40 on DCs (Figure M3A). CpG maturation of DCs had minimal impact on the DC subpopulations present in the culture. Indeed, the fraction of cDC identified by the expression of B220 and CD11c was similar for mature and immature BMDC. (Figure M3B).

### ***Impact of BMDC/ T cell ratio on CD8 T cell activation***

In order to decide the suitable concentration of DCs to be used for the activation of CD8 T cells, the impact of different concentrations of DCs on the proliferation of  $1.5 \times 10^5$  purified CD8 T cells was measured. We found that when above  $1.5 \times 10^4$  DC's, a ratio of DC/T superior to 1/10, the number of DCs didn't significantly influence the number of divided T cells (Figure M4A). Similar results were found when exogenous IL-2 was added (Figure M4B). Different concentrations of DCs had little influence on the expression of EOMES, T-bet and CD25 or the production of IFN- $\gamma$  (Figure M4C). Whether or not in the presence of exogenous IL-2, the expression of EOMES, T-bet and CD25 was not influenced

by the concentration of DCs, except for the production of IFN- $\gamma$  which was increased at the highest concentration of DCs (Figure M4D), in the presence of exogenous IL-2. Based on these results we decided to activate purified CD8 T cells with a ratio of 1DC/10T.

### ***Impact of exogenous IL-2 concentration on CD8 T cell activation***

Because of the well-known impacts of IL-2 on the cell proliferation and survival, different concentrations of IL-2 were used to activate purified naive CD8 T cells. We also compared an in-house produced supernatant containing IL-2 and commercially available recombinant IL-2. Different concentrations of IL-2 had no influence on the number of divided CD8 T cells, this was true whether using supernatant containing IL-2 or recombinant IL-2 (Figure M5A). We also monitored, on day 3, 4 and 5 following activation, the expression of a number of markers associated with CD8 T cells activation or induced by IL-2. IL-2 had little effect on the expression of EOMES and T-bet. In contrast, starting on day 4, the expression of BCL-2 and CD25 was increased in the presence of exogenous-IL-2, while TCF1 was down regulated (see Figure M5B, Figure M5C and Figure M5D) in a dose-dependent manner with a maximal modulation observed using 5% supernatant containing IL-2 or 11.5 ng/ml recombinant IL-2. Based on these results, we decided to use 5% supernatant IL-2 to activate purified naive CD8 T cells.

Final model: Based on the results above, we decided to use DC loaded with peptide to activate purified CD8 in vitro, at a ratio of 1DC/10T with a concentration of 5% IL-2 supernatant.

### ***Capacity of CD8 T cells activated in vitro to differentiate in memory cells upon adoptive transfer in vivo***

In order to explore whether the CD8 T cells activated in vitro could generate memory cells once they were adoptively transferred in vivo, we transferred the CD8 T cells that had been activated in vitro for 4 days in to naive mice. We cultured splenocytes in the presence or absence of 5% supernatant IL-2 at a ratio of 1DC/10T. Memory F5 CD8 T cells were recovered from spleen and lymph nodes on day63. Priming of CD8 T cells in the

presence of exogenous IL-2 directs the generation of more memory cells in both spleen and lymph nodes (Figure M6A).

### ***Model***

At last, we were able to set up the in vitro activation/ in vivo memory generation model (Figure M7). We use DCs to activate CD8 T cells in vitro, and IL-2 supernatant was added or not. On day 4, activated CD8 T cells were transferred into mice where they would differentiate into memory cells. Memory CD8 T cells were recovered from mice at least four weeks after transfer.

### **Material and Methods**

See in section 3.3.

## Figure legends

### **Figure M1. Impact of exogenous IL-2 on the activation of F5 CD8 T cells with different concentration of peptide.**

1.5x10<sup>5</sup> CTV-labelled purified naive F5 CD8 T cells were cultured for 4 days with NP68 peptide. Four concentration of peptide (1nM, 10nM, 100nM or 1000nM) were used. 5% supernatant IL-2 was added or not. Results for triplicates are shown for one representative experiment out of two independent experiments.

A. CD8 T cell division based on CTV dilution following 4 days of culture.

B. Number of divided CD8 T cells on day4.

### **Figure M2. Comparison of naive CD8 T cells activation by soluble peptide or peptide-loaded mature dendritic cells.**

A-B. 1.5x10<sup>5</sup> CTV-labelled purified F5 CD8 T cells were activated with NP68 (10nM) peptide or CpG matured, NP68 peptide (20nM) loaded BMDCs (5x10<sup>4</sup> cDC) for 3 or 4 days in vitro. 5% supernatant IL-2 was added or not. The purified total F5 CD8 T cells contain naive CD8 T cells which are CD44<sup>-</sup> and innate memory CD8 T cells which are CD44<sup>+</sup>. The purification of total and naive F5 CD8 T cells is described in material and methods. Results for triplicates are shown of one experiments. The number of divided CD8 T cells is shown in A. CD8 T cell division based on CTV dilution is plotted in B.

C. CTV-labelled F5 splenocytes containing 1.5x10<sup>5</sup> CD8 T cells were activated with NP68 (10nM) peptide or CpG matured, NP68 peptide (20nM) loaded BMDC (including 5x10<sup>4</sup> cDC) for 3 or 4 days in vitro. 5% supernatant IL-2 was added or not. Results for triplicates are shown of one experiments. The number of divided CD8 T cells is shown.

D. The CTV fluorescent intensity of purified F5 CD8 T cells and F5 splenocytes after 4 days of culture are shown.

### **Figure M3. Characterization of Flt3 generated Bone marrow derived dendritic cells.**

Bone marrow cells were cultured with Flt-3 for 7 days as described in the methods to generate BMDCs. Then BMDCs were cultured with NP68 peptide (20nM) and CpG 1826 (2 µg/mL) or NP68 peptide (20nM) alone overnight, respectively. Results are representative of four independent experiments.

A. Heatmap plot of BMDCs. The percentage of cDCs which are CD11c<sup>+</sup>B220<sup>-</sup> is shown.

B. Overlay of BMDCs cultured with or without CpG 1826. The expression of CD86 and CD40 are shown.

### **Figure M4. Impact of BMDC/ T cell ratio on CD8 T cell activation.**

1.5x10<sup>5</sup> CTV-labelled

purified F5 CD8 T cells were cultured with CpG matured, peptide loaded BMDCs including  $1.5 \times 10^5$ ,  $5 \times 10^4$ ,  $1.5 \times 10^4$  and  $5 \times 10^3$  cDC in the presence or absence of 5% supernatant IL-2 for 4 days in vitro. Results for triplicates are shown for one representative experiment out of four independent experiments.

A. The number of divided CD8 T cells activated with the indicating numbers of DC in the absence of IL-2.

B. The number of divided CD8 T cells activated with the indicating numbers of DC in the presence of IL-2.

C. The expression of EOMES, T-bet, CD25 and the production of IFN- $\gamma$  by CD8 T cells activated with the indicating numbers of DC in the absence of IL-2.

D. The expression of EOMES, T-bet, CD25 and the production of IFN- $\gamma$  by CD8 T cells activated with the indicating numbers of DC in the presence of IL-2.

**Figure M5. Impact of exogenous IL-2 concentration on CD8 T cell activation.**  $1.5 \times 10^5$  CTV-labelled purified naive F5 CD8 T cells were cultured with CpG matured, peptide loaded BMDC including  $1.5 \times 10^4$  cDC in the presence of supernatant or recombinant IL-2 for 3, 4 and 5 days in vitro. Supernatant IL-2 (230ng/mL) was diluted at 4 concentrations (0.5%, 1.5%, 5%, 15%), respectively. Recombinant IL-2 was adjusted to the same concentrations: 1.15ng/mL, 3.45ng/mL, 11.5ng/mL, 34.5ng/mL, respectively. Results for triplicates are shown of one independent experiments.

A. The number of divided CD8 T cells activated with four concentrations of IL-2.

B. The expression of CD25, TCF1, Bcl2, EOMES and T-bet on day3.

C. The expression of CD25, TCF1, Bcl2, EOMES and T-bet on day4.

D. The expression of CD25, TCF1, Bcl2, EOMES and T-bet on day5.

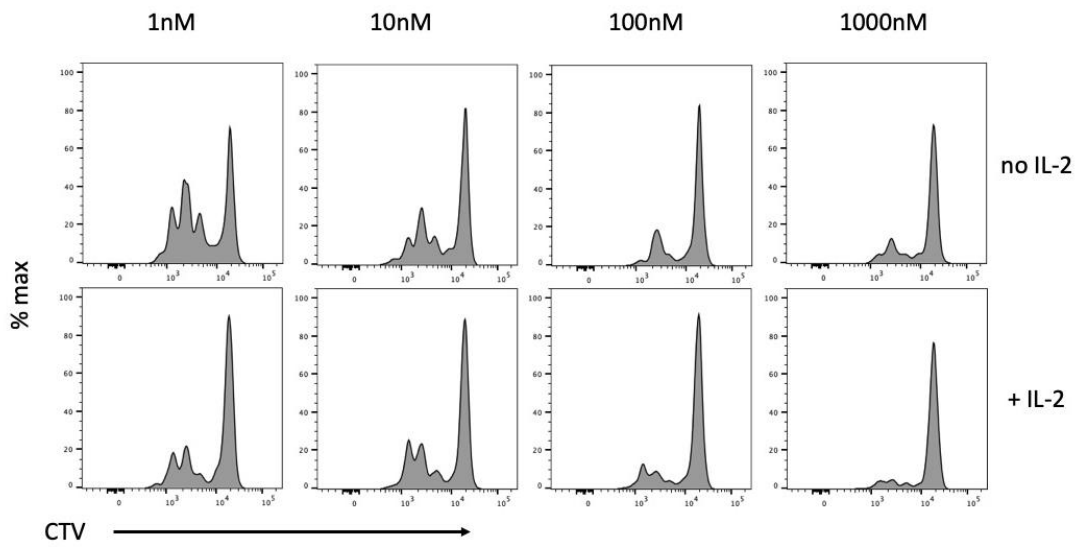
**Figure M6. The capacity of CD8 T cells activated in vitro to differentiate in memory cells upon adoptive transfer in vivo.** CTV-labelled F5 splenocytes, including  $1.8 \times 10^7$  F5 CD8 T cells, were cultured with CpG matured, peptide loaded BMDCs including  $1.8 \times 10^6$  cDC in the presence or absence of 5% supernatant IL-2 for 4 days in vitro. Then, total lymphocytes were isolated and adoptively transferred into C57BL/6J naive mice as described in material and methods. Each mouse received 2.5 million CD8 T cells and every group included 3 mice. Results are representative of one experiments.

A. The number of F5 CD8 T cells in spleen and lymph nodes on day63.

**Figure M7. Experiment model.**

Figure M1.

A



B

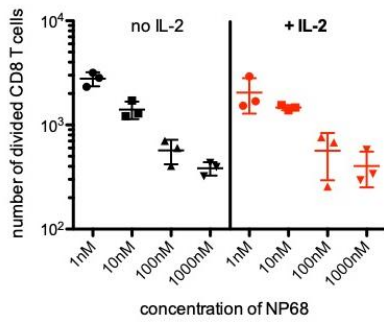


Figure M2.

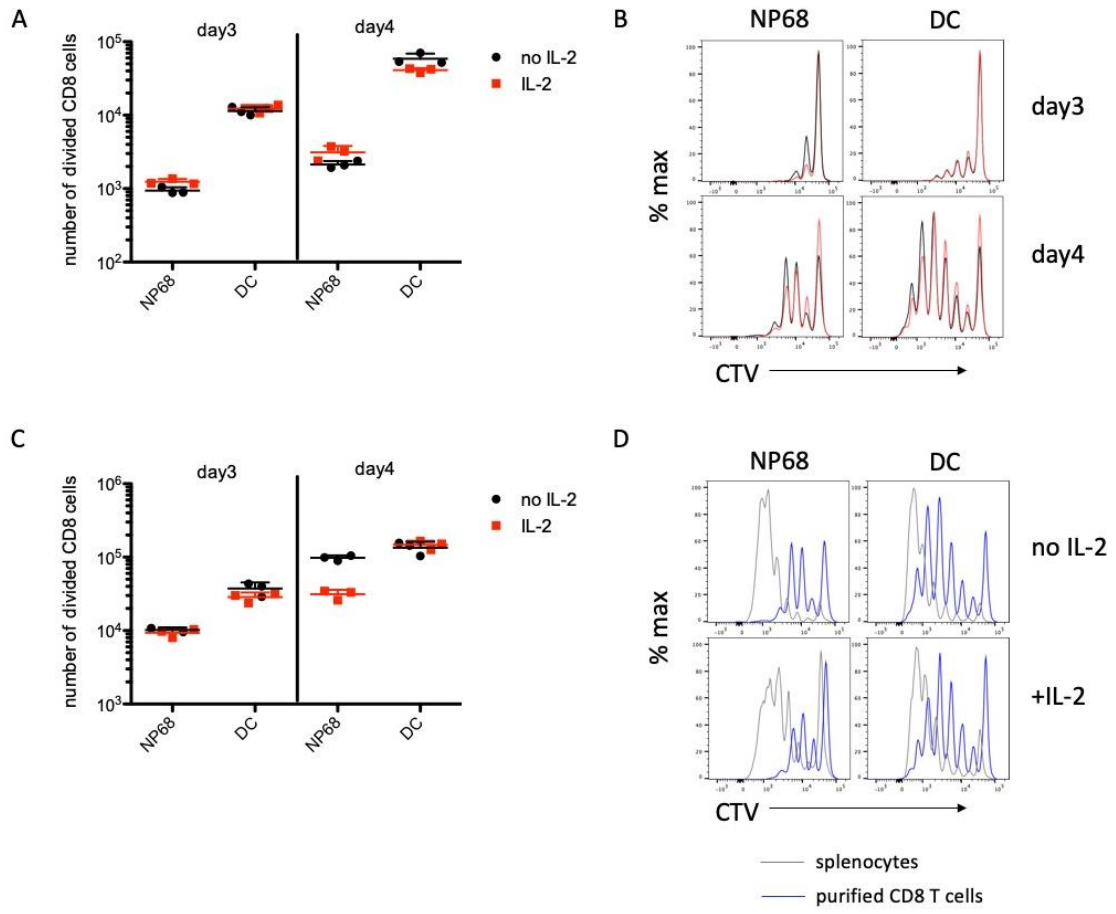
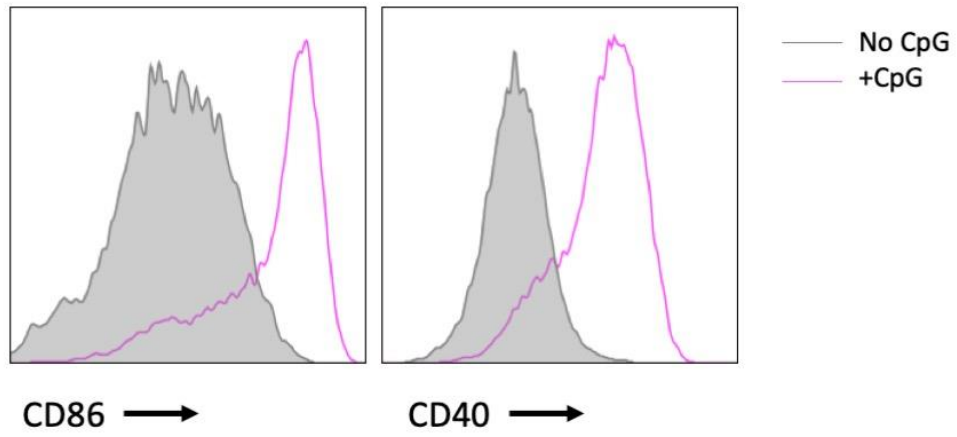


Figure M3.

A



B

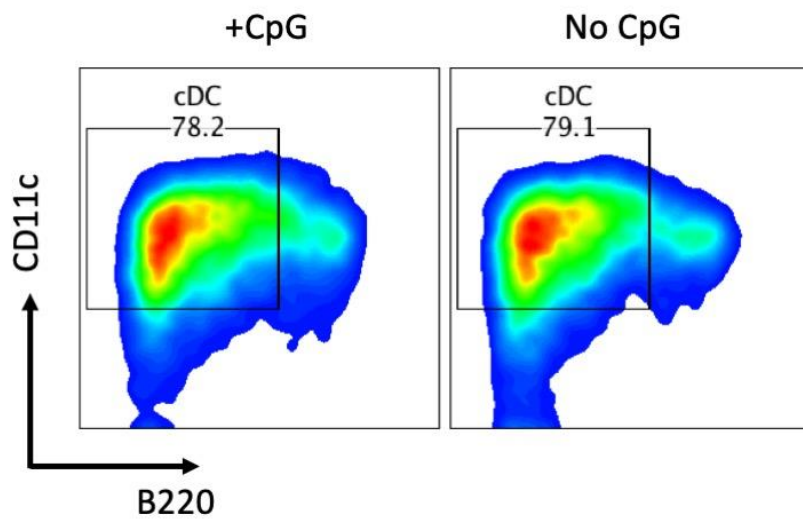


Figure M4.

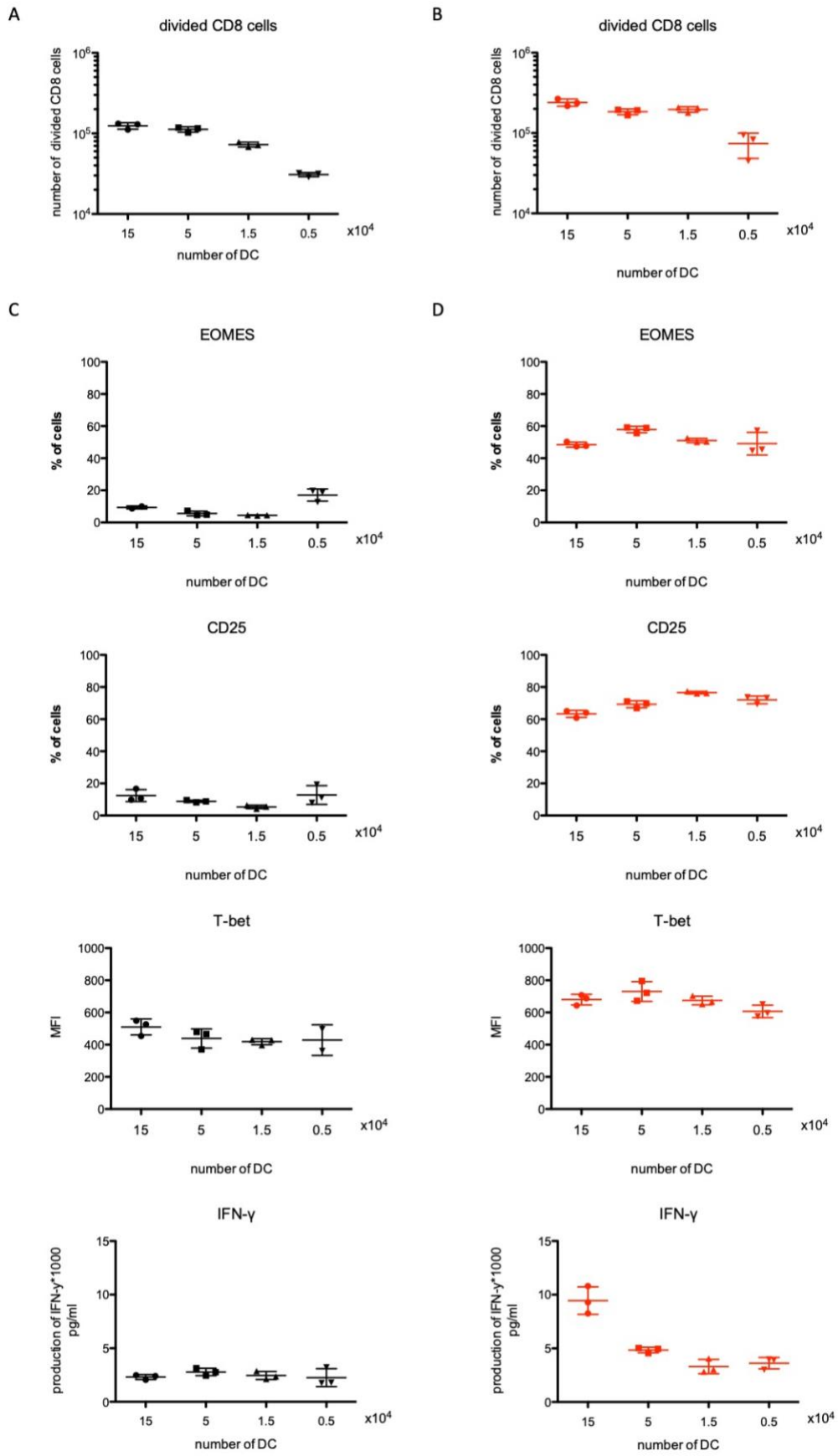


Figure M5.

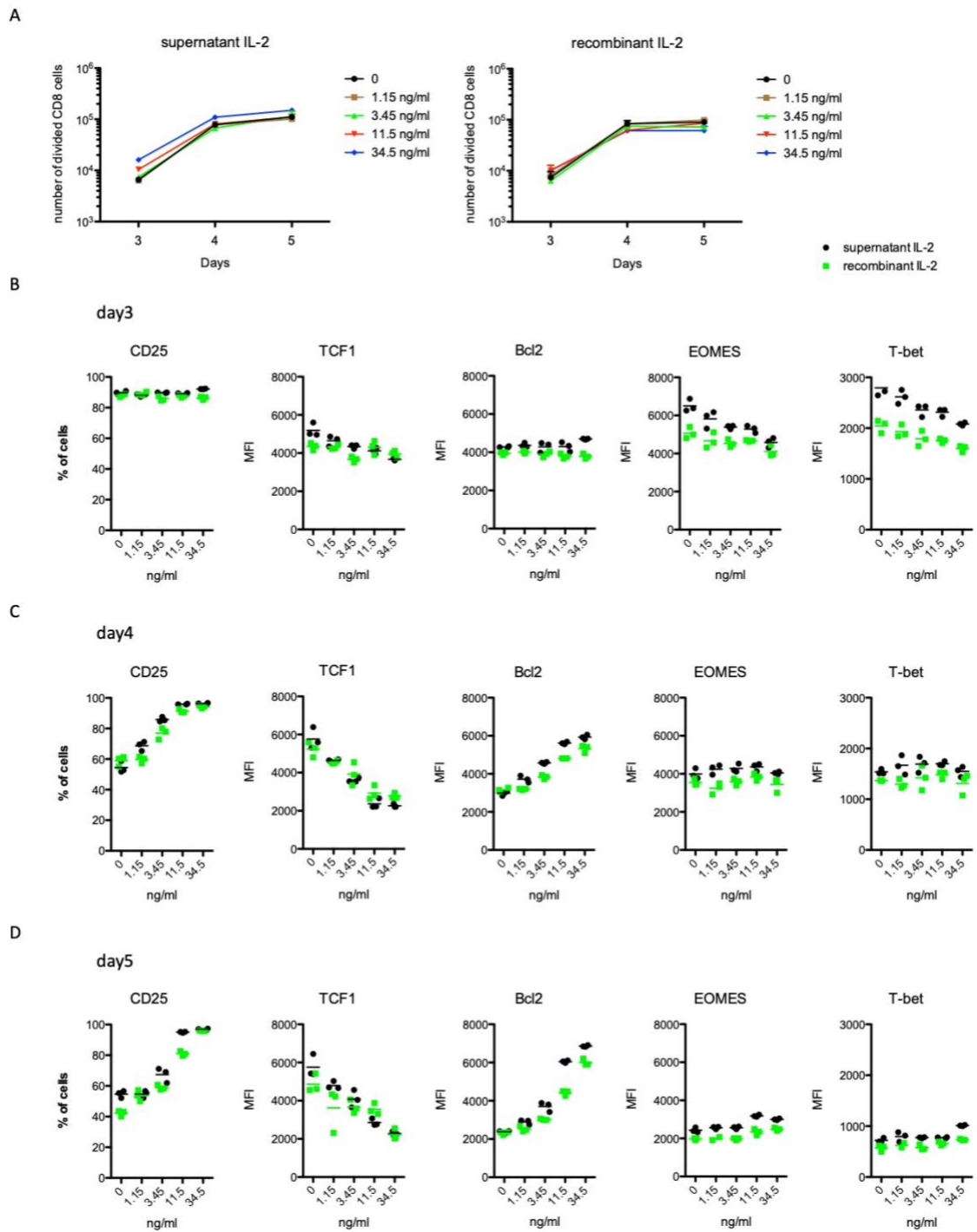


Figure M6.

A

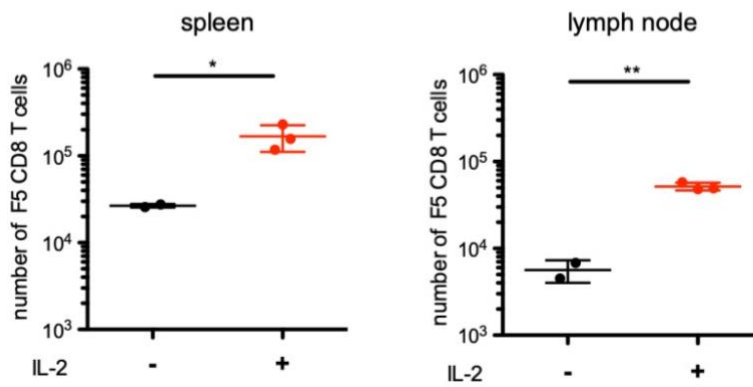
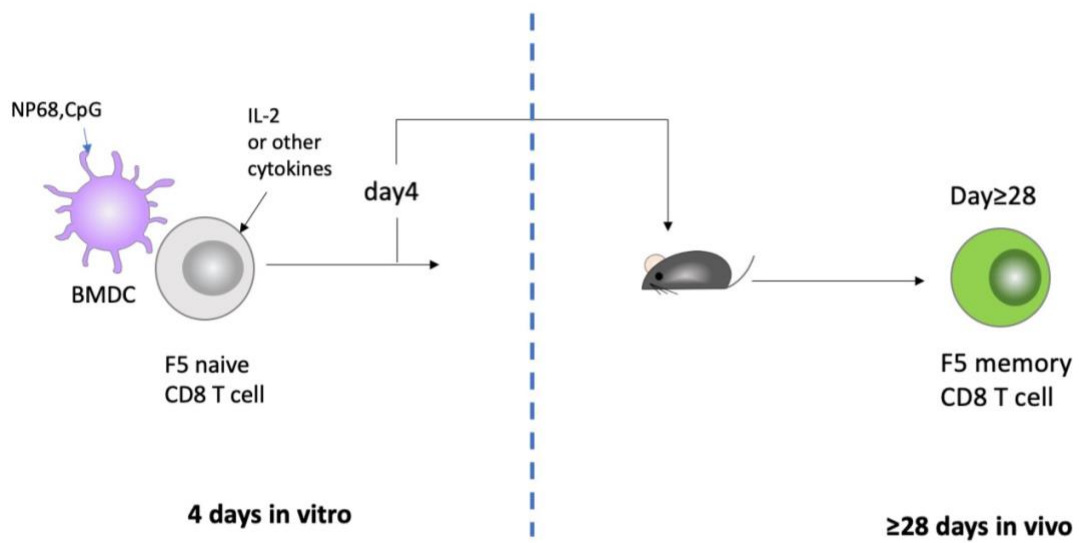


Figure M7.



### **3.3 Article**

**Exogenous IL-2 delays the generation of memory precursor cells and is essential for the generation of memory cells with increased effector functions**

Shaoying Wang, Margaux Prioux, Simon de Bernard, Daphne Laubreton, Sophia Djebali, Maxence Dubois, Christophe Arpin, Camille Fourneaux, Fabien Crauste, Wenzheng Jiang and Jacqueline Marvel

**In preparation (2022)**

## **Exogenous IL-2 delays the generation of memory precursor cells and is essential for the generation of memory cells with increased effector functions**

Shaoying Wang<sup>1, 2</sup>, Margaux Prioux<sup>1, 5</sup>, Simon de Bernard<sup>3</sup>, Daphne Laubreton<sup>1</sup>, Sophia Djebali<sup>1</sup>, Maxence Dubois<sup>1</sup>, Christophe Arpin<sup>1</sup>, Camille Fourneaux<sup>5</sup>, Fabien Crauste<sup>6</sup>, Wenzheng Jiang<sup>2</sup>, Jacqueline Marvel<sup>1</sup>

<sup>1</sup> Centre International de Recherche en Infectiologie, INSERM, U1111, Université Claude Bernard Lyon 1, CNRS, UMR5308, École Normale Supérieure de Lyon, Université de Lyon, Lyon, France

<sup>2</sup> Shanghai Key Laboratory of Regulatory Biology, Institute of Biomedical Sciences and School of Life Sciences, East China Normal University, Shanghai, China

<sup>3</sup> AltraBio, Lyon, France

<sup>4</sup> Inria, Villeurbanne, France

<sup>5</sup> Laboratoire de Biologie et de Modélisation de la cellule, Université de Lyon, ENS de Lyon, CNRS UMR 5239, INSERM U1210, Lyon, France

<sup>6</sup> Laboratoire MAP5 (UMR CNRS 8145), Université Paris Cité, Paris, France

<sup>5</sup> Laboratoire de Biologie et de Modélisation de la cellule, Université de Lyon, ENS de Lyon, CNRS UMR 5239, INSERM U1210, Lyon, France

<sup>6</sup> Laboratoire MAP5 (UMR CNRS 8145), Université de Paris, Paris, France

## Abstract

The encounter of naive CD8 T cells with antigen presenting cells triggers their activation, proliferation and differentiation up to the memory state. To evaluate the impact of exogenous IL-2 (ex-IL-2) on memory precursors differentiation, we have set-up an *in vitro* model of CD8 T cell activation. Our findings indicate that the initial cellular concentration of responding CD8 T cells determines their dependency on IL-2, indeed ex-IL-2 only impacts the number of activated CD8 T cells generated when they are seeded at a low concentration. However, in all culture conditions ex-IL-2 enhances the expression of CD25, EOMES and Bcl2 while downregulating the expression of TCF1. To assess the capacity of the *in vitro* activated CD8 T cells to participated in an ongoing effector response or to directly differentiate in memory cells we have transferred *in vitro* activated CD8 T cells in either virus infected or naive mice. When transferred in virus infected mice, whether IL-2 supplemented or not, activated CD8 cells showed a similar ability to participate in an ongoing immune response and they gave rise to memory cells with a similar phenotype. In contrast, when transferred in a naive host, CD8 T cells activated in the presence of ex-IL-2 generated a higher frequency of memory cells that displayed increased functional memory traits such as integrins expression or cytokines production. Finally, a single-cell transcriptomic analysis of *in vitro* activated CD8 T cells indicates that, in the absence of ex-IL-2, activated CD8 T cells rapidly acquire a memory precursor signature, while in its presence they mainly adopt an effector CD8 T cell signature. Overall, our study shows that ex-IL-2 delays the early transition of activated CD8 T cells into MP cells, allowing them to acquire effector functions that are imprinted in the memory cells they generate.

**Key words:** CD8 T cell, exogenous IL-2, memory precursors

## Introduction

After antigen encounter during an acute infection, naive CD8 T cells are activated and differentiate into antigen-specific effector T cells that proliferate and eradicate the pathogen. The majority of effector cells then die by apoptosis, however, a small fraction survives and give rise to long-lived memory cells able to mount a recall response (Williams and Bevan, 2007). Optimal activation of naive CD8 T cells requires 3 signals which are T cell antigen receptor (TCR) activation, co-stimulation signal and inflammatory cytokines (Williams and Bevan, 2007). Besides these signals, IL-2 has a central role in cellular proliferation, differentiation and survival of CD8 T cells (Kalia and Sarkar, 2018). IL-2 is a member of the common cytokine-receptor  $\gamma$ -chain ( $\gamma$ c) family and its receptor is formed by CD25 (IL-2R $\alpha$ ), CD122 (IL-2R $\beta$ ) and CD132 (IL-2R $\gamma$ ) (Boyman and Sprent, 2012; Shourian et al., 2019). IL-2 signals through STAT5 and phosphoinositide-3-kinase (PI3K)-AKT pathway (Boyman and Sprent, 2012; Crompton et al., 2014; Kalia and Sarkar, 2018). Dendritic cells (DCs) and CD4 T cells are essential for the proliferation and the generation of efficient memory CD8 T cells (Borst et al., 2018; Kalia and Sarkar, 2018).

The role of IL-2 in the activation of CD8 T cells and their differentiation in memory cells has been extensively studied (Feau et al., 2011; Kahan et al., 2022; Kalia et al., 2010; Krämer et al., 1994; Pipkin et al., 2010; Redeker et al., 2015; Williams et al., 2006). IL-2 is essential for the generation of functional memory CD8 T cells. Indeed, when CD25-KO CD8 T cells are activated *in vivo*, their primary response is similar to CD25-WT CD8 T cells as is the number of memory cells generated. However, the CD25-KO memory cells are non-functional and unable to mount an effective recall response (Pipkin *et al.*, 2010; Williams *et al.*, 2006). IL-2 is produced by both CD4 and CD8 T cells, the role of CD8-derived IL-2 has been shown to be critical for CD8 differentiation, as IL-2 deficiency in CD8 T cells but not CD4 T cells impeded the generation of functional memory CD8 T cells (Feau *et al.*, 2011). Similarly, enforced expression of IL-2 by CD8 T cells increased their expansion capacity to primary and secondary viral challenge (Redeker *et al.*, 2015).

The essential role of CD8-derived IL-2, in the generation of memory CD8 T cells, has recently been confirmed by tracing the fate of IL-2-producing CD8 T cells *in vivo*. Indeed,

over the course of an infection, not all CD8 T cells produce IL-2 and it was found that IL-2 producing-CD8 T cells are more prone to differentiate in memory cells (Kahan *et al.*, 2022).

However, the role of IL-2 is ambivalent as too much IL-2 signaling seems to counteract the capacity of CD8 T cells to differentiate in memory cells (Kalia and Sarkar, 2018). Indeed, Kalia *et al.*, using the CD25 expression level as an indicator of the IL-2 signaling strength received by CD8 T cells responding to a viral infection, have shown that CD25-high CD8 T cells tend to differentiate in terminal effector cells, while CD25-low cells give rise to memory cells (Kalia *et al.*, 2010), indicating that a strong IL-2 stimulation drives CD8 T cells towards terminal effector differentiation. These results are in line with experiments showing that high IL-2 concentrations promote the expression of the effector molecules perforin and granzyme B (Pipkin *et al.*, 2010).

The timing of exogenous IL-2 signaling could also impact CD8 T cell differentiation. Indeed, after DC immunization, *in vivo*, administration of IL-2-complexed with an anti-IL-2 antibody early (days 1-3) or late (days 4-6) after priming enhances memory cell formation or promotes CD8 T cell terminal effector cell differentiation respectively (Kim *et al.*, 2016).

The number of responding cells is another parameter that can influence CD8 T cell differentiation. Particularly, CD8 T cells tend to differentiate into central memory cells (TCM) in adoptive transfer experiment when a high number of naive CD8 T cells is transferred (Badovinac *et al.*, 2007; Marzo *et al.*, 2005; Obar *et al.*, 2008). Similarly, the generation of CD44<sup>+</sup>CD62L<sup>+</sup> precursors of central memory cells (pTCM) is promoted when naive CD4 T cells are cultured at a high density (Polonsky *et al.*, 2018).

T cell-transfer-therapy such as CAR-T cells (chimeric antigen receptor–T cell) have been a remarkable achievement in anticancer immunotherapy. The generation of these cells from patient T cells requires their activation and expansion *ex-vivo*, this is usually done by activating cells in culture with anti-CD3, supplemented with IL-2 to support T cell expansion. The robust proliferation and survival of therapeutic T cells *in vivo* are regarded as critical indicators of clinical response in patients with B-cell malignancies and solid tumors (Collinson-Pautz *et al.*, 2019; Sengupta *et al.*, 2018; Yeku *et al.*, 2017). However, a significant fraction of patients relapses after immunotherapy or is refractory to the

treatment. The quality of T cells that are transferred is one of the limiting factors that has been identified (Hinrichs et al., 2009). Experiments in preclinical models have shown that the degree of differentiation of CD8 T cells used to prepare the therapeutic T cells inversely correlated with the magnitude of tumor rejection (Gattinoni et al., 2005; Gattinoni et al., 2011; Hinrichs *et al.*, 2009). The cytokines used to support *in vitro* T cell proliferation also influence the quality of T cells that are generated (Shourian *et al.*, 2019). Hence, one of the potential improvements in the generation of therapeutic T cells is the definition of culture condition that will generate T that are efficient in killing tumor cells and that will persist as memory cells once transferred *in vivo*.

In these contexts, we have reexamined the impact of exogenous IL-2 (ex-IL-2) on the activation and the generation of memory precursor CD8 T cells *in vitro*. We show that the cellular concentration of responding CD8 T cells determines the dependency on ex-IL-2 for their optimal expansion. We assessed the capacity of these *in vitro* activated CD8 T cells to differentiate into memory cells either directly after adoptive transfer in naive recipients or following *in vivo* re-stimulation in virus infected mice. We found that ex-IL-2 promotes direct differentiation into memory of a larger fraction of activated CD8 T cells when transferred in naive mice. Whereas, it does not change the differentiation into effector and memory cells in the viral environment. We characterized transcriptional changes occurring over the course of *in vitro* activation and performed single-cell RNA-seq. We found that cells activated after 4 days without ex-IL-2 split into 2 groups of cells: one that differentiated into quiescent memory precursor cells while the second was composed of cycling cells beginning to express the memory precursor genes. However, cells activated with ex-IL-2 acquired effector functions while maintaining a capacity to generate memory cells with improved effector functions thus suggesting that ex-IL-2 only delays the transition into memory precursors.

## **Result**

### ***Impact of exogenous IL-2 on the *in vitro* activation of CD8 T cells***

To characterize the impact of exogenous IL-2 (ex-IL-2) on CD8 T cells priming, naive F5 CD8 T cells labelled with CTV were activated with NP68-loaded DCs in the presence or absence of ex-IL-2. We measured cell division and characterized the phenotype of CD8 T cells at different time points following activation. The strategy to gate divided CD8 T cells is described in Figure S1A. Ex-IL-2 had no impact on the number of divided cells recovered 4, 5 and 6 days after activation (Figure 1A). In agreement with these results, the number of performed divisions and the level of the Ki67 proliferation marker expression by divided CD8 T cells were similar in the presence or absence of ex-IL-2 (Figure 1B and 1C). Furthermore, ex-IL-2 had no impact on CD8 T cell glucose uptake (Figure S1B). Increasing the dosage of IL-2 from 11.5 ng/ml to 34.5 ng/ml using two different sources of IL-2 did not influence the number of divided CD8 T cells nor CD25 expression (Figure S1C). These results were not due to the usage of TCR transgenic CD8 T cells as similar results were obtained with non-transgenic CD8 T cells following their activation with anti-CD3 and anti-CD28 beads (Figure S1D). CD8 T cells produce IL-2 following antigenic stimulation (Figure S1E), suggesting that, in our conditions, intrinsic IL-2 (int-IL-2) might be sufficient to sustain the initial CD8 T cells proliferation. ex-IL-2 did however impact activated CD8 T cells as it was able to maintain an increased expression of CD25, EOMES and Bcl2 and to induce the decreased expression of TCF1 starting from day 3 onwards (Figure 1D and E). Moreover, ex-IL-2 maintained the phosphorylation of AKT and STAT5 in activated CD8 T cells on day 4 following activation (Figure 1F). These findings suggested that although ex-IL-2 impacts the expression of transcription factors, and bcl2 and maintains the phosphorylation of AKT and STAT5, it does not affect the initial proliferation nor the number of activated CD8 T cells recovered after 4 days of activation.

### ***Impact of responding CD8 T cells concentration on the dependency of ex-IL-2***

A number of studies showed that the local responding-T cell density can modulate T cell differentiation (Badovinac *et al.*, 2007; Marzo *et al.*, 2005; Obar *et al.*, 2008; Polonsky *et al.*, 2018). Therefore, we investigated the impact of ex-IL-2 on the proliferation and differentiation of CD8 T cells activated at different cellular densities. The CD8 T cell concentration at the start of the culture was decreased by 3-fold and 10-fold while maintaining a DC/T ratio of 1/10. To compare the different culture conditions, we

calculated the proliferation index per 100 cells. Decreasing the CD8 T cell density reduced the cell proliferation index in presence, as well as in the absence of ex-IL-2, indicating a degree of cellular cooperation independent of IL-2. However, ex-IL-2 was able to increase the number of divided CD8 T cells recovered 4 days after activation, in a cell density-dependent manner (Figure 2A), low density-cultured cells being especially sensitive to ex-IL-2. To test if the decrease in the proliferation index was due to a decrease survival of cells when grown at low density, we performed the same experiment adding an excess ( $3 \times 10^5$ ) of C57BL/6J splenocytes to the culture. When grown at low density, a similar decrease in the CD8 T cell proliferation index was observed and ex-IL-2 was able to enhanced their proliferation (Figure S2A). This suggests that the ex-IL-2 dependency at low cell density was determined by the number of responding cells rather than the number of total cells in the environment. At lower cell densities, ex-IL-2 increased the number of cells in each division but dividing cells performed on average the same number of divisions (Figure 2B). However, the presence of non-transgenic splenocytes increased the number of divisions at all cell densities regardless of the addition of ex-IL-2 (Figure S2B). Interestingly, this was not due to an increase in the production of intrinsic IL-2 since the IL-2 concentration was lower in the presence of feeders (Figure S2C). The reduction of cell density or the addition of non-transgenic splenocytes did not influence the effect of ex-IL-2 on the expression of Bcl2, CD25 and TCF1 (Figure 2C and S2D). In agreement with what has been observed for CD4 T cells (Polonsky *et al.*, 2018), the expression of CD62L decreased as cell density decreased (Figure 2D). In conclusion, the activation of CD8 T cells is highly dependent on cellular cooperation and the cellular density in the culture influences the dependency on ex-IL-2.

### ***Ability of in vitro activated CD8 T cells to differentiate into effector and memory cells in vivo***

To evaluate the capacity of *in vitro* activated CD8 T cells to participate in the antiviral immune response and therefore, to differentiate into effector and memory cells, we sorted F5 CD8 T cells after 4 days of activation in the presence or absence of ex-IL-2 and transfer them into C57BL/6J mice challenged with vaccinia virus (VV) 4 days earlier (Figure 3A). On day 8 post-activation similar number of effector cells were recovered in the blood

whether cells had been activated with or without ex-IL-2. (Figure 3B). Similarly, after 32 days, F5 CD8 T cells activated with or without ex-IL-2 gave rise to similar numbers of memory CD8 T cells (Figure 3C). This was even true when cells were cultured at low density, a condition where they depend more on ex-IL-2 (Figure 2). Next, we analyzed the phenotype of the memory cells generated. To be able to do this, we in vitro-activated and transferred higher numbers of F5 cells. The presence of ex-IL-2 during priming did not influence the expression of CD62L, NKG2D or integrins essential for tissue migration such as CD29, CD49a and CD49d (Figure 3D). Moreover, memory cells predominantly adopted a CD27<sup>+</sup> CD43<sup>-</sup> phenotype, which was found to be associated with better recall responses (Hikono et al., 2007), following both priming conditions (Figure 3E). Finally, F5 memory cells restimulated with NP68 peptide produce similar level of IFN- $\gamma$  and CCL5 whether ex-IL-2 was added in the in vitro cultures or not.

In summary, these results indicate that cells activated with and without ex-IL-2 have a similar potential to participate in primary immune response and differentiate into memory cells.

#### ***Ability of in vitro activated CD8 T cell to differentiate directly into memory cells in vivo***

To further explore the impact of ex-IL-2 during the primary response on memory cells generation without further antigenic stimulation, we next adoptively transferred F5 CD8 T cells activated with and without ex-IL-2 for 4 days into naive C57BL/6J mice (Figure 4A). The number and phenotype of the cells from the spleen were analyzed 32 days post-activation in the spleen. We found that the addition of ex-IL-2 during priming increased the number of F5 CD8 T cells whether initially activated at low or high density (Figure 3B). Cells activated with ex-IL-2 further differentiated into CD27<sup>+</sup> CD43<sup>+</sup> memory cells while they predominantly adopt a CD27<sup>+</sup>CD43<sup>-</sup> phenotype in the absence of ex-IL-2 during priming (Figure 3C). Furthermore, the presence of ex-IL-2 during priming resulted in higher expression of CD29, CD49a, CD49d and NKG2D (Figure 3D) but did not impact of CD62L expression. Finally, cells activated with ex-IL-2 produced more IFN- $\gamma$  and expressed higher level of CCL5 following NP68 restimulation (Figure 3E).

Overall, these results indicate that the presence of ex-IL-2 during priming *in vitro* promotes, after transfer in naive hosts, the generation of more memory CD8 T cells that displays increased memory traits.

### ***Single-cell RNA-sequencing of in vitro activated CD8 T cell with or without ex-IL-2***

To investigate the transcriptional differences and changes that occur over the course of *in vitro* activation, we performed single-cell RNA-sequencing (scRNA-seq) on F5 CD8 T cells activated with or without ex-IL-2. Cells were first sorted 1, 2 or 3 days post-activation and naive cells were sorted as control. We performed a UMAP to visualize cells in a two-dimensional space (Figure S3A) and observed that cells were essentially grouped by experimental time points. No differences between IL-2 conditions were visible which is in agreement with the phenotypic similarity observed at the protein level using a restricted number of markers after 3 days of activation (see Figure 1E). We then performed scRNA-seq on cells sorted 4 days post-activation. UMAP and clustering partitioned cells into 4 clusters with clusters 0 and 2 enriched in cells activated with ex-IL-2 and clusters 1 and 3 enriched in cells activated without ex-IL-2 (Figure 5A). Clusters 1 and 3 highly expressed genes associated with cell division (*Tuba1b*, *Top2a*, *Mki67*, *Cdk1*, *Pclaf*) and effector functions (*Gzmb*, *Id2*), with the stronger expression measured in cluster 3 (Figure 5B-C). Conversely, cluster 0 completely downregulated these genes and rather highly expressed genes associated with a memory phenotype and quiescence (*Tcf7*, *Id3*, *Slamf6*, *Btg1*). Interestingly, cells in cluster 2 exhibited an intermediate transcriptomic profile with a strong expression of histones and cell cycle genes and weaker expression of memory-related genes. We then classified the cells according to their cell cycle phase (Figure 5D). Interestingly, cells in cluster 0 were classified into the G1 phase while cluster 1, 2 and 3 were composed of a mix of cells that were in S and G2/M phases. We next performed a gene set enrichment analysis (GSEA) using the memory precursors (MP) gene signature from Yao, et al. (Yao et al., 2019) (Figure 5E) and found that approximately 30% of cluster 0 cells were enriched in this signature whereas less than 10% were defined as MP cells in the other clusters. We observed an enrichment of MP signature as soon as D3 of culture

without IL-2 (Figure S3B), although cells were not clearly transcriptionally distinguishable from cells with ex-IL-2 (Figure S3A).

Finally, we used TinGa (Todorov et al., 2020) to infer predicted developmental relationships between IL-2 conditions (Figure 5F). This analysis revealed a complex trajectory with on one side CD8 T cells activated in absence of ex-IL-2 that split into two branches: one of which terminating predominantly cycling cells belonging to cluster 2 the other in quiescent memory precursor cells (cluster 0). On the other side, cells grown in the presence of ex-IL-2 were found with an increasing expression of effector genes going from cluster 1 at the center of the trajectory to cells in cluster 3.

In summary, after 4 days of culture in absence of ex-IL-2, CD8 T cells start acquiring quiescent memory precursor traits while in the presence of ex-IL-2 they start expressing genes coding for effector functions.

## Discussion

IL-2 is regarded as a growth factor driving the proliferation and expansion of T cells (Cheng et al., 2002; Cousens et al., 1995; Smith, 1988). In this paper, we showed that exogenous IL-2 is dispensable for CD8 T proliferation, *in vitro*, when cells are cultured at a high density. Still an increased expression of IL-2 target genes such as CD25 and Bcl-2 and a sustained phosphorylation of STAT5 and AKT was observed when CD8 T cells were cultured in the presence of ex-IL-2, indicating a good degree of IL-2 responsiveness of the cells. Addition of ex-IL-2 was associated with a better CD8 expansion only when cells were cultured at low density. Interestingly, we observed a better differentiation toward a central memory phenotype when CD8 cells are cultured at higher density, similarly to what has been described for CD4 T cells (Polonsky *et al.*, 2018).

Several studies have suggested that the initial encounter and stimulation by antigen is sufficient to drive the proliferation and the differentiation program leading to the generation of effector and memory CD8 T cells (Kaech and Ahmed, 2001; Kalia et al., 2006; Mercado et al., 2000; van Stipdonk et al., 2001; Williams and Bevan, 2007) Naive CD8 T cells that have been activated for a brief period could continue expand and differentiate

in the absence of further stimulation in an autopilot process (van Stipdonk *et al.*, 2001). Here, we show that CD8 T cells activated in the absence of ex-IL-2 indeed proliferate *in vitro* to the same extent as cells activated with ex-IL-2, and this even when activated at low density. This is in agreement with previously published data showing that, *in vivo*, IL-2 knockout and IL-2R $\alpha$  knockout CD8 T cells performed the same number of divisions compared to wild-type CD8 T cells in a context of viral or tumoral immunization (D'Souza and Lefrancois, 2003). Moreover, F5 CD8 T cells activated in the absence or presence of ex-IL-2 were functional and able to participate to an ongoing immune response against vaccinia virus expressing NP68. Furthermore, they gave rise to memory CD8 T cells with identical phenotypes and function.

In contrast, when we allow the *in vitro* activated CD8 T cells to differentiate directly in memory cells by transferring them in naive host, we found that only the memory cells derived from cells activated in the presence of ex-IL-2 expressed antigen-induced associated marker NKG2D and high levels of integrins important for cell homing to lung tissue, such as CD29, CD49a and CD49d (Grau *et al.*, 2018). Memory cells generated from cells activated in the absence of ex-IL-2 did not develop these traits. According to CD27 and CD43 markers, Hikono *et al.*, have described three populations of CD8 T cells and showed that these markers are superior to CD62L to predict the cell capacity to mount a recall response (Hikono *et al.*, 2007). Among these 3 subsets, CD27+/CD43- are supposed to display the strongest recall capacity (Hikono *et al.*, 2007). While the presence of ex-IL-2 during priming activation had no influence on the differentiation of TCM, we showed that ex-IL-2 reduced the formation of CD27+/CD43- subsets but increased the differentiation of CD27+/CD43+ subsets. We also showed that ex-IL-2 increased the ability of CD8 memory cells to produce IFN- $\gamma$  and CCL5. Notably, we recovered more cells following adoptive transfer into naive host when CD8 T cells were activated in the presence of ex-IL-2. This could be due to the increased Bcl-2 expression that is observed in the presence of ex-IL-2. Overall, these results indicate that the presence of ex-IL-2 during the *in vitro* activation did not negatively impact the capacity of CD8 T cells to differentiate in memory cells *in vivo*. This is in contrast to previously published work showing that IL-2 could inhibit this capacity, however the concentration of IL-2 used was at least 50-fold higher than the one used here (Pipkin *et al.*, 2010).

To further characterize the impact of ex-IL-2 on CD8 T cells we performed single-cell transcriptomic analyses on CD8 T cells activated in the presence or absence of ex-IL-2. Our results indicate that in the absence of ex-IL-2, a large fraction of CD8 T cells have acquired a quiescent memory precursor gene expression signature without having acquired the expression of effector genes such as *Gzmb* by day 4. This is in line with the phenotype of memory cells generated when these cells are transferred in naive mice. In contrast, when ex-IL-2 is added to *in vitro* cultures CD8 T cells acquire an effector function transcriptional signature. Moreover, they display a superior capacity to directly differentiate in memory cells with increased memory traits.

Overall, *in vitro*, ex-IL-2 is redundant for the initial CD8 T cell expansion, but mainly supports the acquisition of effector functions without abrogating the memory differentiation potential of activated CD8 T cells.

## Materials and Methods

### *Mice*

C57BL/6J(CD45.2) mice were purchased from Charles River Laboratories (L'Arbresle, France). C57BL/10-Tg (Cd2-TcraF5, CD2-TcrbF5)1Kio/AnuApb mice were provided by Prof. D. Kioussis (National Institute of Medical Research, London, U.K.) and backcrossed on CD45.1 C57BL/6 background (Jubin et al., 2012) to obtain F5 TCR [B6/J-Tg (CD2-TcraF5, CD2-TcrbF5)1Kio/Jmar] transgenic mice. The F5 TCR recognizes the NP68 peptide from influenza A virus (ASNENMDAM) in the context of H2-Db. Mice were bred and housed under SPF conditions in our animal facility (AniRA-PBES, Lyon, France). All experiments were approved by our local ethics committee (CECCAPP, Lyon, France) and accreditations have been obtained from governmental agencies.

### *Virus and reagents*

The recombinant vaccinia virus expressing the NP68 epitope (VV-NP68), was engineered from the Western Reserve strain by Dr. D.Y.-L. Teoh, in Prof. Sir Andrew McMichael's laboratory at the Medical Research Council (Human Immunology Unit, Institute of Molecular Medicine, Oxford, U.K.).

Murine rIL-2 produced using the myeloma clone X63-Ag8.653 cell lines transfected with the mouse IL-2 gene kind gift from Dr F. Melchers, Basel Institute of Immunology, Basel, Switzerland).

Complete RPMI and DMEM mediums consist of DMEM or RPMI medium (Life Technologies) supplemented with 10% FCS, 10 mM HEPES, 50 mg/ml gentamicin, 2 mM L-glutamine (Life Technologies).

### *Bone marrow-derived dendritic cells (BMDCs) cultures*

Mice were sacrificed by cervical dislocation and bone marrow progenitors were washed out from bones (femurs and tibias).  $2 \times 10^6$  cells /ml were incubated in complete RPMI medium with 100 ng/ml Flt-3L (Thermo Fisher) in 6 well-plates. After 7 days, NP68 peptide (20 nM) with or without CpG 1826 (2 ug/ml, Invivogen) was added and cells were cultured overnight. The fraction of cDC (CD11c+, B220+) was measured by flow cytometry and was always > 65%.

### *In vitro stimulation*

CD44<sup>-</sup> naive F5 CD8 T cells were magnetically isolated from splenocytes of F5 TCR transgenic mice by negative selection using a specific CD8a<sup>+</sup> T cell isolation kit (Miltenyi Biotec, # 130-104-075) and autoMACS<sup>®</sup> Pro Separator, according to the manufacturer instructions. Anti-CD44-Biotine antibody (IM7.8.1, 1 $\mu$ l/1,5x10<sup>8</sup> cells) was added to the cocktail of biotin-conjugated monoclonal antibodies. Naive CD8 T cells purity was analysed on FACS LSR Fortessa 4L and was always > 97%.

Purified CD8 T cells were stained with CTV (2,5 mM, Thermofisher) according to manufacturer's instruction. 1.5x10<sup>4</sup> to 1.5x10<sup>5</sup> CTV labelled-naive CD8 T cells were cultured in 250  $\mu$ L complete DMEM medium with respectively 1.5x10<sup>3</sup> to 1,5x10<sup>4</sup> NP68-loaded matured BMDCs (ratio DC:CD8 = 1:10) for up to 6 days at 37°C in 96 well plate-U bottom plates, in the presence or absence of 5% murine rIL-2 supernatant (corresponding to a final concentration of 11.5 ng/mL). In some experiment, 3x10<sup>5</sup> C57BL/6J splenocytes were added or recombinant IL-2 (Miltenyi Biotec) was used.

For some adoptive transfer experiment, 1.8x10<sup>7</sup> CTV labelled-F5 were activated with 1.8x10<sup>6</sup> NP68-loaded matured BMDCs in the presence or absence of 5% murine rIL-2 supernatant, in 30 ml in complete DMEM medium T25 flasks for 4 days.

Naive CD8 T cells (CD44<sup>negative</sup>) were isolated from C57BL/6J spleen and stained with CTV as described above. 1.5x10<sup>5</sup> CTV labelled-naive CD8 T cells were cultured in 250  $\mu$ L complete DMEM medium with anti-CD3/CD28 coated beads at a 1 bead: 4 CD8 T cell ratio for 4 days, at 37°C in 96 well plate-U bottom plates, in the presence or absence of 5% supernatant containing IL-2.

### *In vivo Memory CD8 T cell generation and Restimulation*

Purified naive CD8 T cells were activated in vitro for 4 days. The divided cells 4-days CD8 were sorted by flow cytometry (FACS Aria I, BD biosciences) according to their CD44 expression and CTV dilution (see figure S1A). Purity after sorting was >98%. 1x10<sup>6</sup> or 2x10<sup>4</sup> sorted cells were adoptively transferred by intravenous injection (i.v.) in VV-NP68 infected mice or uninfected mice. For immunization, mice were first anesthetized with an intraperitoneal (i.p.) injection of Ketamine (1.5 mg)/ Xylazine (0.3 mg) in 150  $\mu$ L PBS

(Phosphate Buffer Saline) and then the VV-NP68 ( $2 \times 10^5$  PFU) was intranasally (i.n.) administered in 20  $\mu$ L of PBS. Blood was collected after 4 days. After 28 days, mice were sacrificed by cervical dislocation. Spleen was harvested, mechanically disrupted, and filtered through a sterile 100-mm nylon mesh filter (BD Biosciences). Single cell suspensions were then stained for flow cytometry analysis.

For cytokine production that was detected by flow cytometry,  $3 \times 10^6$  splenocytes were incubated with 10 nM NP68 peptide for 4h at 37°C in the presence of GolgiStop™ (BD Biosciences), according to manufacturer's instructions.

### *Flow cytometry*

In order to count cells, 100  $\mu$ L of Flow-count fluorospheres (Beckman Coulter) were added before staining steps. Cells were first stained with efluor780-coupled Fixable Viability Dye (Thermo Scientific) for 15 minutes at 4°C. Cells were then incubated with an Fc receptor blocking antibody (2.4G2 hybridoma supernatant) for 10 minutes at 4°C followed by surface staining for 30min at 4°C with the appropriate mixture of mAbs diluted in staining buffer (PBS supplemented with 1% FCS [Life Technologies] and 0.09% NaN<sub>3</sub> [Sigma-Aldrich]). For biotin-coupled antibody, streptavidin staining was performed for 10min at 4°C. In some experiments, cells were incubated in 100  $\mu$ L RPMI containing 100  $\mu$ M 2-NBDG (ThermoFisher) for 10 minutes at 37°C before staining, to analyze glucose uptake. Intracellular staining was performed using eBioscience™ Foxp3/Transcription Factor Staining Buffer Set kit (Thermofisher) for the analysis of cytokines and transcription factors, or Lyse/Fix and PermIII buffers (BD Biosciences) for the analysis of phosphorylated proteins, according to manufacturer's instructions.

The following antibodies were used: CD8 (53.6.7), CD62L (MEL-14), CD45.1 (A20), CD45.2 (104), CD11b (M1/70), CD11c (HL3), CD19 (1D3), EOMES (Dan11mag), T-bet (4B10), TCF-7/ TCF-1 (S33-966), STAT5 (47/stat5(pY694)), AKT (55/PKBa/Akt), CD27 (LG.7F9), CD29 (eBioHMb1-1), CD49a (Ha31/8), CD49d (R1-2), NKG2D (CX5), TCR V $\beta$  11(RR3-15), IFN- $\gamma$  (XMG1.2) from BD Biosciences and CD25 (PC61), CD44 (IM7.8.1), Bcl2 (BCL/10C4), CCL5 (2E9) from Biolegend.

All analyses were performed on a BD Biosciences FACS Fortessa and analyzed with FlowJo

software 10.7.1 (Tree Star, Ashland, OR).

#### *Cytokines production measurement (ELISA)*

IFN- $\gamma$  and IL-2 were measured on culture supernatants using IFN- $\gamma$  or IL-2 ELISA MAX™ Standard Set mouse kit (Biolegend), according to manufacturer instructions.

#### *Single cell sorting and RNA sequencing*

$1.5 \times 10^5$  or  $3 \times 10^4$  naive F5 CD8 T cells were activated *in vitro* for 1, 2, 3 and 4 days in the presence or absence of 5% IL-2. Undivided (naive and D1 post-activation cells) and divided (D2 to D4 post-activation) F5 CD8 T cells were index sorted on an FACS Aria I (BD biosciences) according to their CD44 expression and CTV dilution, into 96-well plates containing 4 $\mu$ L of lysis solution and barcoded poly(T) reverse-transcription (RT) primers for single-cell RNA-sequencing (scRNA-seq). Plates were stored at -80°C until processed.

Library construction was performed following MARS-seq protocol (Jaitin et al., 2014). Briefly, mRNAs were reverse transcribed into cDNAs. Second strand cDNA was synthesized and cDNAs were pooled. Unbound poly(T) primers were eliminated with exonuclease I (NEB) and cDNA was purified on AmpureXP beads. Samples were then linearly amplified by *in vitro* transcription and amplified RNAs were fragmented, purified and reverse transcribed using hexamer containing a plate barcode. Illumina sequencing adaptors were added and cDNA was amplified by PCR. Library quality and quantity were tested using DNA high sensitivity D1000 ScreenTape on TapeStation 4200 (Agilent). All libraries were pooled at equimolar concentration and sequenced on an Illumina HiSeq with 8% of PhiX at an average sequencing depth of ~600,000 reads/cells.

#### *Single cell RNA-seq preprocessing*

Raw data were processed with a single-cell data analysis pipeline developed by our collaborators from the “Laboratoire de Biologie et de Modélisation de la Cellule” (LBMC – Lyon) in nextflow version (Di Tommaso et al., 2017). Briefly, the sample was demultiplexed according to plate barcode. Reads that reach the quality standards were aligned to the mouse reference sequence GRCm38.p6 using bowtie2. Genes and artificial RNAs quantification per cell were performed using UMI-tools (Smith et al., 2017) generating a

gene/count matrix. 3 datasets were used; one composed of 4x96 cells sorted on days 0 and 1, 2 and 3 after *in vitro* activation. Cells with less than 500 UMIs and more than 10% of mitochondrial counts were removed. The dataset was normalized using *sctransform* and the integration workflow from Seurat (version 3.2.2) to compensate for a plate effect. The last two datasets comprising activated cells after 4 days, were merge resulting in 6x96 cells. Cell filtering was performed separately for each plate using the scater package (McCarthy et al., 2017). Briefly, cells with a log-library size and a log-transformed number of expressed genes that were more than 3 median absolute deviations (MAD) below the median value were excluded. Then, cells with a log-transformed percentage of expressed mitochondrial genes that were more than 2 MADs above the median value were discarded. Moreover, genes expressed in less than 5 cells were removed. The data were then normalized using the *sctransform* function, features were selected using the *SelectIntegrationFeatures* function and integration to compensate plate effect was performed using canonical correlation analysis (CCA) included in the Seurat v4 package (Hao et al., 2021).

#### *Single-cell RNA-seq analysis*

To cluster the cells, the principal component analysis dimensions were first selected and the Louvain algorithm include in the Seurat package V4 was applied to the data. The clusters were projected onto the UMAP dimension reduction using the same principal component as input to the clustering analysis. Differential expression analysis was made using the Seurat function *FindAllMarkers*. Heatmap and dot plot were generated using the Seurat function *DoHeatmap* and *DotPlot* respectively. The Seurat R package was used to classify cells into G1, S or G2/M phases of the cell cycle. The classifier, relying on a list of genes from Tirosh et al. (Tirosh et al., 2016) contains markers of the G2/M and S phase. A score was attributed to each cell with a certain probability to belong to the S or G2/M phases. Cells expressing no S, G2/M markers are assigned to the G1 class. The AUCell R package (Aibar et al., 2017) was used in order to identify cells with active gene signature. The memory precursor signature was downloaded from Yao et al. paper (Yao *et al.*, 2019). The TinGa (Todorov *et al.*, 2020) method was used to infer a trajectory in the data (Todorov *et al.*, 2020). First, the integrated data was wrapped into a dataset object with the dynwrap R package (Saelens et al., 2019) and TinGa was implemented using the

default parameters. The dynplot R package (Saelens *et al.*, 2019) was then used for an easy visualization of the resulting trajectories on an MDS dimension reduction.

### *Statistical analysis*

Statistical analyses were performed using Graph-pad software Prism 5. Two tailed unpaired t-test and one-way ANOVA Friedman test were used as indicated in the figure legend.

## Figure legends

### **Figure 1. ex-IL-2 impacts the phenotype but not the proliferation of in vitro activated CD8 T cells.**

1.5x10<sup>5</sup> magnetically purified naive F5 CD8 T cells labelled with CTV were cultured with CpG-matured, peptide-loaded cDC at a ratio of cDC:CD8 = 1:10, in the presence or absence of IL-2. **A.** The number of divided CD8 T cells was determined on day 4, 5 and 6.

**B.** CD8 proliferation in the presence (red) or absence (black) of ex-IL-2 was analyzed after 4 days by CTV dilution and represented as overlay histogram.

**C.** Mean of fluorescence intensity (MFI) of Ki67 was measured on divided cells after 4 days.

**D.** Expression of CD25, TCF1, EOMES, T-bet and Bcl2 by divided CD8 T cells was analyzed 4 days after activation. Representative histograms of cells cultured in the presence (red) or absence (black) of IL-2 is shown (D).

**E.** Kinetics of the percentage of EOMES<sup>+</sup> and CD25<sup>+</sup> cells, as well as the level of Bcl-2 expression by divided CD8 T cells.

**F.** Expression of pAkt and pSTAT5 by divided CD8 T cells were analyzed 4 days after activation (right panel). Representative histograms of cells culture in the presence (red) or absence (black) of IL-2 are shown (left panel).

The results are from one out of six independent experiments. The statistical significance of differences was determined by the student t test (\*\*\*\*p<0.0001).

### **Figure 2. Lower CD8 cellular concentration strongly increases the dependency on ex-IL-2.**

1.5x10<sup>5</sup>, 5x10<sup>4</sup> or 1.5x10<sup>4</sup> purified naive F5 CD8 T cells labelled with CTV were cultured with CpG-matured, peptide-loaded cDC at a ratio of cDC:CD8 = 1:10, in the presence or absence of IL-2 for 4 days.

**A.** The number of divided cells was measured and the proliferation index was determined as (the number of divided cells/ the initial number of CD8 T cells) \*100

**B.** CD8 proliferation in the presence (red) or absence (black) of ex-IL-2 was analyzed after 4 days by CTV dilution and represented as overlay histogram.

**C.** Expression of CD25, TCF1, Bcl2 by divided CD8 T cells was measured.

**D.** Expression of CD62L by CD8 T cells activated at different concentrations with IL-2.

The results are expressed as the mean of triplicates  $\pm$  SD for one out of three independent experiments. The statistical significance of differences was determined by the student t test in A, C and one-way ANOVA Friedman test in D (\* $p < 0.05$ , \*\* $p < 0.005$ , \*\*\* $p < 0.0001$ ).

**Figure 3. Cells activated with and without ex-IL-2 have the similar potential to participate in an ongoing immune response.**

**A-F.** CTV-labelled purified naive F5 CD8 T cells, at a concentration of  $1.8 \times 10^7/30\text{ml}$  (B; D-F) or  $1.5 \times 10^5/250 \mu\text{l}$  or  $3 \times 10^4/250 \mu\text{l}$  (C), were cultured with CpG-matured, peptide-loaded cDC at a ratio of cDC:CD8 = 1:10 for 4 days. Divided CD8 cells were sorted by flow cytometry and  $1 \times 10^6$  (B; D-F) or  $2 \times 10^4$  (C) cells were adoptively transferred into vaccine virus infected C57BL/6J mice (4 days post-infection).

**A.** Outline of the experimental scheme

**B-C.** The number of TCR V $\beta$ 11+ F5 CD8 T cell was determined in the blood on day 8 (B) and in the spleen on day32 after activation (C).

**D.** The expression of CD62L, NKG2D, CD29, CD49d and CD49a was analyzed on TCR V $\beta$ 11+ F5 CD8 T cells from spleen on day32 and represented as histogram.

**E.** The expression of CD43 and CD27 was analyzed on TCR V $\beta$ 11+ F5 CD8 T cells from spleen on day32. Representative histograms and individual percentages of CD27+CD43- and CD27+CD43+ cells are depicted.

**F.** On day32,  $3 \times 10^6$  splenocytes were stimulated with NP68 (10nM) for 4 hours. The expression of IFN- $\gamma$  and CCL5 by F5 CD8 T was analyzed by flow cytometry.

Results are from one out of four independent experiments (n=4 mice per group). The statistical significance of differences was determined by the student t test (ns =  $p \geq 0.05$ , \* $p < 0.05$ , Student's test).

**Figure 4. ex-IL-2 promotes direct in vivo memory differentiation of in vitro activated cells.**

**A-E.** CTV-labelled purified naive F5 CD8 T cells at a concentration of  $1.8 \times 10^7/30\text{ml}$  (C-E) or  $1.5 \times 10^5/250\text{ul}$  or  $3 \times 10^4/250\text{ul}$  (B) were cultured with CpG-matured, peptide-loaded cDC

at a ratio of cDC:CD8 = 1:10 for 4 days. Divided CD8 cells were sorted by flow cytometry and  $1 \times 10^6$  (C-E) or  $2 \times 10^4$  (B) cells were adoptively transferred into naive C57BL/6J mice.

**A.** Outline of the experimental scheme

**B.** The number of TCR V $\beta$ 11+ F5 CD8 T cell was determined in the spleen on day32 after activation.

**C.** The expression of CD43 and CD27 was analyzed on TCR V $\beta$ 11+ F5 CD8 T cells from spleen on day32. Representative histograms and individual percentages of CD27+CD43- and CD27+CD43+ cells are depicted.

**D.** The expression of CD62L, NKG2D, CD29, CD49d and CD49a was analyzed on TCR V $\beta$ 11+ F5 CD8 T cells from spleen on day32 and represented as histogram.

**E.** On day32,  $3 \times 10^6$  splenocytes were stimulated with NP68 (10 nM) for 4 hours. The expression of IFN- $\gamma$  and CCL5 by F5 CD8 T was analyzed by flow cytometry.

Results are from one out of four independent experiments (n=4 mice per group). The statistical significance of differences was determined by the student t test (\*p<0.05, \*\*p<0.005, \*\*\*p<0.0001, Student's t test).

**Figure 5. scRNA-seq shows that absence of ex-IL-2 during in vitro activation allows the development of cells with a memory precursor phenotype, while cells cultured with IL-2 display effector trait.**

**A.** Left panel: UMAP projection of cells sorted on day 4 after activation with or without ex-IL-2 and colored according to cluster identification by Seurat cluster. Right panel: cell counts from each culture conditions (with or without ex-IL-2) across the 4 clusters from (A- left panel).

**B.** Heatmap representing the top 15 differentially expressed marker genes for each cluster defined in Figure 5A- left panel.

**C.** Dot plot showing gene expression per cluster (X and Y-axis respectively). The size of the dot represents the percentage of cells from the cluster on the y-axis, expressing the genes indicated on the x-axis; while the color indicates the average expression level across cells in which the gene is detected.

**D.** Classification of cells into one of the cell-cycle phases (G1, S or G2/M) and colored accordingly using the Seurat package. Cell-cycle position was projected onto the UMAP (left panel) or the cell counts for each cell cycle phase in each cluster were plotted (right

panel). The percentages represent the proportion of cells in the G1, S or G2/M phase for the indicated cluster.

**E.** Memory precursor signature enrichment per cluster. The dotted line represents the threshold above which, cells are considered as memory precursors. The legend indicates the percentage of memory precursor cells in each cluster. AUC: area under the curve.

**F.** Trajectory inference (black line) using TinGa for cells projected in a 2D space using multi-dimensional scaling (MDS). The cells were colored according to the Seurat clusters. Numbers along the trajectory correspond to TinGa-defined milestones.

## Supplementary figures

### Figure S1. Extended data for figure 1.

A-B.  $1.5 \times 10^5$  magnetically purified naive F5 CD8 T cells labelled with CTV were cultured with CpG-matured, peptide-loaded cDC at a ratio of cDC:CD8 = 1:10, in the presence or absence of IL-2. **A.** Gating strategy of divided CD8 T cells was shown. **B.** 2-NBDG (glucose uptake indicator) was analyzed on divided CD8. Representative dot plots are shown.

**C.**  $1.5 \times 10^5$  magnetically purified naive F5 CD8 T cells labelled with CTV were cultured with CpG-matured, peptide-loaded cDC at a ratio of cDC:CD8 = 1:10, in the presence of various concentrations of supernatant-containing-IL2 or recombinant-IL-2 for 4 days. Equivalent concentrations of supernatant IL-2 and recombinant IL-2 were used (0.5, 1.5, 5 or 15% equivalent to 1.15, 3.45, 11.5 and 34.5ng/ml respectively). The number of divided CD8 T cells (left panel) and CD25 expression by divided CD8 T cells (right panel) are shown.

The results are expressed as the mean of triplicates  $\pm$  SD from one experiment.

**D.**  $1.5 \times 10^5$  magnetically purified naive C57BL/6J CD8 T cells labelled with CTV were cultured with anti-CD3/CD28 coated beads at a ratio of beads:CD8 = 1:4, in the presence or absence of IL-2 for 4 days. The number of divided CD8 T cells (left panel) and CTV dilution in the presence (red) or absence (black) of IL-2 are shown. CTV fluorescent intensity of the overlay between CD8 T cells activated with and without 5% supernatant IL-2 (right). The results are expressed as the mean of triplicates  $\pm$  SD from one representative out of three independent experiments.

**E.** Secretion of IL-2 by CD8 T cells activated in the absence of exogenous IL-2 as described in A-B was measured by ELISA in the culture supernatant at the indicated days. The results are expressed as the mean triplicates  $\pm$  SD from one representative out of three independent experiments.

### Figure S2. Extended data for figure 2.

$5 \times 10^4$  or  $1.5 \times 10^4$  magnetically purified naive F5 CD8 T cells labelled with CTV were cultured with CpG-matured, peptide-loaded cDC at a ratio of DC:CD8 = 1:10, in the presence or absence of IL-2 for 4 days. And  $3 \times 10^5$  splenocytes from C57BL/6J mice were added to sustain cell viability.

**A.** The number of divided cells was measured on CD8 activated in the presence of C57BL/6J splenocytes and the proliferation index was determined as (the number of divided cells/ the initial number of CD8 T cells) \*100.

**B.** CD8 proliferation was analyzed after 4 days by CTV dilution in the presence (grey) or absence (blue) of splenocytes and represented as overlay histograms.

**C.** Secretion of IL-2 by CD8 T cells activated in the absence of exogenous IL-2 was measured by ELISA in supernatant after 4 days, in the presence (empty triangles) or absence (full circles) of splenocytes.

**D.** Expression of CD25, TCF1, Bcl2 by divided CD8 T cells activated in the presence of C57BL/6J splenocytes.

The results are expressed as the mean of triplicates  $\pm$  SD from one out of two independent experiments. (ns:  $p \geq 0.05$ , \*\* $p < 0.005$ , \*\*\* $p < 0.0001$ , Student's t test).

**Figure S3. Extended data for figure 5.**

**A.** UMAP projection of cells colored according to the experimental time points (0, 1, 2 and 3 days post *in vitro* activation) and culture conditions (with or without ex-IL-2).

**B.** Memory precursor signature enrichment per time points and culture conditions. Cells above the threshold represented by the dotted line, are considered as memory precursors. The legend indicates the percentage of memory precursor cells in each condition. AUC: area under the curve.

**C.** Heatmap representing genes expression of the memory precursor signature of cells sorted at day 4 after activation in each Seurat cluster from Fig 5A.

Figure 1

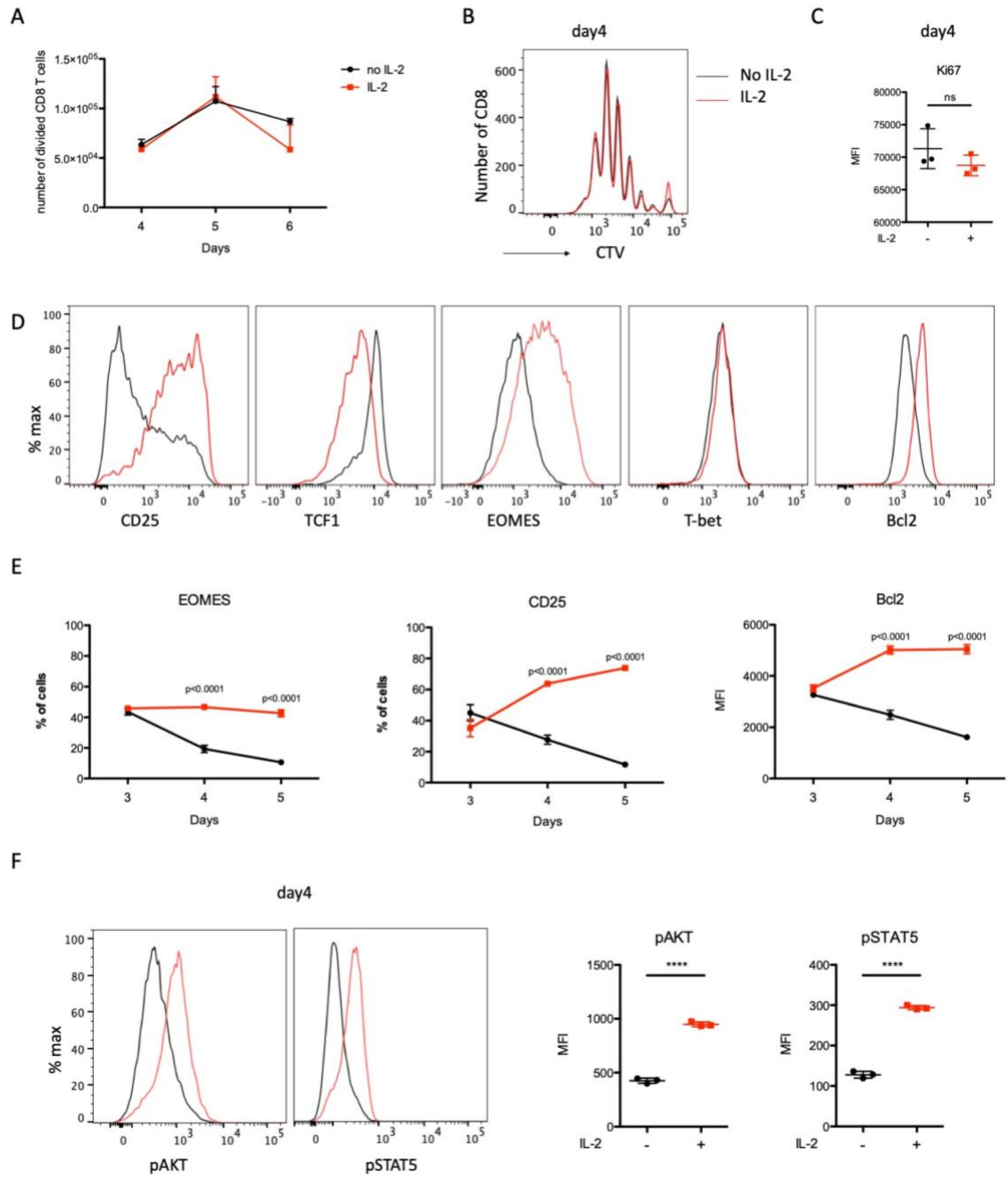


Figure 2

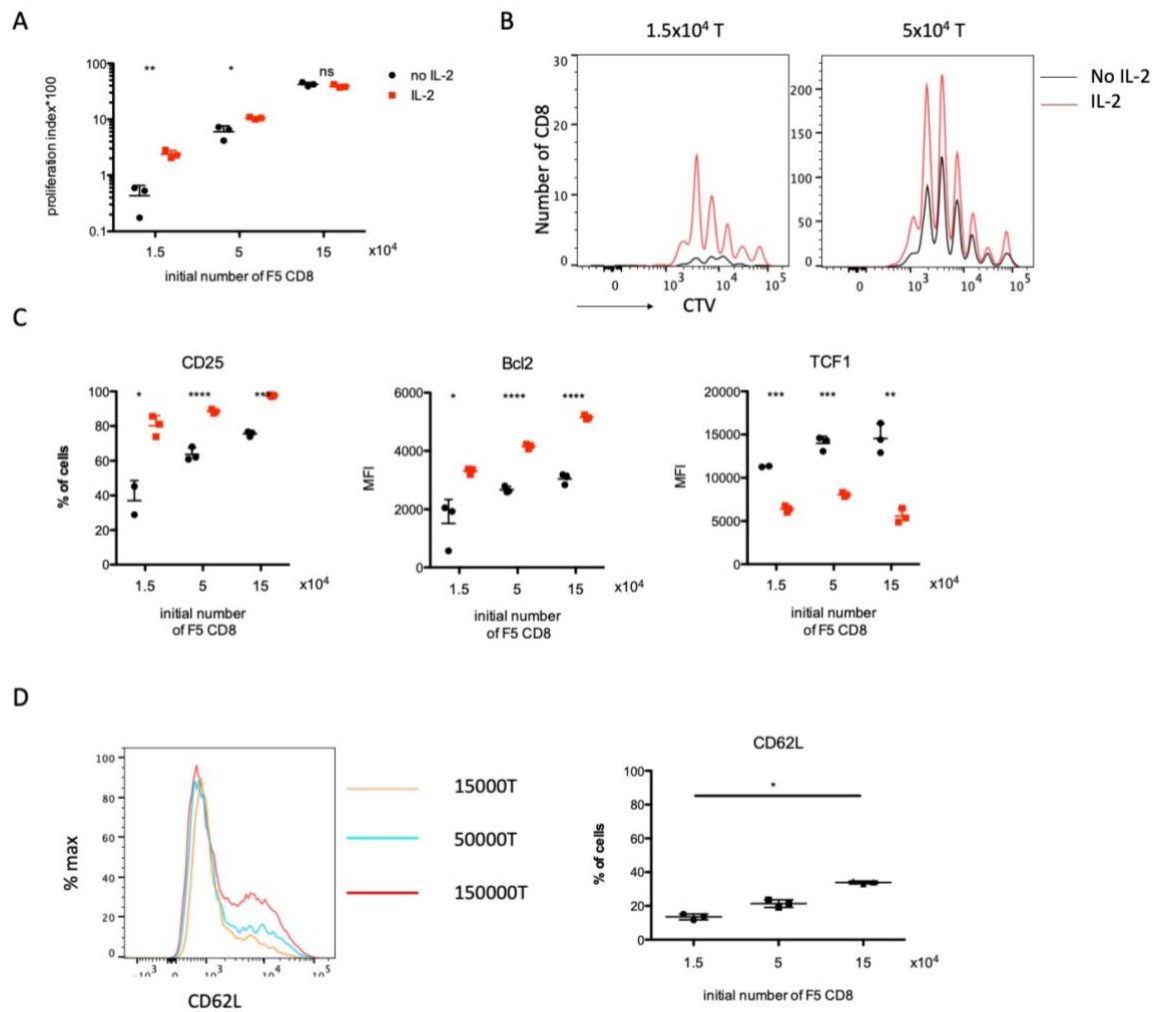


Figure 3

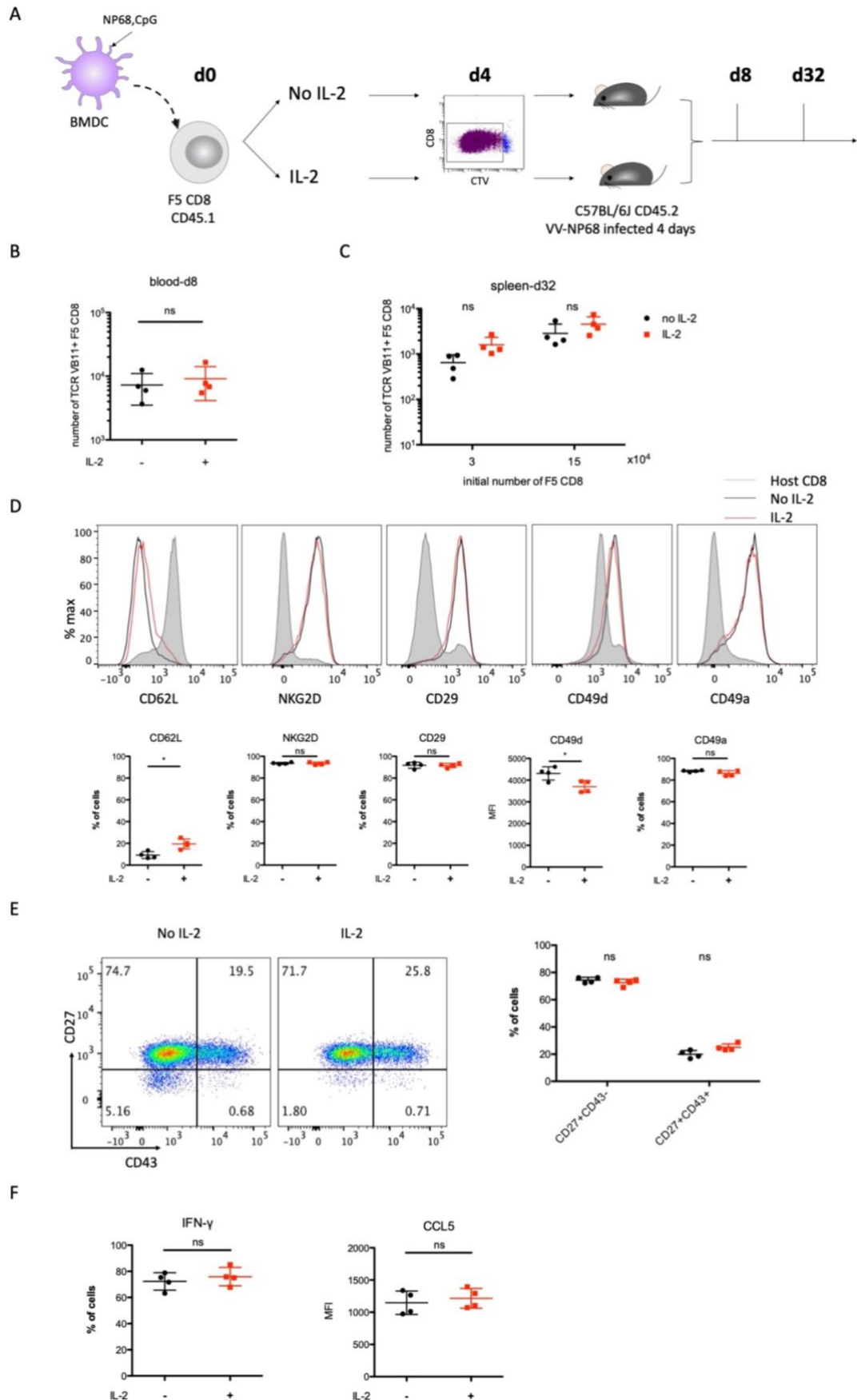


Figure 4

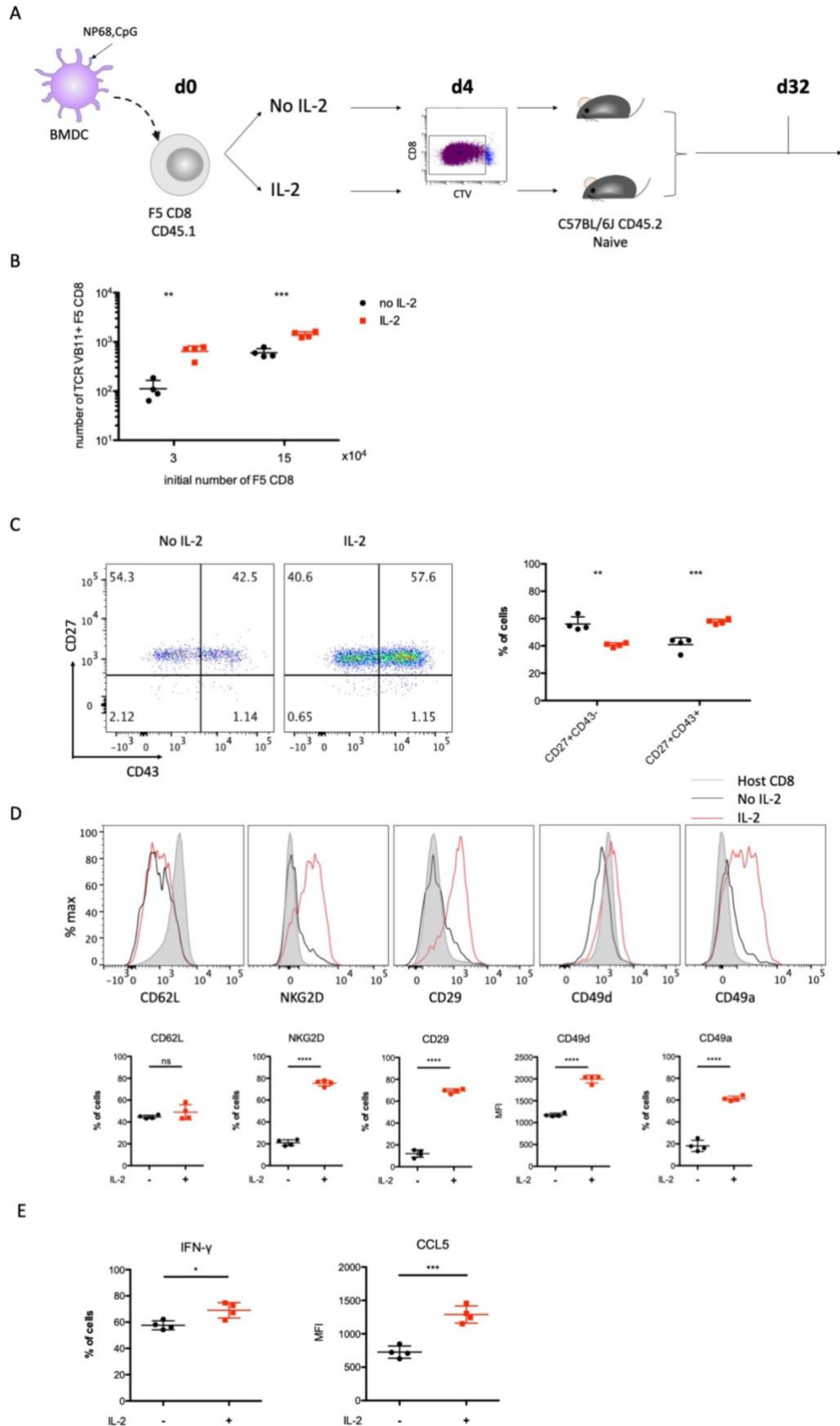


Figure 5

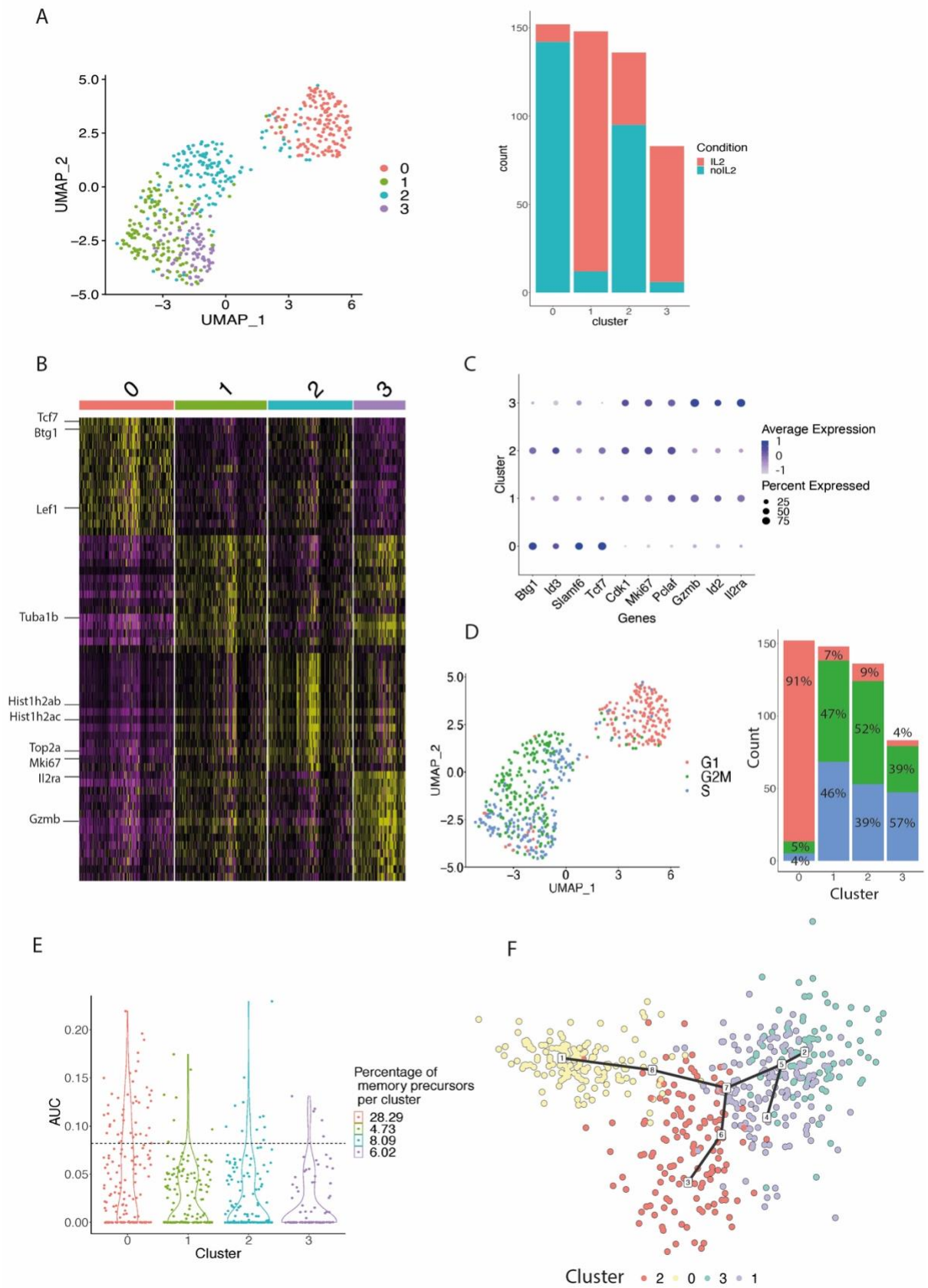


Figure S1

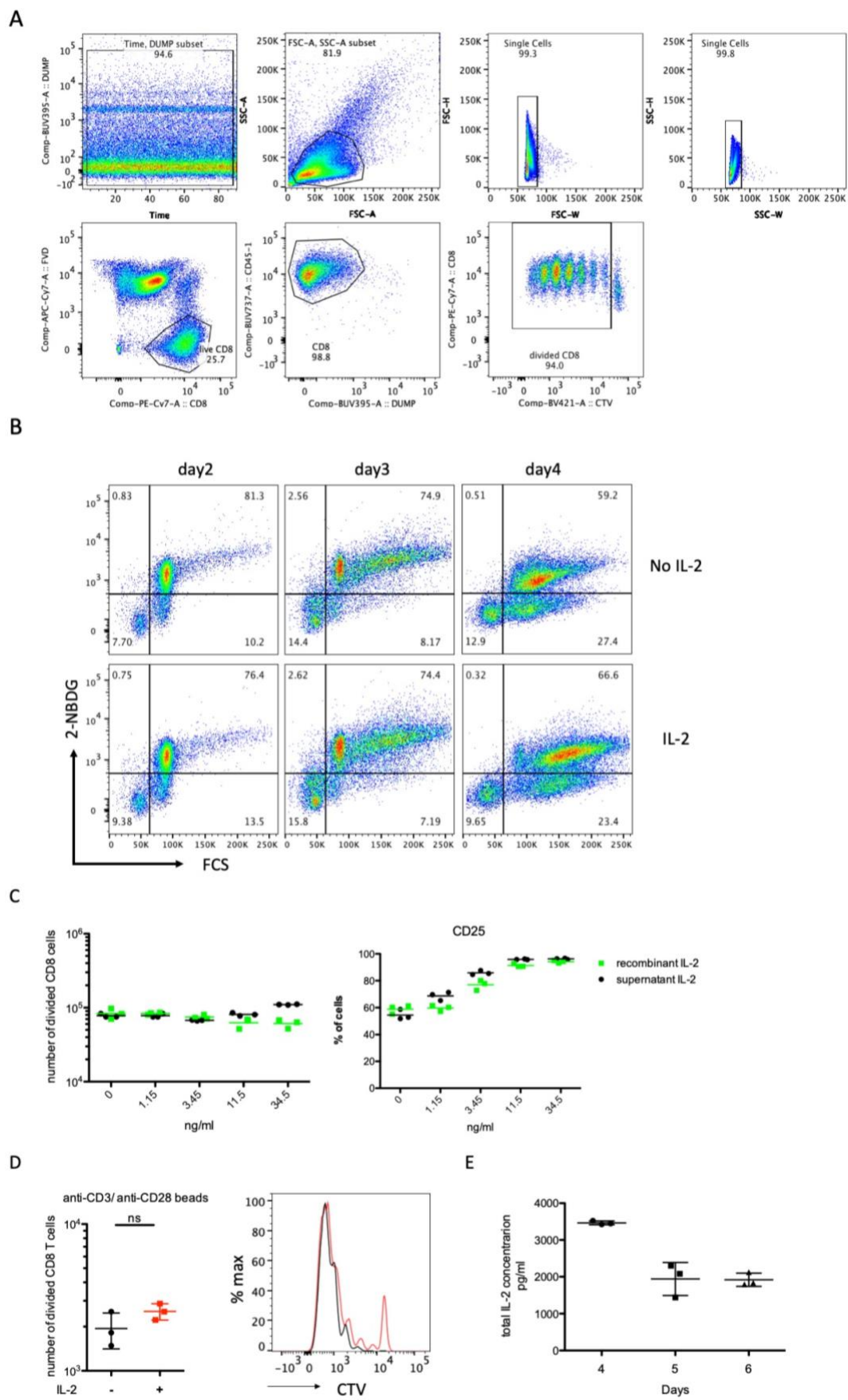


Figure S2

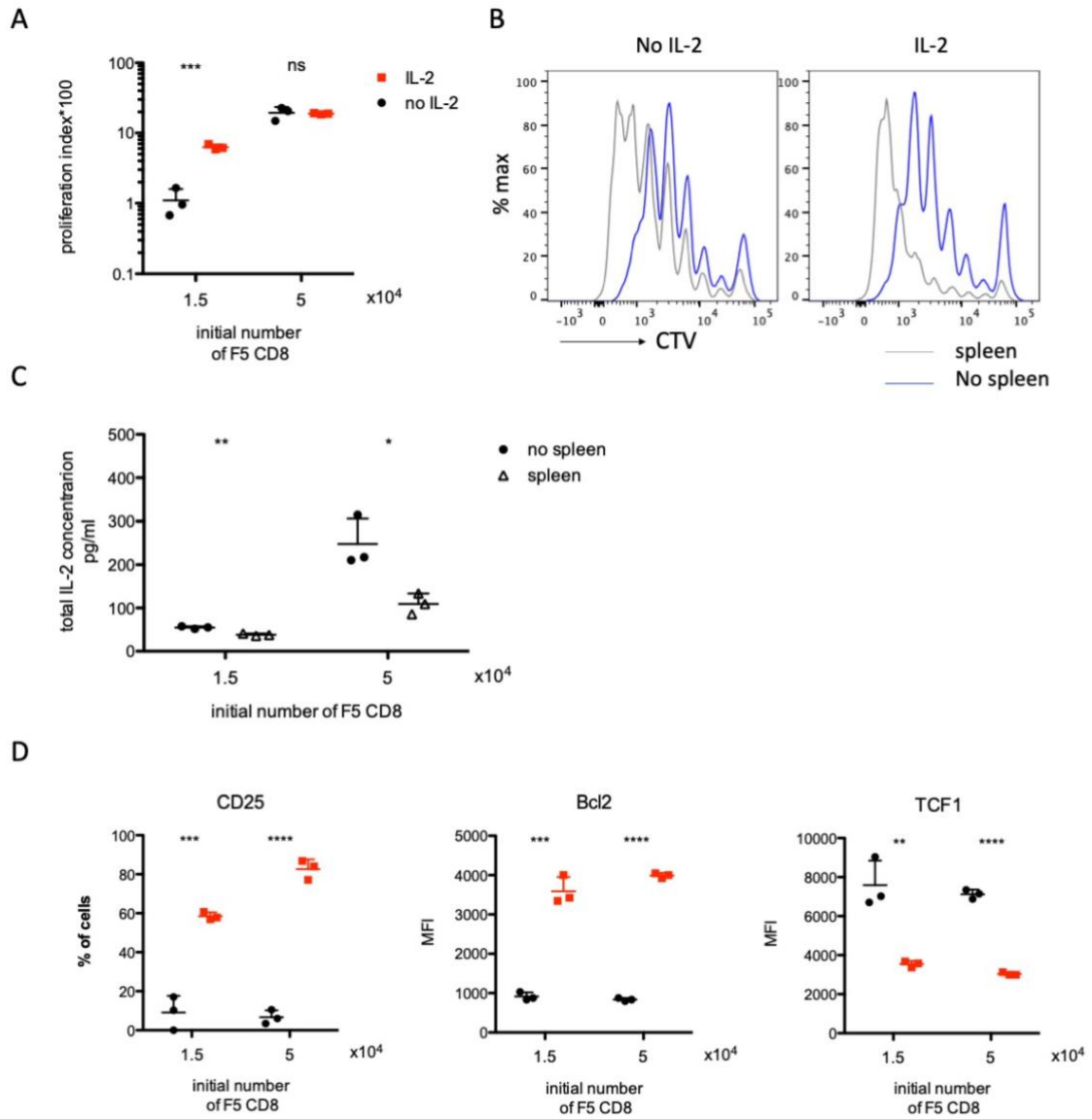
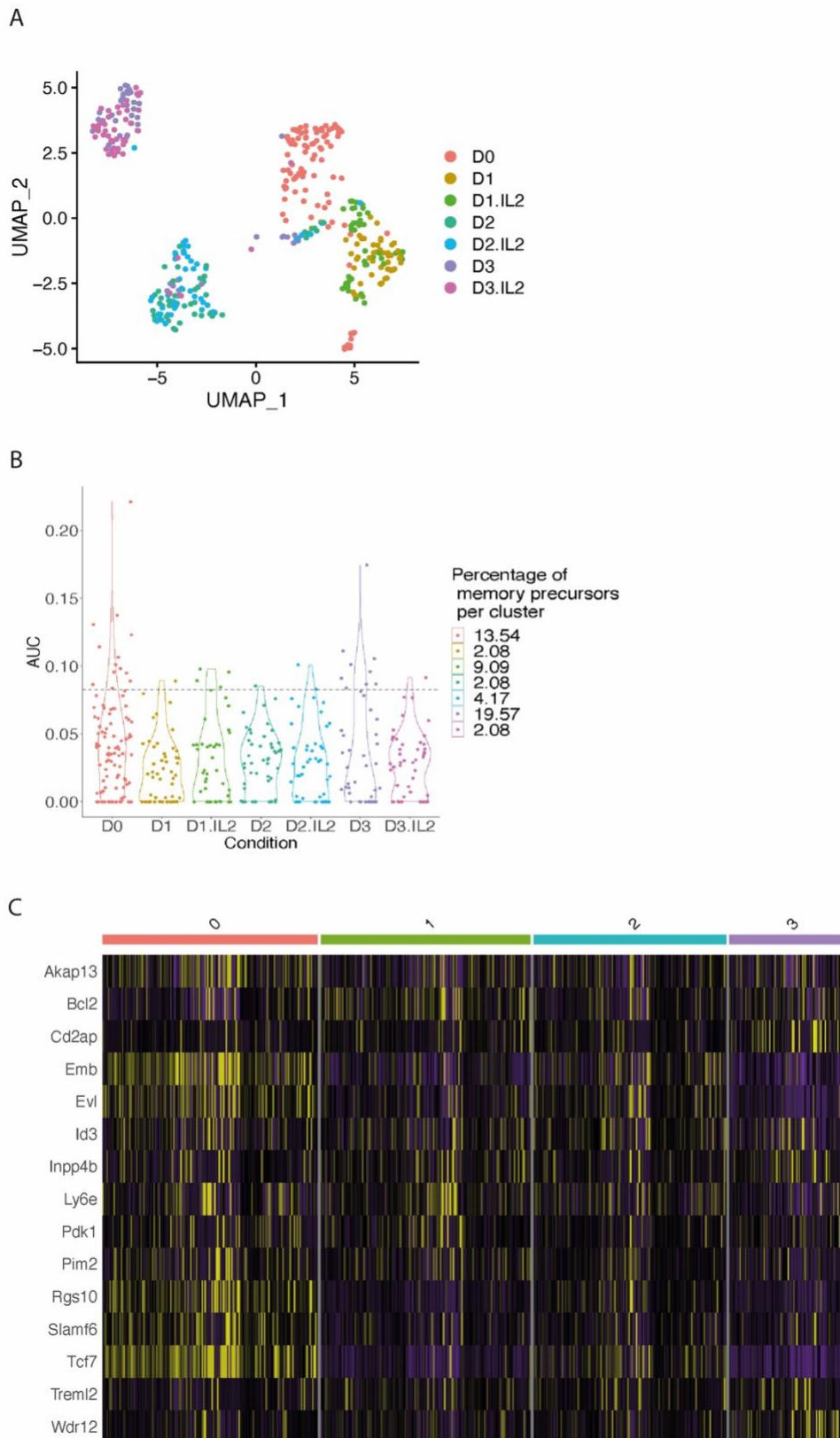


Figure S3



## References

- Aibar, S., Gonzalez-Blas, C.B., Moerman, T., Huynh-Thu, V.A., Imrichova, H., Hulselmans, G., Rambow, F., Marine, J.C., Geurts, P., Aerts, J., et al. (2017). SCENIC: single-cell regulatory network inference and clustering. *Nat Methods* 14, 1083-1086. 10.1038/nmeth.4463.
- Badovinac, V.P., Haring, J.S., and Harty, J.T. (2007). Initial T cell receptor transgenic cell precursor frequency dictates critical aspects of the CD8(+) T cell response to infection. *Immunity* 26, 827-841. 10.1016/j.immuni.2007.04.013.
- Borst, J., Ahrends, T., Babala, N., Melief, C.J.M., and Kastenmuller, W. (2018). CD4(+) T cell help in cancer immunology and immunotherapy. *Nat Rev Immunol* 18, 635-647. 10.1038/s41577-018-0044-0.
- Boyman, O., and Sprent, J. (2012). The role of interleukin-2 during homeostasis and activation of the immune system. *Nat Rev Immunol* 12, 180-190. 10.1038/nri3156.
- Cheng, L.E., Ohlen, C., Nelson, B.H., and Greenberg, P.D. (2002). Enhanced signaling through the IL-2 receptor in CD8+ T cells regulated by antigen recognition results in preferential proliferation and expansion of responding CD8+ T cells rather than promotion of cell death. *Proc Natl Acad Sci U S A* 99, 3001-3006. 10.1073/pnas.052676899.
- Collinson-Pautz, M.R., Chang, W.C., Lu, A., Khalil, M., Crisostomo, J.W., Lin, P.Y., Mahendravada, A., Shinnars, N.P., Brandt, M.E., Zhang, M., et al. (2019). Constitutively active MyD88/CD40 costimulation enhances expansion and efficacy of chimeric antigen receptor T cells targeting hematological malignancies. *Leukemia* 33, 2195-2207. 10.1038/s41375-019-0417-9.
- Cousens, L.P., Orange, J.S., and Biron, C.A. (1995). Endogenous IL-2 contributes to T cell expansion and IFN-gamma production during lymphocytic choriomeningitis virus infection. *J Immunol* 155, 5690-5699.
- Crompton, J.G., Sukumar, M., and Restifo, N.P. (2014). Uncoupling T-cell expansion from effector differentiation in cell-based immunotherapy. *Immunol Rev* 257, 264-276. 10.1111/imr.12135.
- D'Souza, W.N., and Lefrancois, L. (2003). IL-2 is not required for the initiation of CD8 T cell cycling but sustains expansion. *J Immunol* 171, 5727-5735. 10.4049/jimmunol.171.11.5727.
- Di Tommaso, P., Chatzou, M., Floden, E.W., Barja, P.P., Palumbo, E., and Notredame, C. (2017). Nextflow enables reproducible computational workflows. *Nat Biotechnol* 35, 316-319. 10.1038/nbt.3820.
- Feau, S., Arens, R., Togher, S., and Schoenberger, S.P. (2011). Autocrine IL-2 is required for secondary population expansion of CD8(+) memory T cells. *Nat Immunol* 12, 908-913. 10.1038/ni.2079.
- Gattinoni, L., Klebanoff, C.A., Palmer, D.C., Wrzesinski, C., Kerstann, K., Yu, Z., Finkelstein, S.E., Theoret, M.R., Rosenberg, S.A., and Restifo, N.P. (2005). Acquisition of full effector function in vitro paradoxically impairs the in vivo antitumor efficacy of adoptively transferred CD8+ T cells. *J Clin Invest* 115, 1616-1626. 10.1172/JCI24480.
- Gattinoni, L., Lugli, E., Ji, Y., Pos, Z., Paulos, C.M., Quigley, M.F., Almeida, J.R., Gostick, E., Yu, Z., Carpenito, C., et al. (2011). A human memory T cell subset with stem cell-like properties. *Nat Med* 17, 1290-1297. 10.1038/nm.2446.
- Grau, M., Valsesia, S., Mafille, J., Djebali, S., Tomkowiak, M., Mathieu, A.L., Laubreton, D., de Bernard, S., Jouve, P.E., Ventre, E., et al. (2018). Antigen-Induced but Not Innate Memory CD8 T Cells Express NKG2D and Are Recruited to the Lung Parenchyma upon Viral Infection. *J Immunol* 200, 3635-3646. 10.4049/jimmunol.1701698.

- Hao, Y., Hao, S., Andersen-Nissen, E., Mauck, W.M., 3rd, Zheng, S., Butler, A., Lee, M.J., Wilk, A.J., Darby, C., Zager, M., et al. (2021). Integrated analysis of multimodal single-cell data. *Cell* 184, 3573-3587 e3529. 10.1016/j.cell.2021.04.048.
- Hikono, H., Kohlmeier, J.E., Takamura, S., Wittmer, S.T., Roberts, A.D., and Woodland, D.L. (2007). Activation phenotype, rather than central- or effector-memory phenotype, predicts the recall efficacy of memory CD8+ T cells. *J Exp Med* 204, 1625-1636. 10.1084/jem.20070322.
- Hinrichs, C.S., Borman, Z.A., Cassard, L., Gattinoni, L., Spolski, R., Yu, Z., Sanchez-Perez, L., Muranski, P., Kern, S.J., Logun, C., et al. (2009). Adoptively transferred effector cells derived from naive rather than central memory CD8+ T cells mediate superior antitumor immunity. *Proc Natl Acad Sci U S A* 106, 17469-17474. 10.1073/pnas.0907448106.
- Jaitin, D.A., Kenigsberg, E., Keren-Shaul, H., Elefant, N., Paul, F., Zaretsky, I., Mildner, A., Cohen, N., Jung, S., Tanay, A., and Amit, I. (2014). Massively parallel single-cell RNA-seq for marker-free decomposition of tissues into cell types. *Science* 343, 776-779. 10.1126/science.1247651.
- Kaech, S.M., and Ahmed, R. (2001). Memory CD8+ T cell differentiation: initial antigen encounter triggers a developmental program in naïve cells. *Nat Immunol* 2, 415-422. 10.1038/87720.
- Kahan, S.M., Bakshi, R.K., Ingram, J.T., Hendrickson, R.C., Lefkowitz, E.J., Crossman, D.K., Harrington, L.E., Weaver, C.T., and Zajac, A.J. (2022). Intrinsic IL-2 production by effector CD8 T cells affects IL-2 signaling and promotes fate decisions, stemness, and protection. *Sci Immunol* 7, eabl6322. 10.1126/sciimmunol.abl6322.
- Kalia, V., and Sarkar, S. (2018). Regulation of Effector and Memory CD8 T Cell Differentiation by IL-2-A Balancing Act. *Front Immunol* 9, 2987. 10.3389/fimmu.2018.02987.
- Kalia, V., Sarkar, S., Gourley, T.S., Rouse, B.T., and Ahmed, R. (2006). Differentiation of memory B and T cells. *Curr Opin Immunol* 18, 255-264. 10.1016/j.coi.2006.03.020.
- Kalia, V., Sarkar, S., Subramaniam, S., Haining, W.N., Smith, K.A., and Ahmed, R. (2010). Prolonged interleukin-2 $\alpha$  expression on virus-specific CD8+ T cells favors terminal-effector differentiation in vivo. *Immunity* 32, 91-103. 10.1016/j.immuni.2009.11.010.
- Kim, M.T., Kurup, S.P., Starbeck-Miller, G.R., and Harty, J.T. (2016). Manipulating Memory CD8 T Cell Numbers by Timed Enhancement of IL-2 Signals. *J Immunol* 197, 1754-1761. 10.4049/jimmunol.1600641.
- Krämer, S., Mamalaki, C., Horak, I., Schimpl, A., Kioussis, D., and Hüng, T. (1994). Thymic selection and peptide-induced activation of T cell receptor-transgenic CD8 T cells in interleukin-2-deficient mice. *Eur J Immunol* 24, 2317-2322. 10.1002/eji.1830241009.
- Marzo, A.L., Klonowski, K.D., Le Bon, A., Borrow, P., Tough, D.F., and Lefrancois, L. (2005). Initial T cell frequency dictates memory CD8+ T cell lineage commitment. *Nat Immunol* 6, 793-799. 10.1038/ni1227.
- McCarthy, D.J., Campbell, K.R., Lun, A.T., and Wills, Q.F. (2017). Scater: pre-processing, quality control, normalization and visualization of single-cell RNA-seq data in R. *Bioinformatics* 33, 1179-1186. 10.1093/bioinformatics/btw777.
- Mercado, R., Vijh, S., Allen, S.E., Kerksiek, K., Pilip, I.M., and Pamer, E.G. (2000). Early programming of T cell populations responding to bacterial infection. *J Immunol* 165, 6833-6839. 10.4049/jimmunol.165.12.6833.
- Obar, J.J., Khanna, K.M., and Lefrancois, L. (2008). Endogenous naive CD8+ T cell precursor frequency regulates primary and memory responses to infection. *Immunity* 28, 859-869. 10.1016/j.immuni.2008.04.010.

Pipkin, M.E., Sacks, J.A., Cruz-Guilloty, F., Lichtenheld, M.G., Bevan, M.J., and Rao, A. (2010). Interleukin-2 and inflammation induce distinct transcriptional programs that promote the differentiation of effector cytolytic T cells. *Immunity* 32, 79-90. 10.1016/j.immuni.2009.11.012.

Polonsky, M., Rimer, J., Kern-Perets, A., Zaretsky, I., Miller, S., Bornstein, C., David, E., Kopelman, N.M., Stelzer, G., Porat, Z., et al. (2018). Induction of CD4 T cell memory by local cellular collectivity. *Science* 360. 10.1126/science.aaj1853.

Redeker, A., Welten, S.P., Baert, M.R., Vloemans, S.A., Tiemessen, M.M., Staal, F.J., and Arens, R. (2015). The Quantity of Autocrine IL-2 Governs the Expansion Potential of CD8+ T Cells. *J Immunol* 195, 4792-4801. 10.4049/jimmunol.1501083.

Saelens, W., Cannoodt, R., Todorov, H., and Saeys, Y. (2019). A comparison of single-cell trajectory inference methods. *Nat Biotechnol* 37, 547-554. 10.1038/s41587-019-0071-9.

Sengupta, S., Katz, S.C., Sengupta, S., and Sampath, P. (2018). Glycogen synthase kinase 3 inhibition lowers PD-1 expression, promotes long-term survival and memory generation in antigen-specific CAR-T cells. *Cancer Lett* 433, 131-139. 10.1016/j.canlet.2018.06.035.

Shourian, M., Beltra, J.C., Bourdin, B., and Decaluwe, H. (2019). Common gamma chain cytokines and CD8 T cells in cancer. *Semin Immunol* 42, 101307. 10.1016/j.smim.2019.101307.

Smith, K.A. (1988). Interleukin-2: inception, impact, and implications. *Science* 240, 1169-1176. 10.1126/science.3131876.

Smith, T., Heger, A., and Sudbery, I. (2017). UMI-tools: modeling sequencing errors in Unique Molecular Identifiers to improve quantification accuracy. *Genome Res* 27, 491-499. 10.1101/gr.209601.116.

Tirosh, I., Izar, B., Prakadan, S.M., Wadsworth, M.H., 2nd, Treacy, D., Trombetta, J.J., Rotem, A., Rodman, C., Lian, C., Murphy, G., et al. (2016). Dissecting the multicellular ecosystem of metastatic melanoma by single-cell RNA-seq. *Science* 352, 189-196. 10.1126/science.aad0501.

Todorov, H., Cannoodt, R., Saelens, W., and Saeys, Y. (2020). TinGa: fast and flexible trajectory inference with Growing Neural Gas. *Bioinformatics* 36, i66-i74. 10.1093/bioinformatics/btaa463.

van Stipdonk, M.J., Lemmens, E.E., and Schoenberger, S.P. (2001). Naïve CTLs require a single brief period of antigenic stimulation for clonal expansion and differentiation. *Nat Immunol* 2, 423-429. 10.1038/87730.

Williams, M.A., and Bevan, M.J. (2007). Effector and memory CTL differentiation. *Annu Rev Immunol* 25, 171-192. 10.1146/annurev.immunol.25.022106.141548.

Williams, M.A., Tzgnik, A.J., and Bevan, M.J. (2006). Interleukin-2 signals during priming are required for secondary expansion of CD8+ memory T cells. *Nature* 441, 890-893. 10.1038/nature04790.

Yao, C., Sun, H.W., Lacey, N.E., Ji, Y., Moseman, E.A., Shih, H.Y., Heuston, E.F., Kirby, M., Anderson, S., Cheng, J., et al. (2019). Single-cell RNA-seq reveals TOX as a key regulator of CD8(+) T cell persistence in chronic infection. *Nat Immunol* 20, 890-901. 10.1038/s41590-019-0403-4.

Yeku, O., Li, X., and Brentjens, R.J. (2017). Adoptive T-Cell Therapy for Solid Tumors. *Am Soc Clin Oncol Educ Book* 37, 193-204. 10.14694/EDBK\_180328. 10.1200/EDBK\_180328.

### 3.4 Extended results

#### *Impact of gamma c cytokines on the activation of CD8 T cells in vitro*

Other gamma c cytokines, such as IL-4, IL-7, IL-15 and IL-21, also play specific roles in the activation of CD8 T cells. In order to explore whether these cytokines could support CD8 T cells activation, we first compare their impact on CD8 T cells activated at a high cell density in vitro. After 4 days of activation, priming in the presence of gamma c cytokines IL-7, IL-15 and IL-21 did not change the number of divided CD8 T cells obtained except for ex-IL-4 that induced a strong reduction in the number of divided CD8 T (Figure E1A). In line with these results, the number of divisions performed by CD8 T cells was not increased by these cytokines, however, ex-IL-4 lead to a large fraction of undivided cells and a reduced number of CD8 T cells in each cell division (Figure E1B). To further explore whether these cytokines could cooperate with IL-2 to activate CD8 T cells in vitro, we also used these cytokines in combination with ex-IL-2 to activate CD8 T cells. After 4 days of activation, ex-IL4 still led to a reduction in CD8 T cells division (Figure E2A and E2B). Ex-IL-7, IL-15 and IL-21 did not modify CD8 T cell expansion in the presence of ex-IL-2 (Figure E2A, E2B). The impact of gamma c cytokine on activated CD8 T cells phenotype was next analyzed. Ex-IL-4 induced a strong upregulation of CD25 while ex-IL-21 potently down-regulated the expression of CD25 (Figure E1C). Ex-IL-7 and IL-15 had minimal effect on the expression of CD25 (Figure E1C). Ex-IL-4 also decreased the expression of TCF1 to a larger extent than ex-IL-2. Ex-IL-7, IL-15 and IL-21 did not significantly change the expression of TCF1 (Figure E1C). The expression of Bcl2 was enhanced by ex-IL-2 and IL-4, reduced by ex-IL-21, but not influenced by ex-IL-7 and IL-15 (Figure E1C). When ex-IL-2 was combined with ex-IL-7 and IL-15, the expression of CD25, TCF1 or Bcl2 was not modified. While the expression of CD25 was increased, or decreased in co-addition of ex-IL-2 and ex-IL-4 or ex-IL-21 respectively. The expression of TCF1 was still decreased in presence of ex-IL-4 (Figure E2C). Overall, ex-IL-7, IL-15 and IL-21 similarly to ex-IL-2 did not impact CD8 T cell expansion, while ex-IL-4 did induce a strong reduction in the number of activated CD8 even in the presence of ex-IL-2. In terms of phenotype, ex-IL-7 and IL-15 did not modify the phenotype of cells whether IL-2 was present or not. While ex-IL-4 and IL-21 induced different specific cell phenotypes.

### ***Ability of CD8 T cells activated with gamma c cytokines in vitro to differentiate directly into memory cells***

Next, we explored the impact of gamma c cytokines during the primary response on the capacity of cells to directly differentiate into memory cells. Since ex-IL-2 activation was able to enhance the frequency of memory cells generated compared to activation in absence of ex-cytokines, we transferred CD8 T cells activated in presence of ex-IL-4, ex-IL-7 and ex-IL-15, ex-IL-21, in combination with ex-IL-2 into naive mice. The number of F5 memory CD8 T cells recovered from spleen and lymph nodes was analyzed 30 days post-activation. We recovered similar number of memory cells in the spleen and lymph nodes derived from CD8 activated with different gamma c cytokines except for CD8 activated in presence of ex-IL-21 where the number of memory cells formed was strongly decreased (Figure E3A). Moreover, cells activated in presence of ex-IL-21 differentiated into CD27<sup>+</sup>CD43<sup>+</sup> memory cells with a decrease in the frequency of CD27<sup>+</sup>CD43<sup>-</sup> cells (Figure E3B). Ex-IL-4, ex-IL-7 and ex-IL-15 did not influence the expression of CD27 or CD43 (Figure E3B). The expression of CD62L by memory CD8 T cells was decreased by ex-IL-4 and ex-IL-21 but not by ex-IL-7 and ex-IL-15 (Figure E3C). Finally, the ability to produce IFN- $\gamma$  and TNF $\alpha$  by memory CD8 T cells upon re-stimulation was not influenced by ex-IL-4, ex-IL-7 and ex-IL-15 but was decreased by ex-IL-21 (Figure E3D). Therefore, the presence of ex-IL-7 and ex-IL-15 during priming does not affect the activation of CD8 T cells and their capacity to differentiate in memory cells. In contrast, IL-4 strongly impact the activation of CD8 in vitro, but the reduced number of CD8 that are generated are able to differentiate into memory cells. Addition of ex-IL-21 did not affect the number of activated CD8 generated, but these cells were impaired in their capacity to differentiate into memory cells.

## **Extended Methods**

### *Cell culture and stimulation*

CD44<sup>-</sup> naive F5 CD8 T cells CD8 T cells isolation were described in section 3.3 material and method.  $1.5 \times 10^5$  CTV-labelled F5 CD8 T cells were cultured with CpG matured, peptide

loaded BMDC including  $1.5 \times 10^4$  cDC in the presence or absence of 5% murine rIL-2 supernatant (corresponding to 230 ng/mL), 20ng/mL mIL-4; 10ng/mL mIL-7; 20ng/mL mIL-15 or 25ng/mL mIL-21. mIL-4, mIL-7; mIL-15 and mIL-21 were all from Miltenyi Biotec.

#### *Adoptive transfer*

$1.8 \times 10^7$  CTV labelled-F5 were activated with  $1.8 \times 10^6$  NP68-loaded matured BMDCs in the presence of 5% murine rIL-2 supernatant, in T25 flasks for 4 days. 20ng/mL mIL-4; 10ng/mL mIL-7+ 20ng/mL mIL-15 or 25ng/mL mIL-21 were added respectively at the beginning of the culture. Total lymphocytes were isolated using pancoll mouse (PAN-Biotech, P04-64100) following manufacturer's instructions. Then total cells containing 1 million CD8 T cells were adoptively transferred in naive mice by intravenous injection (i.v.).

### **Extended Figure Legends**

**Figure E1. Impact of gamma c cytokines on the activation CD8 T cells in vitro.**  $1.5 \times 10^5$  purified naive F5 CD8 T cells were cultured with CpG matured, peptide loaded BMDC including  $1.5 \times 10^4$  cDC for 4 days in vitro. 5% supernatant IL-2, recombinant IL-4, IL-7, IL-15 and IL-21 were added. Cells activated without any cytokine are regarded as control.

**A.** Numbers of divided CD8 T cells.

**B.** CD8 proliferation was analyzed after 4 days by CTV dilution in the presence of one specific cytokines (black) or no cytokine (grey) and represented as overlay histogram.

**C.** Expression of CD25, TCF1 and Bcl2 by divided CD8 T cells was analyzed 4 days after activation. Representative histograms of cells cultured in the presence of one specific cytokines (black) or no cytokine (grey) and individual expression are shown.

The results are from one out of three independent experiments. The statistical significance of differences was determined by the student t test (\*\*\*\* $p < 0.0001$ ).

**Figure E2. Impact of gamma c cytokines cooperating with IL-2 on the activation CD8 T cells in vitro.**  $1.5 \times 10^5$  purified naive F5 CD8 T cells were cultured with CpG matured, peptide loaded BMDC including  $1.5 \times 10^4$  cDC for 4 days in vitro. 5% supernatant IL-2, 5% supernatant IL-2+recombinant IL-4, 5% supernatant IL-2+recombinant IL-7, 5%

supernatant IL-2+recombinant IL-15 and 5% supernatant IL-2+recombinant IL-21 were added, respectively. Cells activated without any cytokine are regarded as control.

**A.** Numbers of divided CD8 T cells.

**B.** CD8 proliferation was analyzed after 4 days by CTV dilution in the presence of IL-2 alone (red) or IL-2 in combination with one specific cytokines (black) or no cytokine (grey) and represented as overlay histogram.

**C.** Expression of CD25, TCF1 and Bcl2 by divided CD8 T cells was analyzed 4 days after activation. Representative histograms of cells cultured in the presence of IL-2 alone (red) or IL-2 in combination with one specific cytokines (black) or no cytokine (grey) are shown for CD25. Individual expression (MFI or percentage of positive cells) are shown.

**Figure E3. Impact of gamma c cytokines cooperating with IL-2 during activation on the generation of memory CD8 T cells.** F5 Splenocytes, containing  $1.8 \times 10^7$  F5 CD8 T cells, were cultured with CpG matured, peptide loaded BMDC including  $1.8 \times 10^6$  cDC in T25 flask. 5% supernatant IL-2 were added. IL-4, IL-7+ IL-15, IL-21 were added, respectively. After 4 days, total lymphocytes were adoptively transferred into C57BL/6J naive mice. Each mouse received 1 million CD8 T cells.

**A.** Numbers of TCR V $\beta$ 11+ F5 CD8 T cells recovered from spleen and drain lymph node (drain LN) on day30.

**B.** Individual percentages of CD27+CD43- and CD27+CD43+ cells among TCR V $\beta$ 11+ F5 CD8 T cells recovered from spleen on day30.

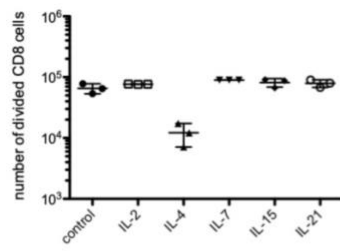
**C.** Expression of CD62L by TCR V $\beta$ 11+ F5 CD8 T cells from spleen on day30.

**D.** On day30,  $3 \times 10^6$  spleen cells were re-stimulated with 10nM NP68 peptide for 4 hours in vitro. The percentage of IFN- $\gamma$  and TNF $\alpha$ -producing F5 CD8 T cells among TCR V $\beta$ 11+ F5 CD8 T cells are shown.

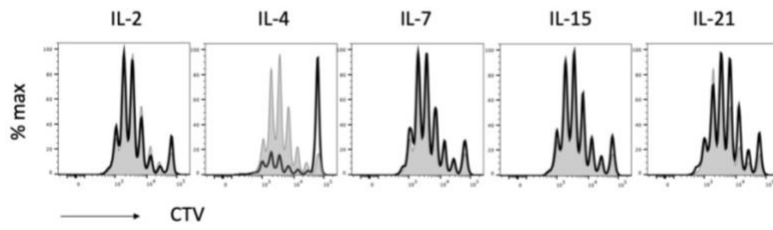
The results are expressed as the mean of triplicates  $\pm$  SD for one experiment (n=5 mice per group). The statistical significance of differences was determined by one-way ANOVA Friedman test (\*p<0.05, \*\*p<0.005, \*\*\*p<0.0001).

Figure E1

A



B



C

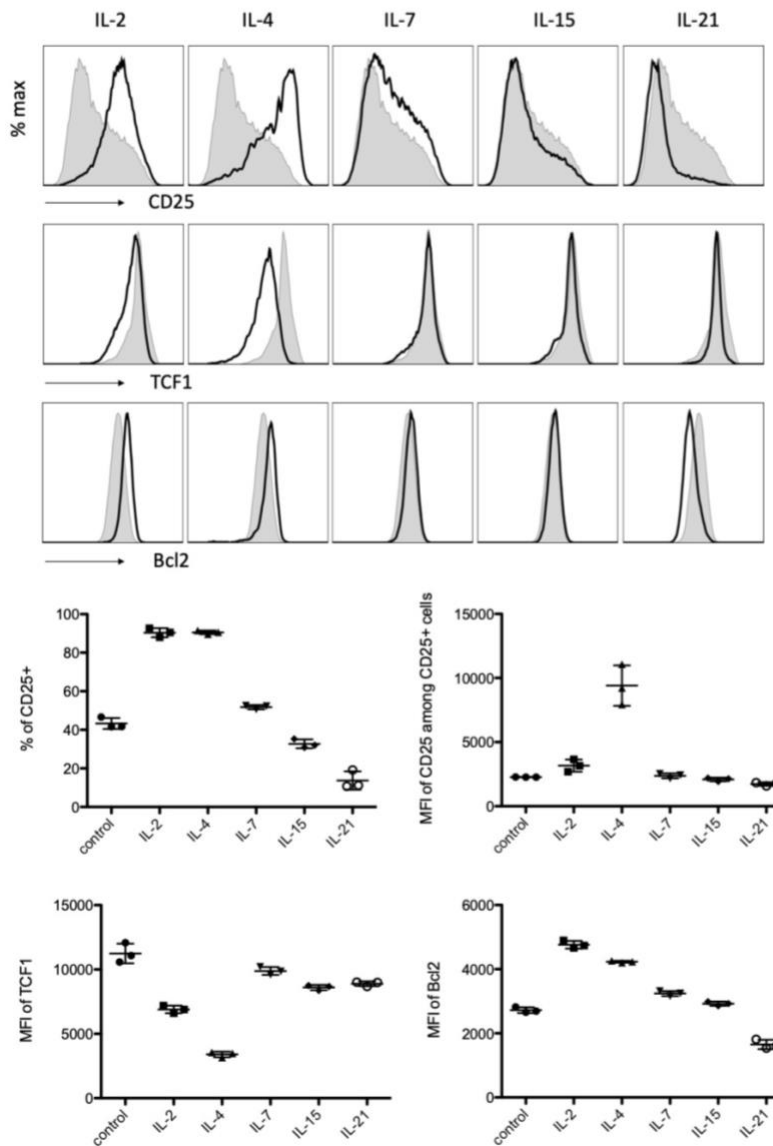
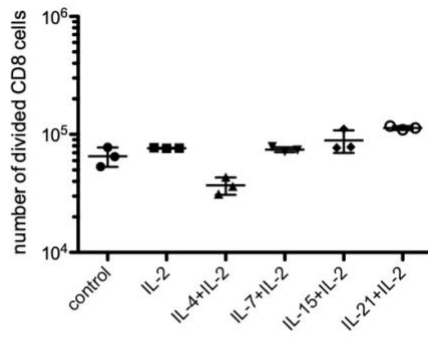
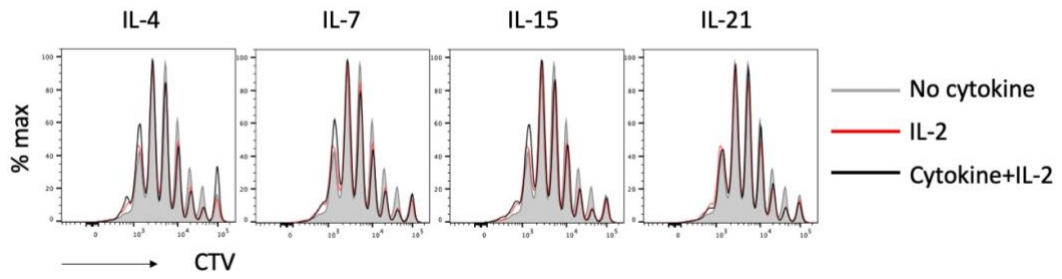


Figure E2

A



B



C

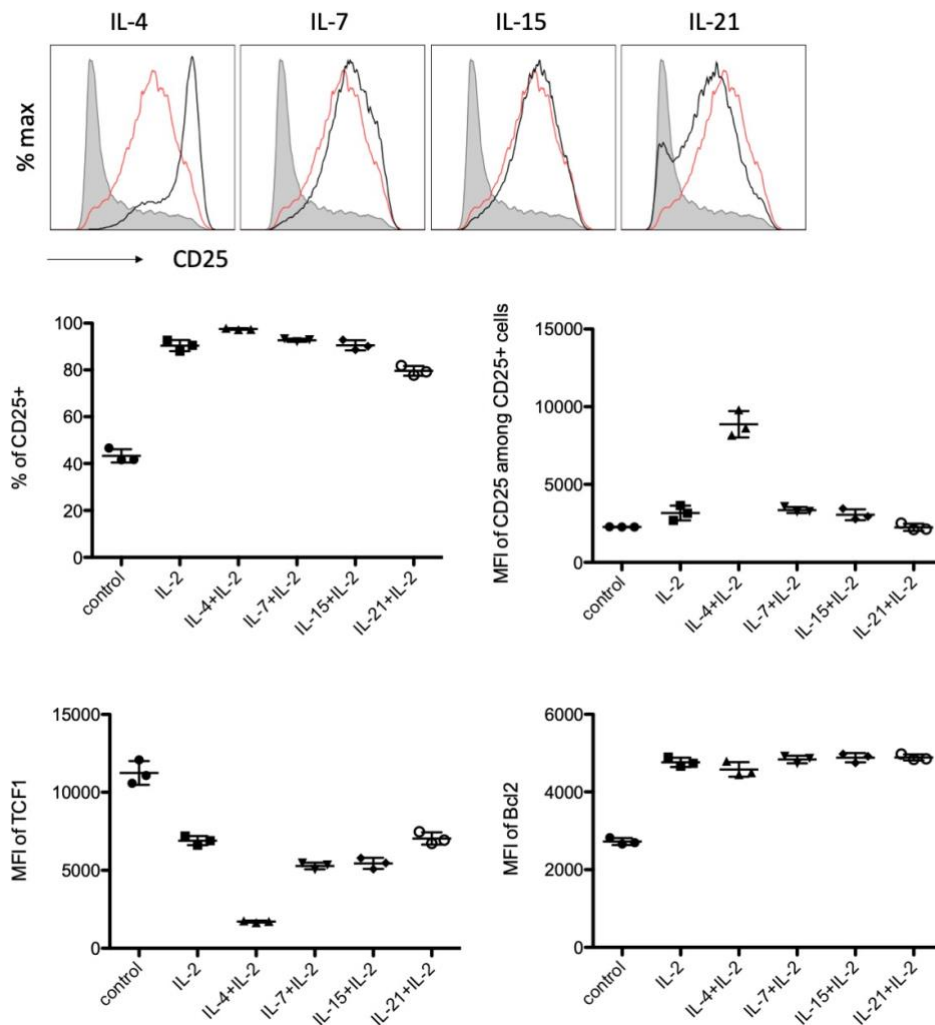
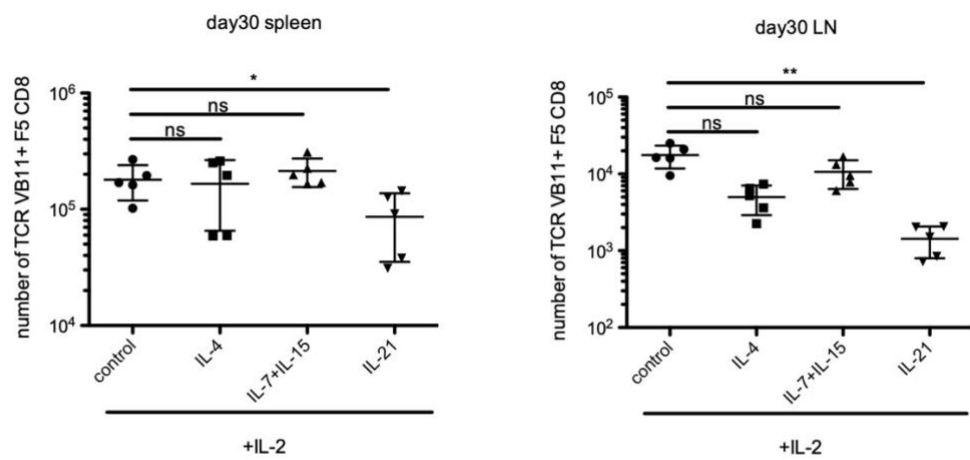
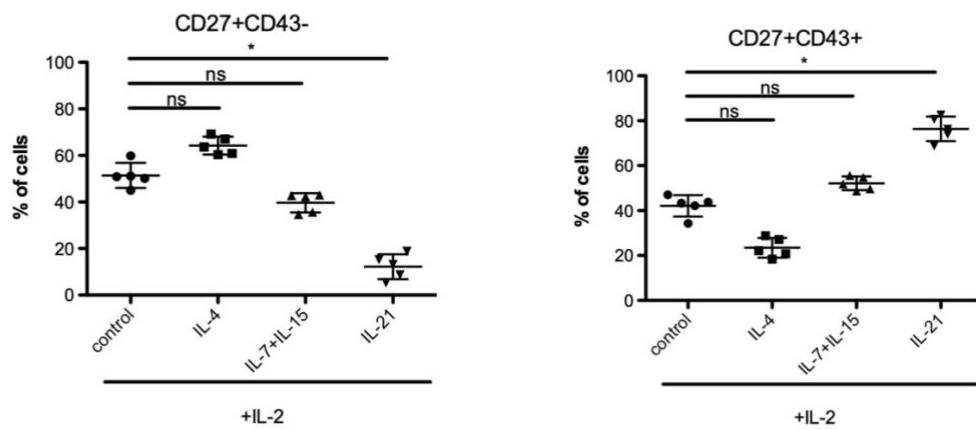


Figure E3

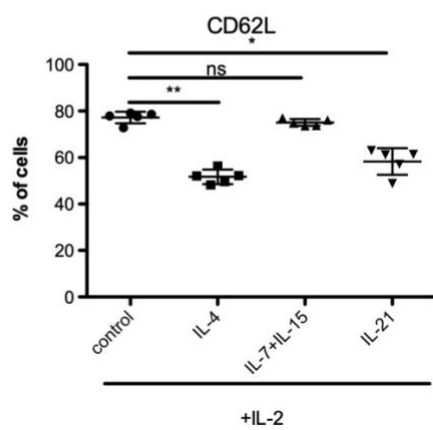
A



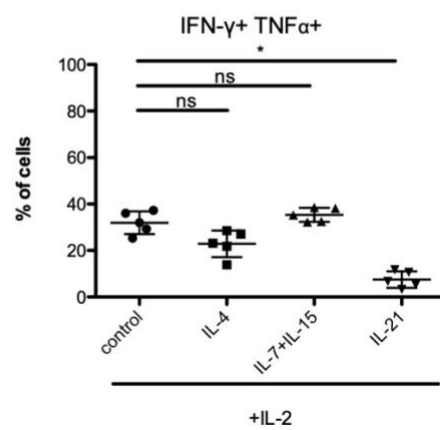
B



C



D



## 4 Discussion and perspectives

T Lymphocytes engineered to express a chimeric antigen receptor (CAR) have become a well-known achievement in anticancer immunotherapy. CAR-T cells modified to recognize CD19 have been shown effective in the therapy of chronic lymphocytic leukemia (CLL) and acute lymphoblastic leukemia (AAL) (Fry et al., 2018; Grupp et al., 2013; Kochenderfer et al., 2010). To design CAR-T cells, patients' T cells are isolated from peripheral blood and modified ex-vivo with the CAR. The CAR-T cells are activated and acquire effector functions such as cytokine production and lytic degranulation when recognizing their targets (Gacerez et al., 2016; Hu et al., 2019; Lim and June, 2017; Srivastava and Riddell, 2015). Before transduction, the T cells are first activated and expanded in vitro usually by culturing with anti-CD3/anti-CD28 beads supplemented with IL-2. The robust proliferation, long-term survival and memory generation of CAR-T cells in vivo are considered as critical predictors of clinical response in patients with B-cell malignancies and solid tumor (Collinson-Pautz *et al.*, 2019; Sengupta *et al.*, 2018; Yeku *et al.*, 2017). The quality of T cells that are transferred is one of the important factors that limit the therapy, indeed T cells can become exhausted following their in vitro expansion leading to decreased persistence and lack of effector functions once in vivo (Gattinoni *et al.*, 2005; Gattinoni *et al.*, 2011; Hinrichs *et al.*, 2009). Hence, the definition of culture condition will be one of the potentials to improve the quality of CAR-T cells generated. In our study, we tested different culture conditions to activate CD8 T cells in vitro and then transferred the activated CD8 T cells in vivo to let them differentiate into memory cells. We mainly focus on the impact of exogenous-IL-2 on the activation of CD8 T cells and the generation of memory CD8 T cells.

### 4.1 Comparison of different culture conditions

TCR signals (signal 1), co-stimulation (signal 2) and inflammatory cytokines (signal 3) play central roles in the activation of CD8 T cells (Williams and Bevan, 2007). Activation signals provided by anti-CD3/anti-CD28 beads and DCs are different (Figure 23). Peptide activation provides a weak signal through TCR receptor. The presence of other spleen cells (containing CD4 T cells, NK cells and so on) may also amplify the strength provided by DCs

and provide more activation signals such as IL-2 and other cytokines.

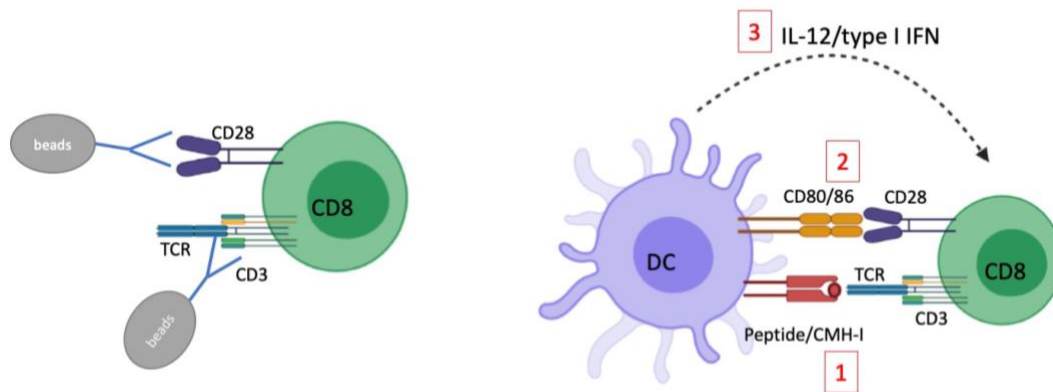


**Figure 23. Activation signals by anti-CD3/anti-CD28 beads and DCs.** Anti-CD3/anti-CD28 beads activate CD8 T cells through signal 1 and signal 2. DCs induce the activation of CD8 T cells through signal 1, signal 2 and signal 3.

Accordingly, the number of activated CD8 T cells generated was different when activating purified CD8 T cells with anti-CD3/anti-CD28 beads or NP68 peptide alone or NP68 pulsed DCs in the absence or presence of feeder cells. The number of divided CD8 T cells increased when different type of signals was present, however, the numbers were never increased by the addition of ex-IL-2 (Figure 24). This also demonstrated that ex-IL-2 was not essential for the initial expansion of naive CD8 T cells when seeded at high a high density of responding cells. It is important to note that activation of TCR transgenic CD8 T cells by their cognate peptide is similar to activation by anti-CD3/CD28 of polyclonal CD8 cells in terms of density of responding cells.

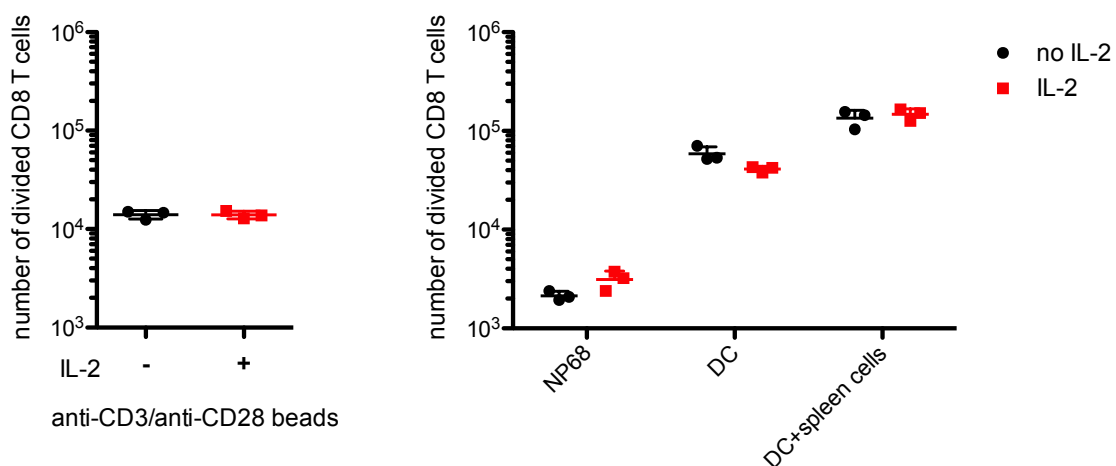


**Figure 24. Number of activated CD8 T cells generated after 4 days following activation in different context.**  $1.5 \times 10^5$  purified naive F5 CD8 T cells were cultured with 10nM NP68 peptide,  $1.5 \times 10^5$  anti-CD3/anti-CD28 beads (ratio of beads: CD8=1:4),  $1.5 \times 10^4$  DCs and  $1.5 \times 10^4$  DCs in supplement with  $3 \times 10^5$  C57BL/6J feeders respectively for 4 days. 5% supernatant IL-2 was added or not. The number of divided CD8 T cells is shown.

Co-stimulation through the interaction of CD80/CD86 and CD28 is required for the generation of CTL responses in mice following the infection by a virus or bacteria (Andreasen et al., 2000; Shedlock et al., 2003; Sigal *et al.*, 1998). The proliferation of CD8 T cells is significantly decreased when they are stimulated by CD80 and CD86 double knockout antigen presenting cells (McAdam *et al.*, 1998). In our study, we used CpG ODNs to mature BMDCs leading to the expression of co-stimulation receptors such as CD86 on the surface of BMDCs. To analyze the activation of CD8 T cells in the absence of co-stimulation we used BMDCs that have not been matured with CpG to activate CD8 T cells. We found that activation with BMDCs that had not been matured with CpG reduced the expansion of CD8 T cells and this reduction could not be compensated by the presence of ex-IL-2 (Figure 25A). After adoptive transfer of CD8 T cells activated with mature or immature BMDCs in the presence of ex-IL-2 into naive mice, activation with immature BMDCs reduced the generation of memory cells. While they had the same potential to participate in the immune response when they were transferred in to vaccinia virus infected mice (Figure 25B). Therefore, ex-IL-2 was unable to compensate the activation provided by the interaction of CD80/CD86 and CD28 to allow direct generation of memory cells in vivo.

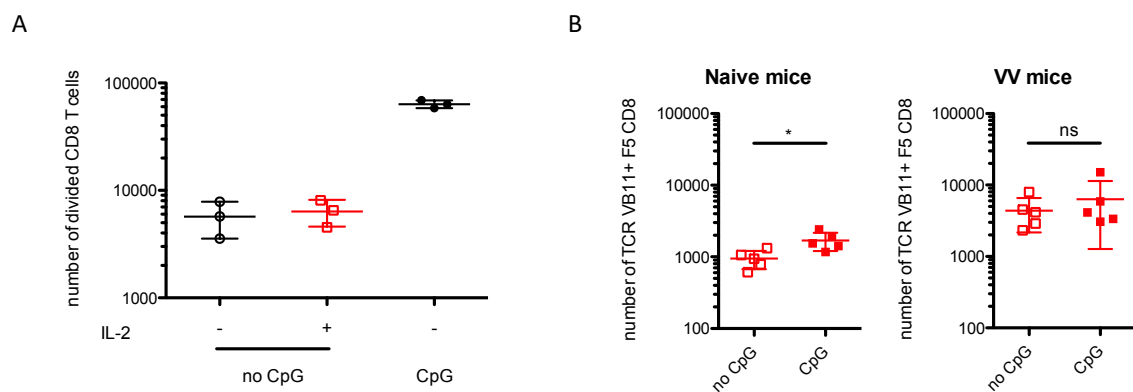


**Figure 25. Activation of CD8 T cells with BMDCs that had been matured with CpG reduced the**

**expansion and memory formation in naive mice. A.**  $1.5 \times 10^5$  purified naive F5 CD8 T cells were cultured with  $1.5 \times 10^4$  BMDCs that had been matured with CpG or not. 5% supernatant IL-2 were added or not. The number of divided CD8 T cells was calculated 4 days after activation. **B.**  $1.5 \times 10^5$  purified naive F5 CD8 T cells were cultured with  $1.5 \times 10^4$  BMDCs that had been matured with CpG or not. 5% supernatant IL-2 were added. Then on day4 divided CD8 T cells were transferred into naive mice or mice that had been infected with vaccinia virus 4 days earlier.

IL-12 and type I IFN produced by DCs serve as signal 3 to activate naive CD8 T cells. IL-12 is essential for the development of enhanced function by effector CD8 T cells and the differentiation in efficient memory CD8 T cells (Curtsinger *et al.*, 2003; Mescher *et al.*, 2006). The presence of IL-12 during the activation of CD8 T cell in vitro enhances the expression of T-bet and drives the differentiation of SLEC (Joshi *et al.*, 2007). In our study, we also found that CD8 T cells activated with ex-IL-12 express higher level of CD25, T-bet but lower level of TCF1 (data not show), indicating that ex-IL-12 promotes the differentiation to effector cells in vitro.

## 4.2 The role of IL-2

### Intrinsic IL-2 (int-IL-2) versus exogenous IL-2 (ex-IL-2)

The IL-2 produced by CD8 T cells (intrinsic IL-2) is considered to be essential for the activation of CD8 T cells (Feau *et al.*, 2011). Indeed, int-IL-2 deficiency potently impedes the generation of protective memory CD8 T cells that could mount a secondary response (Feau *et al.*, 2011). A genetically induced increased in the production of int-IL-2 by CD8 T cells enhances the formation of memory cells and their secondary expansion (Redeker *et al.*, 2015), suggesting that int-IL-2 promotes memory formation. In our study, we found that culturing CD8 T cells with DCs led to the secretion of IL-2 in the supernatant. And the concentration of IL-2 in the supernatant declined following time, suggesting that intrinsic IL-2 in the supernatant was used by activated CD8 T cells. However, the int-IL-2 was unable to maintain the expression of CD25, EOMES and Bcl-2, which were maintained in the presence of ex-IL-2. The role of exogenous-IL-2 was studied in different models. The fact that IL-2 deficiency in CD8 cannot be rescued by the IL-2 produced by CD4 T cells, while IL-2 proficient CD8 T cells generate memory cells without CD4-IL-2 help argues for

a unique role of CD8-intrinsic-IL-2 in the generation of functional memory CD8 (Feau *et al.*, 2011). However, wild-type CD8 T cells generate more memory cells following ex-IL-2 treatment during the contraction phase in LCMV-infected mice (Blattman *et al.*, 2003) indicating that ex-IL-2 can also favor memory CD8 T cell development. Therefore, both int-IL-2 and ex-IL-2 could play a role in promoting the memory CD8 T cell formation. Our results show that wild type CD8 T cells, following DC activation *in vitro*, are able to differentiate to memory cells following transfer in a naive host, however, if they are activated in the presence of ex-IL-2, more memory cells are generated indicating a positive impact of ex-IL-2.

## **Exogenous IL-2 dosage**

Pipkin *et al.* found that the expression of CD25 progressively increases when increasing the dosage of ex-IL-2 from 1U/mL to 10U/mL and to 100U/mL, and CD8 T cells activated with 10 U/mL recombinant IL-2 generate more memory cells than CD8 T cells activated with 100 U/mL recombinant IL-2 following adoptive transfer into naive mice. (Pipkin *et al.*, 2010). This is in agreement with the finding that CD25<sup>hi</sup> cells tend to give rise to terminally differentiated effector cells (Kalia *et al.*, 2010). Thus, these results suggested that increasing the concentration of ex-IL-2 impaired the formation of memory cells. However, the IL-2 used by Pipkin *et al.* is calculated by U/mL, and we don't know whether they refer to international Units and they did not mention the origin of the product. Thereby, it's hard to compare with the concentration of IL-2 we used.

A survey of the literature indicates that the dosage of ex-IL-2 used to culture T cells varies from 30 IU/mL (Yang *et al.*, 2017) to 3000 IU/mL (Sengupta *et al.*, 2018). In another paper, the IL-2 dosage is 100U/mL corresponding to 20ng/mL (Collinson-Pautz *et al.*, 2019). The dosage of ex-IL-2 we used in our study, i.e. 11.5ng/mL (1483.5 IU/mL), is in a similar range and corresponds, in our model, to the lowest concentration giving the maximal expression of CD25. Therefore, the study we have performed is relevant to studies using ex-IL-2 that are currently performed.

## **The impact of ex-IL-2 during primary activation on the differentiation of CD8 T cells in naive host**

Here, we found that CD8 T cells activated with and without ex-IL-2 both differentiate to memory cells upon adoptive transfer in an antigen free environment. This partially corresponds to the finding that weak IL-2 signals during priming drives the differentiation to memory cells (Pipkin *et al.*, 2010). The single-cell transcriptomic data show that CD8 T cells activated without ex-IL-2 become memory precursors as soon as 4 days after activation while CD8 T cells activated with ex-IL-2 acquire effector functions. Moreover, CD8 T cells activated with ex-IL-2 tend to generate more memory cells. This indicates that CD8 T cells activated without ex-IL-2 differentiate in memory precursors earlier, while activation with ex-IL-2 delays their transition to memory precursors (Figure 26).

Accordingly, memory CD8 T cells generated by cells activated in the presence of ex-IL-2 express high level of integrins, such as CD29, CD49a and CD49d and produce more IFN- $\gamma$  and CCL5 upon re-stimulation. This is in line with the finding that following activation memory precursors are constantly generated and memory cells produced at later time point (7 days post infection) express higher level of CCL5 than those differentiate at earlier time points (4,5 days post infection) (Todorov *et al.* submitted 2022).

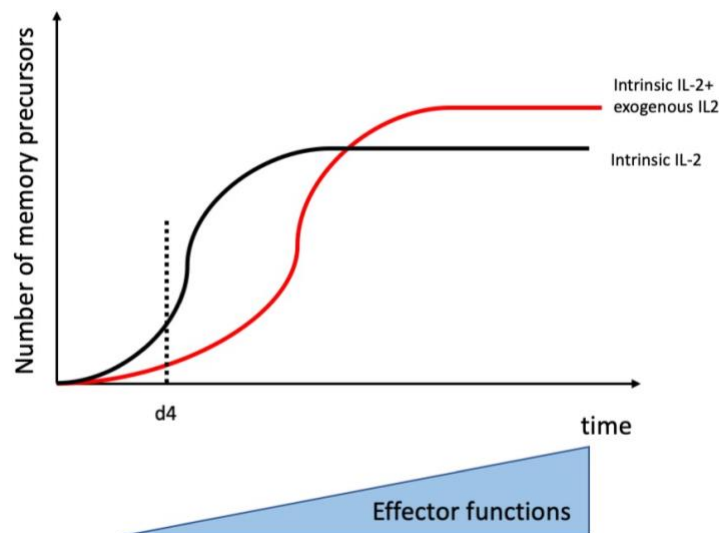


**Figure 26. Impact of ex-IL-2 on the generation of memory precursors with time.** CD8 T cells activated with ex-IL-2 generate memory precursors later than that activated without ex-IL-2. At later time, ex-IL-2 activation induce more memory precursors formation.

Furthermore, the phenotype of memory CD8 T cells generated is impacted by the presence of ex-IL-2. The memory CD8 T cell pool is heterogeneous (Mueller *et al.*, 2013).

CD62L is a marker to discriminate the two well-known memory subsets  $T_{CM}$  and  $T_{EM}$ .  $T_{CM}$  cells express high level of CD62L and  $T_{EM}$  cells have low expression level of CD62L (Sallusto *et al.*, 1999). In our model, CD8 T cells activated with and without ex-IL-2 differentiate in similar number of  $T_{CM}$  and  $T_{EM}$  subsets when they are transferred in naive mice. Based on the expression of CD27 and CD43, memory cells have been subdivided into three subsets: CD27+/CD43+, CD27+/CD43- and CD27-/CD43- subsets. CD27+ CD43+ cells expressed a higher level granzyme B than CD27+ CD43- cells, indicating that CD27+ CD43+ cells develop more effector functions than CD27+ CD43- cells. However, the two subsets: CD27+ CD43- and CD27+ CD43+ produced similar level of IFN- $\gamma$  and TNF- $\alpha$  upon re-stimulation with peptide in vitro for 5h (Hikono *et al.*, 2007). In our study, CD8 T cells activated with ex-IL-2 generate more CD27+/CD43+ and less CD27+/CD43- cells after adoptive transfer in naive mice. This corresponds to the fact that the presence of ex-IL-2 during priming leads to the generation of memory CD8 T cells that have acquired more effector function. However, in contrast to the finding of Hikono *et al.*, we found that after re-stimulation with NP68 peptide for 4h in vitro, they produced more IFN- $\gamma$ . Thus, there isn't a strict correlation between the phenotype and the capacity to produce IFN- $\gamma$ . The expression of CX3CR1 defines three subsets: CX3CR1<sup>hi</sup>, CX3CR1<sup>int</sup>, CX3CR1<sup>-</sup> (Gerlach *et al.*, 2016). In our model the memory cells generated from in vitro activated CD8 T cells with or without ex-IL-2 did not express CX3CR1.

## **The impact of ex-IL-2 during primary activation on the differentiation of CD8 T cells in virus-infected mice**

Early administration of ex-IL-2 to acute virus-infected mice does not influence the generation of memory CD8 T cells (Blattman *et al.*, 2003). Therefore, the presence of ex-IL-2 during priming has minimal effect on the differentiation of memory CD8 T cells in mice following an acute infection by a virus. In DC immunized-mice, administration of IL-2-complexed with an anti-IL-2 antibody to increase the IL-2 half-life early after priming (days 1-3) enhances the memory CD8 T cell formation, while late administration (days 4-6) promotes the terminal differentiation of CD8 T cell (Kim *et al.*, 2016). In our study, when we adoptively transfer the activated CD8 T cells into vaccine virus-infected mice, we found that the CD8 T cells activated in vitro for 4 days are agile and able to expand a lot and

differentiate in memory cells. These cells have a similar phenotype as endogenous cells or F5 CD8 T cells transferred in mice before the viral challenge, indicating that in vitro activated CD8 are able to fully differentiate once restimulated by antigen in a virus induced activation environment. However, CD8 T cells activated with and without ex-IL-2 generate similar number of effector and memory cells with similar phenotype following adoptive transfer into vaccine virus-infected mice.

Importantly, when CD8 activated in the presence of ex-IL-2 are transferred in naive host they give rise to memory cells that have a surface phenotype that is close to the one induced by the virus.

### Can we identify memory precursor cells in vitro?

CD25<sup>hi</sup> cells tend to give rise to terminally differentiated effector cells while the CD25<sup>lo</sup> CD8 T cells are able to differentiate to long lived functional memory cells when they are adoptively transferred into infection-matched recipients (Kalia *et al.*, 2010). TCF1 is an important memory precursor marker (Todorov *et al.* submitted 2022) and is essential for the differentiation of memory CD8 T cells (Zhao *et al.*, 2010). We found CD8 T cells activated with and without ex-IL-2 generate both CD25<sup>+</sup> cells and CD25<sup>-</sup> cells, but ex-IL-2 decreases the expression of TCF1 in both CD25<sup>+</sup> cells and CD25<sup>-</sup> cells. And according to the expression of TCF1, CD25<sup>+</sup> cells can be subdivided into CD25<sup>hi</sup> and CD25<sup>int</sup> cells, and CD25<sup>int</sup> cells express lower level of TCF1 than CD25<sup>hi</sup> cells (Figure 27), indicating that the expression of TCF1 does not completely correlate with the expression of CD25.

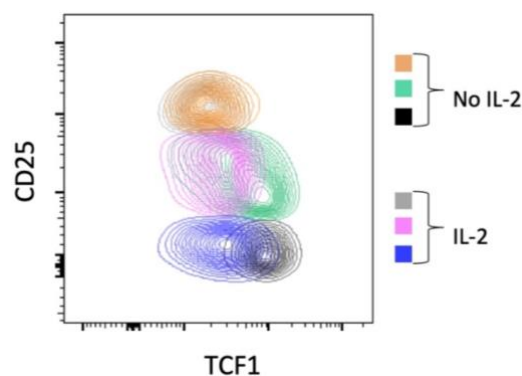


**Figure 27. The expression of CD25 and TCF1 by CD8 T cells 4 days after activation.** 5x10<sup>4</sup> purified naive F5 CD8 T cells were cultured with 5x10<sup>3</sup> BMDCs in the presence or absence of 5%

supernatant IL-2 for 4 days. Co-expression of TCF1 and CD25 as assessed by flow-cytometry is shown.

Ly108/Slamf6 is a surface marker that has been used as a surrogate for the intracellular expression of TCF1 transcription factor (Beltra *et al.*, 2020). In our hands, the expression of Ly108 and TCF1 did not correlate well. Therefore, we have been unable to sort live cells according to the expression of TCF1 in order to test their differentiation potential *in vivo* following transfer.

### **4.3 The role of IL-4, IL-7, IL-15 and IL-21**

Other common  $\gamma$ -chain ( $\gamma$ c) cytokines, such as IL-4, IL-7, IL-15 and IL-21, also play a central role in cellular proliferation, differentiation and survival of CD8 T cells (Shourian *et al.*, 2019). We found ex-IL-4- and ex-IL-21-induced CD8 T cells exhibited different phenotypes from that induced by ex-IL-2. Previous works have shown that IL-4 inhibits the CTL function of CD8 T cells (Croft *et al.*, 1994) and IL-21 induces a less differentiated phenotype on CD8 T cells (Hinrichs *et al.*, 2008). While IL-2 drives the differentiation of terminally differentiated cells (Hinrichs *et al.*, 2008). In presence of IL-2, the addition of ex-IL-4 and ex-IL-21 still altered the phenotype of memory CD8 T cells generated. Thus, IL-4 and IL-21 may be used to generate new subsets. In order to explore the specific role of IL-4 and IL-21 on the generation of memory CD8 T cells, we could activate CD8 T cells with IL-4 or IL-21, respectively and then transfer the activated cells into naive or virus-infected mice and analyze the frequency and phenotype of CD8 T cells.

Ex-IL-7 and ex-IL-15 did neither alter the phenotype of activated CD8 T cells *in vitro* nor influence the generation of memory CD8 T cells when they synergized with ex-IL-2. IL-7 plays a crucial role in mediating the survival of naive and memory CD8 T cells while IL-15 is important for the homeostatic proliferation of memory CD8 T cells (Schluns and Lefrancois, 2003). Therefore, as the presence of ex-IL-7 and ex-IL-15 during the early activation has minimal effect on the activation and differentiation of CD8 T cells, they may play a role at later time point.

## 5 Conclusion

In this research, we mainly focus on the role of ex-IL-2 on the activation of CD8 T cells and the impact of ex-IL-2 activation in vitro on the generation of memory precursor cells. We find that ex-IL-2 activation during priming increases the expansion of CD8 T cells when their initial density is low but does not alter the proliferation of CD8 T cells when the initial density is high. Furthermore, ex-IL-2 induces the CD8 T cells to acquire effector phenotypes 4 days after activation whether CD8 T cell were culture at high or low cell density. CD8 cells cultured at higher density show a better differentiation to T<sub>CM</sub> cells.

CD8 T cells activated without any ex-IL-2 are fit and able to participate in an ongoing, in vivo, immune response. The memory cells that they generated are undistinguishable from those that are derived from cells activated with ex-IL-2 in terms of frequency and phenotype.

In contrast, when we transfer the activated CD8 T cells in naive host to allow them to differentiate directly in memory cells, CD8 T cells activated without ex-IL-2 generate less memory cells than those activated with ex-IL-2. Finally, without ex-IL-2 during priming, memory cells do not express integrin and produce less IFN- $\gamma$  upon re-stimulation, indicating that they are less differentiated (Figure 28).

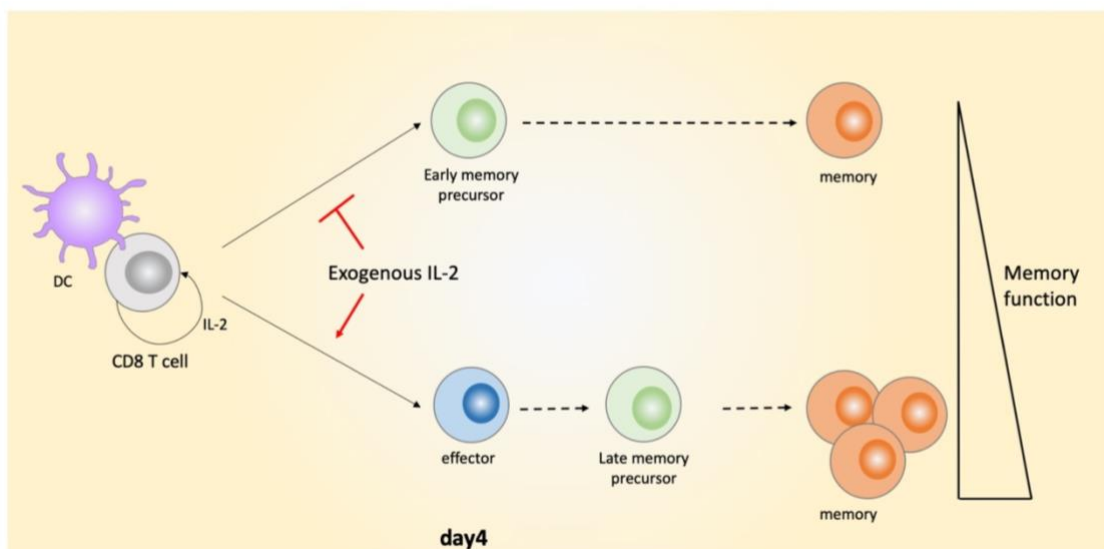


**Figure 28.** The impact of ex-IL-2 in vitro addition on the activation and differentiation of CD8 T

**cells.** Activation with ex-IL-2 decreases the memory precursors formation 4 days after activation but may induce the generation of memory precursors that give rise to memory cells with more imprinted memory functions.

Thus, we propose that ex-IL-2 delays the transition to memory precursors, allowing cells to acquire effector functions that become imprinted in the memory cells generated.

## Reference

- Acacia de Sa Pinheiro, A., Morrot, A., Chakravarty, S., Overstreet, M., Bream, J.H., Irusta, P.M., and Zavala, F. (2007). IL-4 induces a wide-spectrum intracellular signaling cascade in CD8+ T cells. *J Leukoc Biol* 81, 1102-1110. 10.1189/jlb.0906583.
- Acuto, O., and Michel, F. (2003). CD28-mediated co-stimulation: a quantitative support for TCR signalling. *Nat Rev Immunol* 3, 939-951. 10.1038/nri1248.
- Agarwal, P., Raghavan, A., Nandiwada, S.L., Curtsinger, J.M., Bohjanen, P.R., Mueller, D.L., and Mescher, M.F. (2009). Gene regulation and chromatin remodeling by IL-12 and type I IFN in programming for CD8 T cell effector function and memory. *J Immunol* 183, 1695-1704. 10.4049/jimmunol.0900592.
- Ahmadzadeh, M., Johnson, L.A., Heemskerk, B., Wunderlich, J.R., Dudley, M.E., White, D.E., and Rosenberg, S.A. (2009). Tumor antigen-specific CD8 T cells infiltrating the tumor express high levels of PD-1 and are functionally impaired. *Blood* 114, 1537-1544. 10.1182/blood-2008-12-195792.
- Ahrends, T., Spanjaard, A., Pilzecker, B., Babala, N., Bovens, A., Xiao, Y., Jacobs, H., and Borst, J. (2017). CD4(+) T Cell Help Confers a Cytotoxic T Cell Effector Program Including Coinhibitory Receptor Downregulation and Increased Tissue Invasiveness. *Immunity* 47, 848-861 e845. 10.1016/j.immuni.2017.10.009.
- Aibar, S., Gonzalez-Blas, C.B., Moerman, T., Huynh-Thu, V.A., Imrichova, H., Hulselmans, G., Rambow, F., Marine, J.C., Geurts, P., Aerts, J., et al. (2017). SCENIC: single-cell regulatory network inference and clustering. *Nat Methods* 14, 1083-1086. 10.1038/nmeth.4463.
- Alves, N.L., Arosa, F.A., and van Lier, R.A. (2007). Common gamma chain cytokines: dissidence in the details. *Immunol Lett* 108, 113-120. 10.1016/j.imlet.2006.11.006.
- Andreasen, S.O., Christensen, J.E., Marker, O., and Thomsen, A.R. (2000). Role of CD40 ligand and CD28 in induction and maintenance of antiviral CD8+ effector T cell responses. *J Immunol* 164, 3689-3697. 10.4049/jimmunol.164.7.3689.

- Angelosanto, J.M., Blackburn, S.D., Crawford, A., and Wherry, E.J. (2012). Progressive loss of memory T cell potential and commitment to exhaustion during chronic viral infection. *J Virol* 86, 8161-8170. 10.1128/JVI.00889-12.
- Appay, V., Dunbar, P.R., Callan, M., Klenerman, P., Gillespie, G.M., Papagno, L., Ogg, G.S., King, A., Lechner, F., Spina, C.A., et al. (2002). Memory CD8<sup>+</sup> T cells vary in differentiation phenotype in different persistent virus infections. *Nat Med* 8, 379-385. 10.1038/nm0402-379.
- Arsenio, J., Kakaradov, B., Metz, P.J., Kim, S.H., Yeo, G.W., and Chang, J.T. (2014). Early specification of CD8<sup>+</sup> T lymphocyte fates during adaptive immunity revealed by single-cell gene-expression analyses. *Nat Immunol* 15, 365-372. 10.1038/ni.2842.
- Arsenio, J., Metz, P.J., and Chang, J.T. (2015). Asymmetric Cell Division in T Lymphocyte Fate Diversification. *Trends Immunol* 36, 670-683. 10.1016/j.it.2015.09.004.
- Ashton-Rickardt, P.G. (2005). The granule pathway of programmed cell death. *Crit Rev Immunol* 25, 161-182. 10.1615/critrevimmunol.v25.i3.10.
- Bachmann, M.F., Schorle, H., Kühn, R., Müller, W., Hengartner, H., Zinkernagel, R.M., and Horak, I. (1995). Antiviral immune responses in mice deficient for both interleukin-2 and interleukin-4. *J Virol* 69, 4842-4846. 10.1128/JVI.69.8.4842-4846.1995.
- Badovinac, V.P., Haring, J.S., and Harty, J.T. (2007). Initial T cell receptor transgenic cell precursor frequency dictates critical aspects of the CD8(+) T cell response to infection. *Immunity* 26, 827-841. 10.1016/j.immuni.2007.04.013.
- Badovinac, V.P., Messingham, K.A., Jabbari, A., Haring, J.S., and Harty, J.T. (2005). Accelerated CD8<sup>+</sup> T-cell memory and prime-boost response after dendritic-cell vaccination. *Nat Med* 11, 748-756. 10.1038/nm1257.
- Badovinac, V.P., Porter, B.B., and Harty, J.T. (2004). CD8<sup>+</sup> T cell contraction is controlled by early inflammation. *Nat Immunol* 5, 809-817. 10.1038/ni1098.
- Banerjee, A., Gordon, S.M., Intlekofer, A.M., Paley, M.A., Mooney, E.C., Lindsten, T., Wherry, E.J., and Reiner, S.L. (2010). Cutting edge: The transcription factor eomesodermin enables CD8<sup>+</sup> T cells to compete for the memory cell niche. *J Immunol* 185, 4988-4992. 10.4049/jimmunol.1002042.

- Barber, D.L., Wherry, E.J., and Ahmed, R. (2003). Cutting edge: rapid in vivo killing by memory CD8 T cells. *J Immunol* 171, 27-31. 10.4049/jimmunol.171.1.27.
- Barber, D.L., Wherry, E.J., Masopust, D., Zhu, B., Allison, J.P., Sharpe, A.H., Freeman, G.J., and Ahmed, R. (2006). Restoring function in exhausted CD8 T cells during chronic viral infection. *Nature* 439, 682-687. 10.1038/nature04444.
- Beltra, J.C., Bourbonnais, S., Bedard, N., Charpentier, T., Boulange, M., Michaud, E., Boufaied, I., Bruneau, J., Shoukry, N.H., Lamarre, A., and Decaluwe, H. (2016). IL2Rbeta-dependent signals drive terminal exhaustion and suppress memory development during chronic viral infection. *Proc Natl Acad Sci U S A* 113, E5444-5453. 10.1073/pnas.1604256113.
- Beltra, J.C., Manne, S., Abdel-Hakeem, M.S., Kurachi, M., Giles, J.R., Chen, Z., Casella, V., Ngiow, S.F., Khan, O., Huang, Y.J., et al. (2020). Developmental Relationships of Four Exhausted CD8(+) T Cell Subsets Reveals Underlying Transcriptional and Epigenetic Landscape Control Mechanisms. *Immunity* 52, 825-841 e828. 10.1016/j.immuni.2020.04.014.
- Belz, G.T., and Masson, F. (2010). Interleukin-2 tickles T cell memory. *Immunity* 32, 7-9. 10.1016/j.immuni.2010.01.009.
- Bennett, S.R., Carbone, F.R., Karamalis, F., Miller, J.F., and Heath, W.R. (1997). Induction of a CD8+ cytotoxic T lymphocyte response by cross-priming requires cognate CD4+ T cell help. *J Exp Med* 186, 65-70. 10.1084/jem.186.1.65.
- Berard, M., Brandt, K., Bulfone-Paus, S., and Tough, D.F. (2003). IL-15 promotes the survival of naive and memory phenotype CD8+ T cells. *J Immunol* 170, 5018-5026. 10.4049/jimmunol.170.10.5018.
- Biasco, L., Scala, S., Basso Ricci, L., Dionisio, F., Baricordi, C., Calabria, A., Giannelli, S., Cieri, N., Barzaghi, F., Pajno, R., et al. (2015). In vivo tracking of T cells in humans unveils decade-long survival and activity of genetically modified T memory stem cells. *Sci Transl Med* 7, 273ra213. 10.1126/scitranslmed.3010314.

- Blackburn, S.D., Shin, H., Freeman, G.J., and Wherry, E.J. (2008). Selective expansion of a subset of exhausted CD8 T cells by alphaPD-L1 blockade. *Proc Natl Acad Sci U S A* 105, 15016-15021. 10.1073/pnas.0801497105.
- Blackburn, S.D., Shin, H., Haining, W.N., Zou, T., Workman, C.J., Polley, A., Betts, M.R., Freeman, G.J., Vignali, D.A., and Wherry, E.J. (2009). Coregulation of CD8+ T cell exhaustion by multiple inhibitory receptors during chronic viral infection. *Nat Immunol* 10, 29-37. 10.1038/ni.1679.
- Blank, C.U., Haining, W.N., Held, W., Hogan, P.G., Kallies, A., Lugli, E., Lynn, R.C., Philip, M., Rao, A., Restifo, N.P., et al. (2019). Defining 'T cell exhaustion'. *Nat Rev Immunol* 19, 665-674. 10.1038/s41577-019-0221-9.
- Blattman, J.N., Grayson, J.M., Wherry, E.J., Kaech, S.M., Smith, K.A., and Ahmed, R. (2003). Therapeutic use of IL-2 to enhance antiviral T-cell responses in vivo. *Nat Med* 9, 540-547. 10.1038/nm866.
- Boehm, T., and Swann, J.B. (2014). Origin and evolution of adaptive immunity. *Annu Rev Anim Biosci* 2, 259-283. 10.1146/annurev-animal-022513-114201.
- Bonilla, F.A., and Oettgen, H.C. (2010). Adaptive immunity. *J Allergy Clin Immunol* 125, S33-40. 10.1016/j.jaci.2009.09.017.
- Borst, J., Ahrends, T., Babala, N., Melief, C.J.M., and Kastenmuller, W. (2018). CD4(+) T cell help in cancer immunology and immunotherapy. *Nat Rev Immunol* 18, 635-647. 10.1038/s41577-018-0044-0.
- Bottcher, J.P., Beyer, M., Meissner, F., Abdullah, Z., Sander, J., Hochst, B., Eickhoff, S., Rieckmann, J.C., Russo, C., Bauer, T., et al. (2015). Functional classification of memory CD8(+) T cells by CX3CR1 expression. *Nat Commun* 6, 8306. 10.1038/ncomms9306.
- Boulet, S., Daudelin, J.F., and Labrecque, N. (2014). IL-2 induction of Blimp-1 is a key in vivo signal for CD8+ short-lived effector T cell differentiation. *J Immunol* 193, 1847-1854. 10.4049/jimmunol.1302365.

- Bouneaud, C., Garcia, Z., Kourilsky, P., and Pannetier, C. (2005). Lineage relationships, homeostasis, and recall capacities of central- and effector-memory CD8 T cells in vivo. *J Exp Med* 201, 579-590. 10.1084/jem.20040876.
- Boyman, O., Kovar, M., Rubinstein, M.P., Surh, C.D., and Sprent, J. (2006). Selective stimulation of T cell subsets with antibody-cytokine immune complexes. *Science* 311, 1924-1927. 10.1126/science.1122927.
- Brewitz, A., Eickhoff, S., Dahling, S., Quast, T., Bedoui, S., Kroczeck, R.A., Kurts, C., Garbi, N., Barchet, W., Iannacone, M., et al. (2017). CD8(+) T Cells Orchestrate pDC-XCR1(+) Dendritic Cell Spatial and Functional Cooperativity to Optimize Priming. *Immunity* 46, 205-219. 10.1016/j.immuni.2017.01.003.
- Bromley, S.K., Mempel, T.R., and Luster, A.D. (2008). Orchestrating the orchestrators: chemokines in control of T cell traffic. *Nat Immunol* 9, 970-980. 10.1038/ni.f.213.
- Bullock, T.N., and Yagita, H. (2005). Induction of CD70 on dendritic cells through CD40 or TLR stimulation contributes to the development of CD8+ T cell responses in the absence of CD4+ T cells. *J Immunol* 174, 710-717. 10.4049/jimmunol.174.2.710.
- Burkett, P.R., Koka, R., Chien, M., Chai, S., Boone, D.L., and Ma, A. (2004). Coordinate expression and trans presentation of interleukin (IL)-15 $\alpha$  and IL-15 supports natural killer cell and memory CD8+ T cell homeostasis. *J Exp Med* 200, 825-834. 10.1084/jem.20041389.
- Carding, S.R., and Egan, P.J. (2002). Gammadelta T cells: functional plasticity and heterogeneity. *Nat Rev Immunol* 2, 336-345. 10.1038/nri797.
- Carrio, R., Bathe, O.F., and Malek, T.R. (2004). Initial antigen encounter programs CD8+ T cells competent to develop into memory cells that are activated in an antigen-free, IL-7- and IL-15-rich environment. *J Immunol* 172, 7315-7323. 10.4049/jimmunol.172.12.7315.
- Carrio, R., Rolle, C.E., and Malek, T.R. (2007). Non-redundant role for IL-7R signaling for the survival of CD8+ memory T cells. *Eur J Immunol* 37, 3078-3088. 10.1002/eji.200737585.

- Cella, M., Jarrossay, D., Facchetti, F., Alebardi, O., Nakajima, H., Lanzavecchia, A., and Colonna, M. (1999). Plasmacytoid monocytes migrate to inflamed lymph nodes and produce large amounts of type I interferon. *Nat Med* 5, 919-923. 10.1038/11360.
- Cella, M., Scheidegger, D., Palmer-Lehmann, K., Lane, P., Lanzavecchia, A., and Alber, G. (1996). Ligation of CD40 on dendritic cells triggers production of high levels of interleukin-12 and enhances T cell stimulatory capacity: T-T help via APC activation. *J Exp Med* 184, 747-752.
- Chang, J.T., Palanivel, V.R., Kinjyo, I., Schambach, F., Intlekofer, A.M., Banerjee, A., Longworth, S.A., Vinup, K.E., Mrass, P., Oliaro, J., et al. (2007). Asymmetric T lymphocyte division in the initiation of adaptive immune responses. *Science* 315, 1687-1691. 10.1126/science.1139393.
- Chen, Z., Ji, Z., Ngiow, S.F., Manne, S., Cai, Z., Huang, A.C., Johnson, J., Staupe, R.P., Bengsch, B., Xu, C., et al. (2019). TCF-1-Centered Transcriptional Network Drives an Effector versus Exhausted CD8 T Cell-Fate Decision. *Immunity* 51, 840-855 e845. 10.1016/j.immuni.2019.09.013.
- Cheng, L.E., Ohlen, C., Nelson, B.H., and Greenberg, P.D. (2002). Enhanced signaling through the IL-2 receptor in CD8+ T cells regulated by antigen recognition results in preferential proliferation and expansion of responding CD8+ T cells rather than promotion of cell death. *Proc Natl Acad Sci U S A* 99, 3001-3006. 10.1073/pnas.052676899.
- Chevalier, M.F., Julg, B., Pyo, A., Flanders, M., Ranasinghe, S., Soghoian, D.Z., Kwon, D.S., Rychert, J., Lian, J., Muller, M.I., et al. (2011). HIV-1-specific interleukin-21+ CD4+ T cell responses contribute to durable viral control through the modulation of HIV-specific CD8+ T cell function. *J Virol* 85, 733-741. 10.1128/JVI.02030-10.
- Cieri, N., Camisa, B., Cocchiarella, F., Forcato, M., Oliveira, G., Provasi, E., Bondanza, A., Bordignon, C., Peccatori, J., Ciceri, F., et al. (2013). IL-7 and IL-15 instruct the generation of human memory stem T cells from naive precursors. *Blood* 121, 573-584. 10.1182/blood-2012-05-431718.

- Cieri, N., Oliveira, G., Greco, R., Forcato, M., Taccioli, C., Cianciotti, B., Valtolina, V., Noviello, M., Vago, L., Bondanza, A., et al. (2015). Generation of human memory stem T cells after haploidentical T-replete hematopoietic stem cell transplantation. *Blood* 125, 2865-2874. 10.1182/blood-2014-11-608539.
- Ciofani, M., and Zuniga-Pflucker, J.C. (2010). Determining gammadelta versus alpha beta T cell development. *Nat Rev Immunol* 10, 657-663. 10.1038/nri2820.
- Collinson-Pautz, M.R., Chang, W.C., Lu, A., Khalil, M., Crisostomo, J.W., Lin, P.Y., Mahendravada, A., Shinnars, N.P., Brandt, M.E., Zhang, M., et al. (2019). Constitutively active MyD88/CD40 costimulation enhances expansion and efficacy of chimeric antigen receptor T cells targeting hematological malignancies. *Leukemia* 33, 2195-2207. 10.1038/s41375-019-0417-9.
- Colombetti, S., Levy, F., and Chapatte, L. (2009). IL-7 adjuvant treatment enhances long-term tumor-antigen-specific CD8+ T-cell responses after immunization with recombinant lentivector. *Blood* 113, 6629-6637. 10.1182/blood-2008-05-155309.
- Cousens, L.P., Orange, J.S., and Biron, C.A. (1995). Endogenous IL-2 contributes to T cell expansion and IFN-gamma production during lymphocytic choriomeningitis virus infection. *J Immunol* 155, 5690-5699.
- Cox, M.A., Harrington, L.E., and Zajac, A.J. (2011). Cytokines and the inception of CD8 T cell responses. *Trends Immunol* 32, 180-186. 10.1016/j.it.2011.01.004.
- Crauste, F., Mafille, J., Boucinha, L., Djebali, S., Gandrillon, O., Marvel, J., and Arpin, C. (2017). Identification of Nascent Memory CD8 T Cells and Modeling of Their Ontogeny. *Cell Syst* 4, 306-317 e304. 10.1016/j.cels.2017.01.014.
- Croft, M., Carter, L., Swain, S.L., and Dutton, R.W. (1994). Generation of polarized antigen-specific CD8 effector populations: reciprocal action of interleukin (IL)-4 and IL-12 in promoting type 2 versus type 1 cytokine profiles. *J Exp Med* 180, 1715-1728. 10.1084/jem.180.5.1715.
- Cruz-Guilloty, F., Pipkin, M.E., Djuretic, I.M., Levanon, D., Lotem, J., Lichtenheld, M.G., Groner, Y., and Rao, A. (2009). Runx3 and T-box proteins cooperate to establish

- the transcriptional program of effector CTLs. *J Exp Med* 206, 51-59. 10.1084/jem.20081242.
- Cui, W., Liu, Y., Weinstein, J.S., Craft, J., and Kaech, S.M. (2011). An interleukin-21-interleukin-10-STAT3 pathway is critical for functional maturation of memory CD8<sup>+</sup> T cells. *Immunity* 35, 792-805. 10.1016/j.immuni.2011.09.017.
- Curtsinger, J.M., Lins, D.C., and Mescher, M.F. (2003). Signal 3 determines tolerance versus full activation of naive CD8 T cells: dissociating proliferation and development of effector function. *J Exp Med* 197, 1141-1151. 10.1084/jem.20021910.
- Curtsinger, J.M., and Mescher, M.F. (2010). Inflammatory cytokines as a third signal for T cell activation. *Curr Opin Immunol* 22, 333-340. 10.1016/j.coi.2010.02.013.
- Curtsinger, J.M., Valenzuela, J.O., Agarwal, P., Lins, D., and Mescher, M.F. (2005). Type I IFNs provide a third signal to CD8 T cells to stimulate clonal expansion and differentiation. *J Immunol* 174, 4465-4469. 10.4049/jimmunol.174.8.4465.
- D'Souza, W.N., and Hedrick, S.M. (2006). Cutting edge: latecomer CD8 T cells are imprinted with a unique differentiation program. *J Immunol* 177, 777-781. 10.4049/jimmunol.177.2.777.
- D'Souza, W.N., and Lefrancois, L. (2003). IL-2 is not required for the initiation of CD8 T cell cycling but sustains expansion. *J Immunol* 171, 5727-5735. 10.4049/jimmunol.171.11.5727.
- D'Souza, W.N., Schluns, K.S., Masopust, D., and Lefrancois, L. (2002). Essential role for IL-2 in the regulation of antiviral extralymphoid CD8 T cell responses. *J Immunol* 168, 5566-5572. 10.4049/jimmunol.168.11.5566.
- Danilo, M., Chennupati, V., Silva, J.G., Siegert, S., and Held, W. (2018). Suppression of Tcf1 by Inflammatory Cytokines Facilitates Effector CD8 T Cell Differentiation. *Cell Rep* 22, 2107-2117. 10.1016/j.celrep.2018.01.072.
- Darcy, P.K. (2008). IL-21 priming enhances T-cell immunotherapy. *Blood* 111, 5268-5269. 10.1182/blood-2008-03-142505.

- De Rosa, S.C., Herzenberg, L.A., and Roederer, M. (2001). 11-color, 13-parameter flow cytometry: identification of human naive T cells by phenotype, function, and T-cell receptor diversity. *Nat Med* 7, 245-248. 10.1038/84701.
- Di Tommaso, P., Chatzou, M., Floden, E.W., Barja, P.P., Palumbo, E., and Notredame, C. (2017). Nextflow enables reproducible computational workflows. *Nat Biotechnol* 35, 316-319. 10.1038/nbt.3820.
- Dijkgraaf, F.E., Kok, L., and Schumacher, T.N.M. (2021). Formation of Tissue-Resident CD8(+) T-Cell Memory. *Cold Spring Harb Perspect Biol* 13. 10.1101/cshperspect.a038117.
- Dobrzanski, M.J., Reome, J.B., Hollenbaugh, J.A., and Dutton, R.W. (2004). Tc1 and Tc2 effector cell therapy elicit long-term tumor immunity by contrasting mechanisms that result in complementary endogenous type 1 antitumor responses. *J Immunol* 172, 1380-1390. 10.4049/jimmunol.172.3.1380.
- Doering, T.A., Crawford, A., Angelosanto, J.M., Paley, M.A., Ziegler, C.G., and Wherry, E.J. (2012). Network analysis reveals centrally connected genes and pathways involved in CD8+ T cell exhaustion versus memory. *Immunity* 37, 1130-1144. 10.1016/j.immuni.2012.08.021.
- Eickhoff, S., Brewitz, A., Gerner, M.Y., Klauschen, F., Komander, K., Hemmi, H., Garbi, N., Kaisho, T., Germain, R.N., and Kastenmuller, W. (2015). Robust Anti-viral Immunity Requires Multiple Distinct T Cell-Dendritic Cell Interactions. *Cell* 162, 1322-1337. 10.1016/j.cell.2015.08.004.
- Elsaesser, H., Sauer, K., and Brooks, D.G. (2009). IL-21 is required to control chronic viral infection. *Science* 324, 1569-1572. 10.1126/science.1174182.
- Feau, S., Arens, R., Togher, S., and Schoenberger, S.P. (2011). Autocrine IL-2 is required for secondary population expansion of CD8(+) memory T cells. *Nat Immunol* 12, 908-913. 10.1038/ni.2079.
- Feau, S., Garcia, Z., Arens, R., Yagita, H., Borst, J., and Schoenberger, S.P. (2012). The CD4(+) T-cell help signal is transmitted from APC to CD8(+) T-cells via CD27-CD70 interactions. *Nat Commun* 3, 948. 10.1038/ncomms1948.

- Fixemer, J., Hummel, J.F., Arnold, F., Klose, C.S.N., Hofherr, A., Weissert, K., Kogel, T., Kottgen, M., Arnold, S.J., Aichele, P., and Tanriver, Y. (2020). Eomes cannot replace its paralog T-bet during expansion and differentiation of CD8 effector T cells. *PLoS Pathog* 16, e1008870. [10.1371/journal.ppat.1008870](https://doi.org/10.1371/journal.ppat.1008870).
- Frauwirth, K.A., Riley, J.L., Harris, M.H., Parry, R.V., Rathmell, J.C., Plas, D.R., Elstrom, R.L., June, C.H., and Thompson, C.B. (2002). The CD28 signaling pathway regulates glucose metabolism. *Immunity* 16, 769-777. [10.1016/s1074-7613\(02\)00323-0](https://doi.org/10.1016/s1074-7613(02)00323-0).
- Freeman, G.J., Borriello, F., Hodes, R.J., Reiser, H., Gribben, J.G., Ng, J.W., Kim, J., Goldberg, J.M., Hathcock, K., and Laszlo, G. (1993). Murine B7-2, an alternative CTLA4 counter-receptor that costimulates T cell proliferation and interleukin 2 production. *J Exp Med* 178, 2185-2192. [10.1084/jem.178.6.2185](https://doi.org/10.1084/jem.178.6.2185).
- Frohlich, A., Kisielow, J., Schmitz, I., Freigang, S., Shamshiev, A.T., Weber, J., Marsland, B.J., Oxenius, A., and Kopf, M. (2009). IL-21R on T cells is critical for sustained functionality and control of chronic viral infection. *Science* 324, 1576-1580. [10.1126/science.1172815](https://doi.org/10.1126/science.1172815).
- Fry, T.J., Shah, N.N., Orentas, R.J., Stetler-Stevenson, M., Yuan, C.M., Ramakrishna, S., Wolters, P., Martin, S., Delbrook, C., Yates, B., et al. (2018). CD22-targeted CAR T cells induce remission in B-ALL that is naive or resistant to CD19-targeted CAR immunotherapy. *Nat Med* 24, 20-28. [10.1038/nm.4441](https://doi.org/10.1038/nm.4441).
- Gacerez, A.T., Arellano, B., and Sentman, C.L. (2016). How Chimeric Antigen Receptor Design Affects Adoptive T Cell Therapy. *J Cell Physiol* 231, 2590-2598. [10.1002/jcp.25419](https://doi.org/10.1002/jcp.25419).
- Gattinoni, L., Klebanoff, C.A., Palmer, D.C., Wrzesinski, C., Kerstann, K., Yu, Z., Finkelstein, S.E., Theoret, M.R., Rosenberg, S.A., and Restifo, N.P. (2005). Acquisition of full effector function in vitro paradoxically impairs the in vivo antitumor efficacy of adoptively transferred CD8+ T cells. *J Clin Invest* 115, 1616-1626. [10.1172/JCI24480](https://doi.org/10.1172/JCI24480).
- Gattinoni, L., Lugli, E., Ji, Y., Pos, Z., Paulos, C.M., Quigley, M.F., Almeida, J.R., Gostick, E., Yu, Z., Carpenito, C., et al. (2011). A human memory T cell subset with stem cell-like properties. *Nat Med* 17, 1290-1297. [10.1038/nm.2446](https://doi.org/10.1038/nm.2446).

- Gattinoni, L., Speiser, D.E., Lichterfeld, M., and Bonini, C. (2017). T memory stem cells in health and disease. *Nat Med* 23, 18-27. 10.1038/nm.4241.
- Gattinoni, L., Zhong, X.S., Palmer, D.C., Ji, Y., Hinrichs, C.S., Yu, Z., Wrzesinski, C., Boni, A., Cassard, L., Garvin, L.M., et al. (2009). Wnt signaling arrests effector T cell differentiation and generates CD8+ memory stem cells. *Nat Med* 15, 808-813. 10.1038/nm.1982.
- Gautam, S., Fioravanti, J., Zhu, W., Le Gall, J.B., Brohawn, P., Lacey, N.E., Hu, J., Hocker, J.D., Hawk, N.V., Kapoor, V., et al. (2019). The transcription factor c-Myb regulates CD8(+) T cell stemness and antitumor immunity. *Nat Immunol* 20, 337-349. 10.1038/s41590-018-0311-z.
- Gebhardt, T., Palendira, U., Tschärke, D.C., and Bedoui, S. (2018). Tissue-resident memory T cells in tissue homeostasis, persistent infection, and cancer surveillance. *Immunol Rev* 283, 54-76. 10.1111/imr.12650.
- Gebhardt, T., Wakim, L.M., Eidsmo, L., Reading, P.C., Heath, W.R., and Carbone, F.R. (2009). Memory T cells in nonlymphoid tissue that provide enhanced local immunity during infection with herpes simplex virus. *Nat Immunol* 10, 524-530. 10.1038/ni.1718.
- Geginat, J., Lanzavecchia, A., and Sallusto, F. (2003). Proliferation and differentiation potential of human CD8+ memory T-cell subsets in response to antigen or homeostatic cytokines. *Blood* 101, 4260-4266. 10.1182/blood-2002-11-3577.
- Gerlach, C., Moseman, E.A., Loughhead, S.M., Alvarez, D., Zwijnenburg, A.J., Waanders, L., Garg, R., de la Torre, J.C., and von Andrian, U.H. (2016). The Chemokine Receptor CX3CR1 Defines Three Antigen-Experienced CD8 T Cell Subsets with Distinct Roles in Immune Surveillance and Homeostasis. *Immunity* 45, 1270-1284. 10.1016/j.immuni.2016.10.018.
- Gerlach, C., van Heijst, J.W., Swart, E., Sie, D., Armstrong, N., Kerkhoven, R.M., Zehn, D., Bevan, M.J., Schepers, K., and Schumacher, T.N. (2010). One naive T cell, multiple fates in CD8+ T cell differentiation. *J Exp Med* 207, 1235-1246. 10.1084/jem.20091175.

- Germain, R.N. (2002). T-cell development and the CD4-CD8 lineage decision. *Nat Rev Immunol* 2, 309-322. 10.1038/nri798.
- Goldrath, A.W., Sivakumar, P.V., Glaccum, M., Kennedy, M.K., Bevan, M.J., Benoist, C., Mathis, D., and Butz, E.A. (2002). Cytokine requirements for acute and Basal homeostatic proliferation of naive and memory CD8+ T cells. *J Exp Med* 195, 1515-1522. 10.1084/jem.20020033.
- Gordon, S.M., Carty, S.A., Kim, J.S., Zou, T., Smith-Garvin, J., Alonzo, E.S., Haimm, E., Sant'Angelo, D.B., Koretzky, G.A., Reiner, S.L., and Jordan, M.S. (2011). Requirements for eomesodermin and promyelocytic leukemia zinc finger in the development of innate-like CD8+ T cells. *J Immunol* 186, 4573-4578. 10.4049/jimmunol.1100037.
- Grabstein, K.H., Eisenman, J., Shanebeck, K., Rauch, C., Srinivasan, S., Fung, V., Beers, C., Richardson, J., Schoenborn, M.A., and Ahdieh, M. (1994). Cloning of a T cell growth factor that interacts with the beta chain of the interleukin-2 receptor. *Science* 264, 965-968. 10.1126/science.8178155.
- Granucci, F., Vizzardelli, C., Pavelka, N., Feau, S., Persico, M., Virzi, E., Rescigno, M., Moro, G., and Ricciardi-Castagnoli, P. (2001). Inducible IL-2 production by dendritic cells revealed by global gene expression analysis. *Nat Immunol* 2, 882-888. 10.1038/ni0901-882.
- Grau, M., Valsesia, S., Mafille, J., Djebali, S., Tomkowiak, M., Mathieu, A.L., Laubretton, D., de Bernard, S., Jouve, P.E., Ventre, E., et al. (2018). Antigen-Induced but Not Innate Memory CD8 T Cells Express NKG2D and Are Recruited to the Lung Parenchyma upon Viral Infection. *J Immunol* 200, 3635-3646. 10.4049/jimmunol.1701698.
- Green, J.M., Noel, P.J., Sperling, A.I., Walunas, T.L., Gray, G.S., Bluestone, J.A., and Thompson, C.B. (1994). Absence of B7-dependent responses in CD28-deficient mice. *Immunity* 1, 501-508. 10.1016/1074-7613(94)90092-2.
- Grupp, S.A., Kalos, M., Barrett, D., Aplenc, R., Porter, D.L., Rheingold, S.R., Teachey, D.T., Chew, A., Hauck, B., Wright, J.F., et al. (2013). Chimeric antigen receptor-modified T cells for acute lymphoid leukemia. *N Engl J Med* 368, 1509-1518. 10.1056/NEJMoa1215134.

- Hamann, D., Baars, P.A., Rep, M.H., Hooibrink, B., Kerkhof-Garde, S.R., Klein, M.R., and van Lier, R.A. (1997). Phenotypic and functional separation of memory and effector human CD8+ T cells. *J Exp Med* 186, 1407-1418. 10.1084/jem.186.9.1407.
- Hao, Y., Hao, S., Andersen-Nissen, E., Mauck, W.M., 3rd, Zheng, S., Butler, A., Lee, M.J., Wilk, A.J., Darby, C., Zager, M., et al. (2021). Integrated analysis of multimodal single-cell data. *Cell* 184, 3573-3587 e3529. 10.1016/j.cell.2021.04.048.
- Hendriks, J., Gravestein, L.A., Tesselaar, K., van Lier, R.A., Schumacher, T.N., and Borst, J. (2000). CD27 is required for generation and long-term maintenance of T cell immunity. *Nat Immunol* 1, 433-440. 10.1038/80877.
- Hendriks, J., Xiao, Y., and Borst, J. (2003). CD27 promotes survival of activated T cells and complements CD28 in generation and establishment of the effector T cell pool. *J Exp Med* 198, 1369-1380. 10.1084/jem.20030916.
- Hermans, D., Gautam, S., Garcia-Canaveras, J.C., Gromer, D., Mitra, S., Spolski, R., Li, P., Christensen, S., Nguyen, R., Lin, J.X., et al. (2020). Lactate dehydrogenase inhibition synergizes with IL-21 to promote CD8(+) T cell stemness and antitumor immunity. *Proc Natl Acad Sci U S A* 117, 6047-6055. 10.1073/pnas.1920413117.
- Hikono, H., Kohlmeier, J.E., Takamura, S., Wittmer, S.T., Roberts, A.D., and Woodland, D.L. (2007). Activation phenotype, rather than central- or effector-memory phenotype, predicts the recall efficacy of memory CD8+ T cells. *J Exp Med* 204, 1625-1636. 10.1084/jem.20070322.
- Hinrichs, C.S., Borman, Z.A., Cassard, L., Gattinoni, L., Spolski, R., Yu, Z., Sanchez-Perez, L., Muranski, P., Kern, S.J., Logun, C., et al. (2009). Adoptively transferred effector cells derived from naive rather than central memory CD8+ T cells mediate superior antitumor immunity. *Proc Natl Acad Sci U S A* 106, 17469-17474. 10.1073/pnas.0907448106.
- Hinrichs, C.S., Spolski, R., Paulos, C.M., Gattinoni, L., Kerstann, K.W., Palmer, D.C., Klebanoff, C.A., Rosenberg, S.A., Leonard, W.J., and Restifo, N.P. (2008). IL-2 and IL-21 confer opposing differentiation programs to CD8+ T cells for adoptive immunotherapy. *Blood* 111, 5326-5333. 10.1182/blood-2007-09-113050.

- Hofmann, M., and Pircher, H. (2011). E-cadherin promotes accumulation of a unique memory CD8 T-cell population in murine salivary glands. *Proc Natl Acad Sci U S A* 108, 16741-16746. 10.1073/pnas.1107200108.
- Howard, M., Farrar, J., Hilfiker, M., Johnson, B., Takatsu, K., Hamaoka, T., and Paul, W.E. (1982). Identification of a T cell-derived b cell growth factor distinct from interleukin 2. *J Exp Med* 155, 914-923. 10.1084/jem.155.3.914.
- Hu, W., Huang, X., Huang, X., Chen, W., Hao, L., and Chen, Z. (2019). Chimeric antigen receptor modified T cell (CAR-T) co-expressed with ICOSL-41BB promote CAR-T proliferation and tumor rejection. *Biomed Pharmacother* 118, 109333. 10.1016/j.biopha.2019.109333.
- Huang, L.R., Chen, F.L., Chen, Y.T., Lin, Y.M., and Kung, J.T. (2000). Potent induction of long-term CD8+ T cell memory by short-term IL-4 exposure during T cell receptor stimulation. *Proc Natl Acad Sci U S A* 97, 3406-3411. 10.1073/pnas.060026497.
- Hui, E., Cheung, J., Zhu, J., Su, X., Taylor, M.J., Wallweber, H.A., Sasmal, D.K., Huang, J., Kim, J.M., Mellman, I., and Vale, R.D. (2017). T cell costimulatory receptor CD28 is a primary target for PD-1-mediated inhibition. *Science* 355, 1428-1433. 10.1126/science.aaf1292.
- Huster, K.M., Busch, V., Schiemann, M., Linkemann, K., Kerksiek, K.M., Wagner, H., and Busch, D.H. (2004). Selective expression of IL-7 receptor on memory T cells identifies early CD40L-dependent generation of distinct CD8+ memory T cell subsets. *Proc Natl Acad Sci U S A* 101, 5610-5615. 10.1073/pnas.0308054101.
- Hwang, B., Lee, J.H., and Bang, D. (2018). Single-cell RNA sequencing technologies and bioinformatics pipelines. *Exp Mol Med* 50, 1-14. 10.1038/s12276-018-0071-8.
- Intlekofer, A.M., Banerjee, A., Takemoto, N., Gordon, S.M., Dejong, C.S., Shin, H., Hunter, C.A., Wherry, E.J., Lindsten, T., and Reiner, S.L. (2008). Anomalous type 17 response to viral infection by CD8+ T cells lacking T-bet and eomesodermin. *Science* 321, 408-411. 10.1126/science.1159806.
- Intlekofer, A.M., Takemoto, N., Wherry, E.J., Longworth, S.A., Northrup, J.T., Palanivel, V.R., Mullen, A.C., Gasink, C.R., Kaech, S.M., Miller, J.D., et al. (2005). Effector and

- memory CD8<sup>+</sup> T cell fate coupled by T-bet and eomesodermin. *Nat Immunol* 6, 1236-1244. 10.1038/ni1268.
- Isakson, P.C., Puré, E., Vitetta, E.S., and Krammer, P.H. (1982). T cell-derived B cell differentiation factor(s). Effect on the isotype switch of murine B cells. *J Exp Med* 155, 734-748. 10.1084/jem.155.3.734.
- Isogawa, M., Chung, J., Murata, Y., Kakimi, K., and Chisari, F.V. (2013). CD40 activation rescues antiviral CD8<sup>(+)</sup> T cells from PD-1-mediated exhaustion. *PLoS Pathog* 9, e1003490. 10.1371/journal.ppat.1003490.
- Jabri, B., and Abadie, V. (2015). IL-15 functions as a danger signal to regulate tissue-resident T cells and tissue destruction. *Nat Rev Immunol* 15, 771-783. 10.1038/nri3919.
- Jackson, R.J., Ramsay, A.J., Christensen, C.D., Beaton, S., Hall, D.F., and Ramshaw, I.A. (2001). Expression of mouse interleukin-4 by a recombinant ectromelia virus suppresses cytolytic lymphocyte responses and overcomes genetic resistance to mousepox. *J Virol* 75, 1205-1210. 10.1128/JVI.75.3.1205-1210.2001.
- Jaitin, D.A., Kenigsberg, E., Keren-Shaul, H., Elefant, N., Paul, F., Zaretsky, I., Mildner, A., Cohen, N., Jung, S., Tanay, A., and Amit, I. (2014). Massively parallel single-cell RNA-seq for marker-free decomposition of tissues into cell types. *Science* 343, 776-779. 10.1126/science.1247651.
- Jameson, S.C., Lee, Y.J., and Hogquist, K.A. (2015). Innate memory T cells. *Adv Immunol* 126, 173-213. 10.1016/bs.ai.2014.12.001.
- Jameson, S.C., and Masopust, D. (2009). Diversity in T cell memory: an embarrassment of riches. *Immunity* 31, 859-871. 10.1016/j.immuni.2009.11.007.
- Janssen, E.M., Droin, N.M., Lemmens, E.E., Pinkoski, M.J., Bensinger, S.J., Ehst, B.D., Griffith, T.S., Green, D.R., and Schoenberger, S.P. (2005). CD4<sup>+</sup> T-cell help controls CD8<sup>+</sup> T-cell memory via TRAIL-mediated activation-induced cell death. *Nature* 434, 88-93. 10.1038/nature03337.
- Jeannet, G., Boudousquie, C., Gardiol, N., Kang, J., Huelsken, J., and Held, W. (2010). Essential role of the Wnt pathway effector Tcf-1 for the establishment of

- functional CD8 T cell memory. *Proc Natl Acad Sci U S A* 107, 9777-9782. 10.1073/pnas.0914127107.
- Jia, B., Zhao, C., Rakszawski, K.L., Claxton, D.F., Ehmann, W.C., Rybka, W.B., Mineishi, S., Wang, M., Shike, H., Bayerl, M.G., et al. (2019). Eomes(+)T-bet(low) CD8(+) T Cells Are Functionally Impaired and Are Associated with Poor Clinical Outcome in Patients with Acute Myeloid Leukemia. *Cancer Res* 79, 1635-1645. 10.1158/0008-5472.CAN-18-3107.
- Jiang, X., Clark, R.A., Liu, L., Wagers, A.J., Fuhlbrigge, R.C., and Kupper, T.S. (2012). Skin infection generates non-migratory memory CD8<sup>+</sup> T(RM) cells providing global skin immunity. *Nature* 483, 227-231. 10.1038/nature10851.
- Johnson, J.L., Georgakilas, G., Petrovic, J., Kurachi, M., Cai, S., Harly, C., Pear, W.S., Bhandoola, A., Wherry, E.J., and Vahedi, G. (2018). Lineage-Determining Transcription Factor TCF-1 Initiates the Epigenetic Identity of T Cells. *Immunity* 48, 243-257 e210. 10.1016/j.immuni.2018.01.012.
- Johnson, L.D., and Jameson, S.C. (2009). Immunology. A chronic need for IL-21. *Science* 324, 1525-1526. 10.1126/science.1176487.
- Joshi, N.S., Cui, W., Chandele, A., Lee, H.K., Urso, D.R., Hagman, J., Gapin, L., and Kaech, S.M. (2007). Inflammation directs memory precursor and short-lived effector CD8<sup>+</sup> T cell fates via the graded expression of T-bet transcription factor. *Immunity* 27, 281-295. 10.1016/j.immuni.2007.07.010.
- Joshi, N.S., Cui, W., Dominguez, C.X., Chen, J.H., Hand, T.W., and Kaech, S.M. (2011). Increased numbers of preexisting memory CD8 T cells and decreased T-bet expression can restrain terminal differentiation of secondary effector and memory CD8 T cells. *J Immunol* 187, 4068-4076. 10.4049/jimmunol.1002145.
- Kaech, S.M., and Ahmed, R. (2001). Memory CD8<sup>+</sup> T cell differentiation: initial antigen encounter triggers a developmental program in naïve cells. *Nat Immunol* 2, 415-422. 10.1038/87720.
- Kaech, S.M., and Cui, W. (2012). Transcriptional control of effector and memory CD8<sup>+</sup> T cell differentiation. *Nat Rev Immunol* 12, 749-761. 10.1038/nri3307.

- Kaech, S.M., Tan, J.T., Wherry, E.J., Konieczny, B.T., Surh, C.D., and Ahmed, R. (2003). Selective expression of the interleukin 7 receptor identifies effector CD8 T cells that give rise to long-lived memory cells. *Nat Immunol* 4, 1191-1198. 10.1038/ni1009.
- Kahan, S.M., Bakshi, R.K., Ingram, J.T., Hendrickson, R.C., Lefkowitz, E.J., Crossman, D.K., Harrington, L.E., Weaver, C.T., and Zajac, A.J. (2022). Intrinsic IL-2 production by effector CD8 T cells affects IL-2 signaling and promotes fate decisions, stemness, and protection. *Sci Immunol* 7, eabl6322. 10.1126/sciimmunol.abl6322.
- Kakaradov, B., Arsenio, J., Widjaja, C.E., He, Z., Aigner, S., Metz, P.J., Yu, B., Wehrens, E.J., Lopez, J., Kim, S.H., et al. (2017). Early transcriptional and epigenetic regulation of CD8(+) T cell differentiation revealed by single-cell RNA sequencing. *Nat Immunol* 18, 422-432. 10.1038/ni.3688.
- Kalia, V., and Sarkar, S. (2018). Regulation of Effector and Memory CD8 T Cell Differentiation by IL-2-A Balancing Act. *Front Immunol* 9, 2987. 10.3389/fimmu.2018.02987.
- Kalia, V., Sarkar, S., Gourley, T.S., Rouse, B.T., and Ahmed, R. (2006). Differentiation of memory B and T cells. *Curr Opin Immunol* 18, 255-264. 10.1016/j.coi.2006.03.020.
- Kalia, V., Sarkar, S., Subramaniam, S., Haining, W.N., Smith, K.A., and Ahmed, R. (2010). Prolonged interleukin-2Ralpha expression on virus-specific CD8+ T cells favors terminal-effector differentiation in vivo. *Immunity* 32, 91-103. 10.1016/j.immuni.2009.11.010.
- Kallies, A., and Good-Jacobson, K.L. (2017). Transcription Factor T-bet Orchestrates Lineage Development and Function in the Immune System. *Trends Immunol* 38, 287-297. 10.1016/j.it.2017.02.003.
- Kamphorst, A.O., Wieland, A., Nasti, T., Yang, S., Zhang, R., Barber, D.L., Konieczny, B.T., Daugherty, C.Z., Koenig, L., Yu, K., et al. (2017). Rescue of exhausted CD8 T cells by PD-1-targeted therapies is CD28-dependent. *Science* 355, 1423-1427. 10.1126/science.aaf0683.

- Kaur, B.P., and Secord, E. (2019). Innate Immunity. *Pediatr Clin North Am* 66, 905-911. 10.1016/j.pcl.2019.06.011.
- Kieper, W.C., Tan, J.T., Bondi-Boyd, B., Gapin, L., Sprent, J., Ceredig, R., and Surh, C.D. (2002). Overexpression of interleukin (IL)-7 leads to IL-15-independent generation of memory phenotype CD8<sup>+</sup> T cells. *J Exp Med* 195, 1533-1539. 10.1084/jem.20020067.
- Kim, C., Jin, J., Weyand, C.M., and Goronzy, J.J. (2020). The Transcription Factor TCF1 in T Cell Differentiation and Aging. *Int J Mol Sci* 21. 10.3390/ijms21186497.
- Kim, M.T., Kurup, S.P., Starbeck-Miller, G.R., and Harty, J.T. (2016). Manipulating Memory CD8 T Cell Numbers by Timed Enhancement of IL-2 Signals. *J Immunol* 197, 1754-1761. 10.4049/jimmunol.1600641.
- Klebanoff, C.A., Finkelstein, S.E., Surman, D.R., Lichtman, M.K., Gattinoni, L., Theoret, M.R., Grewal, N., Spiess, P.J., Antony, P.A., Palmer, D.C., et al. (2004). IL-15 enhances the in vivo antitumor activity of tumor-reactive CD8<sup>+</sup> T cells. *Proc Natl Acad Sci U S A* 101, 1969-1974. 10.1073/pnas.0307298101.
- Kochenderfer, J.N., Wilson, W.H., Janik, J.E., Dudley, M.E., Stetler-Stevenson, M., Feldman, S.A., Maric, I., Raffeld, M., Nathan, D.A., Lanier, B.J., et al. (2010). Eradication of B-lineage cells and regression of lymphoma in a patient treated with autologous T cells genetically engineered to recognize CD19. *Blood* 116, 4099-4102. 10.1182/blood-2010-04-281931.
- Kovalovsky, D., Yu, Y., Dose, M., Emmanouilidou, A., Konstantinou, T., Germar, K., Aghajani, K., Guo, Z., Mandal, M., and Gounari, F. (2009). Beta-catenin/Tcf determines the outcome of thymic selection in response to alphabetaTCR signaling. *J Immunol* 183, 3873-3884. 10.4049/jimmunol.0901369.
- Kratchmarov, R., Magun, A.M., and Reiner, S.L. (2018). TCF1 expression marks self-renewing human CD8. *Blood Adv* 2, 1685-1690. 10.1182/bloodadvances.2018016279.
- Krämer, S., Mamalaki, C., Horak, I., Schimpl, A., Kioussis, D., and Hüng, T. (1994). Thymic selection and peptide-induced activation of T cell receptor-transgenic CD8 T cells

- in interleukin-2-deficient mice. *Eur J Immunol* 24, 2317-2322. 10.1002/eji.1830241009.
- Kurachi, M. (2019). CD8(+) T cell exhaustion. *Semin Immunopathol* 41, 327-337. 10.1007/s00281-019-00744-5.
- Kwon, H., Thierry-Mieg, D., Thierry-Mieg, J., Kim, H.P., Oh, J., Tunyaplin, C., Carotta, S., Donovan, C.E., Goldman, M.L., Taylor, P., et al. (2009). Analysis of interleukin-21-induced Prdm1 gene regulation reveals functional cooperation of STAT3 and IRF4 transcription factors. *Immunity* 31, 941-952. 10.1016/j.immuni.2009.10.008.
- Lai, D., Zhu, J., Wang, T., Hu-Li, J., Terabe, M., Berzofsky, J.A., Clayberger, C., and Krensky, A.M. (2011). KLF13 sustains thymic memory-like CD8(+) T cells in BALB/c mice by regulating IL-4-generating invariant natural killer T cells. *J Exp Med* 208, 1093-1103. 10.1084/jem.20101527.
- Lalvani, A., Brookes, R., Hambleton, S., Britton, W.J., Hill, A.V., and McMichael, A.J. (1997). Rapid effector function in CD8+ memory T cells. *J Exp Med* 186, 859-865. 10.1084/jem.186.6.859.
- Lang, K.S., Recher, M., Navarini, A.A., Harris, N.L., Lohning, M., Junt, T., Probst, H.C., Hengartner, H., and Zinkernagel, R.M. (2005). Inverse correlation between IL-7 receptor expression and CD8 T cell exhaustion during persistent antigen stimulation. *Eur J Immunol* 35, 738-745. 10.1002/eji.200425828.
- Lanzavecchia, A., and Sallusto, F. (2002). Progressive differentiation and selection of the fittest in the immune response. *Nat Rev Immunol* 2, 982-987. 10.1038/nri959.
- Lee, Y.J., Jameson, S.C., and Hogquist, K.A. (2011). Alternative memory in the CD8 T cell lineage. *Trends Immunol* 32, 50-56. 10.1016/j.it.2010.12.004.
- Lens, S.M., Tesselaar, K., van Oers, M.H., and van Lier, R.A. (1998). Control of lymphocyte function through CD27-CD70 interactions. *Semin Immunol* 10, 491-499. 10.1006/smim.1998.0154.
- Lenschow, D.J., Walunas, T.L., and Bluestone, J.A. (1996). CD28/B7 system of T cell costimulation. *Annu Rev Immunol* 14, 233-258. 10.1146/annurev.immunol.14.1.233.

- Leonard, W.J., and Spolski, R. (2005). Interleukin-21: a modulator of lymphoid proliferation, apoptosis and differentiation. *Nat Rev Immunol* 5, 688-698. 10.1038/nri1688.
- Li, L., Sad, S., Kägi, D., and Mosmann, T.R. (1997). CD8Tc1 and Tc2 cells secrete distinct cytokine patterns in vitro and in vivo but induce similar inflammatory reactions. *J Immunol* 158, 4152-4161.
- Lim, W.A., and June, C.H. (2017). The Principles of Engineering Immune Cells to Treat Cancer. *Cell* 168, 724-740. 10.1016/j.cell.2017.01.016.
- Loschinski, R., Böttcher, M., Stoll, A., Bruns, H., Mackensen, A., and Mougiakakos, D. (2018). IL-21 modulates memory and exhaustion phenotype of T-cells in a fatty acid oxidation-dependent manner. *Oncotarget* 9, 13125-13138. 10.18632/oncotarget.24442.
- Lugli, E., Dominguez, M.H., Gattinoni, L., Chattopadhyay, P.K., Bolton, D.L., Song, K., Klatt, N.R., Brenchley, J.M., Vaccari, M., Gostick, E., et al. (2013). Superior T memory stem cell persistence supports long-lived T cell memory. *J Clin Invest* 123, 594-599. 10.1172/JCI66327.
- Mahnke, Y.D., Brodie, T.M., Sallusto, F., Roederer, M., and Lugli, E. (2013). The who's who of T-cell differentiation: human memory T-cell subsets. *Eur J Immunol* 43, 2797-2809. 10.1002/eji.201343751.
- Marcais, A., Coupet, C.A., Walzer, T., Tomkowiak, M., Ghittoni, R., and Marvel, J. (2006). Cell-autonomous CCL5 transcription by memory CD8 T cells is regulated by IL-4. *J Immunol* 177, 4451-4457. 10.4049/jimmunol.177.7.4451.
- Mariuzza, R.A., Agnihotri, P., and Orban, J. (2020). The structural basis of T-cell receptor (TCR) activation: An enduring enigma. *J Biol Chem* 295, 914-925. 10.1074/jbc.REV119.009411.
- Martin, M.D., and Badovinac, V.P. (2018). Defining Memory CD8 T Cell. *Front Immunol* 9, 2692. 10.3389/fimmu.2018.02692.

- Marzo, A.L., Klonowski, K.D., Le Bon, A., Borrow, P., Tough, D.F., and Lefrancois, L. (2005). Initial T cell frequency dictates memory CD8+ T cell lineage commitment. *Nat Immunol* 6, 793-799. 10.1038/ni1227.
- Mathieu, C., Beltra, J.C., Charpentier, T., Bourbonnais, S., Di Santo, J.P., Lamarre, A., and Decaluwe, H. (2015). IL-2 and IL-15 regulate CD8+ memory T-cell differentiation but are dispensable for protective recall responses. *Eur J Immunol* 45, 3324-3338. 10.1002/eji.201546000.
- McAdam, A.J., Schweitzer, A.N., and Sharpe, A.H. (1998). The role of B7 co-stimulation in activation and differentiation of CD4+ and CD8+ T cells. *Immunol Rev* 165, 231-247. 10.1111/j.1600-065x.1998.tb01242.x.
- McCarthy, D.J., Campbell, K.R., Lun, A.T., and Wills, Q.F. (2017). Scater: pre-processing, quality control, normalization and visualization of single-cell RNA-seq data in R. *Bioinformatics* 33, 1179-1186. 10.1093/bioinformatics/btw777.
- McLane, L.M., Abdel-Hakeem, M.S., and Wherry, E.J. (2019). CD8 T Cell Exhaustion During Chronic Viral Infection and Cancer. *Annu Rev Immunol* 37, 457-495. 10.1146/annurev-immunol-041015-055318.
- Mercado, R., Vijh, S., Allen, S.E., Kerksiek, K., Pilip, I.M., and Pamer, E.G. (2000). Early programming of T cell populations responding to bacterial infection. *J Immunol* 165, 6833-6839. 10.4049/jimmunol.165.12.6833.
- Mescher, M.F., Curtsinger, J.M., Agarwal, P., Casey, K.A., Gerner, M., Hammerbeck, C.D., Popescu, F., and Xiao, Z. (2006). Signals required for programming effector and memory development by CD8+ T cells. *Immunol Rev* 211, 81-92. 10.1111/j.0105-2896.2006.00382.x.
- Miller, C.H., Klawon, D.E.J., Zeng, S., Lee, V., Socci, N.D., and Savage, P.A. (2020). Eomes identifies thymic precursors of self-specific memory-phenotype CD8(+) T cells. *Nat Immunol* 21, 567-577. 10.1038/s41590-020-0653-1.
- Miller, C.L., Hooton, J.W., Gillis, S., and Paetkau, V. (1990). IL-4 potentiates the IL-2-dependent proliferation of mouse cytotoxic T cells. *J Immunol* 144, 1331-1337.

- Mishra, A., Sullivan, L., and Caligiuri, M.A. (2014). Molecular pathways: interleukin-15 signaling in health and in cancer. *Clin Cancer Res* 20, 2044-2050. 10.1158/1078-0432.CCR-12-3603.
- Mo, X.Y., Sangster, M.Y., Tripp, R.A., and Doherty, P.C. (1997). Modification of the Sendai virus-specific antibody and CD8<sup>+</sup> T-cell responses in mice homozygous for disruption of the interleukin-4 gene. *J Virol* 71, 2518-2521. 10.1128/JVI.71.3.2518-2521.1997.
- Molenaar, M., van de Wetering, M., Oosterwegel, M., Peterson-Maduro, J., Godsave, S., Korinek, V., Roose, J., Destrée, O., and Clevers, H. (1996). XTcf-3 transcription factor mediates beta-catenin-induced axis formation in *Xenopus* embryos. *Cell* 86, 391-399. 10.1016/s0092-8674(00)80112-9.
- Moran, T.M., Isobe, H., Fernandez-Sesma, A., and Schulman, J.L. (1996). Interleukin-4 causes delayed virus clearance in influenza virus-infected mice. *J Virol* 70, 5230-5235. 10.1128/JVI.70.8.5230-5235.1996.
- Moroz, A., Eppolito, C., Li, Q., Tao, J., Clegg, C.H., and Shrikant, P.A. (2004). IL-21 enhances and sustains CD8<sup>+</sup> T cell responses to achieve durable tumor immunity: comparative evaluation of IL-2, IL-15, and IL-21. *J Immunol* 173, 900-909. 10.4049/jimmunol.173.2.900.
- Morrot, A., Hafalla, J.C., Cockburn, I.A., Carvalho, L.H., and Zavala, F. (2005). IL-4 receptor expression on CD8<sup>+</sup> T cells is required for the development of protective memory responses against liver stages of malaria parasites. *J Exp Med* 202, 551-560. 10.1084/jem.20042463.
- Mueller, S.N., Gebhardt, T., Carbone, F.R., and Heath, W.R. (2013). Memory T cell subsets, migration patterns, and tissue residence. *Annu Rev Immunol* 31, 137-161. 10.1146/annurev-immunol-032712-095954.
- Murphy, K., and Weaver, C. (2016). *Janeway's Immunobiology* 9<sup>th</sup> edition. Garland Science.
- Muroyama, Y., and Wherry, E.J. (2021). Memory T-Cell Heterogeneity and Terminology. *Cold Spring Harb Perspect Biol*. 10.1101/cshperspect.a037929.

- Namen, A.E., Lupton, S., Hjerrild, K., Wignall, J., Mochizuki, D.Y., Schmierer, A., Mosley, B., March, C.J., Urdal, D., and Gillis, S. (1988). Stimulation of B-cell progenitors by cloned murine interleukin-7. *Nature* 333, 571-573. 10.1038/333571a0.
- Nelms, K., Keegan, A.D., Zamorano, J., Ryan, J.J., and Paul, W.E. (1999). The IL-4 receptor: signaling mechanisms and biologic functions. *Annu Rev Immunol* 17, 701-738. 10.1146/annurev.immunol.17.1.701.
- Obar, J.J., Khanna, K.M., and Lefrancois, L. (2008). Endogenous naive CD8+ T cell precursor frequency regulates primary and memory responses to infection. *Immunity* 28, 859-869. 10.1016/j.immuni.2008.04.010.
- Olsen, T.K., and Baryawno, N. (2018). Introduction to Single-Cell RNA Sequencing. *Curr Protoc Mol Biol* 122, e57. 10.1002/cpmb.57.
- Osborne, L.C., Dhanji, S., Snow, J.W., Priatel, J.J., Ma, M.C., Miners, M.J., Teh, H.S., Goldsmith, M.A., and Abraham, N. (2007). Impaired CD8 T cell memory and CD4 T cell primary responses in IL-7R alpha mutant mice. *J Exp Med* 204, 619-631. 10.1084/jem.20061871.
- Paley, M.A., Kroy, D.C., Odorizzi, P.M., Johnnidis, J.B., Dolfi, D.V., Barnett, B.E., Bikoff, E.K., Robertson, E.J., Lauer, G.M., Reiner, S.L., and Wherry, E.J. (2012). Progenitor and terminal subsets of CD8+ T cells cooperate to contain chronic viral infection. *Science* 338, 1220-1225. 10.1126/science.1229620.
- Pallett, L.J., Davies, J., Colbeck, E.J., Robertson, F., Hansi, N., Easom, N.J.W., Burton, A.R., Stegmann, K.A., Schurich, A., Swadling, L., et al. (2017). IL-2(high) tissue-resident T cells in the human liver: Sentinels for hepatotropic infection. *J Exp Med* 214, 1567-1580. 10.1084/jem.20162115.
- Papaioannou, V.E. (2014). The T-box gene family: emerging roles in development, stem cells and cancer. *Development* 141, 3819-3833. 10.1242/dev.104471.
- Park, S.L., Zaid, A., Hor, J.L., Christo, S.N., Prier, J.E., Davies, B., Alexandre, Y.O., Gregory, J.L., Russell, T.A., Gebhardt, T., et al. (2018). Local proliferation maintains a stable pool of tissue-resident memory T cells after antiviral recall responses. *Nat Immunol* 19, 183-191. 10.1038/s41590-017-0027-5.

- Park, W.R., Park, C.S., Tomura, M., Ahn, H.J., Nakahira, Y., Iwasaki, M., Gao, P., Abe, R., Hamaoka, T., and Fujiwara, H. (2001). CD28 costimulation is required not only to induce IL-12 receptor but also to render janus kinases/STAT4 responsive to IL-12 stimulation in TCR-triggered T cells. *Eur J Immunol* 31, 1456-1464. 10.1002/1521-4141(200105)31:5<1456::AID-IMMU1456>3.0.CO;2-A.
- Patin, E., Hasan, M., Bergstedt, J., Rouilly, V., Libri, V., Urrutia, A., Alanio, C., Scepanovic, P., Hammer, C., Jonsson, F., et al. (2018). Natural variation in the parameters of innate immune cells is preferentially driven by genetic factors. *Nat Immunol* 19, 302-314. 10.1038/s41590-018-0049-7.
- Patsoukis, N., Brown, J., Petkova, V., Liu, F., Li, L., and Boussiotis, V.A. (2012). Selective effects of PD-1 on Akt and Ras pathways regulate molecular components of the cell cycle and inhibit T cell proliferation. *Sci Signal* 5, ra46. 10.1126/scisignal.2002796.
- Pearce, E.L., Mullen, A.C., Martins, G.A., Krawczyk, C.M., Hutchins, A.S., Zediak, V.P., Banica, M., DiCioccio, C.B., Gross, D.A., Mao, C.A., et al. (2003). Control of effector CD8+ T cell function by the transcription factor Eomesodermin. *Science* 302, 1041-1043. 10.1126/science.1090148.
- Pellegrini, M., Calzascia, T., Elford, A.R., Shahinian, A., Lin, A.E., Dissanayake, D., Dhanji, S., Nguyen, L.T., Gronski, M.A., Morre, M., et al. (2009). Adjuvant IL-7 antagonizes multiple cellular and molecular inhibitory networks to enhance immunotherapies. *Nat Med* 15, 528-536. 10.1038/nm.1953.
- Pellegrini, M., Calzascia, T., Toe, J.G., Preston, S.P., Lin, A.E., Elford, A.R., Shahinian, A., Lang, P.A., Lang, K.S., Morre, M., et al. (2011). IL-7 engages multiple mechanisms to overcome chronic viral infection and limit organ pathology. *Cell* 144, 601-613. 10.1016/j.cell.2011.01.011.
- Peperzak, V., Xiao, Y., Veraar, E.A., and Borst, J. (2010). CD27 sustains survival of CTLs in virus-infected nonlymphoid tissue in mice by inducing autocrine IL-2 production. *J Clin Invest* 120, 168-178. 10.1172/JCI40178.

- Pihlgren, M., Dubois, P.M., Tomkowiak, M., Sjögren, T., and Marvel, J. (1996). Resting memory CD8+ T cells are hyperreactive to antigenic challenge in vitro. *J Exp Med* 184, 2141-2151. 10.1084/jem.184.6.2141.
- Pipkin, M.E., Sacks, J.A., Cruz-Guilloty, F., Lichtenheld, M.G., Bevan, M.J., and Rao, A. (2010). Interleukin-2 and inflammation induce distinct transcriptional programs that promote the differentiation of effector cytolytic T cells. *Immunity* 32, 79-90. 10.1016/j.immuni.2009.11.012.
- Polonsky, M., Rimer, J., Kern-Perets, A., Zaretsky, I., Miller, S., Bornstein, C., David, E., Kopelman, N.M., Stelzer, G., Porat, Z., et al. (2018). Induction of CD4 T cell memory by local cellular collectivity. *Science* 360. 10.1126/science.aaj1853.
- Prilliman, K.R., Lemmens, E.E., Palioungas, G., Wolfe, T.G., Allison, J.P., Sharpe, A.H., and Schoenberger, S.P. (2002). Cutting edge: a crucial role for B7-CD28 in transmitting T help from APC to CTL. *J Immunol* 169, 4094-4097. 10.4049/jimmunol.169.8.4094.
- Pritchard, G.H., Kedl, R.M., and Hunter, C.A. (2019). The evolving role of T-bet in resistance to infection. *Nat Rev Immunol* 19, 398-410. 10.1038/s41577-019-0145-4.
- Quigley, M., Pereyra, F., Nilsson, B., Porichis, F., Fonseca, C., Eichbaum, Q., Julg, B., Jesneck, J.L., Brosnahan, K., Imam, S., et al. (2010). Transcriptional analysis of HIV-specific CD8+ T cells shows that PD-1 inhibits T cell function by upregulating BATF. *Nat Med* 16, 1147-1151. 10.1038/nm.2232.
- Rao, R.R., Li, Q., Odunsi, K., and Shrikant, P.A. (2010). The mTOR kinase determines effector versus memory CD8+ T cell fate by regulating the expression of transcription factors T-bet and Eomesodermin. *Immunity* 32, 67-78. 10.1016/j.immuni.2009.10.010.
- Rathmell, J.C., Farkash, E.A., Gao, W., and Thompson, C.B. (2001). IL-7 enhances the survival and maintains the size of naive T cells. *J Immunol* 167, 6869-6876. 10.4049/jimmunol.167.12.6869.
- Redeker, A., Welten, S.P., Baert, M.R., Vloemans, S.A., Tiemessen, M.M., Staal, F.J., and Arens, R. (2015). The Quantity of Autocrine IL-2 Governs the Expansion Potential of CD8+ T Cells. *J Immunol* 195, 4792-4801. 10.4049/jimmunol.1501083.

- Renkema, K.R., Lee, J.Y., Lee, Y.J., Hamilton, S.E., Hogquist, K.A., and Jameson, S.C. (2016). IL-4 sensitivity shapes the peripheral CD8<sup>+</sup> T cell pool and response to infection. *J Exp Med* 213, 1319-1329. 10.1084/jem.20151359.
- Richer, M.J., Pewe, L.L., Hancox, L.S., Hartwig, S.M., Varga, S.M., and Harty, J.T. (2015). Inflammatory IL-15 is required for optimal memory T cell responses. *J Clin Invest* 125, 3477-3490. 10.1172/JCI81261.
- Ridge, J.P., Di Rosa, F., and Matzinger, P. (1998). A conditioned dendritic cell can be a temporal bridge between a CD4<sup>+</sup> T-helper and a T-killer cell. *Nature* 393, 474-478. 10.1038/30989.
- Rochman, Y., Spolski, R., and Leonard, W.J. (2009). New insights into the regulation of T cells by gamma(c) family cytokines. *Nat Rev Immunol* 9, 480-490. 10.1038/nri2580.
- Rolot, M., Dougall, A.M., Chetty, A., Javaux, J., Chen, T., Xiao, X., Machiels, B., Selkirk, M.E., Maizels, R.M., Hokke, C., et al. (2018). Helminth-induced IL-4 expands bystander memory CD8<sup>+</sup> T cells for early control of viral infection. *Nat Commun* 9, 4516. 10.1038/s41467-018-06978-5.
- Romero, P., Zippelius, A., Kurth, I., Pittet, M.J., Touvrey, C., Iancu, E.M., Cortes, P., Devere, E., Speiser, D.E., and Rufer, N. (2007). Four functionally distinct populations of human effector-memory CD8<sup>+</sup> T lymphocytes. *J Immunol* 178, 4112-4119. 10.4049/jimmunol.178.7.4112.
- Roncarolo, M.G., Gregori, S., Lucarelli, B., Ciceri, F., and Bacchetta, R. (2011). Clinical tolerance in allogeneic hematopoietic stem cell transplantation. *Immunol Rev* 241, 145-163. 10.1111/j.1600-065X.2011.01010.x.
- Rossjohn, J., Gras, S., Miles, J.J., Turner, S.J., Godfrey, D.I., and McCluskey, J. (2015). T cell antigen receptor recognition of antigen-presenting molecules. *Annu Rev Immunol* 33, 169-200. 10.1146/annurev-immunol-032414-112334.
- Rubinstein, M.P., Lind, N.A., Purton, J.F., Filippou, P., Best, J.A., McGhee, P.A., Surh, C.D., and Goldrath, A.W. (2008). IL-7 and IL-15 differentially regulate CD8<sup>+</sup> T-cell subsets during contraction of the immune response. *Blood* 112, 3704-3712. 10.1182/blood-2008-06-160945.

- Russell, J.H., and Ley, T.J. (2002). Lymphocyte-mediated cytotoxicity. *Annu Rev Immunol* 20, 323-370. 10.1146/annurev.immunol.20.100201.131730.
- Ryan, K., Garrett, N., Mitchell, A., and Gurdon, J.B. (1996). Eomesodermin, a key early gene in *Xenopus* mesoderm differentiation. *Cell* 87, 989-1000. 10.1016/s0092-8674(00)81794-8.
- Sad, S., Marcotte, R., and Mosmann, T.R. (1995). Cytokine-induced differentiation of precursor mouse CD8+ T cells into cytotoxic CD8+ T cells secreting Th1 or Th2 cytokines. *Immunity* 2, 271-279. 10.1016/1074-7613(95)90051-9.
- Sad, S., and Mosmann, T.R. (1995). Interleukin (IL) 4, in the absence of antigen stimulation, induces an anergy-like state in differentiated CD8+ TC1 cells: loss of IL-2 synthesis and autonomous proliferation but retention of cytotoxicity and synthesis of other cytokines. *J Exp Med* 182, 1505-1515. 10.1084/jem.182.5.1505.
- Saelens, W., Cannoodt, R., Todorov, H., and Saeys, Y. (2019). A comparison of single-cell trajectory inference methods. *Nat Biotechnol* 37, 547-554. 10.1038/s41587-019-0071-9.
- Sakuishi, K., Apetoh, L., Sullivan, J.M., Blazar, B.R., Kuchroo, V.K., and Anderson, A.C. (2010). Targeting Tim-3 and PD-1 pathways to reverse T cell exhaustion and restore anti-tumor immunity. *J Exp Med* 207, 2187-2194. 10.1084/jem.20100643.
- Sallusto, F., Lenig, D., Förster, R., Lipp, M., and Lanzavecchia, A. (1999). Two subsets of memory T lymphocytes with distinct homing potentials and effector functions. *Nature* 401, 708-712. 10.1038/44385.
- Sanchez, P.J., McWilliams, J.A., Haluszczak, C., Yagita, H., and Kedl, R.M. (2007). Combined TLR/CD40 stimulation mediates potent cellular immunity by regulating dendritic cell expression of CD70 in vivo. *J Immunol* 178, 1564-1572. 10.4049/jimmunol.178.3.1564.
- Sandau, M.M., Kohlmeier, J.E., Woodland, D.L., and Jameson, S.C. (2010). IL-15 regulates both quantitative and qualitative features of the memory CD8 T cell pool. *J Immunol* 184, 35-44. 10.4049/jimmunol.0803355.

- Sarkar, S., Kalia, V., Haining, W.N., Konieczny, B.T., Subramaniam, S., and Ahmed, R. (2008). Functional and genomic profiling of effector CD8 T cell subsets with distinct memory fates. *J Exp Med* 205, 625-640. 10.1084/jem.20071641.
- Sasaki, K., Pardee, A.D., Okada, H., and Storkus, W.J. (2008). IL-4 inhibits VLA-4 expression on Tc1 cells resulting in poor tumor infiltration and reduced therapy benefit. *Eur J Immunol* 38, 2865-2873. 10.1002/eji.200838334.
- Schenkel, J.M., Fraser, K.A., Beura, L.K., Pauken, K.E., Vezys, V., and Masopust, D. (2014). T cell memory. Resident memory CD8 T cells trigger protective innate and adaptive immune responses. *Science* 346, 98-101. 10.1126/science.1254536.
- Schenkel, J.M., Fraser, K.A., Vezys, V., and Masopust, D. (2013). Sensing and alarm function of resident memory CD8(+) T cells. *Nat Immunol* 14, 509-513. 10.1038/ni.2568.
- Schenkel, J.M., and Masopust, D. (2014). Tissue-resident memory T cells. *Immunity* 41, 886-897. 10.1016/j.immuni.2014.12.007.
- Schilham, M.W., Wilson, A., Moerer, P., Benaissa-Trouw, B.J., Cumano, A., and Clevers, H.C. (1998). Critical involvement of Tcf-1 in expansion of thymocytes. *J Immunol* 161, 3984-3991.
- Schluns, K.S., Kieper, W.C., Jameson, S.C., and Lefrançois, L. (2000). Interleukin-7 mediates the homeostasis of naïve and memory CD8 T cells in vivo. *Nat Immunol* 1, 426-432. 10.1038/80868.
- Schluns, K.S., Klonowski, K.D., and Lefrancois, L. (2004). Transregulation of memory CD8 T-cell proliferation by IL-15 $\alpha$ <sup>+</sup> bone marrow-derived cells. *Blood* 103, 988-994. 10.1182/blood-2003-08-2814.
- Schluns, K.S., and Lefrancois, L. (2003). Cytokine control of memory T-cell development and survival. *Nat Rev Immunol* 3, 269-279. 10.1038/nri1052.
- Schoenberger, S.P., Toes, R.E., van der Voort, E.I., Offringa, R., and Melief, C.J. (1998). T-cell help for cytotoxic T lymphocytes is mediated by CD40-CD40L interactions. *Nature* 393, 480-483. 10.1038/31002.

- Seddon, B., and Zamoyska, R. (2002). TCR signals mediated by Src family kinases are essential for the survival of naive T cells. *J Immunol* 169, 2997-3005. 10.4049/jimmunol.169.6.2997.
- Seidel, J.A., Vukmanovic-Stejic, M., Muller-Durovic, B., Patel, N., Fuentes-Duculan, J., Henson, S.M., Krueger, J.G., Rustin, M.H.A., Nestle, F.O., Lacy, K.E., and Akbar, A.N. (2018). Skin resident memory CD8(+) T cells are phenotypically and functionally distinct from circulating populations and lack immediate cytotoxic function. *Clin Exp Immunol* 194, 79-92. 10.1111/cei.13189.
- Sengupta, S., Katz, S.C., Sengupta, S., and Sampath, P. (2018). Glycogen synthase kinase 3 inhibition lowers PD-1 expression, promotes long-term survival and memory generation in antigen-specific CAR-T cells. *Cancer Lett* 433, 131-139. 10.1016/j.canlet.2018.06.035.
- Sevilla, N., McGavern, D.B., Teng, C., Kunz, S., and Oldstone, M.B. (2004). Viral targeting of hematopoietic progenitors and inhibition of DC maturation as a dual strategy for immune subversion. *J Clin Invest* 113, 737-745. 10.1172/JCI20243.
- Sharma, D.P., Ramsay, A.J., Maguire, D.J., Rolph, M.S., and Ramshaw, I.A. (1996). Interleukin-4 mediates down regulation of antiviral cytokine expression and cytotoxic T-lymphocyte responses and exacerbates vaccinia virus infection in vivo. *J Virol* 70, 7103-7107. 10.1128/JVI.70.10.7103-7107.1996.
- Shedlock, D.J., Whitmire, J.K., Tan, J., MacDonald, A.S., Ahmed, R., and Shen, H. (2003). Role of CD4 T cell help and costimulation in CD8 T cell responses during *Listeria monocytogenes* infection. *J Immunol* 170, 2053-2063. 10.4049/jimmunol.170.4.2053.
- Shenoy, A.R., Kirschnek, S., and Hacker, G. (2014). IL-15 regulates Bcl-2 family members Bim and Mcl-1 through JAK/STAT and PI3K/AKT pathways in T cells. *Eur J Immunol* 44, 2500-2507. 10.1002/eji.201344238.
- Shourian, M., Beltra, J.C., Bourdin, B., and Decaluwe, H. (2019). Common gamma chain cytokines and CD8 T cells in cancer. *Semin Immunol* 42, 101307. 10.1016/j.smim.2019.101307.

- Shuai, K., and Liu, B. (2003). Regulation of JAK-STAT signalling in the immune system. *Nat Rev Immunol* 3, 900-911. 10.1038/nri1226.
- Sigal, L.J., Reiser, H., and Rock, K.L. (1998). The role of B7-1 and B7-2 costimulation for the generation of CTL responses in vivo. *J Immunol* 161, 2740-2745.
- Sikora, A.G., Jaffarad, N., Hailemichael, Y., Gelbard, A., Stonier, S.W., Schluns, K.S., Frasca, L., Lou, Y., Liu, C., Andersson, H.A., et al. (2009). IFN-alpha enhances peptide vaccine-induced CD8+ T cell numbers, effector function, and antitumor activity. *J Immunol* 182, 7398-7407. 10.4049/jimmunol.0802982.
- Smith, K.A. (1988). Interleukin-2: inception, impact, and implications. *Science* 240, 1169-1176. 10.1126/science.3131876.
- Smith, T., Heger, A., and Sudbery, I. (2017). UMI-tools: modeling sequencing errors in Unique Molecular Identifiers to improve quantification accuracy. *Genome Res* 27, 491-499. 10.1101/gr.209601.116.
- Sokke Umeshappa, C., Hebbandi Nanjundappa, R., Xie, Y., Freywald, A., Deng, Y., Ma, H., and Xiang, J. (2012). CD154 and IL-2 signaling of CD4+ T cells play a critical role in multiple phases of CD8+ CTL responses following adenovirus vaccination. *PLoS One* 7, e47004. 10.1371/journal.pone.0047004.
- Spolski, R., and Leonard, W.J. (2008). Interleukin-21: basic biology and implications for cancer and autoimmunity. *Annu Rev Immunol* 26, 57-79. 10.1146/annurev.immunol.26.021607.090316.
- Sportes, C., Babb, R.R., Krumlauf, M.C., Hakim, F.T., Steinberg, S.M., Chow, C.K., Brown, M.R., Fleisher, T.A., Noel, P., Maric, I., et al. (2010). Phase I study of recombinant human interleukin-7 administration in subjects with refractory malignancy. *Clin Cancer Res* 16, 727-735. 10.1158/1078-0432.CCR-09-1303.
- Srivastava, S., and Riddell, S.R. (2015). Engineering CAR-T cells: Design concepts. *Trends Immunol* 36, 494-502. 10.1016/j.it.2015.06.004.
- Steel, J.C., Waldmann, T.A., and Morris, J.C. (2012). Interleukin-15 biology and its therapeutic implications in cancer. *Trends Pharmacol Sci* 33, 35-41. 10.1016/j.tips.2011.09.004.

- Steinbach, K., Vincenti, I., Kreutzfeldt, M., Page, N., Muschaweckh, A., Wagner, I., Drexler, I., Pinschewer, D., Korn, T., and Merkler, D. (2016). Brain-resident memory T cells represent an autonomous cytotoxic barrier to viral infection. *J Exp Med* 213, 1571-1587. 10.1084/jem.20151916.
- Stemberger, C., Huster, K.M., Koffler, M., Anderl, F., Schiemann, M., Wagner, H., and Busch, D.H. (2007). A single naive CD8<sup>+</sup> T cell precursor can develop into diverse effector and memory subsets. *Immunity* 27, 985-997. 10.1016/j.immuni.2007.10.012.
- Svensson, A., Bergin, A.H., Lowhagen, G.B., Tunback, P., Bellner, L., Padyukov, L., and Eriksson, K. (2008). A 3'-untranslated region polymorphism in the TBX21 gene encoding T-bet is a risk factor for genital herpes simplex virus type 2 infection in humans. *J Gen Virol* 89, 2262-2268. 10.1099/vir.0.2008/001305-0.
- Szabo, S.J., Kim, S.T., Costa, G.L., Zhang, X., Fathman, C.G., and Glimcher, L.H. (2000). A novel transcription factor, T-bet, directs Th1 lineage commitment. *Cell* 100, 655-669. 10.1016/s0092-8674(00)80702-3.
- Søndergaard, H., Galsgaard, E.D., Bartholomaeussen, M., Straten, P.T., Odum, N., and Skak, K. (2010). Intratumoral interleukin-21 increases antitumor immunity, tumor-infiltrating CD8<sup>+</sup> T-cell density and activity, and enlarges draining lymph nodes. *J Immunother* 33, 236-249. 10.1097/CJI.0b013e3181c0c1cb.
- Takaba, H., and Takayanagi, H. (2017). The Mechanisms of T Cell Selection in the Thymus. *Trends Immunol* 38, 805-816. 10.1016/j.it.2017.07.010.
- Takada, K., and Jameson, S.C. (2009). Naive T cell homeostasis: from awareness of space to a sense of place. *Nat Rev Immunol* 9, 823-832. 10.1038/nri2657.
- Takahama, Y. (2006). Journey through the thymus: stromal guides for T-cell development and selection. *Nat Rev Immunol* 6, 127-135. 10.1038/nri1781.
- Takemoto, N., Intlekofer, A.M., Northrup, J.T., Wherry, E.J., and Reiner, S.L. (2006). Cutting Edge: IL-12 inversely regulates T-bet and eomesodermin expression during pathogen-induced CD8<sup>+</sup> T cell differentiation. *J Immunol* 177, 7515-7519. 10.4049/jimmunol.177.11.7515.

- Tan, J.T., Dudl, E., LeRoy, E., Murray, R., Sprent, J., Weinberg, K.I., and Surh, C.D. (2001). IL-7 is critical for homeostatic proliferation and survival of naive T cells. *Proc Natl Acad Sci U S A* 98, 8732-8737. 10.1073/pnas.161126098.
- Tang, Y.W., and Graham, B.S. (1994). Anti-IL-4 treatment at immunization modulates cytokine expression, reduces illness, and increases cytotoxic T lymphocyte activity in mice challenged with respiratory syncytial virus. *J Clin Invest* 94, 1953-1958. 10.1172/JCI117546.
- Taniuchi, I. (2018). CD4 Helper and CD8 Cytotoxic T Cell Differentiation. *Annu Rev Immunol* 36, 579-601. 10.1146/annurev-immunol-042617-053411.
- Taraban, V.Y., Rowley, T.F., and Al-Shamkhani, A. (2004). Cutting edge: a critical role for CD70 in CD8 T cell priming by CD40-licensed APCs. *J Immunol* 173, 6542-6546. 10.4049/jimmunol.173.11.6542.
- Teijaro, J.R., Ng, C., Lee, A.M., Sullivan, B.M., Sheehan, K.C., Welch, M., Schreiber, R.D., de la Torre, J.C., and Oldstone, M.B. (2013). Persistent LCMV infection is controlled by blockade of type I interferon signaling. *Science* 340, 207-211. 10.1126/science.1235214.
- Tian, Y., Cox, M.A., Kahan, S.M., Ingram, J.T., Bakshi, R.K., and Zajac, A.J. (2016). A Context-Dependent Role for IL-21 in Modulating the Differentiation, Distribution, and Abundance of Effector and Memory CD8 T Cell Subsets. *J Immunol* 196, 2153-2166. 10.4049/jimmunol.1401236.
- Tian, Y., and Zajac, A.J. (2016). IL-21 and T Cell Differentiation: Consider the Context. *Trends Immunol* 37, 557-568. 10.1016/j.it.2016.06.001.
- Tirosh, I., Izar, B., Prakadan, S.M., Wadsworth, M.H., 2nd, Treacy, D., Trombetta, J.J., Rotem, A., Rodman, C., Lian, C., Murphy, G., et al. (2016). Dissecting the multicellular ecosystem of metastatic melanoma by single-cell RNA-seq. *Science* 352, 189-196. 10.1126/science.aad0501.
- Todorov, H., Cannoodt, R., Saelens, W., and Saeys, Y. (2020). TinGa: fast and flexible trajectory inference with Growing Neural Gas. *Bioinformatics* 36, i66-i74. 10.1093/bioinformatics/btaa463.

- Todorov, H., Prieux, M., Laubret, D., Bouvier, M., Wang, S., Bernard, S.D., Arpin, C., Cannoodt, R., Saelens, W., Bonnaffoux, A., Gandrillon, O., Crauste, F., Saeys, Y., and Marvel, J. (2022). CD8 memory precursor cells generation is a continuous process. Submitted.
- Tsuda, S., and Pipkin, M.E. (2021). Transcriptional Control of Cell Fate Determination in Antigen-Experienced CD8 T Cells. *Cold Spring Harb Perspect Biol.* 10.1101/cshperspect.a037945.
- Turner, S.J., Bennett, T.J., and Gruta, N.L. (2021). CD8(+) T-Cell Memory: The Why, the When, and the How. *Cold Spring Harb Perspect Biol* 13. 10.1101/cshperspect.a038661.
- van de Ven, K., and Borst, J. (2015). Targeting the T-cell co-stimulatory CD27/CD70 pathway in cancer immunotherapy: rationale and potential. *Immunotherapy* 7, 655-667. 10.2217/imt.15.32.
- van de Wetering, M., Oosterwegel, M., Dooijes, D., and Clevers, H. (1991). Identification and cloning of TCF-1, a T lymphocyte-specific transcription factor containing a sequence-specific HMG box. *EMBO J* 10, 123-132.
- van den Broek, T., Borghans, J.A.M., and van Wijk, F. (2018). The full spectrum of human naive T cells. *Nat Rev Immunol* 18, 363-373. 10.1038/s41577-018-0001-y.
- van Stipdonk, M.J., Lemmens, E.E., and Schoenberger, S.P. (2001). Naïve CTLs require a single brief period of antigenic stimulation for clonal expansion and differentiation. *Nat Immunol* 2, 423-429. 10.1038/87730.
- Veiga-Fernandes, H., Walter, U., Bourgeois, C., McLean, A., and Rocha, B. (2000). Response of naïve and memory CD8+ T cells to antigen stimulation in vivo. *Nat Immunol* 1, 47-53. 10.1038/76907.
- Ventre, E., Brinza, L., Schicklin, S., Mafille, J., Coupet, C.A., Marcais, A., Djebali, S., Jubin, V., Walzer, T., and Marvel, J. (2012). Negative regulation of NKG2D expression by IL-4 in memory CD8 T cells. *J Immunol* 189, 3480-3489. 10.4049/jimmunol.1102954.

- Villacres, M.C., and Bergmann, C.C. (1999). Enhanced cytotoxic T cell activity in IL-4-deficient mice. *J Immunol* 162, 2663-2670.
- Vivien, L., Benoist, C., and Mathis, D. (2001). T lymphocytes need IL-7 but not IL-4 or IL-6 to survive in vivo. *Int Immunol* 13, 763-768. 10.1093/intimm/13.6.763.
- Voskoboinik, I., Whisstock, J.C., and Trapani, J.A. (2015). Perforin and granzymes: function, dysfunction and human pathology. *Nat Rev Immunol* 15, 388-400. 10.1038/nri3839.
- Wakim, L.M., Woodward-Davis, A., and Bevan, M.J. (2010). Memory T cells persisting within the brain after local infection show functional adaptations to their tissue of residence. *Proc Natl Acad Sci U S A* 107, 17872-17879. 10.1073/pnas.1010201107.
- Waldmann, T.A. (2006). The biology of interleukin-2 and interleukin-15: implications for cancer therapy and vaccine design. *Nat Rev Immunol* 6, 595-601. 10.1038/nri1901.
- Weinreich, M.A., Takada, K., Skon, C., Reiner, S.L., Jameson, S.C., and Hogquist, K.A. (2009). KLF2 transcription-factor deficiency in T cells results in unrestrained cytokine production and upregulation of bystander chemokine receptors. *Immunity* 31, 122-130. 10.1016/j.immuni.2009.05.011.
- Weninger, W., Crowley, M.A., Manjunath, N., and von Andrian, U.H. (2001). Migratory properties of naive, effector, and memory CD8(+) T cells. *J Exp Med* 194, 953-966. 10.1084/jem.194.7.953.
- Wherry, E.J., and Kurachi, M. (2015). Molecular and cellular insights into T cell exhaustion. *Nat Rev Immunol* 15, 486-499. 10.1038/nri3862.
- Wherry, E.J., Teichgraber, V., Becker, T.C., Masopust, D., Kaech, S.M., Antia, R., von Andrian, U.H., and Ahmed, R. (2003). Lineage relationship and protective immunity of memory CD8 T cell subsets. *Nat Immunol* 4, 225-234. 10.1038/ni889.
- Williams, M.A., and Bevan, M.J. (2007). Effector and memory CTL differentiation. *Annu Rev Immunol* 25, 171-192. 10.1146/annurev.immunol.25.022106.141548.
- Williams, M.A., Tyznik, A.J., and Bevan, M.J. (2006). Interleukin-2 signals during priming are required for secondary expansion of CD8+ memory T cells. *Nature* 441, 890-893. 10.1038/nature04790.

- Wilson, E.B., and Livingstone, A.M. (2008). Cutting edge: CD4+ T cell-derived IL-2 is essential for help-dependent primary CD8+ T cell responses. *J Immunol* 181, 7445-7448. 10.4049/jimmunol.181.11.7445.
- Wofford, J.A., Wieman, H.L., Jacobs, S.R., Zhao, Y., and Rathmell, J.C. (2008). IL-7 promotes Glut1 trafficking and glucose uptake via STAT5-mediated activation of Akt to support T-cell survival. *Blood* 111, 2101-2111. 10.1182/blood-2007-06-096297.
- Wolchok, J.D., Kluger, H., Callahan, M.K., Postow, M.A., Rizvi, N.A., Lesokhin, A.M., Segal, N.H., Ariyan, C.E., Gordon, R.A., Reed, K., et al. (2013). Nivolumab plus ipilimumab in advanced melanoma. *N Engl J Med* 369, 122-133. 10.1056/NEJMoa1302369.
- Wolkers, M.C., Bensinger, S.J., Green, D.R., Schoenberger, S.P., and Janssen, E.M. (2011). Interleukin-2 rescues helpless effector CD8+ T cells by diminishing the susceptibility to TRAIL mediated death. *Immunol Lett* 139, 25-32. 10.1016/j.imlet.2011.04.011.
- Wolkers, M.C., Gerlach, C., Arens, R., Janssen, E.M., Fitzgerald, P., Schumacher, T.N., Medema, J.P., Green, D.R., and Schoenberger, S.P. (2012). Nab2 regulates secondary CD8+ T-cell responses through control of TRAIL expression. *Blood* 119, 798-804. 10.1182/blood-2011-08-373910.
- Wortzman, M.E., Clouthier, D.L., McPherson, A.J., Lin, G.H., and Watts, T.H. (2013). The contextual role of TNFR family members in CD8(+) T-cell control of viral infections. *Immunol Rev* 255, 125-148. 10.1111/imr.12086.
- Wu, T., Ji, Y., Moseman, E.A., Xu, H.C., Manghani, M., Kirby, M., Anderson, S.M., Handon, R., Kenyon, E., Elkahlon, A., et al. (2016). The TCF1-Bcl6 axis counteracts type I interferon to repress exhaustion and maintain T cell stemness. *Sci Immunol* 1. 10.1126/sciimmunol.aai8593.
- Xin, A., Masson, F., Liao, Y., Preston, S., Guan, T., Gloury, R., Olshansky, M., Lin, J.X., Li, P., Speed, T.P., et al. (2016). A molecular threshold for effector CD8(+) T cell differentiation controlled by transcription factors Blimp-1 and T-bet. *Nat Immunol* 17, 422-432. 10.1038/ni.3410.

- Xin, G., Schauder, D.M., Lainez, B., Weinstein, J.S., Dai, Z., Chen, Y., Esplugues, E., Wen, R., Wang, D., Parish, I.A., et al. (2015). A Critical Role of IL-21-Induced BATF in Sustaining CD8-T-Cell-Mediated Chronic Viral Control. *Cell Rep* 13, 1118-1124. 10.1016/j.celrep.2015.09.069.
- Xu, Y., Zhang, M., Ramos, C.A., Durett, A., Liu, E., Dakhova, O., Liu, H., Creighton, C.J., Gee, A.P., Heslop, H.E., et al. (2014). Closely related T-memory stem cells correlate with in vivo expansion of CAR.CD19-T cells and are preserved by IL-7 and IL-15. *Blood* 123, 3750-3759. 10.1182/blood-2014-01-552174.
- Yajima, T., Yoshihara, K., Nakazato, K., Kumabe, S., Koyasu, S., Sad, S., Shen, H., Kuwano, H., and Yoshikai, Y. (2006). IL-15 regulates CD8+ T cell contraction during primary infection. *J Immunol* 176, 507-515. 10.4049/jimmunol.176.1.507.
- Yang, Y., Kohler, M.E., Chien, C.D., Sauter, C.T., Jacoby, E., Yan, C., Hu, Y., Wanhainen, K., Qin, H., and Fry, T.J. (2017). TCR engagement negatively affects CD8 but not CD4 CAR T cell expansion and leukemic clearance. *Sci Transl Med* 9. 10.1126/scitranslmed.aag1209.
- Yao, C., Sun, H.W., Lacey, N.E., Ji, Y., Moseman, E.A., Shih, H.Y., Heuston, E.F., Kirby, M., Anderson, S., Cheng, J., et al. (2019). Single-cell RNA-seq reveals TOX as a key regulator of CD8(+) T cell persistence in chronic infection. *Nat Immunol* 20, 890-901. 10.1038/s41590-019-0403-4.
- Yeku, O., Li, X., and Brentjens, R.J. (2017). Adoptive T-Cell Therapy for Solid Tumors. *Am Soc Clin Oncol Educ Book* 37, 193-204. 10.14694/EDBK\_180328. 10.1200/EDBK\_180328.
- Yi, J.S., Du, M., and Zajac, A.J. (2009). A vital role for interleukin-21 in the control of a chronic viral infection. *Science* 324, 1572-1576. 10.1126/science.1175194.
- Yi, J.S., Ingram, J.T., and Zajac, A.J. (2010). IL-21 deficiency influences CD8 T cell quality and recall responses following an acute viral infection. *J Immunol* 185, 4835-4845. 10.4049/jimmunol.1001032.

- Zeng, R., Spolski, R., Casas, E., Zhu, W., Levy, D.E., and Leonard, W.J. (2007). The molecular basis of IL-21-mediated proliferation. *Blood* 109, 4135-4142. 10.1182/blood-2006-10-054973.
- Zeng, R., Spolski, R., Finkelstein, S.E., Oh, S., Kovanen, P.E., Hinrichs, C.S., Pise-Masison, C.A., Radonovich, M.F., Brady, J.N., Restifo, N.P., et al. (2005). Synergy of IL-21 and IL-15 in regulating CD8<sup>+</sup> T cell expansion and function. *J Exp Med* 201, 139-148. 10.1084/jem.20041057.
- Zhang, Y., Joe, G., Hexner, E., Zhu, J., and Emerson, S.G. (2005). Host-reactive CD8<sup>+</sup> memory stem cells in graft-versus-host disease. *Nat Med* 11, 1299-1305. 10.1038/nm1326.
- Zhao, D.M., Yu, S., Zhou, X., Haring, J.S., Held, W., Badovinac, V.P., Harty, J.T., and Xue, H.H. (2010). Constitutive activation of Wnt signaling favors generation of memory CD8 T cells. *J Immunol* 184, 1191-1199. 10.4049/jimmunol.0901199.
- Zhao, L., Mei, Y., Sun, Q., Guo, L., Wu, Y., Yu, X., Hu, B., Liu, X., and Liu, H. (2014). Autologous tumor vaccine modified with recombinant new castle disease virus expressing IL-7 promotes antitumor immune response. *J Immunol* 193, 735-745. 10.4049/jimmunol.1400004.
- Zhao, X., Shan, Q., and Xue, H.H. (2021). TCF1 in T cell immunity: a broadened frontier. *Nat Rev Immunol*. 10.1038/s41577-021-00563-6.
- Zhou, F. (2009). Molecular mechanisms of IFN-gamma to up-regulate MHC class I antigen processing and presentation. *Int Rev Immunol* 28, 239-260. 10.1080/08830180902978120.
- Zhou, X., Yu, S., Zhao, D.M., Harty, J.T., Badovinac, V.P., and Xue, H.H. (2010). Differentiation and persistence of memory CD8<sup>(+)</sup> T cells depend on T cell factor 1. *Immunity* 33, 229-240. 10.1016/j.immuni.2010.08.002.
- Zhu, Y., Ju, S., Chen, E., Dai, S., Li, C., Morel, P., Liu, L., Zhang, X., and Lu, B. (2010). T-bet and eomesodermin are required for T cell-mediated antitumor immune responses. *J Immunol* 185, 3174-3183. 10.4049/jimmunol.1000749.

## **Annex**

Article

### **CD8 memory precursor cells generation is a continuous process**

Helena Todorov, Margaux Prioux, Daphné Laubretton, Matteo Bouvier, Shaoying Wang, Simon de Bernard, Christophe Arpin, Robrecht Cannoodt, Wouter Saelens, Arnaud Bonnaffoux, Olivier Gandrillon, Fabien Crauste, Yvan Saeys and Jacqueline Marvel

**Submitted**

# CD8 memory precursor cells generation is a continuous process

## Authors

Helena Todorov\*(1,2,3), Margaux Prioux\*(3,4), Daphné Laubretton(3), Matteo Bouvier(4,5), Shaoying Wang(3), Simon de Bernard (6), Christophe Arpin(3), Robrecht Cannoodt(1,2,7), Wouter Saelens(1,2), Arnaud Bonnaffoux(5), Olivier Gandrillon(4,8), Fabien Crauste (9), Yvan Saeys(1,2) and Jacqueline Marvel(3)

\*Co-first author

1 Department of Applied Mathematics, Computer Science and Statistics, Ghent University, Ghent, Belgium

2 Data Mining and Modeling for Biomedicine, VIB Center for Inflammation Research, Ghent, Belgium

3 Centre International de recherche en Infectiologie, Université de Lyon, INSERM U1111, CNRS UMR 5308, Ecole Normale Supérieure de Lyon, Université Claude Bernard Lyon 1, Lyon, France

4 Laboratoire de Biologie et de Modélisation de la cellule, Université de Lyon, ENS de Lyon, CNRS UMR 5239, INSERM U1210, Lyon, France

5 Vidium, Lyon, France

6 AltraBio, Lyon, France

7 Data Intuitive, Lebbeke, Belgium

8 Inria, Villeurbanne, France

9 Laboratoire MAP5 (UMR CNRS 8145), Université de Paris, Paris, France

## Abstract

In this work, we studied the generation of memory precursor cells following an acute infection by analysing single-cell RNA-seq data that contained CD8 T cells collected during the post-infection expansion phase. We used different tools to reconstruct the developmental trajectory that CD8 T cells followed after activation. Cells that exhibited a memory precursor signature were identified and positioned on this trajectory. We found that memory precursors are generated continuously with increasing numbers being generated over time. Similarly, expression of genes associated with effector functions was also found to be raised in memory precursors at later time points. The ability of cells to enter quiescence to differentiate into memory cells was confirmed by BrdU pulse-chase experiment in vivo. Analysis of cell counts indicates that the vast majority of memory cells are generated at later time points from cells that have extensively divided.

## Introduction

The number of naive CD8 T cells that are specific for a given pathogen is relatively low, ranging from 100 to 1000 cells (Obar et al., 2008; Haluszczak et al., 2009). Upon infection, these pathogen specific CD8 T cells will be recruited and activated. This, under appropriate conditions, leads to their extensive proliferation and differentiation in a large ( $10^6$ - $10^7$  cells) population of effector CD8 T cells that display the capacity to eliminate infected cells. The majority of effector cells will die by apoptosis, except for a smaller subset of memory precursor (MP) cells that will further differentiate to give rise to a long-lived population of memory cells ( $10^5$  to  $10^6$  cells) that will provide protection upon subsequent infection (Murali-Krishna et al., 1998; Crauste et al., 2017). Although these cells are mainly quiescent, they retain the capacity, upon re-exposure to pathogens, to expand and rapidly display effector functions due to epigenetic modifications of genes involved in these processes (Fitzpatrick et al., 1999; Marcais et al., 2006).

In order to better understand the properties of memory cells generated in different settings (Appay et al., 2002), many studies have focused on defining CD8 T cell subsets, relying on a restricted number of surface proteins (Sallusto et al., 1999; Hikono et al., 2007; Jameson and Masopust, 2009). These cell subsets include central and effector memory cells, exhausted memory cells or tissue resident memory cells. Over the years, the study of these subsets has brought a wealth of knowledge on the responsiveness (Wherry et al., 2007; Hikono et al., 2007; Sallusto et al., 1999), homing (Masopust et al., 2001), and self-renewal capacities (Graef et al., 2014; Gattinoni et al., 2012) of memory cells. The molecular pathways sustaining their development have also been largely uncovered. Indeed, the involvement of numerous transcription factors (Intlekofer et al., 2005; Omilusik et al., 2015; Mann et al., 2019; Kaech and Cui, 2012) and epigenetic reprogramming factors (Pace et al., 2018) in the differentiation of different classes of effector and/or memory cells has been described.

The lineage relationship between the different subsets of CD8 T cells (Wherry et al., 2003) and the stage at which activated CD8 T cells diverge from the effector fate to commit to the memory lineage have been extensively studied, with many different experimental approaches leading to results supporting alternative models (Kaech and Cui, 2012). A linear pathway where memory cells are derived from effector cells is supported by early studies using genetic marking of memory cells (Jacob and Baltimore, 1999). A linear model where activated naive cells first differentiate into MP cells that give rise to effector cells has been suggested following in vivo fate mapping of single cells (Buchholz et al., 2013). These early MP cells could correspond to the memory stem cells described in a restricted number of experimental systems (Gattinoni et al., 2012). Fate mapping experiments have highlighted the heterogeneity of effector cells in terms of their functional capacities and their differentiation potential into memory cells (Joshi et al., 2007; Wherry et al., 2007; Sarkar et al., 2008; Kalia et al., 2010). Hence, a new classification of effector cells based on the expression of KLRG1 and CD127 has emerged with, on one side, short-lived effector cells doomed to die at the end of the primary response and, on the other side, MP effector cells that maintain the capacity to differentiate into memory cells (Joshi et al., 2007). In this model

and in the first linear models, memory cells are derived from cells that express fully developed effector functions and that have maintained the potential to differentiate into memory cells (Pace et al., 2018; Youngblood et al., 2017). In contrast, a number of other studies have suggested a separation of MP cells at an earlier stage that precedes the differentiation into effector cells. Indeed, branching as early as following the first division has been proposed based on single cell transcriptome analysis (Arsenio et al., 2014; Kakaradov et al., 2017) and would potentially result from an asymmetric division of antigen-triggered cells (Chang et al., 2007). Although these models agree on the early commitment of activated naive CD8 T cells to the memory lineage, there remains some debate about the existence of an early branching (Flossdorf et al., 2015).

More recently, Crauste et al. (2017), based on the modeling of the generation of memory CD8 T cell counts, demonstrated that the total pool of memory CD8 T cells could mainly be generated by a linear pathway; the majority of quiescent memory cells are generated following the transition of naive cells through an early activation effector stage characterized by active cell cycling followed by a late quiescent effector stage (Crauste et al, 2017). In this model, an early branching of memory cells was permitted but it could not account for the generation of the full supply of memory cells.

Overall, functional studies of memory differentiation routes by genetic ablation or cell fate mapping studies have led to the description of multiple possible pathways that lead to a diversity of effector/memory populations. They suggest that memory commitment could take place at several stages of the primary immune response. However, some of these pathways might represent routes followed by only a few cells that generate a minor fraction of the memory cell pool.

In order to uncover the different trajectories followed by naive CD8 T cells to differentiate into memory cells, we have used new trajectory analysis tools that take into account the large amount of information that is delivered by single cell transcriptomics. Indeed, over the last decades, single-cell RNA sequencing (scRNA-seq) has emerged as a powerful tool and allowed a great advance in the exploration of the heterogeneity of the immune system (Papalexis and Satija, 2018). We analysed gene expression dynamics in CD8 T cells collected during the effector response to an acute infection with the Lymphocytic Choriomeningitis Armstrong virus (LCMV-Arm), generated by (Yao et al., 2019) and (Kurd et al., 2020). We applied trajectory inference on these dataset to identify trajectories leading to the generation of MP cells. Using cell-cycle classification and RNA velocity algorithms we show that the differentiation is driven by cell cycle and immune function genes. To identify the molecular regulatory mechanisms supporting the process, we then performed a gene regulatory network (GRN) inference analysis which allowed us to identify a cluster enriched in cells harbouring transcription factors associated with MP cells. Using a MP gene signature, we confirmed that this cluster was enriched in MP cells, though cells expressing that signature were also found at multiple points along the trajectory. Finally, we used another pathogen infection and BrdU labelling to generalise and validate these results in vivo. Analysis of cell counts confirmed that although memory cells are generated continuously all along the trajectory, the majority of memory cells were derived from cells that had proliferated and acquired effector functions.

## Results

### Trajectory inference of the CD8 T cell response to an acute infection

In order to gain insight into the differentiation dynamics of CD8 T cells in response to an acute infection (LCMV-Arm), we performed trajectory inference on a scRNAseq dataset generated by Yao et al (2019) using two recently published methods, Slingshot (Street et al., 2018) and TinGa (Todorov et al., 2020). This dataset consists of measurements on 20,295 splenic CD8 T cells generated following LCMV-Arm acute infection and isolated at two different time points (4.5 and 7 days post infection (dpi)), in two separate replicates. We identified the 2,000 most highly variable genes in the dataset using variance modelling statistics from the Scran R package (Lun et al., 2016), on which we applied both trajectory inference methods. Slingshot was shown to be very efficient in a study that compared more than 40 methods on a large number of datasets (Saelens et al., 2019). TinGa is a new method for trajectory inference that showed comparable results on simple trajectories and better results on complex trajectories than Slingshot (Todorov et al., 2020). These two methods both share a first step in which the dimensions of the data are reduced, either by principal component analysis for Slingshot, or by multidimensional scaling (MDS) for TinGa. In the two resulting representations of the data, the cells form a continuum from cells taken 4.5 dpi to cells taken 7 dpi (Figure 1A and Figure supplement 2A).

Slingshot first applies clustering to the data and then identifies transitions between these clusters. It identified a linear trajectory starting among cells from day 4.5 post-infection (pi), transitioning through a mix of cells from day 4.5 to 7 pi, and ending in a part of the data that was enriched in cells from day 7 pi (Figure supplement 2B). The genes that varied the most along this trajectory are identified in Figure supplement 2C. The linear Slingshot trajectory seemed to start in early activated cells, in which we identified an overexpression of *Ybx1*, *Rps2*, *Rps8* genes involved in the initiation of transcription. The trajectory then transitioned through a state where the cells seemed to be undergoing divisions (*Tubb4b*, *Tuba1b*, *Ccna2*, *Cks1B* genes) and ended in cells that expressed genes associated with immune functions (such as *Ccl5*, *Hcst*, *B2m*, *H2-D1*). In comparison, the trajectory identified by TinGa started similarly to the Slingshot trajectory, but then split into two branches (Figure 1B). One small branch (identified by the number 3) corresponded to cells that seemed to be in a highly cycling state, whereas the other longer branch ended, after several transitional states, in the effector-memory-like state described in the Slingshot trajectory (Figure supplement 1A). Eight transitional states were identified along the TinGa trajectory. For convenience, these eight transitional populations will be referred to as clusters from now on.

Among the 40 genes that varied the most along the two trajectories defined by Slingshot and TinGa (Figure supplement 1 and 2C), 33 were commonly found in both trajectories. This suggests that, even though TinGa identified an extra small branch that Slingshot included in a linear trajectory, the genes that are mainly driving cells along the two trajectories are similar. Interestingly, when we applied Slingshot and TinGa to a reduced set of 1,300 highly variable genes, both methods recovered a branching trajectory (Figure supplement 1B and Figure supplement 2D). This indicates that the main trajectory uncovered is robust and that the small-branch identified differs only marginally from the neighboring cluster.

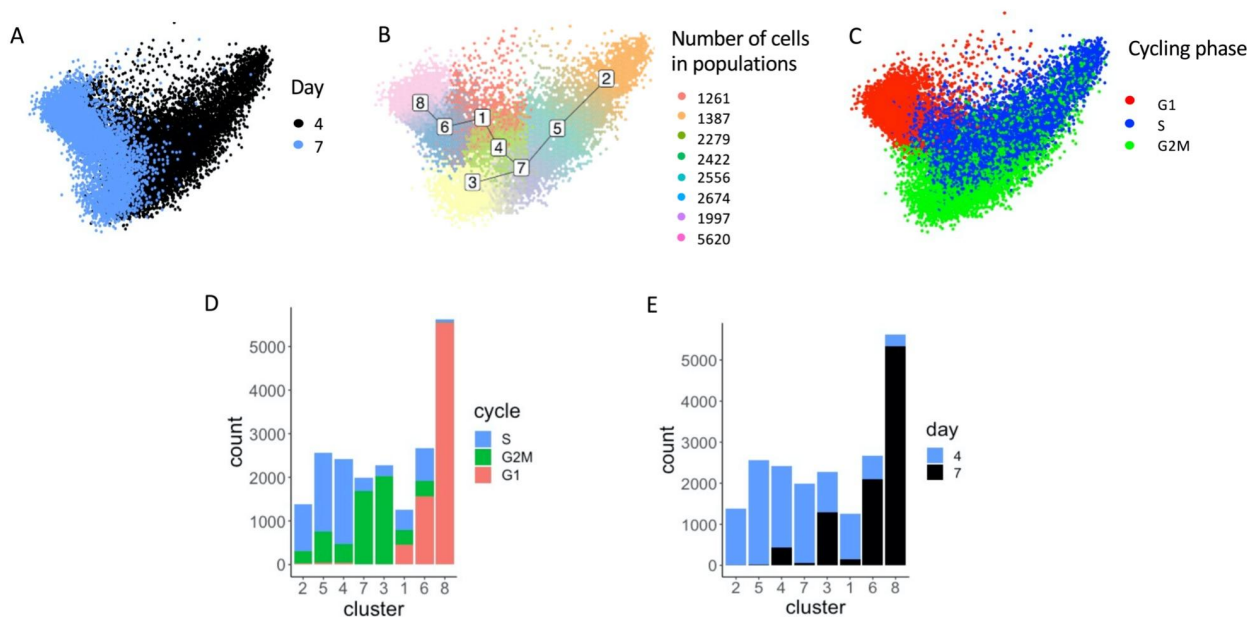


**Figure 1-figure supplement 1-figure supplement 2: TinGa trajectory inference**

**(A-C)** Visualisation of the cells in a 2D space computed by multi-dimensional scaling **(A)** The cells were colored according to the two experimental time points 4.5 and 7 days post LCMV-Armstrong infection. **(B)** The TinGa algorithm identifies a branching trajectory in the data, that is represented by a black line. Milestones along the trajectory can be used to define subgroups of cells that are represented by different colors. They will be referred to as “clusters”. The number of cells in each cluster are indicated. **(C)** The cells were classified into one of the cycling phases (either G1, S, or G2/M) using the Seurat package and colored accordingly. **(D-E)** The number of cells in the G1, S and G2/M phases **(D)** and in the two experimental time points **(E)** are shown for each cluster.

### The inferred trajectories retrace an early-late-memory differentiation pathway

To further characterize the CD8 differentiation trajectory supported by the single cell transcriptomics data, we used the trajectory obtained with TinGa as it identified more transition points along the route and hence might give a more refined definition of differentiation steps. As both the Slingshot and the TinGa trajectories were clearly driven by cell cycle associated genes (Figure supplement 1A and Figure supplement 2C), we used a classifier from the Seurat R package (Tirosh et al., 2016) to allocate cells to the G1, S or G2/M cell-cycle phases (Figure 1C). We identified clear cycling trends along the trajectory. Cells in clusters 2, 5 and 4 were mainly classified in the S phase (Figure 1C-D) while clusters 7 and 3 were de facto classified in the G2/M phase (Figure 1C-D). Cluster 6 was clearly enriched in G1 cells, while cluster 8 contained almost exclusively cells in G1 (Figure 1C-D). Hence, these results showed that the Tinga trajectory consisted of a first cycling effector population that differentiated in a quiescent effector population. Interestingly, TinGa identified three clusters enriched in cells positioned in the S phase (cluster 2, 5 and 4) and two clusters enriched in cells positioned in the G2/M phase (cluster 7 and 3). These clusters, however, differed in terms of sampling days and the two clusters (3 and 4) positioned at a later pseudotime by TinGa contained a larger fraction of cells sampled on day 7 compared to the

earlier clusters with a similar cell cycle position. Thus, to unravel genes driving the trajectory, while overcoming cell cycle gene expression biases, we performed a differential expression analysis between cells from the same cycle phase present in each neighboring cluster along the trajectory (Supplementary Table 1 and Figure supplement 3A). This highlighted the slow transition from early activation markers (Xcl1, Srm) to effector functions (Ccl5, Id2, Gzma/k) and quiescence (Btg1) (Figure supplement 3A right panel).

To further define the dynamics of cell differentiation, we applied the scVelo algorithm (Bergen et al., 2020) that defines RNA velocities. These were projected onto the TinGa embedding (Figure 2A). ScVelo retraced two RNA trajectory dynamics (Figure 2B). The first suggests a circular trajectory that would fit with cells going through the cell cycle. The second corresponds to a linear trajectory of differentiation leading from clusters 5 and 7 to 8. Interestingly, the cells of cluster 3 seemed to join those of cluster 8. Thus, the small branch identified by TinGa could correspond to a transient state composed of cells passing from a state of proliferation to a quiescent state.

A similar dynamic was obtained using only the top 50 genes contributing to the scVelo's dynamical model (Figure supplement 3B, Supplementary Table 2) indicating that they were sufficient to recover the overall cell dynamics (Figure 2A). We then analysed the molecular function associated with these 50 genes and found that they could be broadly classified into three categories (cell cycle, migration and immune function) (Supplementary Table 2). To compare the contribution of these genes to the dynamic, the RNA velocities associated with cell cycle/migration related genes or immune function genes were calculated and projected onto the TinGa embedding (Figure 2C-D). The cell cycle and migration genes clearly defined the first circular dynamics found at the start of the trajectory and also contributed to the differentiation process (Figure 2C) while the immune genes recapitulated a linear trajectory going from cluster 2 to 8 (Figure 2D). By looking at individual gene dynamics, we found that genes act on different parts of the cell differentiation trajectory. Genes such as Id2 have an early effect, with stronger contribution to the global velocities in clusters 4, 5 and 7, while genes such as IL18r1 and Gimap6 start to act at later pseudotime with stronger velocities in the final clusters of the trajectory (Figure supplement 3C).

The trajectory inference based on single cell transcriptomic data seems to recapitulate the two effector compartments that we have previously described, i.e. a first set of early effector cells that are cycling followed by a set of late effector cells that are quiescent and express increased levels of genes encoding immune effector functions (Crauste et al., 2017).

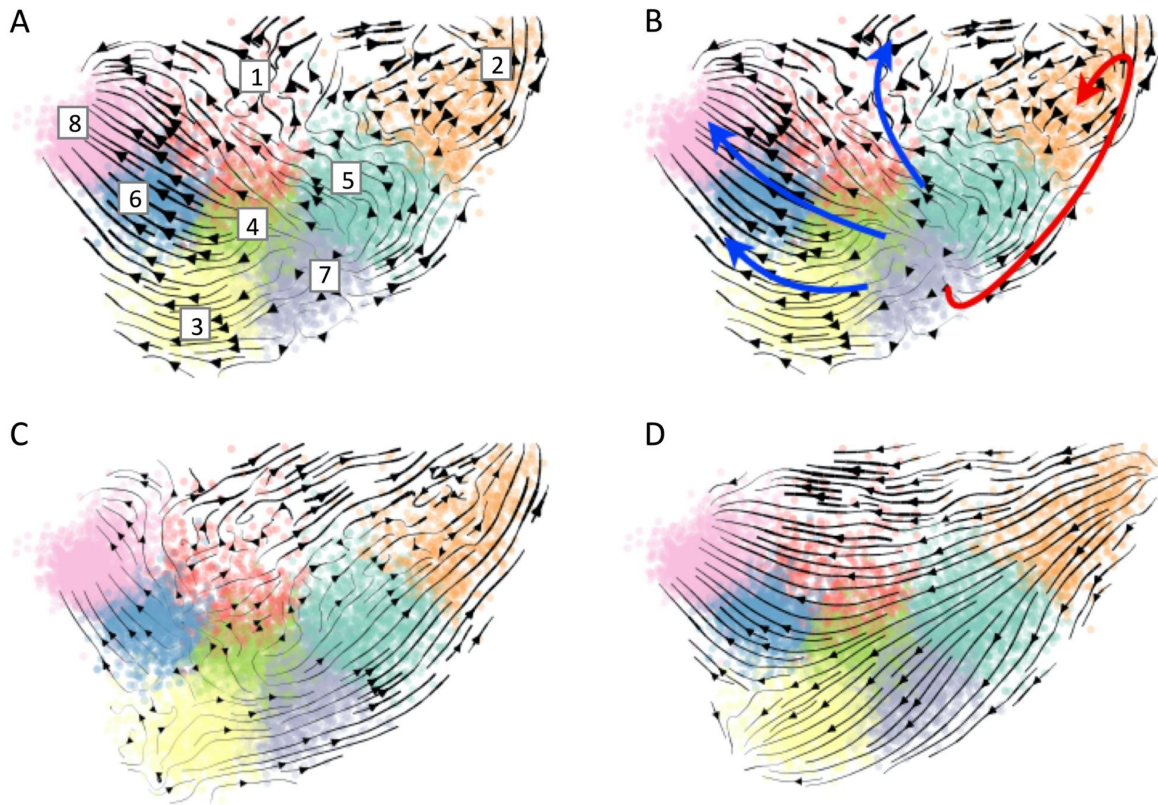


**Figure 2-figure supplement 3:** Gene expression dynamics along the differentiation trajectories. RNA velocities are projected onto the TinGa embedding. The cells in the trajectory were colored according to their TinGa milestones. **(A)** Velocities were calculated using all genes. Numbers correspond to TinGa clusters. **(B)** The RNA velocities show two distinct dynamics. In clusters 2, 5 and 7, cells are cycling (red arrow) but can commit to the differentiation dynamic (blue arrows) by leaving clusters 5 and 7 to reach cluster 8. **(C-D)** RNA velocities based only on cell cycle and migration **(C)** or immune function-related **(D)** genes.

### Gene regulatory interaction analysis

To further characterise the transitional stages defined along the TinGa trajectory, we identified regulatory interactions between transcription regulators and their target genes in the dataset using the BRED tool (Cannoodt et al., 2019). We identified six main GRN-modules, that we defined as groups of target genes gathered around a regulator (Figure 3A). As expected, based on previous results on the cell cycle, three of these modules (Pcna, Hmgb2, Cenpf) were strongly enriched in genes involved in cell cycle regulation. The Ybx1 GRN-module contained two groups of genes. One coding for proteins involved in RNA and protein synthesis metabolism that were up-regulated in the cells from the cluster 2-5-7 branch, the other for immune functions that were enriched in clusters 6 and 8 (Figure supplement 4). Two GRN-modules were composed essentially of genes associated with the immune response. The GRN module Spi1 was expressed in very few cells along the trajectory (Figure supplement 5). In contrast, the Tcf7/Id2/Phb2 GRN-module contained genes coding for transcription factors and immune functions, associated with the

differentiation of CD8 T cells in memory cells. These genes were expressed in different clusters along the trajectory (Figure supplement 6). Interestingly, cluster 1 was enriched in cells that coexpressed genes from the Tcf7/Id2/Phb2 modules which were associated with a MP cell phenotype as defined by a number of studies (Yao et al., 2019; Wu et al., 2016; Utzschneider et al., 2016; Chen et al., 2019). Indeed, they expressed Tcf7 and Id3, two transcription factors that were previously associated with a MP potential (Yao et al., 2019). Two target genes, Slamf6 and Tnfsf8, were found to be positively correlated with the presence of Tcf7 in the Tcf7/Id2/Phb2 module. In contrast, the Id2 transcription factor, that has previously been associated with an effector fate (Omilusik et al., 2018), was repressed in these cells, as was the effector associated gene Gzmb (Figure 3B and Figure supplement 6).

In summary, cluster 1 seemed to contain an interesting set of cells in which effector functions were down-regulated, while genes associated with a memory precursor signature were over-expressed. We thus decided to further characterize the cells in cluster 1.

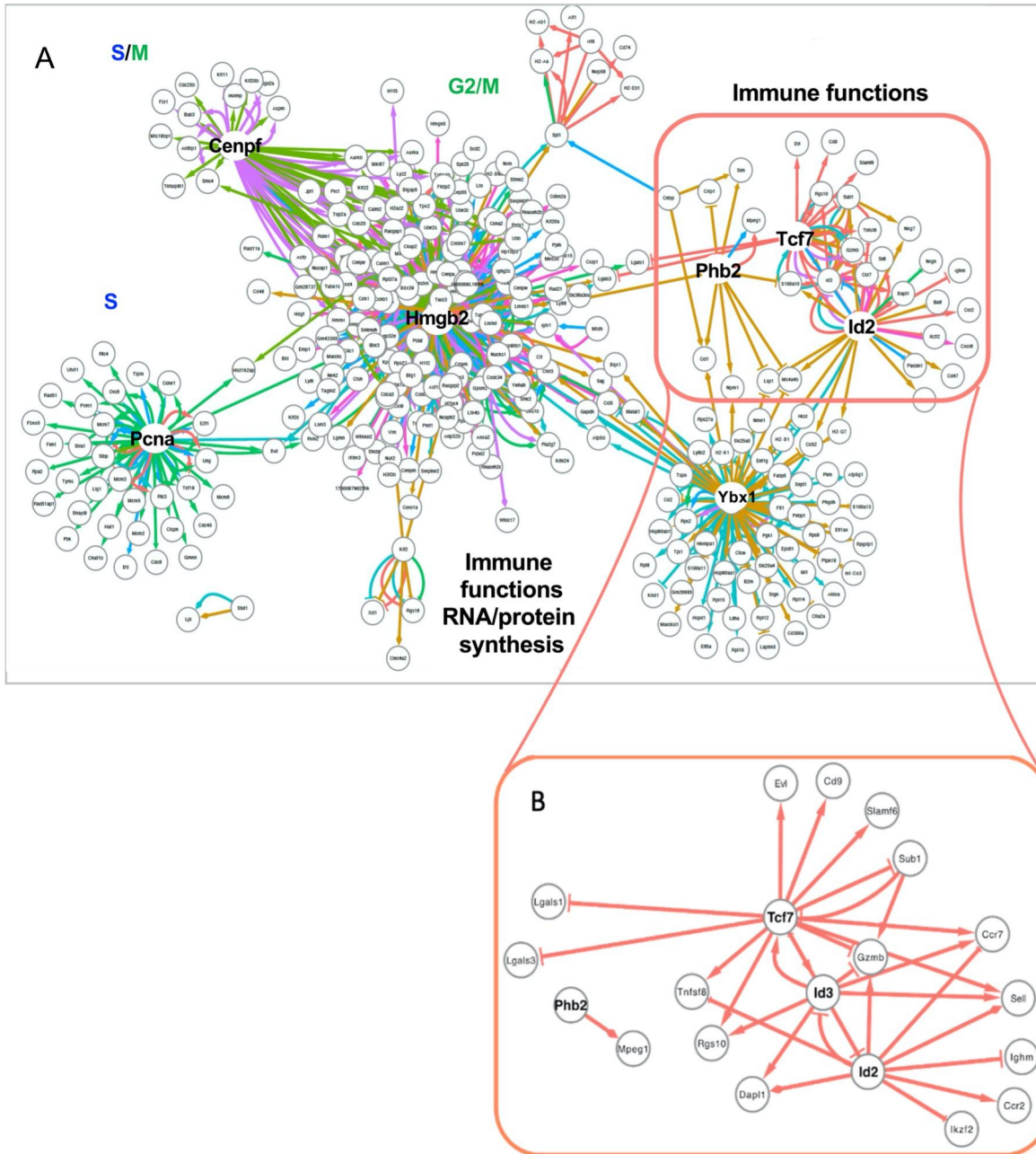


**Figure 3- figure supplement 4-figure supplement 5-figure supplement 6:** Gene regulatory interactions

**(A)** Gene regulatory network identified with BRED. In this GRN, regulatory processes are symbolised by arrows that are directed from transcription factors to their target genes, or to other transcription factors. The top 100 interactions per TinGa cluster are represented, and are colored according to the cluster in which they are occurring. The shape of the arrow indicated whether the interaction was an activation (->) or an inhibition (-|). **(B)** Zoom on the Id2/Tcf7/Id3 module identified by BRED. Only the interactions occurring in cluster 1 in the TinGa trajectory are represented.

## **TinGa identifies distinct clusters associated with a memory-precursor phenotype**

Cluster 1 was mainly composed of cells from day 4.5 pi, a large fraction of which (40%) was classified as being in the G1 phase of the cell cycle (Figure 1D-E, Figure supplement 7A). This contrasted with other clusters enriched in cells from day 4.5 pi, such as clusters 2 and 5, that contained very few cells classified as being in G1 (Figure 1D-E).

To ascertain that cells in cluster 1 had been activated, we compared their transcriptome with the genes expressed in cluster 2 positioned at the beginning of the trajectory. Results in Figure supplement 7B showed that the cells in cluster 1 expressed an increased amount of genes coding for effector functions such as *Ccl5* and *Gzma* compared to cluster 2, indicating that these cells had been activated as they had started to acquire effector functions. Cells in cluster 1 also expressed interferon-induced genes such as *Ifi271a*, *Ifi203*, *Ifi47* (colored in red in Supplementary Fig 7B), indicating that these cells had responded to the pathogen-induced innate response. We thus concluded that cluster 1 contained cells from day 4.5 pi that had been activated but already displayed traits of quiescence.

Cluster 1 cells expressed increased amounts of *Tcf7*, *Id3* and *Ltb* as compared to all other cells in the trajectory, while *Klrg1*, a gene associated with terminal differentiation, was down-regulated in these cells (Figure supplement 7C). This was in agreement with the activation of the *Tcf7/Id2/Phb2* module, containing genes associated with a MP potential in these cells.

To confirm the MP genetic program of cells in cluster 1 and to identify all MP cells along the trajectory, we performed a gene set enrichment analysis (GSEA) using the MP gene signature recently defined in (Yao et al., 2019) (Supplementary Table 3 and Figure 4A). We identified 833 MP cells that were mainly localized in clusters 1 and 8 (Figure 4A-B). Unsurprisingly, cluster 1 was the most enriched in the MP signature with 15% of the cells presenting the signature. Cluster 8 also contained a significant fraction (9%) of MP cells. However, the majority of MP cells were associated with cluster 8 that contained 3 times more MP cells than cluster 1 (Figure 4B-C). The majority of MP in cluster 1 and 8 were associated with the G1 phase of the cell cycle compared to those in the other clusters that were mainly in S and G2/M phase (Figure 4C).

To determine the number of MP cells that had effectively been found on each sampling day, we recalculated the number of MP cells present in the spleen of animals at the two experimental time points (see Methods section). Based on the number of LCMV-Arm specific CD8 T cells present in the spleen on day 4.5 and 7 pi, we could estimate the number of cells with a MP gene signature on these two days to be 3,850 and 643,000. This indicated that the number of MP cells generated 4.5 days after infection is more than 150 times lower than the number of MP cells generated 7 days after infection, in agreement with values estimated in (Crauste et al., 2017).

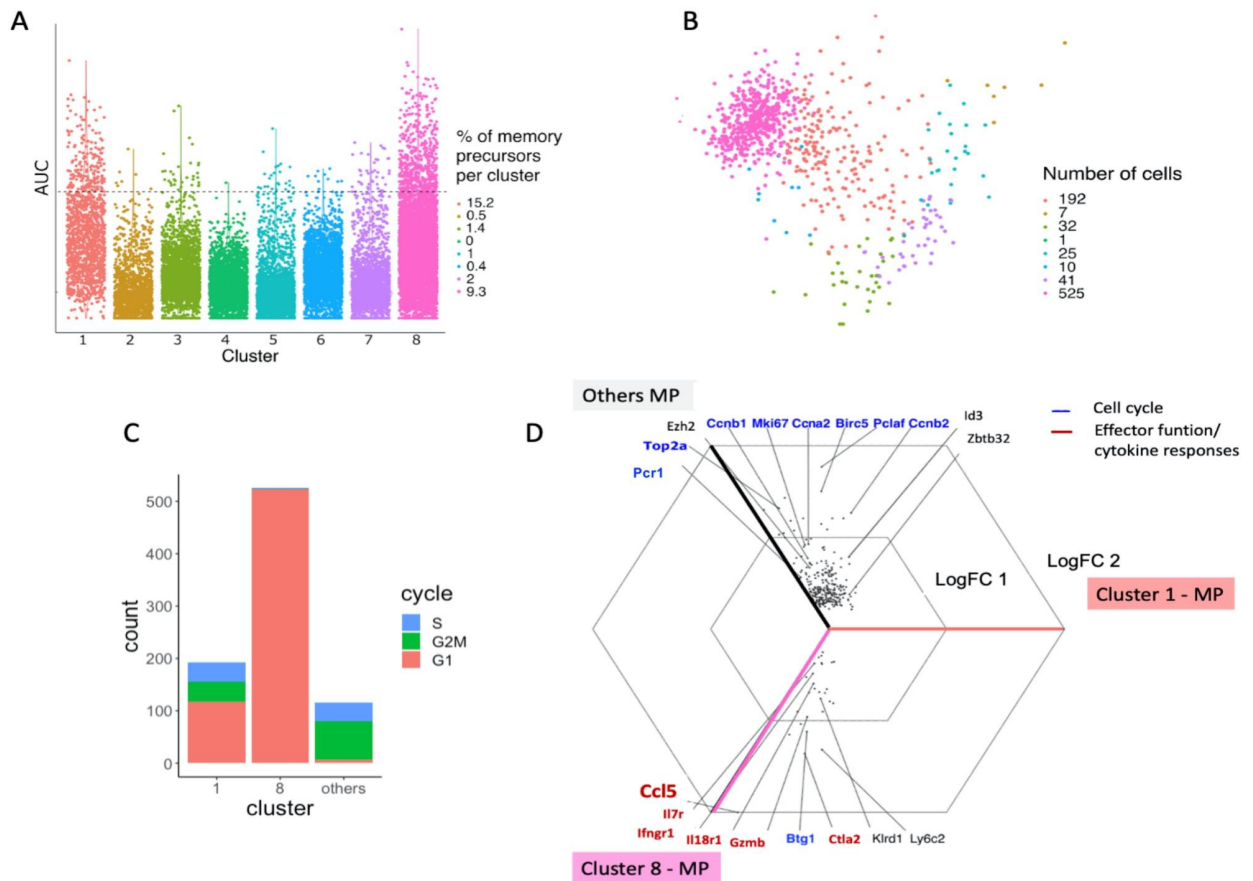


**Figure 4-figure supplement 7-figure supplement 8:** Memory precursor cell identification and characterization. **(A)** Memory precursor signature enrichment in each cluster along TinGa's trajectory. The cells above the threshold represented as a dotted line are considered as memory precursors. The percentage of cells with a memory precursor signature in each cluster is indicated. AUC: area under the curve **(B)** The cells with a memory precursor signature were represented on the TinGa map and colored according to the cluster they came from. The number of cells with a memory precursor signature in each cluster is indicated. **(C)** Distribution in the G1, S and G2/M cell cycle phases of cells with a memory precursor signature from clusters 1, 8 or all others. **(D)** Triwise plot of the log fold-change expression of genes that were differentially expressed between the memory precursor cells found in cluster 1, 8, and all other memory precursors. Only the genes that were differentially expressed with a p-value < 0.05 are represented. The internal hexagon corresponds to a log fold-change of 1, the external hexagon corresponds to a log fold-change of 2.

To investigate differences between MP cells generated at day 4.5 and at day 7 pi, we compared the gene expression profiles of cluster 1 to cluster 8 MP cells respectively, and to the profiles of MP from all the other clusters (Figure 4D). Both clusters 1 and 8 MP cells showed a decreased expression of genes driving the cell cycle compared to the other MP, in agreement with their position in G1 phase (Figure 4C-D). Cluster 8 MP cells have an increased expression of genes coding for proteins involved in effector functions (Gzmb, Ctla2, Ccl5) or cytokine response (Il7r, Il18r1, Ifngr1) compared to cluster 1 MP cells, indicating that, although they display a MP gene signature, they have also acquired effector cell properties. This was in agreement with the data showing that effector cells could dedifferentiate into quiescent memory cells (Youngblood2017). Interestingly, cycling MP (i.e.,

MP from clusters other than 1 and 8) expressed genes coding for transcription factors (Zbtb32, Id3) or histone modifier (Ezh2) involved in the regulation of the developmental switch between effector and MP cells, suggesting that cycling MP are still oscillating between these two fates (Kakaradov et al., 2017; Shin et al., 2017; Yang et al., 2011).

To confirm the continuous generation of MP cells, we analysed a second transcriptomic dataset generated by Kurd et al. that contained cells sampled at multiple time points during the primary response (day 4, 5, 6, 7 and 10 post-LCMV infection). Highly variable genes expressed by the 9,614 cells were selected and TinGa was applied (Figure supplement 8A). The trajectory obtained is similar to the Yao et al.'s data (Yao et al., 2019) with the first part of the trajectory being enriched in cycling cells (cluster 1, 3, 8, 6 and 4) which were sampled on day 4, 5, 6 and 7 pi. The second part contained quiescent cells sampled on day 6, 7 and 10 pi (Figure supplement 8A-B-C). Similarly, 574 MP cells were found by GSEA all along the TinGa trajectory (Figure supplement 8D-E).

Overall, these results suggested that MP cells with different functional and differentiation statuses, from activated cycling cells to quiescent effector cells, were present at different points along the trajectory.

### **In vivo validation of memory cell generation at different time points following activation of CD8 T cells**

Our in-silico analyses strongly suggest that CD8 T cells become quiescent and differentiate into memory cells at different stages following activation in response to acute viral infection. To validate this result in vivo, we used BrdU pulse-chase experiments. Indeed, these allow tracking cells that proliferate during the pulse time and stop soon thereafter, thus maintaining their BrdU labelling in the memory phase. This way we can identify MP cells present at the time of pulse. We also wanted to extend the data to other experimental systems so we used vaccinia virus (VV) that induces a local acute infection in the lung when inoculated intranasally. Thus, mice were infected intranasally with a VV harboring the NP68 epitope and we followed the activation of TCR transgenic F5 cells (Crauste et al., 2017). Mice were given one injection of BrdU on days 4, 7 and 11 pi and BrdU labelling was analysed after 24 hours in the spleen and the lymph nodes draining the lung and nasal cavity (Figure supplement 9A).

Following VV infection, TCR transgenic F5 CD8 T cells increased in proportion and numbers over time in both spleen and draining lymph nodes (dLN), with a peak 8 dpi (Figure 5A-B). The percentage of BrdU labelled cells, representative of proliferating CD8 T cells, was maximal 5 dpi in the dLN and 8 dpi in the spleen, reflecting the local initiation of the CD8 T cells immune response following intranasal infection (Figure 5C-D). The number of BrdU labelled cells was maximal both in spleen and dLN 8 dpi and started to decrease thereafter with a limited number of cycling cells detected 12 dpi.

Using data from three independent experiments we next estimated (see Methods section) the proliferation and differentiation rates of cycling effector cells (Crauste et al., 2017) on days 4, 5, 7 and 11 pi. In agreement with the BrdU labelling profile of total CD8 T cells we found that the proliferation rate of effector cells peaks on days 4-5 before quickly decreasing both in dLN and spleen (Figure 5E). This is in agreement with previous results (Crauste et al., 2017) obtained on blood samples. In contrast, their differentiation rates to quiescent effector cells is

very low on days 4-5 pi, increasing on day 7 pi with the highest rate being observed on day 11 pi, once proliferation has drastically vanished, in both spleen and dLN (Fig 5F).

We then measured the fraction and number of BrdU-labelled CD8 T cells in the memory phase (39 dpi) in order to evaluate the MP cells present on day 4, 7 or 11 pi of the response (Figure 5G-H). As predicted by the single cell transcriptomic data, we found that memory cells could derive from activated/effector cells at all investigated times. However, the largest fraction of memory cells was derived from cells labelled on day 7 or later (Figure 5I). Importantly the few cells that were labelled with BrdU between days 11 and 12 gave rise to a significant fraction of the memory cell pool in agreement with their increased differentiation rates (Figure 5F).

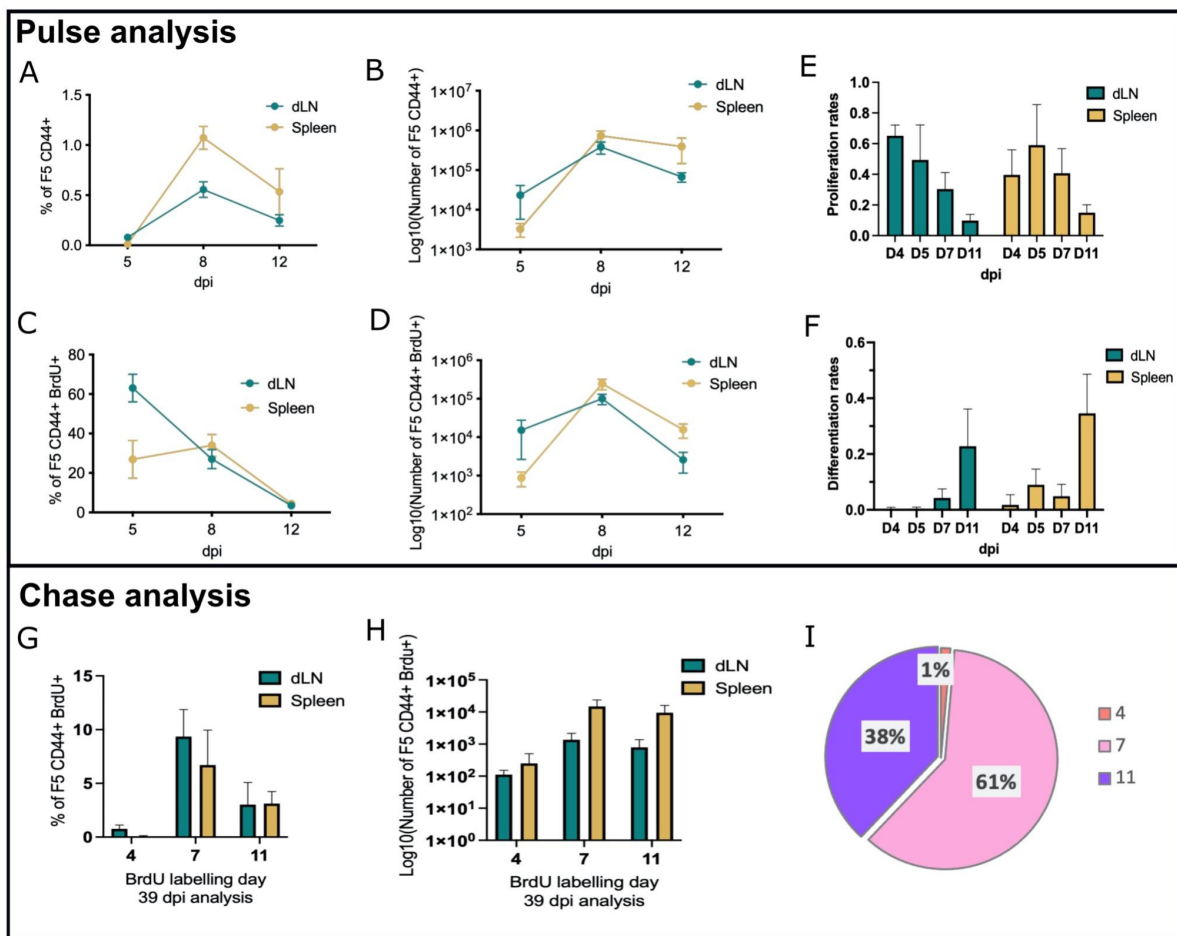


**Figure 5-figure supplement 9:** In vivo identification of memory precursors using BrdU labelling. (A-D) The percentages (A, C) and numbers (B, D) of total F5 CD44+ (A, B) and BrdU+ F5 CD44+ (C, D) CD8 T cells were determined 24h after BrdU injection (pulse) in the indicated organs. (E) Proliferation rates of Early Effector (EE) cells in the indicated organs from day 4 to day 11 post-infection. (F) Differentiation rates of EE cells into Late Effector (LE) cells in the indicated organs from day 4 to day 11 post-infection. (G-H) The percentages (G) and numbers (H) of BrdU+ F5 CD8 memory T cells originating from cells labelled on days 4, 7 or 11 pi was determined 39 days after BrdU injection (chase) in the indicated organs. (I) Proportion of memory cells originating from MP labelled at days 4, 7 or 11 pi normalized to the total number of recovered BrdU+ F5 CD8 memory T cells. Data are representative of 3 independent experiments.

Finally, we compared protein expression of memory cells generated on day 4.5 or day 7 pi. We thus performed a BrdU chase experiment (Figure supplement 9B) and measured the expression of proteins encoded by genes that were differentially expressed in the single cell transcriptomic dataset (Figure 4D and Supplementary Table 4). We found that CCL5, which was the most differentially expressed gene in late d7 MP cluster 8 (Figure 4D), was also expressed at a higher protein level by F5 memory cells generated at 7 dpi (Figure 6A). The expression of CCL5 was also measured on endogenous antigen-induced BrdU positive memory cells, identified based on their CD49d expression (Grau et al., 2018) (Figure supplement 9C). Similarly, we found a significant increase of CCL5 expression on BrdU+ endogenous memory cells generated at 7 dpi in the dLN and spleen (Figure 6B-C).

Overall these results show that although memory cells are generated continuously after activation, the majority of memory cells are generated late during the effector phase (Figure 7).

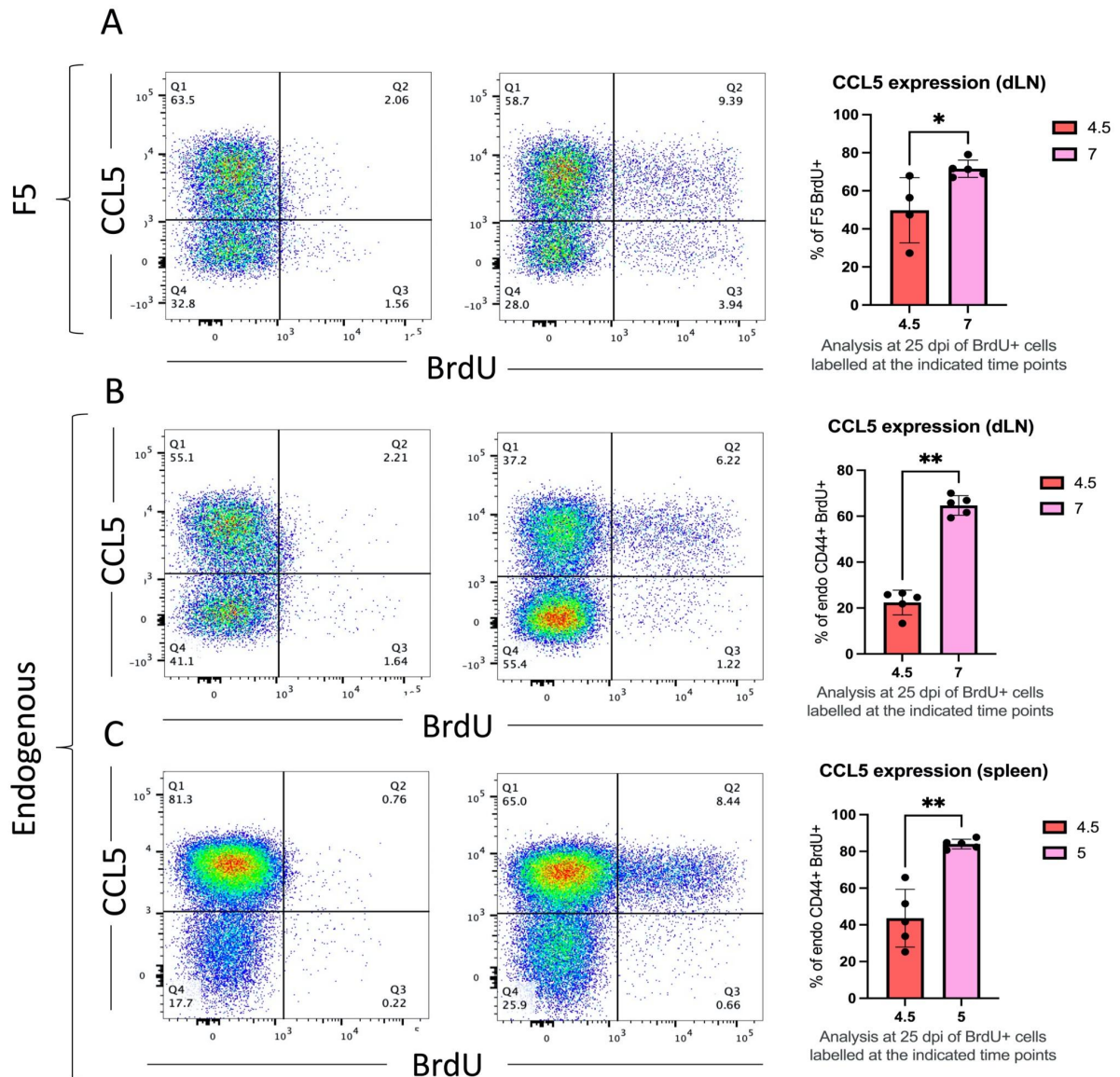
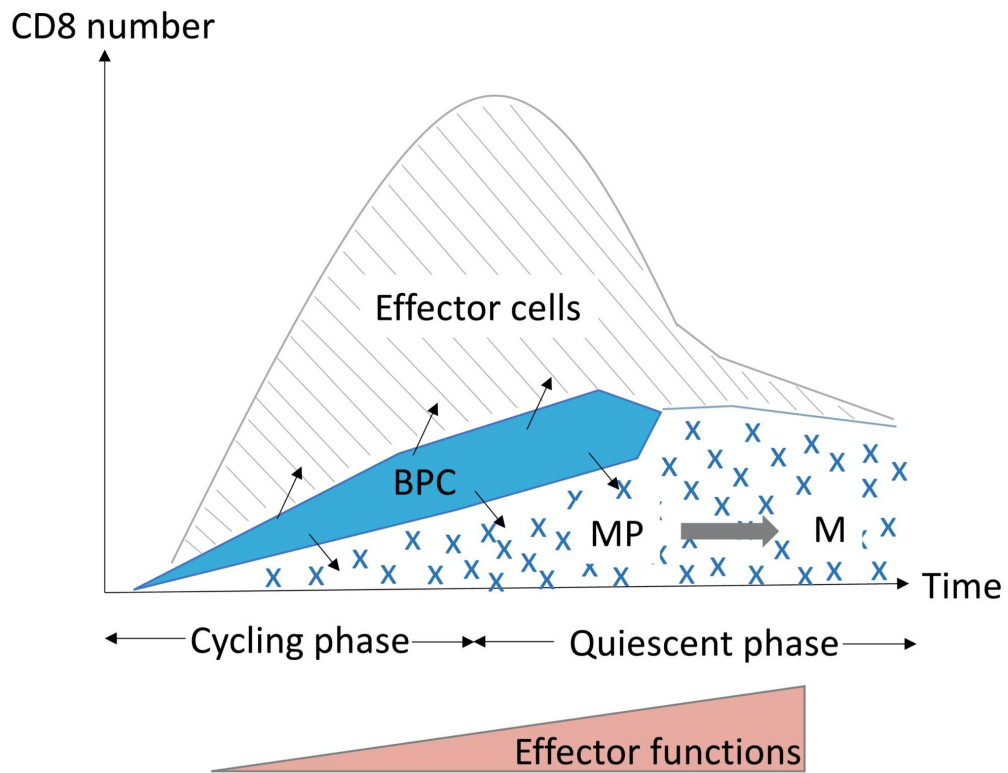


**Figure 6-figure supplement 9:** CCL5 expression of early and late generated memory cells by flow cytometry. **(A)** Flow-cytometry plots and quantification of BrdU+ F5 memory cells expressing CCL5 labelled on day 4.5 and 7 with BrdU was assessed. **(B, C)** Flow-cytometry plots and quantification of CD44+ CD49d+ BrdU+ endogenous memory cells expressing CCL5 labelled on day 4.5 and 7 with BrdU was assessed in the draining lymph node **(B)** and in the spleen **(C)**.

\* $p < 0.05$  (Mann-Whitney test). Data are representative of 2 independent experiments.



BPC: bipotent cells; MP: memory precursor; M: memory

**Figure 7:** Using *in silico* analysis of single cell transcriptomics and *in vivo* tracing of memory precursors coupled to mathematical modeling, we demonstrate that MP are generated continuously during the primary response with the largest fraction being generated at the peak of the expansion phase.

## Discussion

In this study, we have used trajectory inference tools to analyse the generation of memory precursor CD8 T cells during a primary response against an acute viral infection. A single cell transcriptomic dataset (Yao et al., 2019) generated at two timepoints during the primary response, was analysed using two recently developed trajectory inference algorithms (Slingshot (Street et al., 2018) and TinGa (Todorov et al., 2020)). These tools allow modeling gradual transitions between cell states, as they tend to preserve the local similarities between cells, thus predicting the likely differentiation path followed by cells activated *in vivo* by the virus (Saelens et al., 2019). Trajectory inference tools have become essential as they allow to predict the fate of cells that have to be lysed to analyse their cellular content and/or transcriptome. Although different dimensionality reduction and trajectory computation approaches were used, the trajectories identified by both algorithms were driven by similar sets of genes and displayed a consistent trajectory starting among cells from day 4.5 post-infection that were mainly cycling and ending among cells from day 7 post-infection that were mainly quiescent. Importantly, there was a significant overlap between cells collected on each day as clusters in the middle of the trajectory contained cells from both time points. This indicates that the differentiation process although continuous is heterogeneous in its duration as for example some cells exit the cell cycle at early time points or acquire effector functions more rapidly. This is in agreement with experiments tracking the fate of single T cells in mice that have shown that the clonal size of memory cells generated from a naïve CD8<sup>+</sup> T cell is heterogeneous (Buchholz et al., 2013; Gerlach et al., 2013). The trajectory identified by TinGa was more refined as it identified 8 transitional stages, one of which (cluster 1) was strongly enriched in MP cells identified using a gene signature derived from Yao et al. (2019).

We also applied scVelo (Bergen et al., 2020), a method that uses the splicing state of transcripts to calculate RNA velocities. The projection of RNA velocities on the TinGa-generated map evidenced two cellular behaviours with early cycling cells that remain on a circular trajectory and later cells that follow a linear path. These two behaviours were associated with cell cycle and immune function genes, respectively. Importantly, the linear trajectory driven by the immune effector genes started in early (d4.5) cells underpinning cycling and quiescent cells, thus reflecting the progressive expression of effector functions by activated CD8 T cells. These results are in agreement with the two effector compartments previously described, namely the early cycling effector cells and late quiescent effector cells expressing genes encoding immune effector functions, through which most MP cells have to go to generate the full pool of memory CD8 T cells (Crauste et al., 2017).

We herein found that MP are present at all pseudo-times, with an enrichment in clusters 1 and 8. The majority of MP cells in clusters 1 and 8 were in the G1 phase of the cell cycle suggesting that they were on their way to become quiescent memory cells. We confirmed the continuous generation of MP cells on another dataset from Kurd, et al. (2020). Importantly, we estimate that the number of MP cells generated on day 7 pi is around 100-fold higher than the number generated on day 4.5 pi. *In vivo* pulse-chase BrdU experiment confirmed that CD8 T cells became quiescent memory cells at different stages of an acute infection and that the differentiation rate of early effector cells increased over time. Overall, our data support a model where MP cells are generated continuously over the duration of the expansion phase and beyond, with the majority generated at the peak of the

response. Memory precursors identified on day 7 (cluster 8) differ from MP cells generated earlier in the response, mainly by their expression of genes coding for CD8 effector functions (*Gzmb*, *Ccl5*) and we confirm that CCL5 is expressed at higher protein level by memory cells generated at 7 dpi compared to cells generated at 4.5 dpi. This is in agreement with the gradual acquisition of epigenetic modifications that lead to a poised transcriptional state of the effector molecule loci in memory CD8 T cells (Dogra et al., 2016; Henning et al., 2018). Based on differential gene expression, we searched for surface markers that could distinguish memory precursor CD8 T cells generated early or late in the response. Unfortunately, we have been unable to identify such markers which would have allowed us to compare the functions and self-renewal capacities of these cells.

The continuous generation of MP over the duration of the effector phase could be explained by the sustained proliferation of MP generated early in the response. These cells would maintain self-renewing capacity while opening the chromatin at effector function gene loci. This would fit with the increased expression of mRNA coding for effector functions in MP identified on day 7. We estimate that cycling MP cells represent only about 15% of all MP cells. Interestingly, these cells differ from quiescent memory precursors by the expression of the transcription factors *Zbtb32* and *Ezh2*, which encodes a catalytic subunit of the polycomb repressive complex 2 (PRC2) (Gray et al., 2017). *Zbtb32*, which is transiently expressed during the effector phase has recently been shown to control the magnitude of effector cells and the generation of memory cells (Shin et al., 2017). Epigenetic modification by *Ezh2* controls the survival and cytokine production of effector cells. Also, it would be involved in the developmental switch between terminal effector cells and memory cells by depositing H3K27me3 in T effector cells (Gray et al., 2017; Kakaradov et al., 2017). Thus, proliferating MP cells could represent bipotential cells that oscillate between two fates: the terminally differentiated effector fate that is associated with the repression of the self-renewing capacity and the activation of effector function loci and the memory precursor fate that maintains the self-renewing capacity while acquiring bivalent chromatin modification marks on gene encoding effector functions. This hypothesis would be in line with a recent study by Pace et al. (2018) suggesting that cycling cells may represent bipotent differentiation intermediates expressing both effector and stem/memory potential. A similar differentiation pattern has recently been found in a hematopoietic stem cell differentiation model (Moussy et al., 2017). Importantly in that model and similarly to our data, the number of divisions performed by bipotent cells before arresting and stabilising in one or the other fate is heterogenous. Such a continuous bivalent model could reconcile a number of previously proposed conflicting models that positioned memory precursor cells at either early or late stages following activation (Arsenio et al., 2014; Buchholz et al., 2013; Flossdorf et al., 2015; Jacob and Baltimore, 1999; Kakaradov et al., 2017) (Figure 7). Importantly, it could account for the diverse sizes of clones derived from a single cell, observed in fate mapping experiments (Buchholz et al., 2013; Gerlach et al., 2013) while being in agreement with the dynamical modelling of memory CD8 T cells generation (Crauste et al., 2017). Finally, it would allow the deposition of epigenetic fingerprints on genes that encode effector functions and are poised for rapid expression in memory cells.

## Methods

- Experimental procedures

**Mice:** C57BL/6J mice were purchased from the Charles River Laboratories. F5 TCR [B6/J-Tg(CD2-TcraF5,CD2-TcrbF5) 1Kio/Jmar] transgenic mice were provided by Prof. D. Kioussis (National Institute of Medical Research, London, U.K.) and backcrossed on CD45.1 C57BL/6 background (Jubin et al., 2012). Mice were bred or housed under specific pathogen free conditions in our animal facility (AniRA-PBES, Lyon, France). All experiments were approved by our local ethics committee (CECCAPP, Lyon, France) and accreditations have been obtained from governmental agencies.

**BrdU labelling:** Mice received  $2 \cdot 10^5$  naive CD45.1 F5-Tg CD8 T cells by intravenous (i.v.) injection one day prior intranasal (i.n.) infection with VV-NP68 ( $2 \cdot 10^5$  pfu under  $20 \mu\text{L}$ ). Mice then received one intraperitoneal (i.p.) BrdU injection (2 mg, Sigma). BrdU labelling was analyzed 24h after BrdU administration or 25 and 39 days post infection (dpi).

**Cell analyses:** Mice were sacrificed by cervical dislocation and spleen and draining lymph nodes (cervical and mediastinal) were collected. Flow cytometry staining was performed on single-cell suspensions from each organ. Briefly, cells were first incubated with efluor780-coupled Fixable Viability Dye (Thermo Scientific) for 20 minutes at  $4^\circ\text{C}$  to label dead cells. Surface staining was then performed for 45 minutes at  $4^\circ\text{C}$  in PBS (TFS) supplemented with 1% FBS (BioWest) and 0.09% NaN<sub>3</sub> (Sigma-Aldrich). Cells were then fixed and permeabilized in 96 wells plates using 200  $\mu\text{L}$  of BrdU staining solution from the BrdU Staining Kit for Flow Cytometry APC (ThermoScientific) according to manufacturer instructions. The following mAbs(clones) were used: CD8(53.6.7), CD45.1 (A20) from BD Biosciences, CD44(IM7.8.1), Bcl2 (BCL/10C4) and CCL5 (2E9) from Biolegend and Ki67 (SolA15) and CD49d (R1-2) from Thermofischer Scientific. Samples were acquired on a FACS LSR Fortessa (BD biosciences) and analyzed with FlowJo software (TreeStar).

- Estimation of proliferation and differentiation rates of early effector CD8+ T cells

Neglecting CD8+ CD44+ effector cells death over the 24 hours period between BrdU injection and sample collection, we consider that early effector (CD44+ Bcl2- Ki67+, Crauste et al., 2017) CD8 T cells can either proliferate or differentiate. Upon BrdU injection, proliferating cells incorporate BrdU, therefore early effector cell proliferation rate can be approximated by the ratio:  $\frac{\#CD44+ \text{ BrdU}+ \text{ cells}}{\#CD44+ \text{ Bcl2- Ki67}+ \text{ cells}}$  (which is equivalent to assuming a linear proliferation rate and that all proliferating cells are BrdU+). The number of BrdU+ late effector (CD44+ Bcl2- Ki67-, Crauste et al., 2017) cells one day after BrdU injection corresponds to the fraction of BrdU+ early effector cells that have differentiated following BrdU injection. Hence, the differentiation rate of early effector cells into late effector cells is approximated by the ratio:  $\frac{\#CD44+ \text{ Bcl2- Ki67- BrdU}+ \text{ cells}}{\#CD44+ \text{ Bcl2- BrdU}+ \text{ cells}}$ .

- In vivo memory precursor cell number calculation

The number of MP present in the spleen of animals at each time point was estimated for each cluster by multiplying the number of cells recovered at this time point (given by the number of cells collected in Yao et al. (2019) by the percentage of cells in the given cluster

(given by the TinGa analysis) and the percentage of MP cells among these (given by the GSEA analysis). Then the number of MP was summed for all 8 clusters to yield the number of MP present in the spleen at a given time point.

- Data preprocessing

- Single-cell RNAseq data preprocessing

Existing single cell data from Yao et al. (2019) were used (GEO, accession no. GSE119943). A feature-barcode matrix by replicate was generated using the Cell Ranger v.3.1 software (10X genomics) and only effector CD8 T cells in acute infection sampled at day 4.5 and day 7 post infection were kept for the analysis. The two replicates were pooled since no batch effect was observed. The cell filtering was made with the scater package (McCarthy et al., 2016). Briefly, cells with a log-library size and a log-transformed number of expressed genes that were more than 3 median absolute deviations below the median value were excluded. The cells with less than 5 % of mitochondrial counts were kept. These criteria were applied separately on the cells from day 4.5 and day 7 leading to 20,295 cells that were kept in total. The data was then normalized using the sctransform function in Seurat (Hafemeister et al., 2019) and variable genes were selected based on variance modelling statistics from the modelGeneVar function in Scrn (Lun et al., 2016). The log-normalized expression values of the 2,000 highly variable genes were used for downstream analysis.

To validate our results, a second dataset from Kurd, et al. were used (GEO, accession no. GSE131847). Pre-processed count matrices of cells sampled at day 4, 5, 6, 7 and 10 (replicate 1 only) were pooled (9,614 total cells) and genes detected in less than 1% of the total cells were removed. The data was then normalized using sctransform function and 1,573 highly variable genes were selected by setting the *variable.features.rv.th* parameter to 1.3 (default value).

- Cell type classification

The cells were automatically annotated and the cell type to which they best corresponded was defined using the SingleR R package (Aran et al., 2019). The labelled normalized expression values of 830 microarray samples of pure mouse immune cells, generated by the Immunologic Genome Project (ImmGen), were used as reference. Cells that were clearly identified as non-T cells (7 B cells, 2 dendritic cells, 3 fibroblasts, 25 macrophages and 62 monocytes) were removed before further analyses were applied.

- Advanced analyses

- Cell-cycle assignment

The Seurat R package was used to classify cells into G1, S or G2/M phases. The classifier relies on a list of genes from Tirosh et al. (2016), that contains markers of the G2/M and S phase. It attributes a class to each cell with a certain probability, with the possibility to attribute the G1 class to cells for which the G2/M or S scores were low.

- Trajectory inference

Two recently published trajectory inference tools, Slingshot and TinGa, were used to identify a trajectory in the data. The normalised data was first wrapped into a dataset object with the dynwrap R package. The slingshot implementation in dynwrap, as found on the [github/dynverse/dynwrap](https://github.com/dynverse/dynwrap) github page, was applied to the data using the default parameters.

The TinGa implementation as found on the [github/Helena-todd/TInGa](https://github.com/Helena-todd/TInGa) repository was applied to the data using the default parameters. The dynplot R package was then used for an easy visualisation of the resulting trajectories.

- Generating heatmaps of gene expression along trajectories

We used the `plot_heatmap()` function from the dynplot package to visualise the expression of specific genes along the Slingshot and TinGa trajectories. We either used the function as a discovery tool to identify the top *n* genes that varied the most along the trajectories, or we provided lists of genes associated with a certain signature to see in which parts of the trajectories these genes were the most expressed.

- Differential expression analysis

The transitional populations that were identified along the TinGa trajectory were used as clusters defining similar cells. Differential expression analysis was performed between these clusters using the Seurat R package. Wilcoxon rank sum tests were applied and genes were selected as differentially expressed if the difference in the fraction of detection of the gene between the two compared groups of cells was higher than 0.25, and if the log fold-change difference between the two groups was higher than 0.3. The differentially expressed genes were then visualised using the triwise R package (VanLaar et al., 2016) and in a volcano plot that was generated manually in R with the ggplot2 R package.

- Gene Set Enrichment Analysis

Gene rankings were computed in cells using the AUCell R package. This allowed to identify cells that showed specific gene signatures. Of the 122 genes described as associated with a memory-precursor signature by (Yao et al., 2019), only 42 genes were present in the 2,000 HVGs that we selected. We thus decided to use all genes available instead of restricting ourselves to the 2,000 HVGs for this analysis. 833 cells out of the 20,196 studied acute responding CD8 T cells were assigned to a memory precursor signature.

- Inferring the number of memory precursors in the spleen

The number of memory precursors in the spleen was calculated based on the percentage of memory precursors identified by gene set enrichment among total day 4.5 or day 7 cells and the average number of CD8 T cells found in the spleen of mice on those same days ( $\text{Number of MP on day } x = \% \text{ of MP among single cell from day } X * \text{ average total number of CD8 T cells in spleen on day } X$ ).

- RNA velocity

Counts of spliced and unspliced abundances were obtained using the Kallisto and Bustools workflow (Melsted et al., 2021). Raw fastq files were pseudo-aligned on Ensembl's *Mus musculus* reference transcriptome using release 97. Only cells which passed previously described preprocessing steps were kept. To infer RNA velocities and predict cell-specific trajectories, scVelo version 0.2.3 (Bergen et al., 2020) was used. As described in Bergen et al. (2020), velocities were estimated using the dynamical model and the neighborhood graph was computed on the PCA representation using 50 components. The velocity graph was computed with parameter *n\_neighbors* set to 20. Other parameters were set to default values. Per-cell MDS coordinates obtained in TinGa were imported into scVelo to project RNA velocities in the same reduced embedding. The 50 genes best fitting scVelo's model were selected and divided into *Cell-Cycle*, *Migration* and *Immune Functions* categories

according to their function. Finally, figures were obtained by applying the *velocity\_embedding\_stream* function.

- Gene regulatory network inference

The BRED R package was used to identify regulatory interactions between a list of transcription factors (that was identified among the 2,000 HVGs using the database in the *org.Mm.eg.db* R package, and manually curated), and the 2000 target genes. The scaled importances corresponding to these interactions were filtered, and the top 100 interactions corresponding to the 8 populations identified in the TinGa trajectory were selected, resulting in a gene regulatory network containing 800 interactions. A layout of these interactions was then generated using Cytoscape. In the resulting gene regulatory network, we define modules as groups of target genes linked to one central transcription factor.

## **Supplementary materials**

### **Supplementary figures**

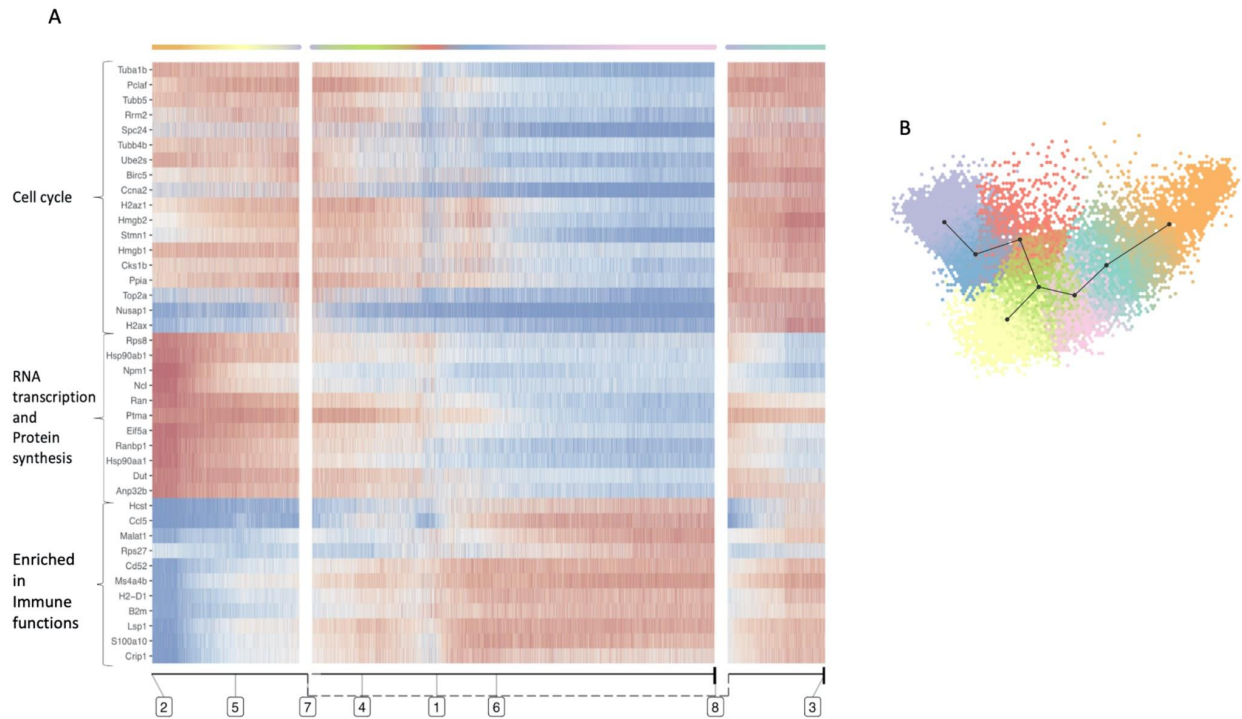


**Figure supplement 1: (A)** Heatmap of the 40 main genes that were associated with the TinGa trajectory. The genes are represented in rows and the cells are represented in columns and are ordered along the TinGa trajectory. The three branches of the trajectory can be identified with milestone colors on top of the heatmap and numbers at the bottom of the heatmap. Gene expression is depicted from low (blue) to high (red) values in the heatmap. **(B)** Trajectory identified by TinGa when the top 10 percent (= 1300) of the most highly variable genes instead of the 2000 HVGs used in **(A)** and other figures.

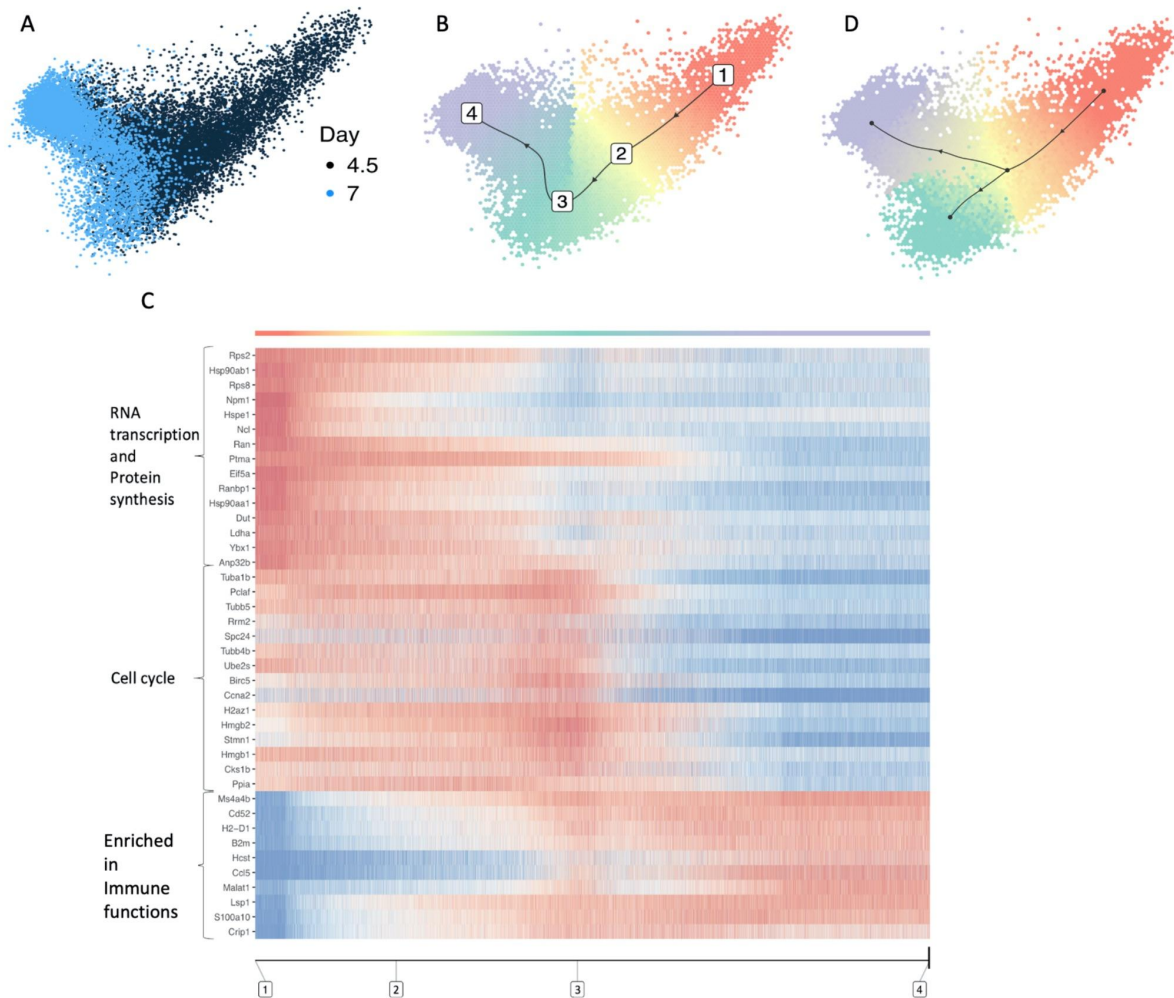


**Figure supplement 2: Slingshot trajectory.** (A, B) Visualisation of the cells in a 2D space computed by principal component analysis. (A) The cells were colored according to the two experimental time points 4.5 and 7 days post LCMV-Armstrong infection. (B) Slingshot recovered a linear trajectory that is represented by a black directed line. Numbers along the trajectory are used as milestones. (C) Heatmap of the 40 main genes that were associated with the Slingshot trajectory. The genes are represented in rows and the cells are represented in columns, re-ordered along the trajectory. The trajectory milestone structure is reported at the bottom of the heatmap as a visual support, and the cluster associated colors are represented at the top of the heatmap. Gene expression is depicted from low (blue) to high (red) values in the heatmap. (D) Trajectory identified by Slingshot using the top 10 percent (= 1300) of the most highly variable genes instead of the 2000 HVGs described in this paper.

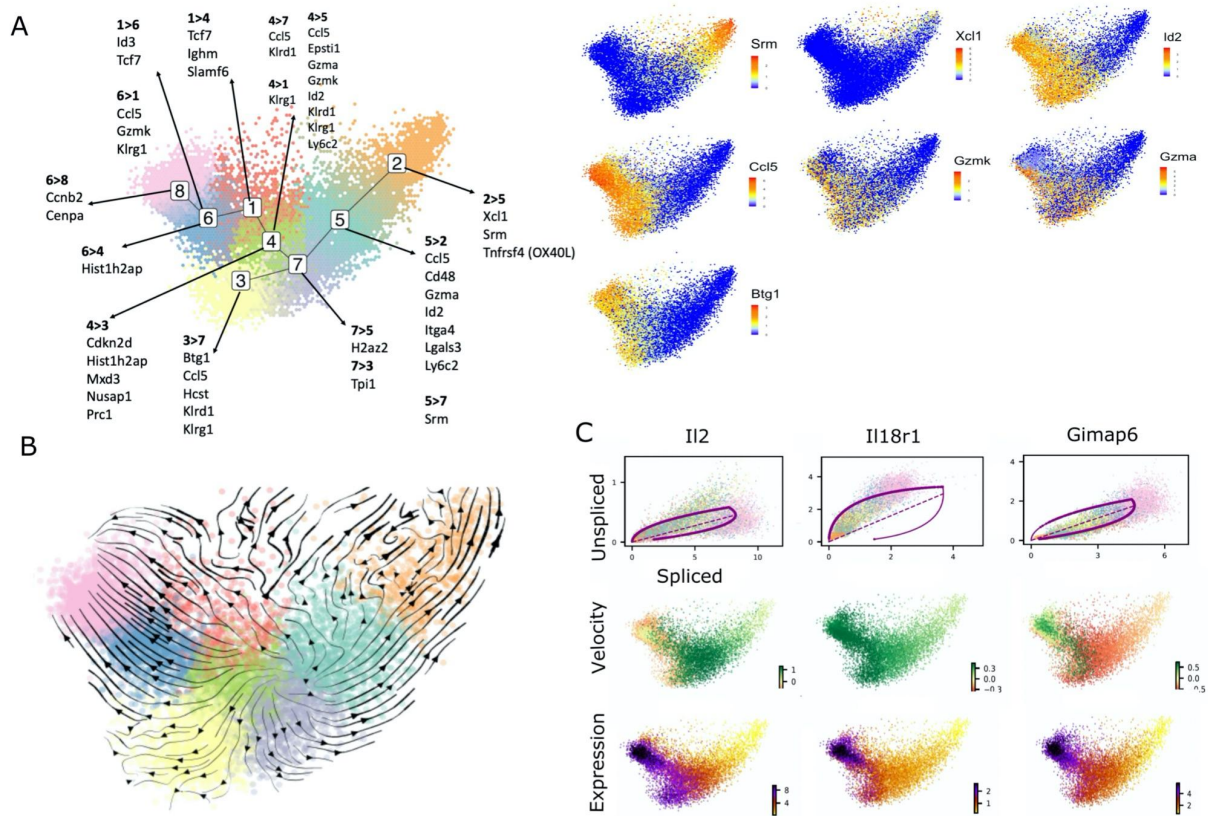


**Figure supplement 3: (A)** Left panel: Differential expression analysis between two clusters of cells in the same phase of the cell cycle along the TinGa trajectory. Only the genes that are shared between the phases of the cycle were kept. The genes over-represented in paired neighbour-cluster comparative analyses are listed. Right panel: expression of some representative genes were highlighted on the TinGa trajectory. **(B)** Velocities were calculated using the top 50 genes best fitting the dynamical model. **(C)** Illustration of the genetic dynamics of 3 immune function-related genes. Left column: scVelo's dynamical model fitting on the spliced and unspliced counts. Middle column: velocity vectors obtained for each cell on a single gene, positive (green) values indicate cells moving towards regions of higher expression, negative (red) values indicate cells moving towards lower expression. Right column: First moment ('Ms' matrix) of expression levels (spliced counts) for each cell across its nearest neighbors (local mean) for the indicated gene.

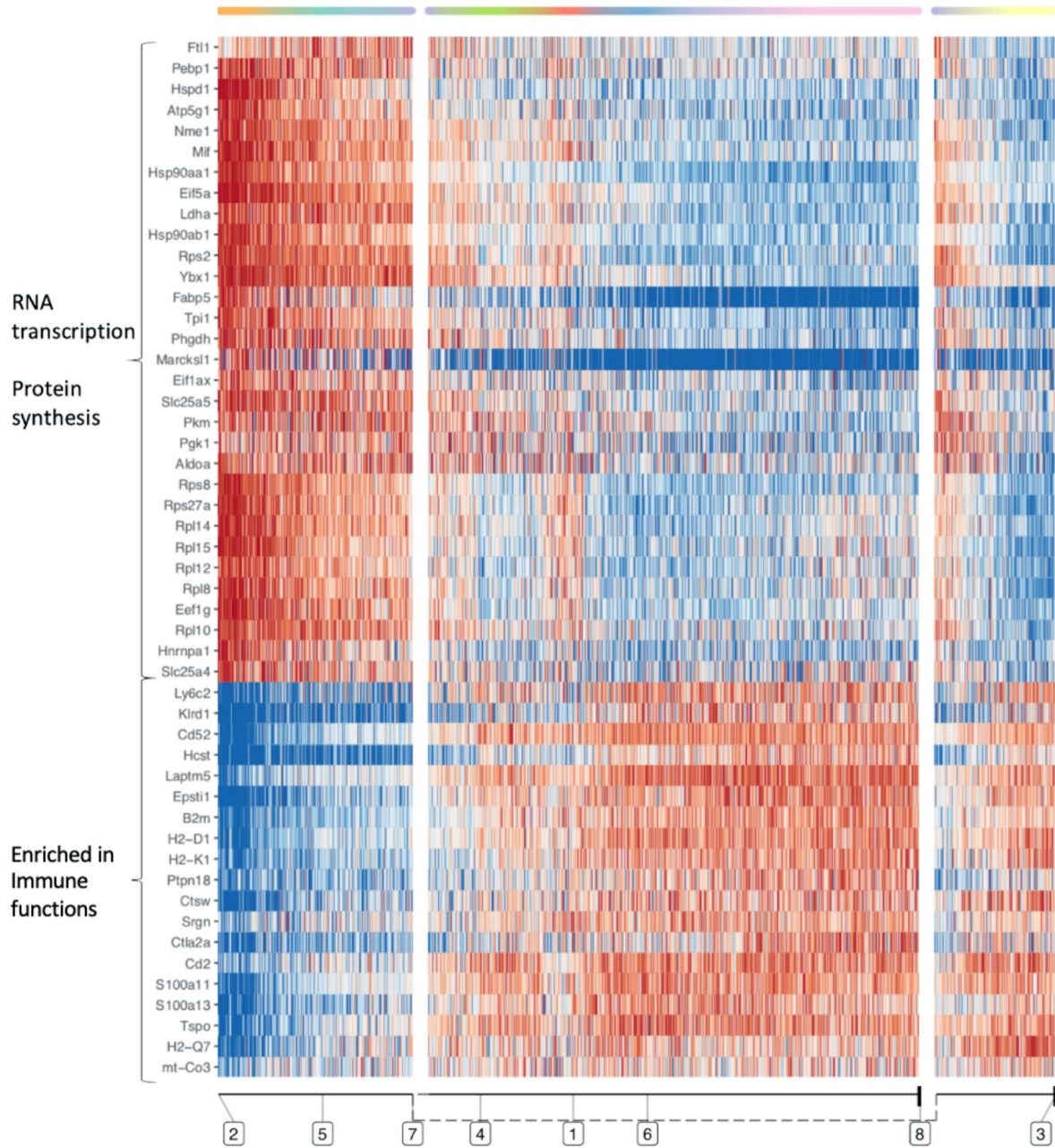


**Figure supplement 4:** Ybx1 gene module heatmap along TinGa's trajectory represented as explained in the legend to Figure supplement 1. Two different groups of genes can be identified. Genes at the top of the heatmap are enriched at the beginning of the trajectory and are involved in RNA and protein synthesis. Genes at the bottom of the heatmap are expressed at the end of the trajectory (in clusters 6 and 8) and code for immune receptors.

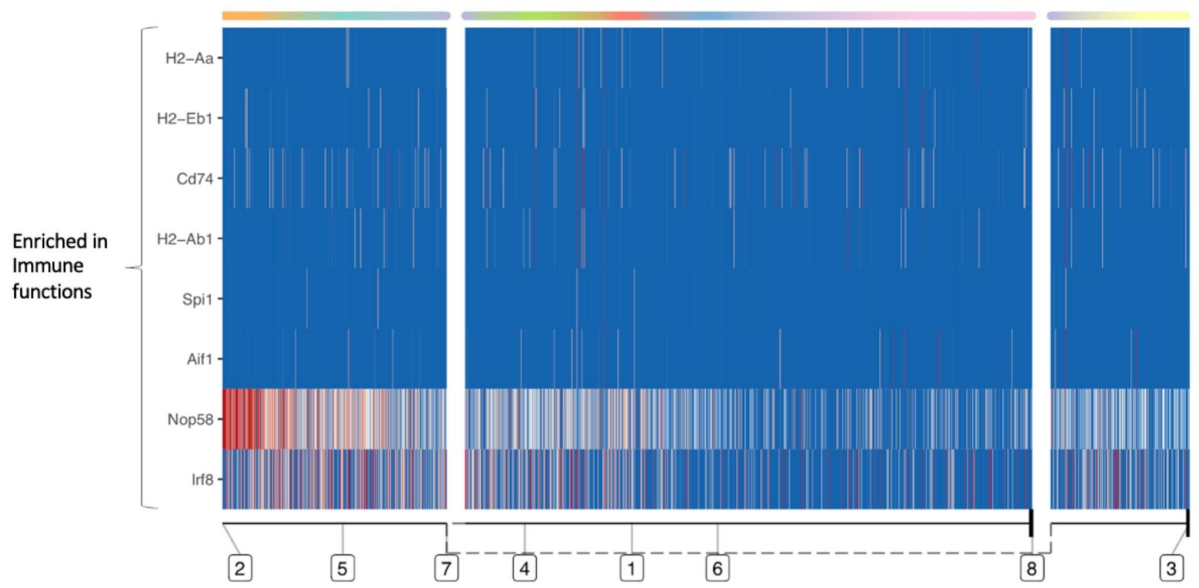


**Figure supplement 5:** Spi1 gene module heatmap along TinGa's trajectory represented as explained in the legend to Figure supplement 1.

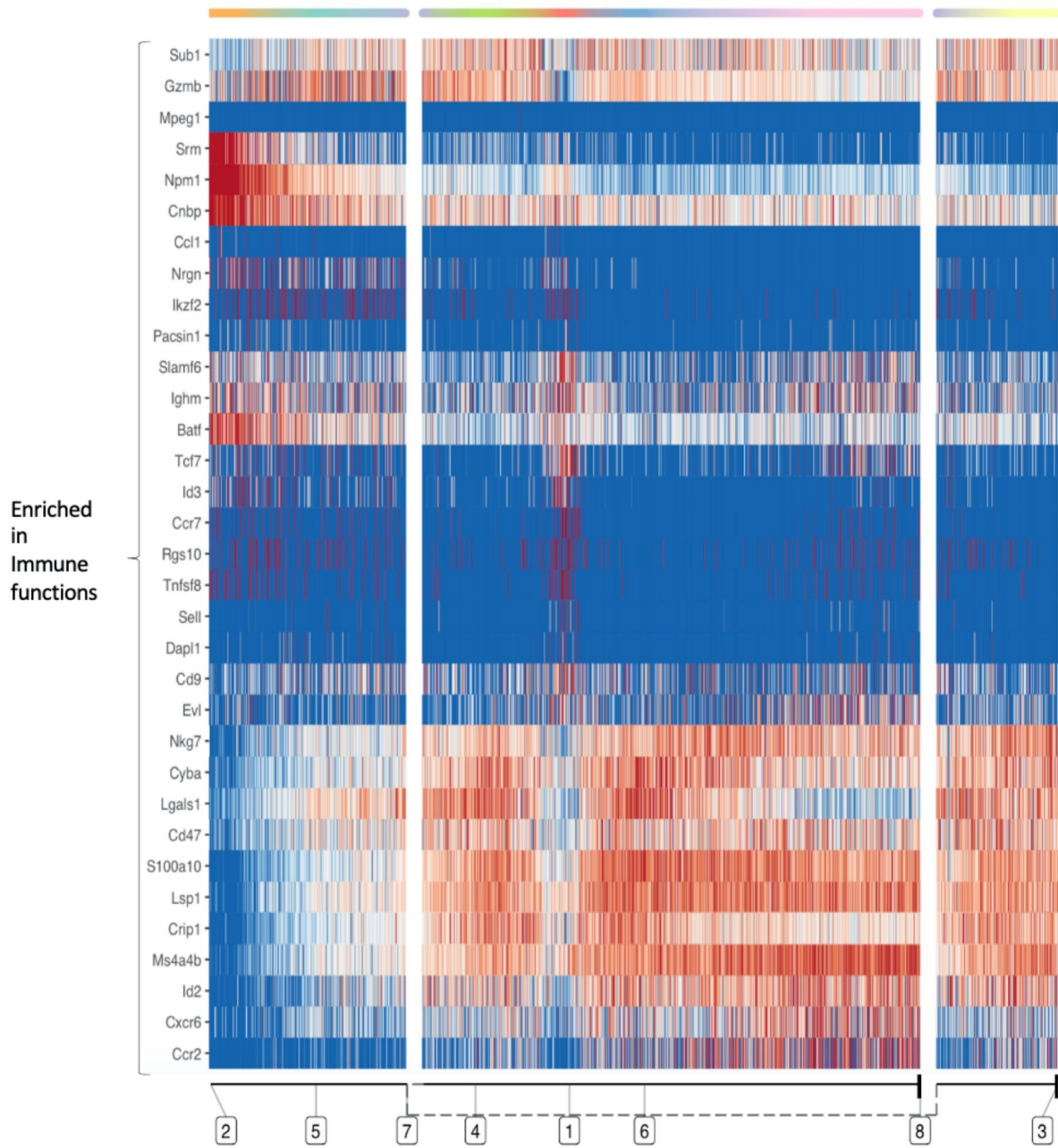


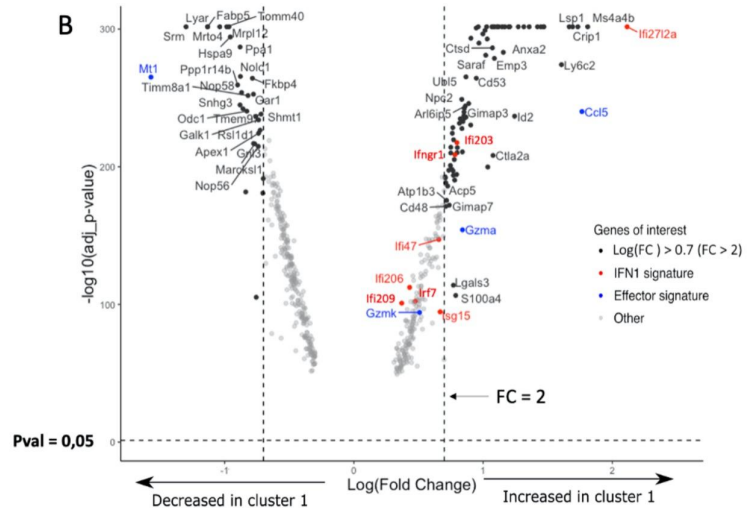
**Figure supplement 6:** Tcf7/Id2/Phb2 gene module heatmap along TinGa's trajectory represented as explained in the legend to Figure supplement 1.

**A**

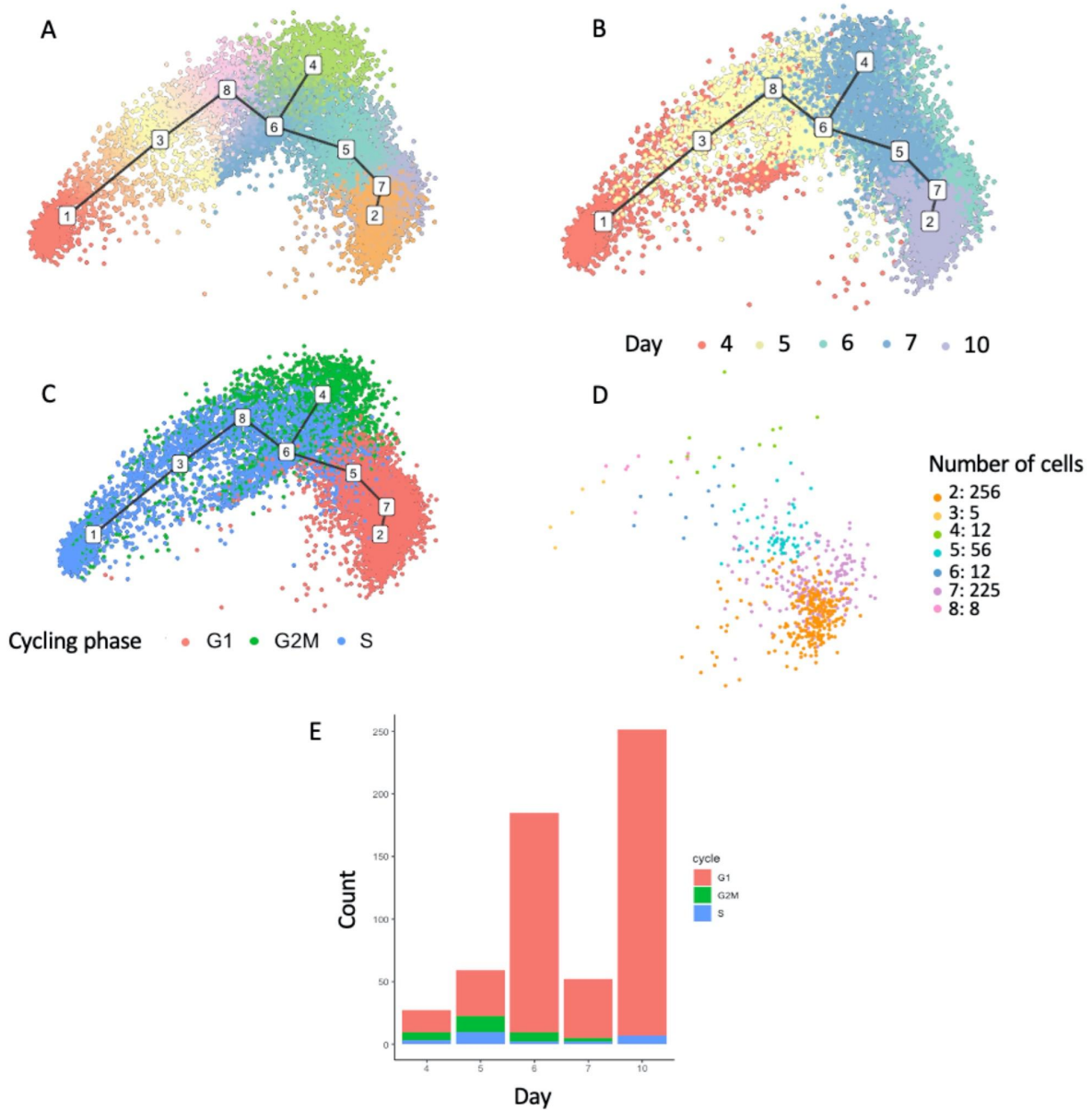
| Day   | G1  | G2/M | S   | Total |
|-------|-----|------|-----|-------|
| 4.5   | 407 | 296  | 416 | 1119  |
| 7     | 53  | 29   | 60  | 142   |
| Total | 460 | 325  | 476 | 1261  |

**C**

| Gene  | p_val     | avg_logFC | p_val_adj |
|-------|-----------|-----------|-----------|
| Tcf7  | 0         | 0.68      | 0         |
| Id3   | 9.62e-220 | 0.54      | 1.92e-216 |
| Ltb   | 4.30e-130 | 0.49      | 8.61e-86  |
| Klrg1 | 1.02e-89  | -0.57     | 2.04e-86  |



**Figure supplement 7: Analysis of Cluster 1. (A)** The distribution of the cells from cluster 1 in the cycle phases at each experimental time point. **(B)** Volcano plot of the genes that were differentially expressed between cluster 1 and cluster 2. The genes that change by a fold-change < -2 or > 2 are pointed in black. The genes associated with a type 1 IFN signature are colored in red and the genes that are associated with an effector signature are colored in blue. **(C)** Four genes were differentially expressed in cluster 1 compared to the rest of the cells. The p-values, averaged log fold-changes and the adjusted p-values are reported in this table. Positive values of averaged log fold-changes indicate that the feature is highly expressed in the cluster 1.



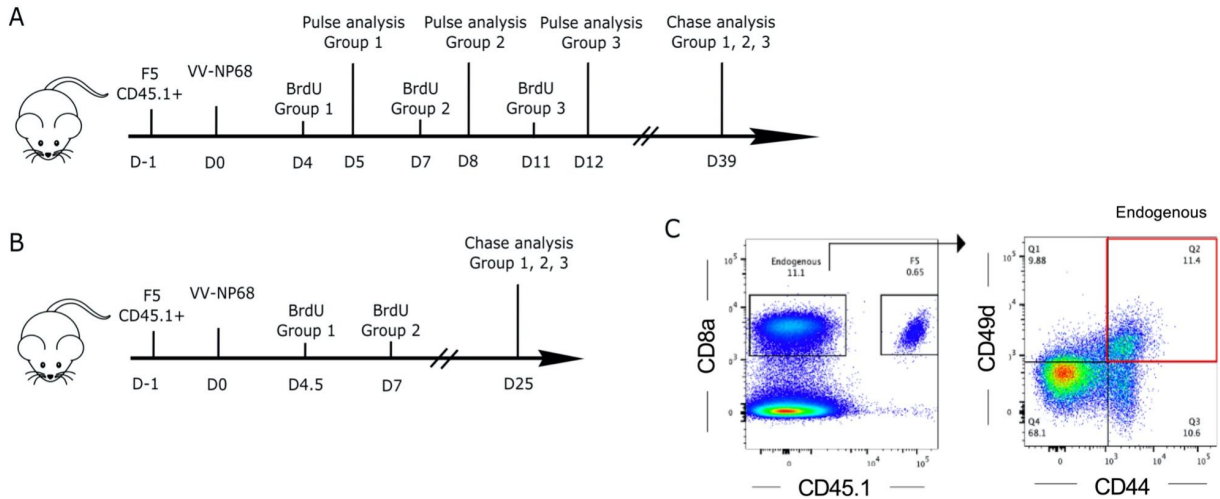


**Figure supplement 9: (A)** Naive CD45.1 F5 TCR-tg CD8 T cells were transferred to C57BL/6 congenic recipients (n = 5 per group) one day prior i.n. infection with VV-NP68. Mice then received one BrdU injection (2 mg i.p.) on day 4 (Group1), day 7 (Group2) or day 11 (Group3). BrdU labelling was determined by flow cytometry on cells collected 24h after BrdU injection (pulse) or 39 days post infection (chase). **(B)** Naive CD45.1 F5 TCR-tg CD8 T cells were transferred to C57BL/6 congenic recipients (n = 5 per group) one day prior i.n. infection with VV-NP68. Mice then received one BrdU injection (2 mg i.p.) on day 4.5 (Group1) or day 7 (Group2). BrdU labelling was determined by flow cytometry on cells collected 25 days (chase) after infection. **(C)** Gating strategy for the identification of antigen-specific endogenous memory CD8 T cells

## Supplementary tables

**Supplementary Table 1:** differential expression analysis between two clusters of cells in the same phase of the cell cycle along the TinGa trajectory. Only the genes that are shared between the phases of the cycle were kept.

| gene          | p_val      | avg_logFC  | pct.1 | pct.2 | p_val_adj   | Comparison        |
|---------------|------------|------------|-------|-------|-------------|-------------------|
| 1500009L16Rik | 1,83E-185  | -0,9245634 | 0,405 | 0,875 | 3,6603E-182 | S_clust_2_vs_5    |
| 1500009L16Rik | 7,3236E-45 | -0,8358373 | 0,426 | 0,832 | 1,46472E-41 | G2M_clust_2_vs_5  |
| AA467197      | 2,3113E-40 | -0,5588995 | 0,187 | 0,564 | 4,62251E-37 | S_clust_1_vs_6    |
| AA467197      | 2,48E-19   | -0,5216    | 0,157 | 0,475 | 4,97E-16    | G2M_clust_1_vs_6  |
| AA467197      | 2,3337E-33 | -0,5589105 | 0,139 | 0,436 | 4,6674E-30  | G1_clust_1_vs_6   |
| Abrac1        | 1,936E-184 | -0,6519145 | 0,711 | 0,976 | 3,8727E-181 | S_clust_2_vs_5    |
| Abrac1        | 3,0943E-43 | -0,5346784 | 0,709 | 0,967 | 6,18852E-40 | G2M_clust_2_vs_5  |
| Anxa2         | 0          | -1,1958255 | 0,459 | 0,98  | 0           | S_clust_2_vs_5    |
| Anxa2         | 2,7269E-81 | -1,0162313 | 0,491 | 0,972 | 5,45373E-78 | G2M_clust_2_vs_5  |
| Anxa6         | 1,292E-201 | -0,746947  | 0,411 | 0,898 | 2,5848E-198 | S_clust_2_vs_5    |
| Anxa6         | 1,2107E-45 | -0,5937352 | 0,436 | 0,859 | 2,42136E-42 | G2M_clust_2_vs_5  |
| Arl6ip5       | 6,878E-115 | -0,5175268 | 0,479 | 0,828 | 1,3757E-111 | S_clust_2_vs_5    |
| Arl6ip5       | 1,7935E-31 | -0,5145371 | 0,422 | 0,752 | 3,5871E-28  | G2M_clust_2_vs_5  |
| Btg1          | 3,28E-37   | -0,69769   | 0,201 | 0,7   | 6,55E-34    | S_clust_7_vs_3    |
| Btg1          | 6,425E-238 | -0,8264548 | 0,274 | 0,762 | 1,285E-234  | G2M_clust_7_vs_3  |
| Ccnb2         | 1,019E-295 | 0,78872048 | 0,777 | 0,365 | 2,0375E-292 | G1_clust_6_vs_8   |
| Cenpa         | 3,192E-172 | 0,6539074  | 0,796 | 0,534 | 6,3849E-169 | G1_clust_6_vs_8   |
| Ccl5          | 9,3103E-74 | -0,9638835 | 0,055 | 0,354 | 1,86205E-70 | S_clust_2_vs_5    |
| Ccl5          | 1,4015E-18 | -0,8803983 | 0,045 | 0,298 | 2,80295E-15 | G2M_clust_2_vs_5  |
| Ccl5          | 7,05E-75   | -2,85729   | 0,473 | 0,96  | 1,41E-71    | S_clust_7_vs_3    |
| Ccl5          | 1,595E-286 | -2,1074316 | 0,492 | 0,902 | 3,1907E-283 | G2M_clust_7_vs_3  |
| Ccl5          | 5,2372E-65 | -1,6667965 | 0,473 | 0,863 | 1,04744E-61 | S_clust_7_vs_4    |
| Ccl5          | 2,621E-86  | -1,2309854 | 0,492 | 0,934 | 5,24205E-83 | G2M_clust_7_vs_4. |
| Ccl5          | 1,361E-148 | -2,4206412 | 0,603 | 0,988 | 2,7228E-145 | S_clust_1_vs_6    |
| Ccl5          | 1,48E-90   | -2,41001   | 0,735 | 0,994 | 2,96E-87    | G2M_clust_1_vs_6  |
| Ccl5          | 1,506E-174 | -2,6118703 | 0,73  | 0,994 | 3,0123E-171 | G1_clust_1_vs_6   |
| Ccl5          | 7,994E-121 | 1,93999434 | 0,934 | 0,298 | 1,5989E-117 | G2M_clust_4_vs_5  |
| Ccl5          | 9,845E-304 | 2,00673666 | 0,863 | 0,354 | 1,9691E-300 | S_clust_4_vs_5    |
| Cd48          | 9,492E-226 | -0,8214374 | 0,714 | 0,978 | 1,8984E-222 | S_clust_2_vs_5    |
| Cd48          | 1,8146E-54 | -0,6720766 | 0,713 | 0,968 | 3,62929E-51 | G2M_clust_2_vs_5  |
| Cdkn2d        | 1,0934E-81 | -0,6580124 | 0,572 | 0,908 | 2,18688E-78 | G2M_CLUST_3_VS_   |

|        |            |            |       |       |             |                  |
|--------|------------|------------|-------|-------|-------------|------------------|
|        |            |            |       |       |             | 4                |
| Cdkn2d | 6,8909E-35 | -0,5079278 | 0,495 | 0,787 | 1,37819E-31 | S_CLUST_3_VS_4   |
| Crip1  | 0          | -1,2732093 | 0,683 | 0,999 | 0           | S_clust_2_vs_5   |
| Crip1  | 9,1661E-93 | -1,0942829 | 0,734 | 1     | 1,83323E-89 | G2M_clust_2_vs_5 |
| Ctsd   | 1,525E-205 | -0,9144151 | 0,305 | 0,841 | 3,0495E-202 | S_clust_2_vs_5   |
| Ctsd   | 1,1768E-44 | -0,7333975 | 0,336 | 0,773 | 2,35361E-41 | G2M_clust_2_vs_5 |
| Ctsw   | 4,2573E-50 | 0,5229673  | 0,899 | 0,582 | 8,51468E-47 | G2M_clust_4_vs_5 |
| Ctsw   | 3,755E-169 | 0,53874008 | 0,893 | 0,603 | 7,5091E-166 | S_clust_4_vs_5   |
| Emp3   | 4,994E-260 | -0,9913708 | 0,332 | 0,919 | 9,9881E-257 | S_clust_2_vs_5   |
| Emp3   | 2,0129E-64 | -0,8513857 | 0,381 | 0,891 | 4,02574E-61 | G2M_clust_2_vs_5 |
| Epsti1 | 2,25E-147  | -0,650919  | 0,083 | 0,577 | 4,5004E-144 | S_clust_2_vs_5   |
| Epsti1 | 2,0845E-37 | -0,5771634 | 0,069 | 0,507 | 4,16893E-34 | G2M_clust_2_vs_5 |
| Epsti1 | 3,003E-103 | 0,88980637 | 0,976 | 0,507 | 6,0057E-100 | G2M_clust_4_vs_5 |
| Epsti1 | 4,26E-295  | 0,81061416 | 0,945 | 0,577 | 8,5208E-292 | S_clust_4_vs_5   |
| Fabp5  | 4,5695E-79 | -0,7346459 | 0,487 | 0,902 | 9,13897E-76 | G2M_clust_4_vs_5 |
| Fabp5  | 1,311E-213 | -0,6087867 | 0,599 | 0,906 | 2,6226E-210 | S_clust_4_vs_5   |
| Gmfg   | 1,128E-217 | -0,826008  | 0,398 | 0,906 | 2,2556E-214 | S_clust_2_vs_5   |
| Gmfg   | 1,5299E-52 | -0,7070077 | 0,391 | 0,866 | 3,0597E-49  | G2M_clust_2_vs_5 |
| Gnl3   | 4,689E-153 | 0,58313772 | 0,907 | 0,536 | 9,3775E-150 | S_clust_2_vs_5   |
| Gnl3   | 3,4974E-36 | 0,51692839 | 0,827 | 0,471 | 6,99478E-33 | G2M_clust_2_vs_5 |
| Gzma   | 9,591E-115 | -1,6245031 | 0,121 | 0,539 | 1,9182E-111 | S_clust_2_vs_5   |
| Gzma   | 3,442E-32  | -1,5232171 | 0,125 | 0,526 | 6,88392E-29 | G2M_clust_2_vs_5 |
| Gzma   | 1,1918E-84 | 1,59653422 | 0,965 | 0,526 | 2,38355E-81 | G2M_clust_4_vs_5 |
| Gzma   | 1,002E-184 | 1,41031454 | 0,887 | 0,539 | 2,0041E-181 | S_clust_4_vs_5   |
| Gzmk   | 6,6426E-32 | -0,5720413 | 0,447 | 0,714 | 1,32853E-28 | S_clust_1_vs_6   |
| Gzmk   | 1,46E-29   | -0,69876   | 0,474 | 0,791 | 2,93E-26    | G2M_clust_1_vs_6 |
| Gzmk   | 7,0983E-48 | -0,6531595 | 0,435 | 0,738 | 1,41967E-44 | G1_clust_1_vs_6  |
| Gzmk   | 6,8159E-44 | 0,60011157 | 0,729 | 0,36  | 1,36319E-40 | G2M_clust_4_vs_5 |
| Gzmk   | 1,5531E-89 | 0,50335221 | 0,712 | 0,438 | 3,10618E-86 | S_clust_4_vs_5   |
| H1f5   | 3,5178E-27 | 0,70369207 | 0,348 | 0,039 | 7,03565E-24 | G2M_CLUST_4_VS_6 |
| H1f5   | 7,786E-98  | 0,75391824 | 0,575 | 0,13  | 1,55721E-94 | S_CLUST_4_VS_6   |
| H2-Q7  | 1,059E-188 | -0,7608977 | 0,596 | 0,953 | 2,1174E-185 | S_clust_2_vs_5   |
| H2-Q7  | 7,6701E-45 | -0,6301942 | 0,63  | 0,94  | 1,53403E-41 | G2M_clust_2_vs_5 |
| H2az2  | 2,2492E-52 | -0,5492847 | 0,608 | 0,906 | 4,49833E-49 | S_clust_5_vs_7   |
| H2az2  | 4,70E-107  | -0,62533   | 0,554 | 0,894 | 9,40E-104   | G2M_clust_5_vs_7 |
| H2az2  | 1,21E-68   | 0,6588974  | 0,927 | 0,554 | 2,42007E-65 | G2M_clust_4_vs_5 |
| H2az2  | 6,511E-209 | 0,5912805  | 0,93  | 0,608 | 1,3022E-205 | S_clust_4_vs_5   |

|           |            |            |       |       |             |                   |
|-----------|------------|------------|-------|-------|-------------|-------------------|
| Hcst      | 7,38E-65   | -1,0769    | 0,423 | 0,941 | 1,48E-61    | S_clust_7_vs_3    |
| Hcst      | 3,286E-282 | -0,8936202 | 0,429 | 0,879 | 6,5728E-279 | G2M_clust_7_vs_3  |
| Hcst      | 4,3728E-91 | 0,69403379 | 0,755 | 0,181 | 8,74569E-88 | G2M_clust_4_vs_5  |
| Hcst      | 2,967E-218 | 0,6561389  | 0,717 | 0,229 | 5,9331E-215 | S_clust_4_vs_5    |
| Hist1h2ap | 5,2973E-26 | 0,74382089 | 0,452 | 0,117 | 1,05947E-22 | G2M_CLUST_4_VS_6  |
| Hist1h2ap | 5,234E-103 | 0,99339733 | 0,613 | 0,166 | 1,0468E-99  | S_CLUST_4_VS_6    |
| Hist1h2ap | 4,2524E-64 | -0,9532653 | 0,452 | 0,781 | 8,5048E-61  | G2M_CLUST_3_VS_4  |
| Hist1h2ap | 1,9486E-70 | -0,8244259 | 0,613 | 0,996 | 3,89718E-67 | S_CLUST_3_VS_4    |
| ld2       | 2,2274E-96 | -0,7869124 | 0,14  | 0,513 | 4,45479E-93 | S_clust_2_vs_5    |
| ld2       | 3,7608E-37 | -0,8960688 | 0,166 | 0,601 | 7,52158E-34 | G2M_clust_2_vs_5  |
| ld2       | 1,5111E-83 | 0,96857233 | 0,969 | 0,601 | 3,02217E-80 | G2M_clust_4_vs_5  |
| ld2       | 9,675E-197 | 0,91671013 | 0,879 | 0,513 | 1,935E-193  | S_clust_4_vs_5    |
| ld3       | 6,6528E-73 | 0,7720574  | 0,437 | 0,029 | 1,33056E-69 | S_clust_1_vs_6    |
| ld3       | 1,15E-23   | 0,507683   | 0,274 | 0,011 | 2,30E-20    | G2M_clust_1_vs_6  |
| ld3       | 3,215E-128 | 0,77259907 | 0,376 | 0,008 | 6,4296E-125 | G1_clust_1_vs_6   |
| lfi27l2a  | 1,722E-103 | -0,7268999 | 0,242 | 0,666 | 3,4435E-100 | S_clust_2_vs_5    |
| lfi27l2a  | 8,1541E-21 | -0,662013  | 0,298 | 0,615 | 1,63082E-17 | G2M_clust_2_vs_5  |
| lghm      | 6,75E-58   | -0,66228   | 0,411 | 0,725 | 1,35E-54    | S_clust_4_vs_1    |
| lghm      | 2,25E-35   | -0,84282   | 0,336 | 0,708 | 4,51E-32    | G2M_clust_4_vs_1  |
| ltga4     | 1,273E-131 | -0,5953305 | 0,24  | 0,7   | 2,5455E-128 | S_clust_2_vs_5    |
| ltga4     | 1,5437E-41 | -0,6253756 | 0,263 | 0,713 | 3,08749E-38 | G2M_clust_2_vs_5  |
| ltgb7     | 4,035E-224 | -0,8612255 | 0,216 | 0,829 | 8,07E-221   | S_clust_2_vs_5    |
| ltgb7     | 4,01E-56   | -0,7546848 | 0,173 | 0,74  | 8,02001E-53 | G2M_clust_2_vs_5  |
| ltm2b     | 1,593E-188 | -0,6823005 | 0,704 | 0,973 | 3,1852E-185 | S_clust_2_vs_5    |
| ltm2b     | 6,672E-47  | -0,5740743 | 0,699 | 0,963 | 1,3344E-43  | G2M_clust_2_vs_5  |
| Jak1      | 3,2171E-58 | 0,60116348 | 0,856 | 0,421 | 6,43425E-55 | G2M_clust_4_vs_5  |
| Jak1      | 8,01E-166  | 0,5956979  | 0,826 | 0,479 | 1,602E-162  | S_clust_4_vs_5    |
| Klf2      | 5,042E-143 | -0,7974653 | 0,467 | 0,879 | 1,0084E-139 | S_clust_2_vs_5    |
| Klf2      | 9,8936E-47 | -0,8134536 | 0,471 | 0,864 | 1,97872E-43 | G2M_clust_2_vs_5  |
| Klrd1     | 5,05E-37   | -0,93213   | 0,467 | 0,854 | 1,01E-33    | S_clust_7_vs_3    |
| Klrd1     | 1,167E-178 | -0,7614834 | 0,443 | 0,839 | 2,3338E-175 | G2M_clust_7_vs_3  |
| Klrd1     | 4,9769E-32 | -0,6510008 | 0,467 | 0,747 | 9,95388E-29 | S_clust_7_vs_4    |
| Klrd1     | 5,6012E-45 | -0,5192762 | 0,443 | 0,812 | 1,12024E-41 | G2M_clust_7_vs_4. |
| Klrd1     | 4,9481E-94 | 0,93209529 | 0,812 | 0,213 | 9,89622E-91 | G2M_clust_4_vs_5  |
| Klrd1     | 2,863E-204 | 0,87798679 | 0,747 | 0,288 | 5,7268E-201 | S_clust_4_vs_5    |
| Klrg1     | 1,67E-42   | 0,583865   | 0,436 | 0,099 | 3,34E-39    | S_clust_4_vs_1    |

|         |            |            |       |       |             |                  |
|---------|------------|------------|-------|-------|-------------|------------------|
| Klrg1   | 2,77E-23   | 0,531668   | 0,421 | 0,095 | 5,54E-20    | G2M_clust_4_vs_1 |
| Klrg1   | 2,00E-26   | -0,69734   | 0,157 | 0,549 | 3,99E-23    | S_clust_7_vs_3   |
| Klrg1   | 1,0749E-98 | -0,5549525 | 0,19  | 0,512 | 2,14978E-95 | G2M_clust_7_vs_3 |
| Klrg1   | 1,5089E-62 | -0,8236819 | 0,099 | 0,572 | 3,01777E-59 | S_clust_1_vs_6   |
| Klrg1   | 3,76E-45   | -0,91912   | 0,095 | 0,612 | 7,52E-42    | G2M_clust_1_vs_6 |
| Klrg1   | 1,5652E-69 | -0,917388  | 0,072 | 0,539 | 3,13041E-66 | G1_clust_1_vs_6  |
| Klrg1   | 8,3743E-39 | 0,55707628 | 0,421 | 0,104 | 1,67486E-35 | G2M_clust_4_vs_5 |
| Klrg1   | 2,8863E-95 | 0,53399858 | 0,436 | 0,141 | 5,77254E-92 | S_clust_4_vs_5   |
| Laptm5  | 7,961E-149 | -0,6065037 | 0,494 | 0,891 | 1,5921E-145 | S_clust_2_vs_5   |
| Laptm5  | 1,3947E-32 | -0,5079673 | 0,505 | 0,832 | 2,78945E-29 | G2M_clust_2_vs_5 |
| Lgals3  | 6,084E-259 | -1,3783836 | 0,385 | 0,928 | 1,2168E-255 | S_clust_2_vs_5   |
| Lgals3  | 2,8358E-63 | -1,1798041 | 0,398 | 0,891 | 5,67154E-60 | G2M_clust_2_vs_5 |
| Lsp1    | 8,843E-300 | -1,1557533 | 0,281 | 0,924 | 1,7687E-296 | S_clust_2_vs_5   |
| Lsp1    | 2,3402E-79 | -1,0174308 | 0,273 | 0,878 | 4,68034E-76 | G2M_clust_2_vs_5 |
| Ly6c2   | 1,7267E-85 | -0,8666487 | 0,191 | 0,563 | 3,45332E-82 | S_clust_2_vs_5   |
| Ly6c2   | 3,5098E-18 | -0,7055798 | 0,215 | 0,507 | 7,01968E-15 | G2M_clust_2_vs_5 |
| Ly6c2   | 2,5392E-81 | 1,08112565 | 0,953 | 0,507 | 5,07849E-78 | G2M_clust_4_vs_5 |
| Ly6c2   | 7,259E-194 | 0,94753361 | 0,907 | 0,563 | 1,4518E-190 | S_clust_4_vs_5   |
| Ms4a4b  | 2,117E-289 | -1,1802288 | 0,603 | 0,993 | 4,2331E-286 | S_clust_2_vs_5   |
| Ms4a4b  | 2,6039E-81 | -1,0945078 | 0,644 | 0,988 | 5,20788E-78 | G2M_clust_2_vs_5 |
| Ms4a6b  | 4,791E-213 | -0,8238616 | 0,618 | 0,974 | 9,5822E-210 | S_clust_2_vs_5   |
| Ms4a6b  | 2,9387E-65 | -0,8053935 | 0,616 | 0,957 | 5,87748E-62 | G2M_clust_2_vs_5 |
| Mxd3    | 2,641E-55  | -0,5001029 | 0,369 | 0,764 | 5,28208E-52 | G2M_CLUST_3_VS_4 |
| Mxd3    | 7,1515E-52 | -0,5140897 | 0,354 | 0,791 | 1,4303E-48  | S_CLUST_3_VS_4   |
| Nusap1  | 1,55E-151  | -1,0559958 | 0,384 | 0,943 | 3,0996E-148 | G2M_CLUST_3_VS_4 |
| Nusap1  | 8,166E-123 | -0,9255125 | 0,307 | 0,933 | 1,6332E-119 | S_CLUST_3_VS_4   |
| Pglyrp1 | 1,625E-137 | -0,6186261 | 0,101 | 0,569 | 3,25E-134   | S_clust_2_vs_5   |
| Pglyrp1 | 4,6929E-31 | -0,513608  | 0,093 | 0,485 | 9,3858E-28  | G2M_clust_2_vs_5 |
| Prc1    | 1,096E-101 | -0,7593231 | 0,325 | 0,865 | 2,19192E-98 | G2M_CLUST_3_VS_4 |
| Prc1    | 1,2673E-56 | -0,5685751 | 0,353 | 0,806 | 2,53456E-53 | S_CLUST_3_VS_4   |
| Prr13   | 1,228E-182 | -0,7533671 | 0,347 | 0,836 | 2,4565E-179 | S_clust_2_vs_5   |
| Prr13   | 2,308E-36  | -0,5852993 | 0,37  | 0,755 | 4,61609E-33 | G2M_clust_2_vs_5 |
| Pycard  | 1,31E-242  | -0,9710085 | 0,64  | 0,977 | 2,6202E-239 | S_clust_2_vs_5   |
| Pycard  | 5,3463E-58 | -0,8122259 | 0,657 | 0,961 | 1,06927E-54 | G2M_clust_2_vs_5 |
| Rasgrp2 | 6,195E-193 | -0,8072175 | 0,533 | 0,936 | 1,2389E-189 | S_clust_2_vs_5   |
| Rasgrp2 | 1,2827E-43 | -0,6813132 | 0,512 | 0,896 | 2,56535E-40 | G2M_clust_2_vs_5 |

|         |            |            |       |       |             |                  |
|---------|------------|------------|-------|-------|-------------|------------------|
| Reep5   | 1,895E-172 | -0,6061037 | 0,675 | 0,964 | 3,7899E-169 | S_clust_2_vs_5   |
| Reep5   | 1,4153E-42 | -0,5245702 | 0,64  | 0,94  | 2,83057E-39 | G2M_clust_2_vs_5 |
| S100a10 | 0          | -1,2224133 | 0,648 | 0,999 | 0           | S_clust_2_vs_5   |
| S100a10 | 2,9984E-90 | -0,9777056 | 0,72  | 0,997 | 5,99686E-87 | G2M_clust_2_vs_5 |
| S100a11 | 2,601E-200 | -0,8298955 | 0,374 | 0,881 | 5,2025E-197 | S_clust_2_vs_5   |
| S100a11 | 6,5153E-50 | -0,7071857 | 0,408 | 0,861 | 1,30306E-46 | G2M_clust_2_vs_5 |
| S100a13 | 8,2011E-75 | 0,64793529 | 0,953 | 0,645 | 1,64021E-71 | G2M_clust_4_vs_5 |
| S100a13 | 1,356E-203 | 0,56764529 | 0,943 | 0,689 | 2,7114E-200 | S_clust_4_vs_5   |
| S1pr4   | 1,162E-157 | -0,6850742 | 0,213 | 0,717 | 2,3246E-154 | S_clust_2_vs_5   |
| S1pr4   | 8,3464E-42 | -0,6223805 | 0,19  | 0,673 | 1,66928E-38 | G2M_clust_2_vs_5 |
| Selplg  | 2,286E-231 | -0,9045231 | 0,42  | 0,903 | 4,5717E-228 | S_clust_2_vs_5   |
| Selplg  | 3,7618E-58 | -0,7594169 | 0,401 | 0,86  | 7,52366E-55 | G2M_clust_2_vs_5 |
| Slamf6  | 3,46E-53   | -0,56024   | 0,353 | 0,653 | 6,93E-50    | S_clust_4_vs_1   |
| Slamf6  | 1,58E-31   | -0,6482    | 0,271 | 0,643 | 3,15E-28    | G2M_clust_4_vs_1 |
| Snhg3   | 1,184E-173 | 0,65036631 | 0,923 | 0,63  | 2,3683E-170 | S_clust_2_vs_5   |
| Snhg3   | 4,8113E-44 | 0,54016998 | 0,889 | 0,55  | 9,62259E-41 | G2M_clust_2_vs_5 |
| Sp100   | 1,7462E-74 | 0,66771967 | 0,908 | 0,468 | 3,49244E-71 | G2M_clust_4_vs_5 |
| Sp100   | 1,702E-169 | 0,55067055 | 0,867 | 0,536 | 3,4043E-166 | S_clust_4_vs_5   |
| Srm     | 8,802E-259 | 0,99147562 | 0,96  | 0,578 | 1,7605E-255 | S_clust_2_vs_5   |
| Srm     | 9,0731E-67 | 0,80595265 | 0,972 | 0,655 | 1,81462E-63 | G2M_clust_2_vs_5 |
| Tcf7    | 1,50E-143  | -0,80465   | 0,059 | 0,506 | 3,00E-140   | S_clust_4_vs_1   |
| Tcf7    | 7,60E-53   | -0,81434   | 0,04  | 0,523 | 1,52E-49    | G2M_clust_4_vs_1 |
| Tcf7    | 3,3458E-77 | 0,81234021 | 0,506 | 0,058 | 6,69162E-74 | S_clust_1_vs_6   |
| Tcf7    | 2,36E-41   | 0,776952   | 0,523 | 0,067 | 4,73E-38    | G2M_clust_1_vs_6 |
| Tcf7    | 5,516E-179 | 0,99614784 | 0,63  | 0,056 | 1,1032E-175 | G1_clust_1_vs_6  |
| Tnfrsf4 | 9E-158     | 0,74203089 | 0,613 | 0,162 | 1,8001E-154 | S_clust_2_vs_5   |
| Tnfrsf4 | 1,5438E-38 | 0,67534608 | 0,564 | 0,186 | 3,08757E-35 | G2M_clust_2_vs_5 |
| Top2a   | 4,463E-28  | 0,79439014 | 0,661 | 0,313 | 8,92599E-25 | G2M_CLUST_4_VS_6 |
| Top2a   | 1,8891E-65 | 0,57134516 | 0,795 | 0,544 | 3,77814E-62 | S_CLUST_4_VS_6   |
| Tpi1    | 4,41E-47   | 0,694298   | 0,987 | 0,708 | 8,82E-44    | S_clust_7_vs_3   |
| Tpi1    | 5,863E-231 | 0,6416271  | 0,949 | 0,678 | 1,1727E-227 | G2M_clust_7_vs_3 |
| Tspo    | 1,086E-191 | -0,7370557 | 0,24  | 0,811 | 2,1721E-188 | S_clust_2_vs_5   |
| Tspo    | 1,809E-49  | -0,6568932 | 0,256 | 0,756 | 3,61791E-46 | G2M_clust_2_vs_5 |
| Tuba1a  | 1,796E-190 | -0,7681033 | 0,395 | 0,878 | 3,5913E-187 | S_clust_2_vs_5   |
| Tuba1a  | 1,1071E-49 | -0,6546187 | 0,398 | 0,838 | 2,21416E-46 | G2M_clust_2_vs_5 |
| Xcl1    | 8,958E-93  | 0,81585298 | 0,599 | 0,242 | 1,7916E-89  | S_clust_2_vs_5   |
| Xcl1    | 8,8195E-22 | 0,90336876 | 0,595 | 0,294 | 1,76391E-18 | G2M_clust_2_vs_5 |



**Supplementary Table 2:** top 50 genes used for RNA velocity analysis

|          |     |
|----------|-----|
| Selenoh  | CC  |
| Nasp     | CC  |
| Pola1    | CC  |
| Lockd    | CC  |
| Nap1l1   | CC  |
| Cenpp    | CC  |
| Dut      | CC  |
| Top2a    | CC  |
| Rrm2     | CC  |
| Gmnn     | CC  |
| Smc4     | CC  |
| Tacc3    | CC  |
| Clspn    | CC  |
| Ckap5    | CC  |
| Lmnb1    | CC  |
| Pop5     | CC  |
| Ddx39    | CC  |
| Kif11    | CC  |
| Tipin    | CC  |
| Hsp90ab1 | CC  |
| Rnaseh2b | CC  |
| Epsti1   | IM  |
| Il18r1   | IM  |
| Cmtm7    | IM  |
| Apbb1ip  | IM  |
| Skap1    | IM  |
| Lck      | IM  |
| Park7    | IM  |
| Anxa1    | IM  |
| Id2      | IM  |
| Lgals1   | IM  |
| Rnf138   | IM  |
| Gimap6   | IM  |
| Lsp1     | IM  |
| Malat1   | IM  |
| Gmfg     | MIG |

|               |           |
|---------------|-----------|
| Gramd3        | MIG       |
| Bin2          | MIG       |
| Actb          | MIG       |
| Cotl1         | MIG       |
| Glpr2         | MIG       |
| Ppp1r12a      | MIG       |
| Ezh2          | EPIG      |
| Sp100         | EPIG      |
| Cbx5          | EPIG      |
| 1500009L16Rik | Other     |
| Crip1         | other     |
| Mrps28        | Other     |
| Etfb          | Other     |
| Gimap4        | apoptosis |

CC: cell cycle; IM: immune; MIG: migration; EPIG: epigenetic

### Supplementary Table 3: MP gene signature

"Abca3";"Abl2";"Acpp";"Actn1";"Aff3";"Afp";"Akap13";"Als2cl";"Ar";"Arhgap5";"Armcx2";"Axl";"Bach2";"Bcl2";"Btd11";"Btla";"Ccr6";"Ccr7";"Cd2ap";"Cd55";"Cd7";"Cd86";"Cd9";"Cmpk2";"Cpm";"Ctla4";"Cxcr5";"Dapl1";"Ddr1";"Ddx60";"Dhx58";"Dock9";"Elovl6";"Emb";"Evl";"F2rl1";"Faah";"Fam101b";"Fam102a";"Fam134b";"Fam169b";"Fam26f";"Fam46c";"Fchsd2";"Fcrl1";"Filip1l";"Gpr183";"Hdgfrp3";"Hipk2";"Hvcn1";"Id3";"Ier3";"Ifitm3";"Ikbke";"Il7r";"Inpp4b";"Ipo4";"Jmjd1c";"Kbtbd11";"Lta";"Ltb";"Ly6e";"Lypd6b";"Lysmd2";"Mcoln2";"Myc";"Ncoa7";"Nrp1";"Nt5e";"Oas3";"Pacsin1";"Pak6";"Parp12";"Parp8";"Pde4b";"Pdk1";"Pfn2";"Pgs1";"Pik3lp1";"Pim2";"Plekha1";"Pou2af1";"Pou6f1";"Ptger2";"Ptpn3";"Qtrtd1";"Rab37";"Rgs10";"Rnf144a";"Rnf213";"Rtp4";"Sell";"Sgms1";"Sh3bp5";"Sirt5";"Slamf6";"Slc11a2";"Smad1";"Socs3";"Socs5";"Spint2";"Ssbp2";"St6gal1";"St8sia1";"Tacc2";"Taf4b";"Tbc1d4";"Tcf7";"Tlr1";"Tnfrsf25";"Tox";"Tpd52";"Traf1";"Trem1";"Trib2";"Trmt61a";"Tsc22d1";"Vav3";"Vwa5a";"Wdr12";"Wfikkn2";"Zc3h12d"

**Supplementary Table 4:** list of antibodies tested to characterise BrdU+ memory CD8 T cells generated at day 4 or 7 post-infection.

| Antibody                            | Source         | Identifier      | Dilution |
|-------------------------------------|----------------|-----------------|----------|
| PE anti-mouse CCL5 (2E9)            | Biolegend      | cat# 149103     | 1/400    |
| Biotin anti-mouse Ly6c (AL21)       | BD Biosciences | cat# 557359     | 1/800    |
| Biotin anti-mouse Ly108 (13G3-19D)  | ebiosciences   | cat# 13-1508    | 1/50     |
| BV650 anti-Rat/Mouse CD49a (Ha31/8) | BD Biosciences | cat# 740519     | 1/50     |
| PE-Cy7 anti-mouse CD127 (A7R34)     | Ebiosciences   | cat# 25-1271    | 1/100    |
| BV510 anti-mouse CD62L (MEL-14)     | Biolegend      | cat# 104441     | 1/200    |
| FITC anti-mouse KLRG1 (2F1)         | Ebiosciences   | cat# 11-5893-82 | 1/100    |
| BV421 anti-mouse CXCR3 (CXCR3-173)  | Biolegend      | cat# 126521     | 1/100    |

## Acknowledgment

We thank C. Yao (NIAMS) , J. O'shea (NIAMS), P. Schwartzberg (NIAID) and T. Wu (department of Immunology and Microbiology, University of Colorado School of Medicine) for sharing data and their advice. We acknowledge the contribution of SFR BioSciences (UAR3444/CNRS, US8/Inserm, École Normale Supérieure de Lyon, Université de Lyon) and of the CELPHEDIA infrastructure (<http://www.celphedia.eu/>), especially the center AniRA in Lyon (AniRA-Cytométrie and AniRA-PBES facilities). This work was supported by INSERM, CNRS, Université de Lyon, ENS Lyon, région Auvergne-Rhône-Alpes (Ingerence pack ambition) and ANR (MEMOIRE ANR-18-CE45-0001). Margaux Prieux has a région Auvergne-Rhône-Alpes PhD fellowship.

## Competing interests

The authors declare no competing financial interests.

## Bibliography

Appay V, Dunbar PR, Callan M, Klenerman P, Gillespie GM, Papagno L, Ogg GS, King A, Lechner F, Spina CA, Little S, Havlir DV, Richman DD, Gruener N, Pape G, Waters A, Easterbrook P, Salio M, Cerundolo V, McMichael AJ, Rowland-Jones SL (2002). Memory CD8+ T cells vary in differentiation phenotype in different persistent virus infections. *Nat Med.* Apr;8(4):379-85. doi: 10.1038/nm0402-379

Aran D, Looney AP, Liu L, Wu E, Fong V, Hsu A, Chak S, Ram P, Naikawadi, Wolters PJ, Abate AR, Butte AJ, Bhattacharya M (2019). Reference-based analysis of lung single-cell sequencing reveals a transitional profibrotic macrophage. *Nat. Immunol.* 20 (2): 163–72 doi.org/10.1038/s41590-018-0276-y

Arsenio J, Kakaradov B, Metz PJ, Kim SH, Yeo GW, Chang JT (2014). Early specification of CD8+ T lymphocyte fates during adaptive immunity revealed by single-cell gene-expression analyses. *Nat Immunol.* 15(4), 365-372. doi:10.1038/ni.2842

Bergen V, Lange M, Peidli S, Wolf FA, and Theis FJ (2020). Generalizing RNA velocity to transient cell states through dynamical modeling. *Nature biotechnology* 38, no. 12: 1408-1414.

Buchholz VR, Flossdorf M, Hensel I, Kretschmer L, Weissbrich B, Gräf P, Verschoor A, Schiemann M, Höfer T, Busch DH (2013). Disparate individual fates compose robust CD8+ T cell immunity. *Science.* May 3;340(6132):630-5. doi: 10.1126/science.1235454

Chang JT, Palanivel VR, Kinjyo I, Schambach F, Intlekofer AM, Banerjee A, Longworth SA, Vinup KE, Mrass P, Oliaro J, Killeen N, Orange JS, Russell SM, Weninger W, Reiner SL (2007). Asymmetric T lymphocyte division in the initiation of adaptive immune responses. *Science.* Mar 23;315(5819):1687-91. doi: 10.1126/science.1139393

Chen Z, Ji Z, Ngiow SF, Manne S, Cai Z, Huang AC, Johnson J, Staube RP, Bengsch B, Xu C, Yu S, Kurachi M, Herati RS, Vella LA, Baxter AE, Wu JE, Khan O, Beltra JC, Giles JR, Stelekati E, McLane LM, Lau CW, Yang X, Berger SL, Vahedi G, Ji H, Wherry EJ (2019). TCF-1-Centered Transcriptional Network Drives an Effector versus Exhausted CD8 T Cell-Fate Decision. *Immunity.* Nov 19;51(5):840-855.e5. doi: 10.1016/j.immuni.2019.09.013

Crauste F, Mafille J, Boucinha L, Djebali S, Gandrillon O, Marvel J, Arpin C (2017). Identification of Nascent Memory CD8 T Cells and Modeling of Their Ontogeny. *Cell Syst.* 4 (3), 306-317.e4. doi:10.1016/j.cels.2017.01.014

Eberlein J, Davenport B, Nguyen TT, Victorino F, Jhun K, van der Heide V, Kuleshov M, Ma'ayan A, Kedl R, Homann D (2020). Chemokine Signatures of Pathogen-Specific T Cells I: Effector T Cells. *J Immunol.* 2020 Oct 15;205(8):2169-2187. doi: 10.4049/jimmunol.2000253

Fitzpatrick DR, Shirley KM, Kelso A (1999). Cutting edge: stable epigenetic inheritance of regional IFN-gamma promoter demethylation in CD44<sup>high</sup>CD8<sup>+</sup> T lymphocytes. *J Immunol.* May 1;162(9):5053-7

Flossdorf M, Rössler J, Buchholz V, Busch DH, Höfer T (2015). CD8<sup>+</sup> T cell diversification by asymmetric cell division. *Nat Immunol.* 16, 891–893. doi: 10.1038/ni.3235

Gattinoni L, Klebanoff CA, Restifo NP (2012). Paths to stemness: building the ultimate antitumour T cell. *Nat Rev Cancer.* Oct;12(10):671-84. doi: 10.1038/nrc3322.

Gerlach C, Rohr JC, Perié L, van Rooij N, van Heijst JW, Velds A, Urbanus J, Naik SH, Jacobs H, Beltman JB, de Boer RJ, Schumacher TN (2013) Heterogeneous differentiation patterns of individual CD8<sup>+</sup> T cells. *Science.* May3;340(6132):635-9. doi: 10.1126/science.1235487.

Graef P, Buchholz VR, Stemberger C, Flossdorf M, Henkel L, Schiemann M, Drexler I, Höfer T, Riddell SR, Busch DH (2014). Serial transfer of single-cell-derived immunocompetence reveals stemness of CD8(+) central memory T cells. *Immunity.* Jul 17;41(1):116-26. doi: 10.1016/j.immuni.2014.05.018

Grau M, Valsesia S, Mafille J, Djebali S, Tomkowiak M, Mathieu AL, Laubretton D, de Bernard S, Jouve PE, Ventre E, Buffat L, Walzer T, Leverrier Y, Marvel J (2018). Antigen-Induced but Not Innate Memory CD8 T Cells Express NKG2D and Are Recruited to the Lung Parenchyma upon Viral Infection. *J Immunol.* 200(10),3635–3646. doi:10.4049/jimmunol.1701698

Gray SM, Amezcua RA, Guan T, Kleinstein SH, Kaech SM (2017). Polycomb Repressive Complex 2-Mediated Chromatin Repression Guides Effector CD8<sup>+</sup> T Cell Terminal Differentiation and Loss of Multipotency. *Immunity.* 2017 Apr 18;46(4):596-608. doi: 10.1016/j.immuni.2017.03.012

Hafemeister C, Satija R (2019). Normalization and variance stabilization of single-cell RNA-seq data using regularized negative binomial regression. *Genome Biol* 20, 296. //doi.org/10.1186/s13059-019-1874-1

Haluszczak C, Akue AD, Hamilton SE, Johnson LD, Pujanauski L, Teodorovic L, Jameson SC, Kedl RM (2009). The antigen-specific CD8<sup>+</sup> T cell repertoire in unimmunized mice includes memory phenotype cells bearing markers of homeostatic expansion. *J Exp Med* Feb 16;206(2):435-48. doi: 10.1084/jem.20081829.

Hikono H, Kohlmeier JE, Takamura S, Wittmer ST, Roberts AD, Woodland DL (2007). Activation phenotype, rather than central- or effector-memory phenotype, predicts the recall efficacy of memory CD8<sup>+</sup> T cells. *J Exp Med.* Jul 9;204(7):1625-36. doi: 10.1084/jem.20070322

Intlekofer AM, Takemoto N, Wherry EJ, Longworth SA, Northrup JT, Palanivel VR, Mullen AC, Gasink CR, Kaech SM, Miller JD, Gapin L, Ryan K, Russ AP, Lindsten T, Orange JS,

Goldrath AW, Ahmed R, Reiner SL (2005). Effector and memory CD8+ T cell fate coupled by T-bet and eomesodermin. *Nat Immunol.* Dec;6(12):1236-44. doi: 10.1038/ni1268.

Jacob J, Baltimore D (1999). Modelling T-cell memory by genetic marking of memory T cells in vivo. *Nature.* Jun 10;399(6736):593-7. doi: 10.1038/21208

Jameson SC, Masopust D (2009). Diversity in T cell memory: an embarrassment of riches. *Immunity.* Dec 18;31(6):859-71. doi: 10.1016/j.immuni.2009.11.007

Joshi NS, Cui W, Chandele A, Lee HK, Urso DR, Hagman J, Gapin L, Kaech SM (2007). Inflammation directs memory precursor and short-lived effector CD8(+) T cell fates via the graded expression of T-bet transcription factor. *Immunity,* 27 (2), 281-295. doi:10.1016/j.immuni.2007.07.010

Jubin V, Ventre E, Leverrier Y, Djebali S, Mayol K, Tomkowiak M, Mafille J, Teixeira M, Teoh DY, Walzer T, Arpin C and Marvel J (2012). T inflammatory memory CD8 T cells participate to antiviral response and generate secondary memory cells with an advantage in XCL1 production. *Immunol Res* 52, 284–293. DOI: 10.1007/s12026-012-8340-4

Kaech SM, Cui W. Transcriptional control of effector and memory CD8+ T cell differentiation (2012). *Nat Rev Immunol.* Nov;12(11):749-61. doi: 10.1038/nri3307

Kakaradov B, Arsenio J, Widjaja CE, He Z, Aigner S, Metz PJ, Yu B, Wehrens EJ, Lopez J, Kim SH, Zuniga EI, Goldrath AW, Chang JT and Yeo GW (2017). Early transcriptional and epigenetic regulation of CD8+T cell differentiation revealed by single-cell RNA sequencing. *Nat immunol.* 18 (4), 422–432. doi:10.1038/ni.3688

Kalia V, Sarkar S, Subramaniam S, Haining WN, Smith KA, Ahmed R (2010). Prolonged interleukin-2 $\alpha$  expression on virus-specific CD8+ T cells favors terminal-effector differentiation in vivo. *Immunity.* Jan 29;32(1):91-103. doi: 10.1016/j.immuni.2009.11.010

Kurd NS, He Z, Louis TL, Milner JJ, Omilusik KD, Jin W, Tsai MS, Widjaja CE, Kanbar JN, Olvera JG, Tysl T, Quezada LK, Boland BS, Huang WJ, Murre C, Goldrath AW, Yeo GW, Chang JT (2020). Early precursors and molecular determinants of tissue-resident memory CD8+T lymphocytes revealed by single-cell RNA sequencing. *Sci Immunol.* 15; 5(47):eaaz6894. doi: 10.1126/sciimmunol.aaz6894

Lun ATL, McCarthy DJ, Marioni JC (2016). A step-by-step workflow for low-level analysis of single-cell RNA-seq data with Bioconductor. *F1000Res.*, 5, 2122. doi: 10.12688/f1000research.9501.2

Marcais A, Coupet CA, Walzer T, Tomkowiak M, Ghittoni R, Marvel J (2006). Cell-autonomous CCL5 transcription by memory CD8 T cells is regulated by IL-4. *J Immunol.* Oct 1;177(7):4451-7. doi: 10.4049/jimmunol.177.7.4451

Mann TH, Kaech SM (2019). Tick-TOX, it's time for T cell exhaustion. *Nat Immunol.* Sep;20(9):1092-1094. doi: 10.1038/s41590-019-0478-y

Masopust D, Vezys V, Marzo AL, Lefrançois L (2001). Preferential localization of effector memory cells in nonlymphoid tissue. *Science*. Mar 23;291(5512):2413-7. doi: 10.1126/science.1058867

McCarthy DJ, Campbell KR, Lun ATL, Willis QF (2017). Scater: pre-processing, quality control, normalisation and visualisation of single-cell RNA-seq data in R. *Bioinformatics*, 33, 1179-1186. doi: 10.1093/bioinformatics/btw777

Melsted, P, Boeshaghi A.S, Liu L, Gao F, Lu L, Min KH, Da Veiga Beltrame E, Hjorleifsson KE, Gehring J, Pachter L (2021). Modular, efficient and constant-memory single-cell RNA-seq preprocessing. *Nat Biotechnol* 39, 813–818. doi.org/10.1038/s41587-021-00870-2

Moussy A, Cosette J, Parmentier R, da Silva C, Corre G, Richard A, Gandrillon O, Stockholm D, Páldi A (2017). Integrated time-lapse and single-cell transcription studies highlight the variable and dynamic nature of human hematopoietic cell fate commitment. *PLoS Biol*. Jul 27;15(7):e2001867. doi: 10.1371/journal.pbio.2001867.

Obar JJ, Khanna KM, Lefrançois L (2008). Endogenous naive CD8+ T cell precursor frequency regulates primary and memory responses to infection. *Immunity*. Jun;28(6):859-69. doi: 10.1016/j.immuni.2008.04.010. Epub 2008

Omilusik KD, Best JA, Yu B, Goossens S, Weidemann A, Nguyen JV, Seuntjens E, Stryjewska A, Zweier C, Roychoudhuri R, Gattinoni L, Bird LM, Higashi Y, Kondoh H, Huylebroeck D, Haigh J, Goldrath AW (2015). Transcriptional repressor ZEB2 promotes terminal differentiation of CD8+ effector and memory T cell populations during infection. *J Exp Med*. Nov 16;212(12):2027-39. doi: 10.1084/jem.20150194.

Omilusik KD, Nadsombati MS, Shaw LA, Yu B, Milner JJ, Goldrath AW (2018). Sustained Id2 regulation of E proteins is required for terminal differentiation of effector CD8+ T cells. *J Exp Med*. Mar 5;215(3):773-783. doi: 10.1084/jem.20171584

Pace L, Goudot C, Zueva E, Gueguen P, Burgdorf N, Waterfall JJ, Quivy JP, Almouzni G, Amigorena S (2018). The epigenetic control of stemness in CD8+ T cell fate commitment. *Science*. Jan 12;359(6372):177-186. doi: 10.1126/science.aah6499

Papalexii E, Satija R (2018). Single-cell RNA sequencing to explore immune cell heterogeneity. *Nat Rev Immunol* 18, 35–45. doi.org/10.1038/nri.2017.76

Saelens W, Cannood, R, Todorov H, Saeys Y (2019). A comparison of single-cell trajectory inference methods. *Nat Biotechnol* 37, 547–554 doi.org/10.1038/s41587-019-0071-9

Sarkar S, Kalia V, Haining WN, Konieczny BT, Subramaniam S, Ahmed R (2008). Functional and genomic profiling of effector CD8 T cell subsets with distinct memory fates. *J Exp Med*. Mar 17;205(3):625-40. doi: 10.1084/jem.20071641

Sallusto F, Lenig D, Förster R, Lipp M, Lanzavecchia A (1999). Two subsets of memory T lymphocytes with distinct homing potentials and effector functions. *Nature* Oct 14;401(6754):708-12. doi: 10.1038/44385. PMID: 10537110.

Shin HM, Kapoor VN, Kim G, Li P, Kim HR, Suresh M, Kaech SM, Wherry EJ, Selin LK, Leonard WJ, Welsh RM, Berg LJ (2017). Transient expression of ZBTB32 in anti-viral CD8+

T cells limits the magnitude of the effector response and the generation of memory. *PLoS Pathog.* Aug 21;13(8):e1006544. doi: 10.1371/journal.ppat.1006544

Street KY, Risso D, Fletcher RB, Das D, Ngai J, Yosef N, Purdom E, and Dudoit S (2018). Slingshot: Cell lineage and pseudotime inference for single-cell transcriptomics. *BMC Genomics*, 19(1):1–16. doi: 10.1186/s12864-018-4772-0

Tirosh I, Izar B, Prakadan SM, Wadsworth MH 2nd, Treacy D, Trombetta JJ, Rotem A, Rodman C, Lian C, Murphy G, Fallahi-Sichani M, Dutton-Regester K, Lin JR, Cohen O, Shah P, Lu D, Genshaft AS, Hughes TK, Ziegler CG, Kazer SW, Gaillard A, Kolb KE, Villani AC, Johannessen CM, Andreev AY, Van Allen EM, Bertagnolli M, Sorger PK, Sullivan RJ, Flaherty KT, Frederick DT, Jané-Valbuena J, Yoon CH, Rozenblatt-Rosen O, Shalek AK, Regev A, Garraway LA (2016). Dissecting the multicellular ecosystem of metastatic melanoma by single-cell RNA-seq. *Science*. Apr 8;352(6282):189-96. doi: 10.1126/science.aad0501

Todorov H, Cannoodt R, Saelens W, Saeys Y (2020). TinGa: fast and flexible trajectory inference with Growing Neural Gas. *Bioinformatics*, 36, i66-i74. doi: 10.1093/bioinformatics/btaa463

Utzschneider DT, Charmoy M, Chennupati V, Pousse L, Ferreira DP, Calderon-Copete S, Danilo M, Alfei F, Hofmann M, Wieland D, Pradervand S, Thimme R, Zehn D, Held W (2016). T Cell Factor 1-Expressing Memory-like CD8(+) T Cells Sustain the Immune Response to Chronic Viral Infections. *Immunity*. Aug 16;45(2):415-27. doi: 10.1016/j.immuni.2016.07.021

Van de Laar L, Saelens W, De Prijck S, Martens L, Scott CL, Van Isterdael G, Hoffmann E, Beyaert R, Saeys Y, Lambrecht BN, Guillems M (2016). Yolk Sac Macrophages, Fetal Liver, and Adult Monocytes Can Colonize an Empty Niche and Develop into Functional Tissue-Resident Macrophages. *Immunity*. Apr 19;44(4):755-68. doi: 10.1016/j.immuni.2016.02.017

Wherry EJ, Blattman JN, Murali-Krishna K, van der Most R, Ahmed R (2003). Viral persistence alters CD8 T-cell immunodominance and tissue distribution and results in distinct stages of functional impairment. *J Virol*. Apr;77(8):4911-27. doi: 10.1128/jvi.77.8.4911-4927

Wherry EJ, Ha SJ, Kaech SM, Haining WN, Sarkar S, Kalia V, Subramaniam S, Blattman JN, Barber DL, Ahmed R (2007). Molecular signature of CD8+ T cell exhaustion during chronic viral infection. *Immunity*. Oct;27(4):670-84. doi: 10.1016/j.immuni.2007.09.006

Wu T, Ji Y, Moseman EA, Xu HC, Manghani M, Kirby M, Anderson SM, Handon R, Kenyon E, Elkahloun A, Wu W, Lang PA, Gattinoni L, McGavern DB, Schwartzberg PL (2016). The TCF1-Bcl6 axis counteracts type I interferon to repress exhaustion and maintain T cell stemness. *Sci Immunol*. Dec 23;1(6):eaai8593. doi: 10.1126/sciimmunol.aai8593

Yang CY Best JA, Knell J, Yang E, Sheridan AD, Jesionek AK, Li2 HS, Rivera RR, Lind KC, M D'Cruz L, Watowich SS, Murre C and Goldrath AW (2011). The transcriptional regulators Id2 and Id3 control the formation of distinct memory CD8+ T cell subsets. *Nat. Immunol.*, 12, 1221–1229. doi:10.1038/ni.2158

Yao, C., Sun, H.W, Lacey, N.E, Ji, Y, Moseman, E.A & al (2019). Single-cell RNA-seq reveals TOX as a key regulator of CD8+ T cell persistence in chronic infection. *Nat. Immunol.*, 20, 890-901. doi: 10.1038/s41590-019-0403-4

Youngblood B, Hale JS, Kissick HT, Ahn E, Xu X, Wieland A, Araki K, West EE, Ghoneim HE, Fan Y, Dogra P, Davis CW, Konieczny BT, Antia R, Cheng X, Ahmed R (2017). Effector CD8 T cells dedifferentiate into long-lived memory cells. *Nature*. 2017 Dec 21;552(7685):404-409. doi: 10.1038/nature25144